

INTEGRAL EQUATION TECHNIQUES
IN GROUNDWATER FLOW

A thesis
submitted in partial fulfilment
of the requirements for the Degree
of
Doctor of Philosophy in Civil Engineering
at the
University of Canterbury
by
PHILIP H. MITCHELL

University of Canterbury,
Christchurch, New Zealand.

January 1984.

TABLE OF CONTENTS

CHAPTER		PAGE
	TABLE OF CONTENTS	i.
	ABSTRACT	iii.
	ACKNOWLEDGEMENTS	iv.
	LIST OF FIGURES	v.
	LIST OF TABLES	xii.
	LIST OF SYMBOLS	xiii.
1	INTRODUCTION	
	1.1 General Discussion	1.
	1.2 Scope of the Thesis	3.
2	LITERATURE REVIEW	
	2.1 The History of Integral Equation Techniques	5.
	2.2 Unsteady Seepage Through Embankments . .	11.
	2.3 The Unsteady Dupuit Equation	14.
3	UNSTEADY SEEPAGE THROUGH EMBANKMENTS	
	3.1 Introduction	22.
	3.2 Integral Equation Formulation	22.
	3.3 Problem Formulation	24.
	3.4 Numerical Solution	27.
	3.5 Experimental Solution	31.
	3.6 Dupuit Approximation Solution	31.
4	EVALUATION OF THE TECHNIQUES GIVEN IN CHAPTER 3	
	4.1 Introduction	35.
	4.2 Seepage Through a Homogeneous, Isotropic Embankment	35.
5	SOLUTIONS OF THE UNSTEADY DUPUIT EQUATION	
	5.1 Introduction	50.
	5.2 Formulation for a Homogeneous Region That Contains No Wells	51.
	5.3 Numerical Solutions	55.
	5.4 Inclusion of Wells in a Homogeneous Region	77.
	5.5 Calculation of h at Internal Points . .	80.
	5.6 Composite Regions	81.

TC
176
M682
1984

CHAPTER		PAGE
6	COMPARISONS BETWEEN THE NUMERICAL TECHNIQUES OF CHAPTER 5	
6.1	Introduction.	84.
6.2	Flows in Homogeneous Regions That Contain No Wells.	86.
6.3	Flows in Homogeneous Regions That Include Wells	117.
6.4	Flow in Composite Regions	137.
7	CONCLUSIONS	
7.1	Summary	161.
7.2	Unsteady Seepage Through Embankments. .	161.
7.3	The Unsteady Dupuit Equation.	161.
	BIBLIOGRAPHY	163.
	APPENDICES	
APPENDIX A	Estimation of Boundary Layer Thickness for the Hele-Shaw Experiment.	A1.
APPENDIX B	Fortran Computer Programs Derived from Methods 1 and 2 of Chapter 5.	B1.

ABSTRACT

In this study, integral equation techniques are developed to solve two different types of groundwater flow problem. The first formulation, based on the Cauchy integral theorem, is used to obtain numerical solutions for unsteady, two-dimensional flow through a homogeneous, isotropic embankment. Free surface profiles following instantaneous drawdown of an upstream reservoir are presented in dimensionless form. The results from an unsteady, parallel-plate, viscous-flow experiment are included to check the accuracy of one of the numerical solutions and to show the limitations of the experimental approach. The numerical results are also compared with the simpler results obtained by making the Dupuit approximation, the inadequacies of which are also discussed.

In aquifers where horizontal dimensions are orders of magnitude greater than vertical dimensions the Dupuit approximation is valid, and a three-dimensional problem is reduced to two dimensions in the horizontal plane. An integral equation technique for solving such problems is presented, in which time-dependent fundamental solutions of the governing partial differential equation are distributed around the flow boundary so that the initial and boundary conditions are satisfied. Two numerical methods of solving the integral equation are compared for a wide range of problems in both homogeneous and zoned regions. Each region may, or may not, contain wells. Comparisons with the finite-difference method are also made for certain problems.

ACKNOWLEDGEMENTS

This study was performed in the Department of Civil Engineering, University of Canterbury, under the guidance of Professor R. Park.

I am indebted to my supervisor, Dr. B. Hunt, for his invaluable assistance, thought-provoking ideas and friendship.

I would also like to thank the following most sincerely for their help during the course of this project;

The Ministry of Works and Development for their financial support;

Mrs. V. Grey and Mr. B. Bishop for their draughting expertise;

Mr. L. Gardner for the photographic work;

Mrs. C. Currie and Mrs. J.E. Stewart for their excellent work in typing the manuscript and;

My fellow students for their help and encouragement.

Finally, I would like to thank my parents for their support, and my wife, Susan, for her inspiration.

LIST OF FIGURES

<u>Figure</u>		<u>Page</u>
3.1	Definition Diagram for Seepage Through an Embankment.	25.
3.2	Flow Chart for Calculation of Unsteady Free Surface Profiles.	29.
3.3	Typical Steady-State Nodal Arrangement.	30.
3.4	Typical Nodal Arrangement Following Drawdown.	30.
4.1	Dimensionless Free Surface Profiles for $H_0/L = 0.1667$.	36.
4.2	Dimensionless Free Surface Profiles for $H_0/L = 0.1389$.	37.
4.3	Dimensionless Free Surface Profiles for $H_0/L = 0.1111$.	38.
4.4	Comparison Between Numerical and Experimental Solutions for $H_0/L = 0.1667$.	39.
4.5	Comparison Between Numerical and Linearized Dupuit Solutions for $H_0/L = 0.1667$.	42.
4.6	Comparison Between Numerical and Linearized Dupuit Solutions for $H_0/L = 0.1111$.	43.
4.7	Comparison Between Numerical and Non-linear Dupuit Solutions for $H_0/L = 0.1667$.	47.
4.8	Comparison Between Numerical and Non-linear Dupuit Solutions for $H_0/L = 0.1111$.	48.
5.1	Definition Diagram for Two-Dimensional Flow.	50.
5.2	Boundary Node Geometry.	54.
5.3	Typical Nodal Arrangement for Homogeneous Region.	55.

<u>Figure</u>		<u>Page</u>
5.4	Definition Diagram for Numerical Calculation of Eqn. 5.30.	58.
5.5	Definition Diagram for Numerical Calculation of Eqn. 5.44.	62.
5.6	Definition Diagram for Calculating $\int_{\Gamma' + \Gamma''} \frac{\cos(r, n)}{r} ds$	65.
5.7	Typical Composite Region.	81.
5.8	Typical Nodal Arrangement for Composite Region.	82.
6.1	Nodal Arrangement for Square Region.	85.
6.2	Nodal Arrangement for Quarter Circle.	85.
6.3	Distribution of h' on $y' = 0$, following instantaneous unit rise in h' at $x' = 1.0$.	88.
6.4	Variation of h' with time at two internal points for the problem shown in Fig. 6.3.	89.
6.5	Variation of $\frac{\partial h'}{\partial n}$ with time at (1.0, 0.5) for the problem shown in Fig. 6.3.	90.
6.6	Distribution of h' , on $y' = 0$ when $h'(x' = 1.0, t') = 1 - e^{-500t'}$, $t' > 0$.	93.
6.7	Variation of h' with time at two internal points for the problem shown in Fig. 6.6.	94.
6.8	Variation of $\frac{\partial h'}{\partial n}$ with time at (1.0, 0.5) for the problem shown in Fig. 6.6.	95.
6.9	Distribution of h' on $y' = 0$ when $h'(x' = 1.0, t') = 1 - e^{-t'}$, $t' > 0$.	96.

<u>Figure</u>		<u>Page</u>
6.10	Variation of h' with time at two internal points for the problem shown in Fig. 6.9.	97.
6.11	Variation of $\frac{\partial h'}{\partial n}$ with time at (1.0, 0.5) for the problem shown in Fig. 6.9.	98.
6.12	Distribution of h' on $y' = 0$ when $h'(x' = 1.0, t') = \sin\left[\frac{\pi t'}{2}\right], t' > 0.$	100.
6.13	Variation of h' with time at two internal points for the problem shown in Fig. 6.12.	101.
6.14	Variation of $\frac{\partial h'}{\partial n}$ with time at (1.0, 0.5) for the problem shown in Fig. 6.12.	102.
6.15	Comparison between Method 2 and Finite-Difference solutions when $h'(x' = 1.0, t') = 1 - e^{-500t'}, t' > 0.$	104.
6.16	Comparison between Method 2 and Finite Difference solutions when $h'(x' = 1.0, t') = 1 - e^{-t'}, t' > 0.$	105.
6.17	Distribution of h' on the radial boundaries following instantaneous rise in h' at $r' = 1.0.$	107.
6.18	Variation of h' with time at three internal points for the problem shown in Fig. 6.17.	108.
6.19	Variation of $\frac{\partial h'}{\partial n}$ with time on the circumferential boundary for the problem shown in Fig. 6.17.	109.
6.20	Distribution of h' on the radial boundary when $h'(r' = 1.0, t') = 1 - e^{-500t'}, t' > 0.$	111.
6.21	Variation of h' with time at three internal points for the problem shown in Fig. 6.20.	112.

<u>Figure</u>		<u>Page</u>
6.22	Variation of $\frac{\partial h'}{\partial n}$ with time on the circumferential boundary for the problem shown in Fig. 6.20.	113.
6.23	Distribution of h' on the radial boundary when $h'(r' = 1.0, t') = 1 - e^{-t'}$, $t' > 0$.	114.
6.24	Variation of h' with time at three internal points for the problem shown in Fig. 6.23.	115.
6.25	Variation of $\frac{\partial h'}{\partial n}$ with time on the circumferential boundary for the problem shown in Fig. 6.23.	116.
6.26	Distribution of h' on the radial boundary when $h'(r' = 1.0, t') = \sin\left(\frac{\pi t'}{2}\right)$, $t' > 0$.	118.
6.27	Variation of h' with time at two internal points for the problem shown in Fig. 6.26.	119.
6.28	Variation of $\frac{\partial h'}{\partial n}$ with time on the circumferential boundary for the problem shown in Fig. 6.26.	120.
6.29	Distribution of h' on $y' = 0$ when $h'(x' = 1.0, t') = 1 - e^{-t'}$, $t' > 0$ and there is a well of strength $\frac{Q'}{4\pi} = 0.1$ at $(0.5, 0.5)$.	123.
6.30	Variation of h' with time at three internal points for the problem shown in Fig. 6.29.	124.
6.31	Variation of $\frac{\partial h'}{\partial n}$ with time at $(1.0, 0.2)$ for the problem shown in Fig. 6.29.	125.
6.32	Comparison between Method 2 and Finite-Difference Solutions on $y' = 0$ for the problem shown in Fig. 6.29.	126.
6.33	Distribution of h' on $y' = 0$ when $h'(x' = 1.0, t') = 1 - e^{-500t'}$, $t' > 0$ and there is a well of strength $\frac{Q'}{4\pi} = 0.1$ at $(0.5, 0.5)$.	128.

<u>Figure</u>		<u>Page</u>
6.34	Variation of h' with time at three internal points for the problem shown in Fig. 6.33.	129.
6.35	Variation of $\frac{\partial h'}{\partial n}$ with time at (1.0, 0.2) for the problem shown in Fig. 6.33.	130.
6.36	Distribution of h' on $y' = 0$ when $h'(x' = 1.0, t') = 1 - e^{-t'}$, $t' > 0$ and there is a well of strength $\frac{Q'}{4\pi} = 0.1$ at (0.25, 0.25).	131.
6.37	Distribution of h' on $x' = 0$ for the problem shown in Fig. 6.36.	132.
6.38	Variation of h' with time at three internal points for the problem shown in Fig. 6.36.	133.
6.39	Variation of $\frac{\partial h'}{\partial n}$ with time at two points on $x' = 1.0$ for the problem shown in Fig. 6.36.	134.
6.40	Comparison between Method 2 and Finite-Difference solutions on $y' = 1.0$ for the problem shown in Fig. 6.36.	135.
6.41	Distribution of h' on $y' = x'$ when $\frac{\partial h'}{\partial n}(x' = y') = 0$ and h' on the permeable portion of the boundary is given by Eqn. 6.23.	138.
6.42	Variation of h' with time at three internal points for the problem shown in Fig. 6.41.	139.
6.43	Variation of $\frac{\partial h'}{\partial n}$ with time at various points on the boundary contour for the problem shown in Fig. 6.41.	140.
6.44	Distribution of h' on $y' = 0$ when $h'(x' = -1.0) = 1.0$ and $h'(x' = 1.0) = 0$.	142.
6.45	Variation of h' with time at two points within each zone for the problem shown in Fig. 6.44.	143.

<u>Figure</u>		<u>Page</u>
6.46	Variation of $\frac{\partial h'}{\partial n}$ with time at $x' = -0.5$, $x' = 0.5$ and $x' = 0$ for the problem shown in Fig. 6.44.	144.
6.47	Distribution of h' on $y' = 0$ when $h'(x' = -1.0) = 1.0$, $h'(x' = 1.0) = 0$ and the boundary contour is irregular.	145.
6.48	Variation of h' with time at three internal points for the problem shown in Fig. 6.47.	146.
6.49	Variation of $\frac{\partial h'}{\partial n}$ with time on the boundary contour for the problem shown in Fig. 6.46.	147.
6.50	Variation of $\frac{\partial h'}{\partial n}$ with time on the boundary contour for the problem shown in Fig. 6.47.	148.
6.51	Distribution of h' on $y' = 0$ when $h'(x' = 1.0, t') = 1 - e^{-t'}$, $t' > 0$ and the solution domain consists of two zones.	150.
6.52	Variation of h' with time at one point within each zone for the problem shown in Fig. 6.51.	151.
6.53	Variation of $\frac{\partial h'}{\partial n}$ with time at $(0.5, 0.5)$ and $(1.0, 0.5)$ for the problem shown in Fig. 6.51.	152.
6.54	Distribution of h' on $y' = 0$ when $h'(x' = 1.0, t') = 1 - e^{-t'}$, $t' > 0$ and there is a well of strength $\frac{Q'}{4\pi} = 0.1$. (The solution domain consists of two zones).	154.
6.55	Distribution of h' on $y' = 1.0$ for the problem shown in Fig. 6.54.	155.
6.56	Distribution of h' on $x' = 0$ for the problem shown in Fig. 6.54.	156.

<u>Figure</u>		<u>Page</u>
6.57	Distribution of h' on $x' = 0.5$ for the problem shown in Fig. 6.54.	157.
6.58	Variation of h' with time at three internal points for the problem shown in Fig. 6.54.	158.
6.59	Variation of $\frac{\partial h'}{\partial n}$ with time at $(0.5, 0.2)$ and $(0.5, 0.8)$ for the problem shown in Fig. 6.54.	159.
6.60	Variation of $\frac{\partial h'}{\partial n}$ with time at $(1.0, 0.2)$ and $(1.0, 0.8)$ for the problem shown in Fig. 6.54.	160.

LIST OF TABLES

<u>Table</u>		<u>Page</u>
4.1	Comparison of Steady-State Flow Rates for Numerical and Dupuit Solutions.	41.
4.2	Comparison of Horizontal and Vertical Velocities from Linearized Dupuit Solution.	46.
6.1	Incremental Time Schemes used in the Numerical Calculations.	87.

LIST OF SYMBOLS

Note: Only the commonly used symbols are listed.

Chapters 3 and 4

B	Plate spacing in Hele-Shaw experiment
\hat{e}_n	Outward pointing normal to the free surface
g	Acceleration due to gravity
h	Piezometric head
H_0	Reservoir depth
K	Permeability
L	Embankment base width
n	Arc length perpendicular to the free surface
P	Pressure
q	Two-dimensional flow rate
\underline{r}	Position vector of (x,y)
s	Arc length along the free surface
t	Time
t_0	Time for reservoir to reach zero depth
u, v	Velocity components
u'	Function defined in Appendix A
w	Complex potential, $\phi + i\psi$
x,y	Cartesian coordinates
z	Complex number, $x + iy$
ϵ	Ratio of reservoir depth to embankment base width
δ	Boundary layer thickness
ν	Kinematic viscosity
σ	Porosity
ρ	Mass density
ϕ	Velocity potential function
ψ	Stream function
Γ	Exterior boundary of the flow region
ζ	Point on the boundary
Ω	Angle between the boundary tangents at ζ_i
θ	Angle between the straight lines joining ζ_{i-1} - ζ_i and ζ_i and ζ_{i+1}
β	Ratio of horizontal coordinate of the intersection between upstream face of the embankment with the reservoir free surface; to the embankment base width, L
η	Square of piezometric head.

Chapters 5 and 6

a^2	Ratio of transmissivity to storage coefficient
E_1	Exponential integral function
f, g	Specified boundary conditions
F, G	Specified functions
h	Piezometric head
$h^k(I)$	Value of h at point I at time t_k
h'	Dimensionless piezometric head
$J_p(x)$	Bessel function of the first kind of order p
K	Permeability
L	Representative length
M	Number of boundary nodes
n	Arc length normal to the boundary contour
n_I	Value of n at point I
N	Number of time steps
Q	Three-dimensional flow rate
Q'	Dimensionless three-dimensional flow rate
r	Distance between two points
r_I	Distance from singular point P to point I
r'	Dimensionless distance between two points
s	Arc length along the boundary contour
S	Storage Coefficient
t	Time
t'	Dimensionless time
T	Transmissivity
u	Time-dependent fundamental solution
x, y	Cartesian coordinates
x', y'	Dimensionless Cartesian coordinates
α, β, ϵ	Constants
τ	Time
γ	Euler's constant
ζ, η	Cartesian coordinates.

Chapter 1

INTRODUCTION

1.1 GENERAL DISCUSSION

The flow of groundwater is of great importance in Civil Engineering, and its influence extends over a wide range of disciplines including; drainage, irrigation, soil stability, and water resource management. In order to find the distribution of piezometric head, h , throughout an aquifer, it is necessary to solve a partial differential equation subject to specified initial and boundary conditions. It is desirable to calculate analytical solutions to these problems, but this is seldom possible due, often, to irregularities in the shape of aquifer boundaries. Consequently, approximate solutions must be calculated either by analogue methods, which are based on the similarity between groundwater flow and other physical systems obeying the same partial differential equation, or by numerical techniques.

The emergence of powerful, high-speed computers capable of storing and manipulating large amounts of data has led to the virtual abandonment of analogue methods and to the development and refinement of a wide range of numerical techniques which can be used to solve both steady and time-dependent groundwater flow problems. Probably the simplest and most widely used of these is the finite-difference method, in which the aquifer under consideration is represented by a finite number of discrete points arranged in a regular pattern or grid. The value of the dependent variable at each point in the grid is approximated with a polynomial of predetermined order, the coefficients of which are written in terms of the values of the dependent variable at adjacent nodes. An algebraic approximation to the partial differential equation at each node is then calculated from this polynomial, and the resulting set of equations solved simultaneously to give values of the

dependent variable throughout the solution domain. Specific details of some finite-difference techniques are given by Bear (1979) and Hunt (1983, at press).

A second numerical technique is the finite-element method, in which the solution domain is subdivided into a finite number of zones or "elements". For steady flows, the distribution of the dependent variable in each element is approximated by a polynomial whose coefficients are determined from values of the dependent variable at the nodes of the element. The numerical solution is then obtained by substituting each polynomial into a definite integral which is equivalent to the partial differential equation and then solving the set of equations simultaneously, either by weighted residual techniques, Galerkin approximations, least squares residual approximations or by the calculus of variations. These techniques are described in detail by Norrie and de Vries (1978). Time-dependent problems are usually solved with the finite-element method by using a finite-difference approximation for the time derivative that appears in the governing partial differential equation. This leads to an elliptic partial differential equation that must be solved at the end of each time step, a procedure which is similar to obtaining a series of steady-state solutions that are small time intervals apart.

If a groundwater flow problem is described by a linear partial differential equation with constant coefficients, then the solution can be calculated using integral equation techniques. For steady flows, fundamental solutions to the partial differential equation are used as weighting functions in an integral equation that is equivalent to the partial differential equation. The unknowns that appear in the integral equation are only those values that occur on the exterior boundary of the solution domain. Numerical solutions are obtained by representing the exterior boundary with a finite number of nodes and writing an integral equation at each node. The set of equations is then solved simultaneously.

Solutions to transient flow problems may be calculated by using Laplace transforms to remove the time dependence from the governing partial differential equation and then using integral equation techniques to solve the transformed problem. This solution must be inverted numerically to obtain the solution in the physical domain. Another more direct method of solving time-dependent problems with integral equations is to write the time derivative in finite-difference form. In this way, the solution at one time can be calculated from the solution at a previous time in terms of an integral equation containing only boundary data and a surface integral over the entire solution domain. A third method is to use a time-dependent fundamental solution as a weighting function in the integral equation. This can sometimes be done in a way that eliminates the need for calculating a surface integral over the solution domain.

The principal advantage of integral equation techniques is that if only boundary data is used in the calculations the dimensionality of the problem is essentially reduced by one. Thus, the amount of data preparation is considerably less than that required by either the finite-difference or finite-element methods. Solutions within the flow region can readily be calculated from an integral equation solution, as will be shown in Chapters 3 and 5, and the advantage of reduced data preparation is still significant because only points at which the solution is required need to be specified.

1.2 SCOPE OF THE THESIS

The aim of this study is to present integral equation formulations that can be used to solve a variety of unsteady groundwater flow problems. A review of the relevant literature, including a brief history of integral equation techniques, is given in Chapter 2.

In Chapter 3 the Cauchy integral theorem is used to obtain a formulation that describes unsteady, two-dimensional

flow through homogeneous, isotropic embankments. An experimental analogue solution, the Hele-Shaw model, is also described, as is the analytical solution that is obtained by making the Dupuit approximation. Free surface profiles following the instantaneous drawdown of an upstream reservoir are presented in dimensionless form in Chapter 4. The results calculated with the integral equation formulation are compared with the less sophisticated Dupuit solutions, and the Hele-Shaw experiment is used to check the accuracy of one integral equation solution.

The flow of groundwater is essentially a three-dimensional problem, but in many real situations the horizontal dimension of an aquifer are much greater than the vertical dimensions. In such cases it is possible to make the Dupuit approximation, which assumes that flow is horizontal. Consequently, the problem is reduced to two dimensions in the horizontal plane. Chapter 5 is concerned with the solution of these problems for both homogeneous and zoned regions, which may, or may not, include wells. These methods are discussed and, in some cases, compared with finite-difference solutions in Chapter 6.

Chapter 2

LITERATURE REVIEW

2.1 THE HISTORY OF INTEGRAL EQUATION TECHNIQUES

The theory of integral equations is well known in classical potential theory and is described in texts like Kellogg (1929), Sternberg and Smith (1946), Muskhelishvili (1946) and many others. With the advent of computers and the associated research of numerical methods, the techniques have progressed from being a mathematical concept to a valuable engineering and scientific tool.

Integral equation methods have been developed to solve a variety of problems ever since the pioneering work of Smith and Pierce (1958) in steady-state aeronautics. They and subsequent authors including; Hess and Smith (1962, 1967), Jaswon (1963), Symm (1963), Giesing (1964, 1966) and Massonnet (1965) used an indirect method of solving the Laplace equation, whereby a Fredholm integral equation of the second kind was formulated in terms of a distribution of unknown source densities on the external boundary of the region under consideration. The solutions for the source densities were then used to generate the required physical solution on the boundary and at any points of interest within the region. This technique is described in some detail by Jaswon and Symm (1977), and, although it can be applied to either the Neumann or Dirichlet problems, it does not appear to have been used to solve the mixed boundary-value problems that occur in groundwater flow.

A direct formulation in which the boundary data act as source densities appears in Kellogg's book (1929), but was probably first applied by Jaswon (1963). A brief outline of the solution method for two-dimensional problems is presented here, although three-dimensional problems may be treated in a similar manner. If two functions U and V are continuously differentiable throughout the solution

domain, R , then Green's second identity;

$$\int_R \left[V \nabla^2 U - U \nabla^2 V \right] dA = \int_{\Gamma} \left[V \frac{\partial U}{\partial n} - U \frac{\partial V}{\partial n} \right] ds \quad (2.1)$$

holds, in which Γ defines the boundary contour of the region R , n = arc length in the direction of the outward pointing normal, and s = arc length measured along the boundary contour. If V is a harmonic function in R , and if;

$$U = \ln r(P, Q) \quad (2.2)$$

in which $r(P, Q)$ is the distance from a fixed point, P , to a variable point, Q , both within the solution domain, then;

$$\begin{aligned} \nabla^2 V &= 0 \\ \nabla^2 U &= 2\pi \delta[x(Q) - x(P)] \delta[y(Q) - y(P)] \end{aligned} \quad (2.3)$$

in which δ is the Dirac delta function, and $x(P)$, $y(P)$, $x(Q)$, $y(Q)$ are the Cartesian coordinates of P and Q , respectively. Substituting Eqns. 2.2 and 2.3 into the left side of Eqn. 2.1 gives;

$$V(P) = \frac{1}{2\pi} \int_{\Gamma} \left[V(Q) \frac{\partial}{\partial n(Q)} [\ln r(P, Q)] - \ln r(P, Q) \frac{\partial V(Q)}{\partial n(Q)} \right] ds(Q) \quad (2.4)$$

in which Q is now a point on the boundary contour. The final integral equation is obtained from Eqn. 2.4 by letting the point P approach a point on the boundary contour. In the limit,

$$V(P) = \frac{1}{\pi} \int_{\Gamma} \left[V(Q) \frac{\partial}{\partial n(Q)} [\ln r(P, Q)] - \ln r(P, Q) \frac{\partial V(Q)}{\partial n(Q)} \right] ds(Q) \quad (2.5)$$

in which the boundary tangent is assumed to turn continuously at P , and the integral is calculated as a Cauchy principal value. Eqn. 2.5 becomes an integral equation of the second kind when P is a point on a boundary of specified $\frac{\partial V}{\partial n}$ and an integral equation of the first kind when P is a point on a boundary of specified V . Unfortunately, the set of

simultaneous equations that result from approximating Eqn. 2.5 around the boundary contour may become ill-conditioned, as verified by Liggett (1977).

Integral equations were first used to solve time-dependent problems by Cruse and Rizzo (1968), who used Laplace transforms to remove the time derivative from the partial differential equation governing transient elastodynamics. Having solved a steady-state problem in the transformed space, the solution was inverted numerically to obtain the solution in terms of the physical variables. The Laplace transform method was also used by Rizzo and Shippy (1970) and, more recently, by Liggett and Liu (1979b) to solve the diffusion equation. (Although Rizzo and Shippy (1970) studied heat conduction and Liggett and Liu (1979b) examined transient groundwater flow, both systems are governed by the same partial differential equation). A brief outline of the method follows.

The two-dimensional diffusion of a physical property, V , through a homogeneous, isotropic region, R , that is bounded by a contour, $\Gamma = \Gamma' + \Gamma''$, is described by;

$$a^2 \nabla_{x,y}^2 V = \frac{\partial V}{\partial t} \quad (2.6)$$

$$V(x,y, t = 0) = V_0(x,y) \quad (2.7)$$

$$V(x,y,t) = f(x,y,t) \text{ for } (x,y) \text{ on } \Gamma' \in \Gamma \quad (2.8)$$

$$\frac{\partial V}{\partial n}(x,y,t) = g(x,y,t) \text{ for } (x,y) \text{ on } \Gamma'' \in \Gamma \quad (2.9)$$

in which a^2 = the relevant diffusion parameter, (x,y) = Cartesian coordinates and t = time. Eqn. 2.6 is the governing partial differential equation, Eqn. 2.7 the initial condition and Eqns. 2.8 and 2.9 the boundary conditions. The Laplace transforms, χ^* of a function χ is defined as

$$\chi^*(x,y,w) \equiv \int_0^{\infty} \chi(x,y,t) e^{-wt} dt \quad (2.10)$$

in which w is real and positive. Thus, taking the Laplace transforms of Eqns. 2.6 - 2.9 gives;

$$a^2 \nabla^2 V^*(x, y, w) - w V^*(x, y, w) + V_0^*(x, y, w) = 0 \quad (2.11)$$

$$V^*(x, y, w) = f^*(x, y, w) \text{ for } (x, y) \text{ on } \Gamma' \in \Gamma \quad (2.12)$$

$$\frac{\partial V^*}{\partial n}(x, y, w) = g^*(x, y, w) \text{ for } (x, y) \text{ on } \Gamma'' \in \Gamma \quad (2.13)$$

If it is assumed that $V_0 = 0$, the function;

$$U^*(P, Q, w) = \frac{1}{a^2} K_0 \left[\left(\frac{w}{a^2} \right)^{\frac{1}{2}} r(P, Q) \right] \quad (2.14)$$

is a fundamental solution of Eqn. 2.11, in which K_0 is a modified Bessel function of the second kind of order zero, and $r(P, Q)$ is the distance from the point P within the solution domain to a point Q on the boundary contour. Applying Green's second identity to U^* and a sufficiently smooth V^* gives;

$$V^*(P, w) = \frac{a^2}{2\pi} \int_{\Gamma=\Gamma'+\Gamma''} \left[U^*(P, Q, w) \frac{\partial V^*(Q, w)}{\partial n(Q)} - V^*(Q, w) \frac{\partial U^*(P, Q, w)}{\partial n(Q)} \right] ds(Q) \quad (2.15)$$

By letting the point P approach a point on the boundary contour, as described previously, the final form of the equation is;

$$V^*(P, w) = \frac{a^2}{\pi} \int_{\Gamma=\Gamma'+\Gamma''} \left[U^*(P, Q, w) \frac{\partial V^*(Q, w)}{\partial n(Q)} - V^*(Q, w) \frac{\partial U^*(P, Q, w)}{\partial n(Q)} \right] ds(Q) \quad (2.16)$$

in which the boundary tangent is assumed to turn continuously at P , and the integral is calculated as a Cauchy principal value.

By writing Eqn. 2.16 at a finite number of points on the boundary contour and using a standard quadrature formula to evaluate the integrals, the resulting set of equations can be solved simultaneously to give the distributions of

V^* and $\frac{\partial V^*}{\partial n}$ on the boundary contour in the transformed space. Direct substitution in Eqn. 2.15 then enables V^* to be calculated at any internal point of interest in the transformed space. The solution at these points in the physical space is calculated by numerically inverting the transformed solution. The inversion technique adopted by Rizzo and Shippy (1970) was developed by Schapery (1962) and assumes that $V(x,y,t)$ can be written in the form;

$$V(x,y,t) = A + Bt + \sum_{i=1}^M a_i e^{-b_i t} \quad (2.17)$$

in which A , B , a_i and b_i are constants and M is a finite integer selected by the analyst. Taking the Laplace transform of Eqn. 2.17 and multiplying by w gives;

$$wV^*(P,w) = A + \frac{B}{w} + \sum_{i=1}^M \frac{a_i}{1 + \frac{b_i}{w}} \quad (2.18)$$

By selecting M values of b_i and $M+2$ values of w means that $M+2$ equations are obtained to be solved simultaneously for the $M+2$ unknowns, namely, A, B and M values of a_i . Substitution of these quantities into the right side of Eqn. 2.17 yields the approximate solution to the problem in the physical domain. Liggett and Liu (1979b) reported that "Choosing too many values of w may make (Eqn. 2.18) unstable, while too few values would not represent the curve adequately." They also stated that "A clever choice of the time function, which depends on the 'feel' that the analyst has for his particular problem, is more important than the selection of a large number of points." Thus, it would appear that the technique is best suited to experienced, skilled personnel who are aware of its limitations.

The use of a step-by-step finite-difference approximation to the time derivative in the diffusion equation is discussed by Brebbia and Walker (1979) and has been expanded upon by Lafe et al (1981). For example, Brebbia and Walker (1979) calculated solutions to the following

form of the two-dimensional heat conduction equation;

$$\nabla^2 V = \frac{\partial V}{\partial t} \quad (2.19)$$

$$V(x, y, t = 0) = V_0(x, y) \text{ for } (x, y) \in R \quad (2.20)$$

$$V(x, y, t) = f(x, y, t) \text{ for } (x, y) \text{ on } \Gamma' \in \Gamma \quad (2.21)$$

$$\frac{\partial V}{\partial n}(x, y, t) = g(x, y, t) \text{ for } (x, y) \text{ on } \Gamma'' \in \Gamma \quad (2.22)$$

in which V = temperature and t = time. Eqn. 2.20 is the initial condition which must be satisfied throughout the solution domain R , and Eqns. 2.21 and 2.22 are the boundary conditions which must be satisfied on the boundary contour, $\Gamma = \Gamma' + \Gamma''$. If the time derivative in Eqn. 2.19 is replaced with a backward-difference approximation, Eqn. 2.19 can be rewritten as;

$$\nabla^2 V(t + \Delta t) - \frac{V(t + \Delta t) - V(t)}{\Delta t} = - \frac{V(t)}{\Delta t} \quad (2.23)$$

in which the values of V at $t + \Delta t$ on the left side of Eqn. 2.23 are unknowns. The fundamental solution of $\nabla^2 U - \frac{U}{\Delta t} = 0$ is given by;

$$U(P, Q) = - K_0 \left[\frac{r(P, Q)}{\sqrt{\Delta t}} \right] \quad (2.24)$$

in which $r(P, Q)$ = distance between a fixed point, P , within the solution domain, and another point, Q . Eqn. 2.23 can be written in integral equation form as;

$$\begin{aligned} & V(P, t + \Delta t) \\ &= \frac{1}{2\pi} \int_{\Gamma} \left[V(Q, t + \Delta t) \frac{\partial U(P, Q)}{\partial n(Q)} - U(P, Q) \frac{\partial V(Q, t + \Delta t)}{\partial n(Q)} \right] ds(Q) \\ &- \frac{1}{2\pi\Delta t} \int_R U(P, Q) V(Q, t) dA \end{aligned} \quad (2.25)$$

If the point P is a point on the boundary contour;

$$\theta V(P, t+\Delta t)$$

$$= \int_{\Gamma} \left[V(Q, t+\Delta t) \frac{\partial U(P, Q)}{\partial n(Q)} - U(P, Q) \frac{\partial V(Q, t+\Delta t)}{\partial n(Q)} \right] ds(Q) \\ - \frac{1}{\Delta t} \int_R U(P, Q) V(Q, t) dA \quad (2.26)$$

in which θ = angle between the boundary tangents at P. The last term in Eqn. 2.26 requires the calculation of an integral over the solution domain for each time step.

Time-dependent fundamental solutions to the diffusion equation have also been used to develop integral equation techniques. This method removes the need for Laplace transforms or finite difference approximations to the time derivative and sometimes can be used to obtain an integral equation that does not require any integration over the solution domain. First presented by Chang et al (1973) this technique forms the basis of Chapter 5 of this study and is discussed both there and in Section 2.3.

2.2 UNSTEADY SEEPAGE THROUGH EMBANKMENTS

The behaviour of unsteady flow through embankments apparently has not been investigated systematically. The non-linearity of the unsteady, free-surface boundary condition, plus the fact that the free surface itself is an inherent unknown, makes exact analytical solutions very difficult to obtain. These difficulties are so great that only experimental or numerical solutions have succeeded in the past. For example, France et al (1971), Desai (1972, 1977) and Desai and Li (1983a, 1983b) have presented solutions using the finite-element method, but the results are in dimensional form and are valid for only one particular choice of permeability, porosity and embankment geometry. Stephenson (1978), on the other hand, has produced results in dimensionless form by using the Dupuit approximation, but these solutions neglect vertical velocities and surfaces of seepage. In particular, it will be shown in Chapter 4

that vertical velocities can not be neglected in this type of problem. Thus, despite the fact that previous investigators have obtained numerical approximations for specific cases, a general dimensionless tabulation of unsteady solutions for seepage through an embankment has yet to appear in the literature.

Liggett's (1977) formulation for this type of problem uses boundary values of a velocity potential and its normal derivative as unknowns in Eqn. 2.5, to give;

$$\phi(P) = \frac{1}{\pi} \int_{\Gamma} \left[\phi(Q) \frac{\partial}{\partial n(Q)} [\ln r(P,Q)] - \ln r(P,Q) \frac{\partial \phi(Q)}{\partial n(Q)} \right] ds(Q) \quad (2.27)$$

in which P and Q are points on the boundary contour and ϕ is defined by Liggett as;

$$\phi = \frac{P}{\rho g} + y \quad (2.28)$$

in which P = pressure, ρ = mass density of water, g = acceleration due to gravity and y is directed vertically upwards. During steady flow, the boundary conditions on a free surface are given by;

$$\phi = y^* \text{ and,} \quad (2.29)$$

$$\frac{\partial \phi}{\partial n} = 0 \quad (2.30)$$

in which y^* = free surface elevation. Because Eqns. 2.29 and 2.30 can not be solved simultaneously using numerical techniques, an iterative process must be used to locate the free surface. Liggett's (1977) method of solution is to make an estimate of the free surface profile and solve Eqn. 2.27 subject to Eqn. 2.30 and the relevant boundary conditions on the remainder of the boundary. If the values of ϕ calculated from Eqn. 2.27 agree with those of Eqn. 2.29 then the assumed free surface is correct. If the two solutions do not agree, a new estimate is made and the above process repeated until successive solutions agree

to within a preselected tolerance. Liggett (1977) states that the two solutions converge quickly (four cycles in his sample problem). However the rate of convergence depends on the accuracy of the initial estimate to the free surface profile.

For unsteady, two-dimensional free-surface flow, pressures are atmospheric on the free surface and Eqn. 2.29 holds. The second boundary condition, which is essentially a conservation of mass statement, is written by Liggett as;

$$\frac{\partial y^*}{\partial t} = \frac{-K}{\sigma \cos \beta} \frac{\partial \phi}{\partial n} \quad (2.31)$$

in which K = permeability, σ = porosity, and β = angle between the free surface and the horizontal. The substitution of Eqn. 2.29 into the left side of Eqn. 2.31 enables Eqn. 2.31 to be given in finite-difference form as;

$$\phi(x, t+\Delta t) = \phi(x, t) - \frac{K\Delta t}{\sigma \cos \beta} \left[\alpha \frac{\partial \phi}{\partial n}(x, t+\Delta t) + (1-\alpha) \frac{\partial \phi}{\partial n}(x, t) \right] \quad (2.32)$$

in which α = a weighting function that determines the variation in $\frac{\partial \phi}{\partial n}$ between time t , at which the solution is known, and time $t+\Delta t$. Eqn. 2.27 can then be written for time $t+\Delta t$, and this, together with Eqn. 2.32 and the boundary conditions on the rest of the boundary, is sufficient to obtain the complete solution at time $t+\Delta t$. It is also assumed that β , and the values of $\ln[r(P, Q)]$ and $\frac{\partial}{\partial n(Q)} [\ln r(P, Q)]$ which appear in Eqns. 2.32 and 2.27, respectively, are constant over each time step, an assumption which is only reasonable if the time step, Δt , is sufficiently small. Liggett and various co-workers have extended the method to solve a variety of steady and time-dependent solutions in two and three dimensions. A complete list of these works is given in the bibliography.

Hunt and Isaacs (1981) have developed an alternative integral equation formulation which has the velocity

potential and stream function on the flow boundary as unknowns and which is applicable to two-dimensional groundwater flow problems. This formulation has advantages of simplicity and compactness but as yet has not been used to solve unsteady free-surface problems. By examining unsteady flow through an embankment following an instantaneous drawdown, it is hoped to verify the suitability of the Hunt-Isaacs formulation for solving unsteady, two-dimensional flows through porous media.

2.3 THE UNSTEADY DUPUIT EQUATION

The horizontal dimensions of many aquifers are orders of magnitude larger than vertical dimensions. In such cases, it is possible to make use of the Dupuit approximation, which assumes that velocities are horizontal and that piezometric heads are constant along a vertical line. Under these conditions, unconfined flows satisfy the following partial differential equation;

$$\nabla \cdot (T \nabla h) = S \frac{\partial h}{\partial t} + \sum_i Q_i \delta(x-x_i) \delta(y-y_i) + R' \quad (2.33)$$

in which S = storage coefficient or effective porosity, Q_i = flow rate in well i located at (x_i, y_i) , and the rate of recharge, R' , is positive for evaporation and negative for replenishment. The transmissivity, T , is given by;

$$T(x, y, t) = \int_{Z_0}^{Z_0+B} K(x, y, z) dz \quad (2.34)$$

in which $Z_0(x, y)$ = elevation of the bottom boundary of the aquifer and $B(x, y, t)$ = saturated aquifer thickness (which depends on h for unconfined flows).

If the Dupuit approximation is made, confined flows satisfy;

$$\nabla \cdot (T \nabla h) = S \frac{\partial h}{\partial t} + \sum_i Q_i \delta(x-x_i) \delta(y-y_i) + R' \quad (2.35)$$

in which the storage coefficient, S , is a function of the elasticity of the aquifer and is usually three to six orders of magnitude smaller than the storage coefficient that appears in Eqn. 2.33. The transmissivity, T , is again given by Eqn. 2.34, but the aquifer thickness, B , is constant at any point. Consequently, Eqn. 2.33 is non-linear in h , while Eqn. 2.35 is linear. However, if Eqn. 2.33 is linearized by assuming that T is independent of changes in h , then both confined and unconfined flows will obey a partial differential equation of the same form. Furthermore, if the aquifer is homogeneous and isotropic, both confined and unconfined flows are governed by;

$$TV^2h = S \frac{\partial h}{\partial t} + \sum_i Q_i \delta(x-x_i) \delta(y-y_i) + R' \quad (2.36)$$

in which T and S are constants.

Lafe et al (1981) used integral equation techniques to analyse problems with combinations of leaky, layered, confined, unconfined, and nonisotropic aquifers under steady-state conditions. Although a method of solution was presented for unsteady flows by using finite-differences to approximate the time derivative, no numerical results were included. To illustrate the basic technique for unsteady flows, consider unconfined flow through a homogeneous, anisotropic, non-leaky region, R , that is bounded by a contour, Γ , and in which the principal axes of seepage are parallel to the x and y axes. If the permeabilities for directions parallel to the x and y axes are given by k_x and k_y , respectively, and if there is no recharge, Eqn. 2.33 can be written as;

$$\frac{\partial^2 h^2}{\partial x_*^2} + \frac{\partial^2 h^2}{\partial y_*^2} = \frac{2S}{k_x} \frac{\partial h}{\partial t} \quad (2.37)$$

in which $x_* = x$, and $y_* = \sqrt{\frac{k_x}{k_y}} y$. If a backward-difference approximation is adopted for the time derivative, Eqn. 2.37 may be rewritten as;

$$\nabla_{x_*, y_*}^2 \left[h(t+\Delta t) \right]^2 - \frac{2S}{\Delta t k_x} h(t+\Delta t) = \frac{-2S}{\Delta t k_x} h(t) \quad (2.38)$$

in which values of h at time t are known and at time $t+\Delta t$ are unknown. In order to solve Eqn. 2.38 by integral equation techniques, it must be linearized, and Lape et al (1981) suggest the following;

$$\nabla_{x_*, y_*}^2 \left[h(t+\Delta t) \right]^2 - \frac{2S}{\Delta t k_x \bar{h}(t+\Delta t)} \left[h(t+\Delta t) \right]^2 = \frac{-2S}{\Delta t k_x} h(t) \quad (2.39)$$

in which $\bar{h}(t+\Delta t)$ is an average value of h over the region. Eqn. 2.39 is of similar form to Eqn. 2.23, and, thus, it can be shown that;

$$\begin{aligned} & \theta h(P, t+\Delta t) \\ &= \int_{\Gamma} \left[h(Q, t+\Delta t) \frac{\partial U(P, Q)}{\partial n(Q)} - U(P, Q) \frac{\partial h(Q, t+\Delta t)}{\partial n(Q)} \right] ds(Q) \\ & - \frac{2S}{\Delta t k_x} \int_R U(P, Q) h(Q, t) dA \end{aligned} \quad (2.40)$$

in which;

$$U(P, Q) = -K_0 \left[\sqrt{\frac{2S}{\Delta t k_x \bar{h}(t+\Delta t)}} r(P, Q) \right] \quad (2.41)$$

and $r(P, Q)$ = distance from a fixed point, P , on the boundary to another point, Q . The variable, θ , = angle between the boundary tangents at P . The solution is obtained iteratively by assuming a value of $\bar{h}(t+\Delta t)$ and then solving Eqn. 2.40. The estimate of $\bar{h}(t+\Delta t)$ is then revised and the process repeated until there is essentially no change in successive solutions. The obvious disadvantage of such a formulation is that because the final term on the right side of Eqn. 2.40 is non-zero, in general, integrations must be performed throughout the solution domain at each time step. Thus, although the method can be extended to solve problems in leaky aquifers with recharge, it does not have the advantage of reducing the dimensionality of the problem.

The use of time-dependent fundamental solutions to solve problems having the same form as Eqn. 2.36 was first presented by Chang, Kang and Chen (1973), who analysed transient heat conduction through an anisotropic medium. The method has since been used by Brebbia and Walker (1979), Brebbia and Wrobel (1979), and Wrobel and Brebbia (1979a,b) who presented solutions to the following form of the heat conduction equation;

$$C\nabla^2 V = \frac{\partial V}{\partial t} \quad (2.42)$$

$$V(x,y, t = 0) = V_0(x,y) \text{ for } (x,y) \in R \quad (2.43)$$

$$V(x,y,t) = f(x,y,t) \text{ for } (x,y) \text{ on } \Gamma' \in \Gamma \quad (2.44)$$

$$\frac{\partial V}{\partial n}(x,y,t) = g(x,y,t) \text{ for } (x,y) \text{ on } \Gamma'' \in \Gamma \quad (2.45)$$

in which V = temperature, C = thermal diffusivity, and Eqn. 2.42 is a special form of Eqn. 2.36, Eqn. 2.43 is the initial condition which must be satisfied throughout the solution domain, R , and Eqns. 2.44 and 2.45 are the boundary conditions which must be satisfied on the respective portions of the boundary contour, $\Gamma = \Gamma' + \Gamma''$. A full description of the results which follow is presented in Chapter 5. A fundamental solution, u , of Eqn. 2.42 is given by;

$$\begin{aligned} u[x(Q) - x(P), y(Q) - y(P), t-\tau] &= u[r(P,Q), t-\tau] \\ &= \frac{1}{4\pi C(t-\tau)} e^{-\frac{[r(P,Q)]^2}{4C(t-\tau)}} \end{aligned} \quad (2.46)$$

in which $r(P,Q)$ = distance from a fixed point, P , within R , to another point, Q , and $0 \leq \tau \leq t$. It will be shown in Chapter 5 that the integral equation representation of Eqn. 2.42 is;

$$\begin{aligned}
V(P, t) = & \int_0^t \int_{\Gamma' + \Gamma''} C \left[u[r(P, Q), t - \tau] \frac{\partial V(Q, \tau)}{\partial n(Q)} \right. \\
& - V(Q, \tau) \left. \frac{\partial u[r(P, Q), t - \tau]}{\partial n(Q)} \right] ds(Q) d\tau \\
& + \int_R \left[u[r(P, Q), t] V(Q, \tau=0) \right] dA
\end{aligned} \tag{2.47}$$

If P is a point on the boundary contour;

$$\begin{aligned}
\frac{\theta}{2\pi} V(P, t) = & \int_0^t \int_{\Gamma' + \Gamma''} C \left[u[r(P, Q), t - \tau] \frac{\partial V(Q, \tau)}{\partial n(Q)} \right. \\
& - V(Q, \tau) \left. \frac{\partial u[r(P, Q), t - \tau]}{\partial n(Q)} \right] ds(Q) d\tau \\
& + \int_R \left[u[r(P, Q), t] V(Q, \tau=0) \right] dA
\end{aligned} \tag{2.48}$$

in which θ = angle between the boundary tangents at P .

Brebbia and Walker (1979) and Brebbia and Wrobel (1979a,b)

calculated solutions of Eqn. 2.48 by assuming that V and

$\frac{\partial V}{\partial n}$ remained constant over a sufficiently small time step and by performing the time integrations stepwise. Using this assumption in Eqn. 2.48 and changing the order of integration gives;

$$\begin{aligned}
\frac{\theta}{2\pi} V(P, t_2) = & \int_{\Gamma' + \Gamma''} C \left[\frac{\partial V(Q, t_2)}{\partial n(Q)} \int_{t_1}^{t_2} u[r(P, Q), t_2 - \tau] d\tau \right. \\
& - V(Q, t_2) \left. \int_{t_1}^{t_2} \frac{\partial u[r(P, Q), t_2 - \tau]}{\partial n(Q)} d\tau \right] ds(Q) \\
& + \int_R \left[u[r(P, Q), t_2 - t_1] V(Q, \tau=t_1) \right] dA
\end{aligned} \tag{2.49}$$

The time integrals on the right side of Eqn. 2.49 can be

evaluated analytically, and it can be shown that;

$$\int_{t_1}^{t_2} u(r(P,Q), t_2 - \tau) d\tau = \frac{1}{4\pi C} E_1 \left[\frac{r(P,Q)^2}{4C(t_2 - t_1)} \right] \quad (2.50)$$

in which E_1 is the exponential function; and

$$\int_{t_1}^{t_2} \frac{\partial u[r(P,Q), t_2 - \tau]}{\partial n(Q)} d\tau = \frac{-\cos(r,n)}{2\pi C r(P,Q)} e^{\frac{-[r(P,Q)]^2}{4C(t_2 - t_1)}} \quad (2.51)$$

in which (r,n) is the angle between $r(P,Q)$ and the unit normal at point Q .

The obvious disadvantage of using Eqn. 2.49 is that, as with the formulation of Lafe et al (1981), a surface integral must be calculated at the start of each time step, and thus negating, to some extent, the advantage of integral equations over the more traditional techniques. However, the methods do retain their accuracy, and both Wrobel and Brebbia (1981b) and Lafe et al (1981) claim that the grid spacing used to calculate surface integrals can be greater than that used in a finite-element solution. Wrobel and Brebbia (1981b) have used time-dependent fundamental solutions to solve axisymmetric problems and have also used linear time interpolation functions in Eqn. 2.49 in an effort to improve accuracy, (1981a).

An alternative formulation for the solution of Eqn. 2.48 was presented by Liggett and Liu (1979) who, unlike Brebbia and Wrobel (1979) and Wrobel and Brebbia (1979-1981), calculated the contour integrals by assuming that V and $\frac{\partial V}{\partial n}$ varied linearly along a straight line joining adjacent nodes and integrating the expression analytically around the boundary. The trapezium rule was used to calculate integrals in the time domain. Liu and Liggett concluded that the initial portions of the time integrations were critical and had to be calculated accurately to avoid the introduction

of a consistent error into the solution. This formulation, also, required the evaluation of an integral over the solution domain.

A solution of Eqn. 2.48 may be obtained by dividing the time interval $0 \leq \tau \leq t$ into N time steps and reversing the order of integration to give;

$$\begin{aligned} \frac{\theta}{2\pi} V(P, t) = & \int_{\Gamma' + \Gamma''} C \sum_{k=2}^N \left[\int_{t_1}^{t_2} \left(u[r(P, Q), t-\tau] \frac{\partial V(Q, \tau)}{\partial n(Q)} \right. \right. \\ & \left. \left. - V(Q, \tau) \frac{\partial u[r(P, Q), t-\tau]}{\partial n(Q)} \right) d\tau \right] ds(Q) \\ & + \int_R \left[u[r(P, Q, t)] V(Q, \tau=0) \right] dA \end{aligned} \quad (2.52)$$

in which $t_1 = 0$ and $t_N = t$. At first glance, it may appear that Eqn. 2.52 is no better than any of the previous formulations because of the surface integral that appears on the right side. However, because the governing partial differential equation, Eqn. 2.42, is linear with constant coefficients, the principle of superposition can be applied. If;

$$V' \equiv V - V_0 \quad (2.53)$$

in which V_0 is the initial condition at $t = 0$, given by Eqn. 2.43, then;

$$\begin{aligned} \frac{\theta}{2\pi} V'(P, t) = & \int_{\Gamma' + \Gamma''} C \sum_{k=2}^N \left[\int_{t_1}^{t_2} \left(u[r(P, Q), t-\tau] \frac{\partial V'(Q, \tau)}{\partial n(Q)} \right. \right. \\ & \left. \left. - V'(Q, \tau) \frac{\partial u[r(P, Q), t-\tau]}{\partial n(Q)} \right) d\tau \right] ds(Q) \end{aligned} \quad (2.54)$$

which must be solved subject to the following boundary conditions;

$$V'(x,y,t) = f(x,y,t) - V_0(x,y) \text{ for } (x,y) \text{ on } \Gamma' \in \Gamma \quad (2.55)$$

$$\frac{\partial V'}{\partial n}(x,y,t) = g(x,y,t) - \frac{\partial V_0}{\partial n}(x,y) \text{ for } (x,y) \text{ on } \Gamma'' \in \Gamma \quad (2.56)$$

Although the amount of data storage and computational effort required is greater for this method than for the others discussed, the advantage of reduced data preparation is very significant.

Dubois and Buysse (1981) have used Eqn. 2.52 to analyse problems of thermal shock by assuming that V and $\frac{\partial V}{\partial n}$ remain constant throughout each time step. In this work, such a solution will be used as a starting point for the solution of the linearized groundwater flow equation, (Eqn. 2.36), for h when $R' = 0$. A second formulation, in which h and $\frac{\partial h}{\partial n}$ vary linearly with time, will be used in an equation analogous to Eqn. 2.52 and the results compared with those obtained when h and $\frac{\partial h}{\partial n}$ are assumed constant over each time step. These techniques will then be applied to composite regions in which T and S are constant within each zone but vary from one zone to the next. The solution domain may or may not include wells.

Chapter 3

UNSTEADY SEEPAGE THROUGH EMBANKMENTS3.1 INTRODUCTION

Hunt and Isaacs (1981) have developed an integral equation formulation which has been applied to two-dimensional, steady groundwater flow problems. In this chapter solutions will be presented in dimensionless form for calculations of unsteady seepage through an embankment. In so doing it is hoped to verify that the Hunt-Isaacs formulation is general enough to enable the solution of unsteady two-dimensional flows through porous media. Because the problem is relatively complicated with many variables, attention will be restricted to the case of an instantaneous drawdown next to an isotropic, homogeneous embankment with side slopes of 2:1. More general cases, including finite reservoir drawdown rates, different side slopes, anisotropy and zoned embankments, can be handled with the same technique, but the extra variables introduced by these additional degrees of freedom make it impossible to present the results systematically in a generalized way.

3.2 INTEGRAL EQUATION FORMULATION

Suppose $\phi(x,y)$ and $\psi(x,y)$ are the velocity potential and stream function in a groundwater flow problem. Since the flow region is assumed to be homogeneous and isotropic, and the flow two-dimensional, a solution of the form;

$$w(z) = \phi(x,y) + i\psi(x,y) \quad (3.1)$$

will be sought, in which $i = \sqrt{-1}$, $z = x+iy$, and $w(z)$ = a complex-valued analytic function.

The integral equation formulation used by Hunt and Isaacs (1981) uses the Cauchy integral theorem to seek a solution of the form;

$$w(z) = \frac{1}{2\pi i} \oint_{\Gamma} \frac{w(\zeta)}{\zeta - z} d\zeta \quad (3.2)$$

in which Γ defines the exterior boundary contour of the flow region, z = coordinate of a point inside Γ , and ζ = coordinate of a point on Γ . The integral equation is obtained from Eqn. 3.2 by letting z approach a point on the boundary contour and then deforming the boundary slightly so that z lies within the flow region. In the limit as this deformation tends to zero;

$$w(z) = \frac{(P)}{\Omega i} \oint_{\Gamma} \frac{w(\zeta)}{\zeta - z} d\zeta \quad (3.3)$$

in which z is a point on Γ , (P) denotes the Cauchy principal value of the integral, and Ω = the exterior angle between the boundary tangents at z . At points where the boundary turns continuously, $\Omega = \pi$. The boundary contour, Γ , is divided into M segments and a node placed at the end of each segment. The nodal spacing is less in regions where ϕ or ψ change rapidly and is increased where the variations in ϕ or ψ are smaller. It is assumed that $w(\zeta)$ is a piecewise linear function of the complex variable, ζ , along each of the boundary segments, and so on the segment joining nodes ζ_j and ζ_{j+1} , $w(\zeta)$ is approximated with;

$$w(\zeta) = \frac{\zeta - \zeta_j}{\zeta_{j+1} - \zeta_j} w_{j+1} + \frac{\zeta_{j+1} - \zeta}{\zeta_{j+1} - \zeta_j} w_j \quad (3.4)$$

If $z = \zeta_i$ and $i \neq j$, or $i \neq j+1$, Eqn. 3.4 can be substituted into Eqn. 3.3 and integrated over the boundary segment joining ζ_j and ζ_{j+1} to give;

$$\begin{aligned} \int_{\zeta_j}^{\zeta_{j+1}} \frac{w(\zeta)}{\zeta - \zeta_i} d\zeta &= \left[1 + \left(\frac{\zeta_i - \zeta_j}{\zeta_{j+1} - \zeta_j} \right) \ln \left(\frac{\zeta_{j+1} - \zeta_i}{\zeta_j - \zeta_i} \right) \right] w_{j+1} \\ &- \left[1 + \left(\frac{\zeta_i - \zeta_{j+1}}{\zeta_{j+1} - \zeta_j} \right) \ln \left(\frac{\zeta_{j+1} - \zeta_i}{\zeta_j - \zeta_i} \right) \right] w_j \end{aligned} \quad (3.5)$$

The complex logarithms that appear in Eqn. 3.5 are multiple-valued, but problems can be avoided by choosing the arguments of all complex numbers to be in the range $-\pi \rightarrow \pi$. Eqn. 3.5 cannot be used to calculate the contribution to the integral of the two elements on each side of the singular node at $z = \zeta_i$. For this case, calculation of the Cauchy principal values gives;

$$(P) \int_{\zeta_{i-1}}^{\zeta_{i+1}} \frac{w(\zeta)}{\zeta - \zeta_i} d\zeta = w_{i+1} - w_{i-1} + \left[\ln \left| \frac{\zeta_{i+1} - \zeta_i}{\zeta_{i-1} - \zeta_i} \right| + i(\Omega - \theta) \right] w_i \quad (3.6)$$

in which Ω = angle between the boundary tangents at ζ_i and θ = angle between the straight lines joining ζ_{i-1} - ζ_i and ζ_i - ζ_{i+1} . Thus the numerical solution of Eqn. 3.3, calculated from Eqn. 3.6 is given by;

$$w_i = \frac{w_{i+1} - w_{i-1} + \sum_{j=1}^{i-2} \int_{\zeta_j}^{\zeta_{j+1}} \frac{w(\zeta)}{\zeta - \zeta_i} d\zeta + \sum_{j=i+1}^M \int_{\zeta_j}^{\zeta_{j+1}} \frac{w(\zeta)}{\zeta - \zeta_i} d\zeta}{\ln \left| \frac{\zeta_{i-1} - \zeta_i}{\zeta_{i+1} - \zeta_i} \right| + i\theta} \quad (3.7)$$

in which the integrals on the right side of Eqn. 3.7 are calculated from Eqn. 3.5. Eqn. 3.7 is applied successively to each boundary node, and the resulting set of equations, together with the appropriate boundary conditions, solved by Gauss elimination to give the solution for w , and hence ϕ and ψ at each node.

3.3 PROBLEM FORMULATION

Consider the problem of seepage through the homogeneous, isotropic embankment shown in Fig. 3.1.

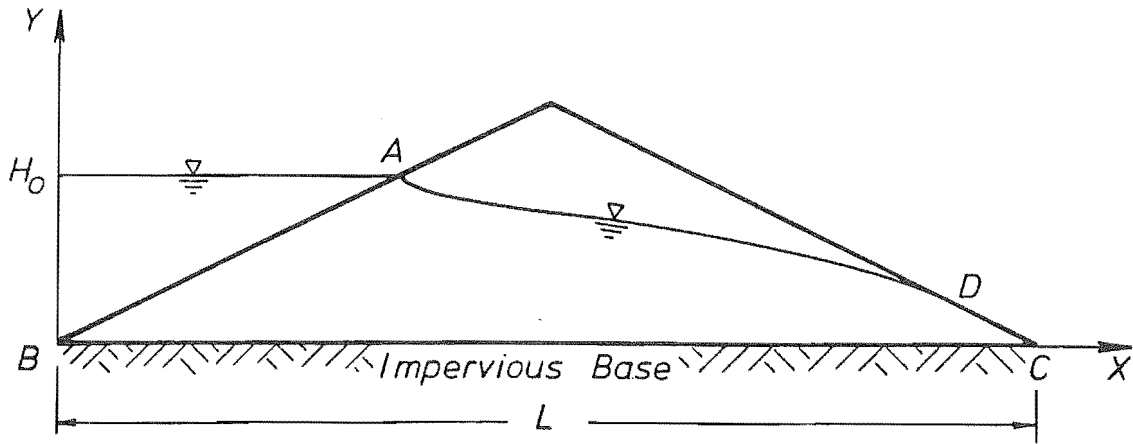


Fig. 3.1 Definition Diagram for Seepage Through an Embankment.

The upstream reservoir level falls instantaneously from a depth of H_0 to zero at time $t = 0$.

The piezometric head, h , is defined as;

$$h \equiv \frac{P}{\rho g} + y \quad (3.8)$$

in which P = pressure, ρ = mass density of water, g = gravitational acceleration, and y = free surface elevation. A velocity potential, ϕ , is defined as;

$$\phi \equiv -Kh \quad (3.9)$$

in which K = permeability of the embankment. The velocity components u and v in the x and y directions, respectively, are given by;

$$u = \frac{\partial \phi}{\partial x} \quad (3.10)$$

$$v = \frac{\partial \phi}{\partial y} \quad (3.11)$$

and the stream function; ψ , is defined in the usual manner from the Cauchy-Riemann equations;

$$u = \frac{\partial \psi}{\partial y} \quad (3.12)$$

$$v = -\frac{\partial \psi}{\partial x} \quad (3.13)$$

Flow through the embankment is governed by the following boundary conditions:

$$\phi = -Ky \text{ for } (x,y) \text{ on AB} \quad (3.14)$$

$$\psi = 0 \text{ for } (x,y) \text{ on AB} \quad (3.15)$$

$$\phi = -Ky \text{ for } (x,y) \text{ on CD} \quad (3.16)$$

$$\phi = -Ky \text{ for } (x,y) \text{ on DA} \quad (3.17)$$

$$\frac{1}{\sigma} \frac{\partial \phi}{\partial n} = \frac{d\tilde{\mathbf{r}}}{dt} \cdot \hat{\mathbf{e}}_n \text{ for } (x,y) \text{ on DA} \quad (3.18)$$

in which n = arc length normal to the free surface, $\tilde{\mathbf{r}}$ = position vector of a point on the free surface, σ = porosity, and $\hat{\mathbf{e}}_n$ = the outward pointing unit normal to the free surface. Eqns. 3.14, 3.16, and 3.17 require pressures to be atmospheric in the upstream face, downstream face and free surface, respectively, while Eqn. 3.15 requires that the impermeable base be a streamline. Eqn. 3.18 states that a fluid particle on the free surface must remain in contact with the free surface as the free surface geometry changes with time. The initial position of the free surface prior to drawdown is found by solving the steady flow problem in which y is replaced with H_0 on the right side of Eqn. 3.14 to give;

$$\phi = -K H_0 \text{ for } (x,y) \text{ on AB} \quad (3.19)$$

and Eqn. 3.18 is replaced with;

$$\psi = q \text{ for } (x,y) \text{ on DA} \quad (3.20)$$

in which q = steady, two-dimensional flow rate through the embankment. Eqn. 3.19 requires pressures to be hydrostatic along the upstream face, while Eqn. 3.20 states that the free surface is a streamline during steady flow.

The coordinates of the free surface, as a function of time are most generally presented by using the following dimensionless variables:

$$\frac{y}{L} = f\left(\frac{x}{L}, \frac{H_0}{L}, \frac{Kt}{\sigma L}\right) \quad (3.21)$$

in which x and y are the horizontal and vertical coordinates, respectively, of a point on the free surface, L is the embankment base width, t = time and f is a functional relationship. Eqn. 3.21 can be obtained either by using dimensional analysis or by formally introducing dimensionless variables into Eqns. 3.14 - 3.19 and then noting which dimensionless variables and parameters would appear in a solution for the free surface.

3.4 NUMERICAL SOLUTION

The first step in any instantaneous drawdown problem is to find the initial steady-state solution. This is done relatively easily by first assuming a free surface profile and solving Eqn. 3.7 subject to the boundary conditions given by Eqns. 3.15, 3.16, 3.19 and 3.20 to give values of ϕ and ψ over the entire boundary of the flow region. The assumed free surface is correct if the values of ϕ calculated above agree with those obtained using Eqn. 3.17. If the two solutions do not agree, a new estimate is made and the process repeated until they do. Provided a realistic estimate of the free surface is made initially, the correct solution results in about four or five iterations.

When the upstream reservoir level drops to zero, Eqn. 3.7 must be solved subject to the appropriate boundary conditions (Eqns. 3.14 - 3.17). Because the free surface profile is known at the instant that drawdown occurs, only one free surface boundary condition is required to solve Eqn. 3.7. The extra free surface boundary condition, Eqn. 3.18, which is controlled by the normal derivative of ϕ along the free surface, is used to calculate changes in the free surface profile. However, since the normal derivative of ϕ has a magnitude that is equal to the tangential derivative of ψ (from the Cauchy-Riemann equations), and since the formulation calculates values of ψ along the free surface, it is more convenient to

substitute the tangential derivative of ψ for the normal derivative of ϕ in Eqn. 3.18. Thus a finite-difference approximation to Eqn. 3.18 can be written in the form;

$$|\Delta n| = \frac{\Delta t}{\sigma} \frac{\partial \psi}{\partial s} \quad (3.22)$$

in which Δn = arc length normal to the free surface, Δt = small time increment and $\frac{\partial \psi}{\partial s}$ = tangential derivative of ψ . For every node i on the free surface a second-order polynomial in x is written for both the distribution of ψ , and for the free surface elevation, in the vicinity of node i using values at $i-1$, i and $i+1$. These equations are used to calculate the value $\frac{\partial \psi}{\partial s}$ and the normal to the free surface at node i and are then substituted into Eqn. 3.22 to give a first approximation to the free surface at the end of the time step. Because $\frac{\partial \psi}{\partial s}$ and the free surface profile change continuously, an improved solution can be achieved by using averages of both $\frac{\partial \psi}{\partial s}$ and the normal direction throughout the time step. Thus Eqn. 3.7 is used to calculate ϕ and ψ on the first approximation to the flow boundary at the end of the time step, and both $\frac{\partial \psi}{\partial s}$ and normal direction are calculated. The average of these values and those at the beginning of the time step are substituted into Eqn. 3.22 to get a better approximation to the free surface profile at the end of the time step. This process is repeated until successive solutions agree to within a pre-selected tolerance. As successive approximations to the free surface profile are calculated, nodal positions are altered so that the horizontal coordinate of each node is the same as it was at the beginning of the time step. This is done by assuming that the free surface profile at the end of the time step in the vicinity of node i is a second order function of x , calculated using data from nodes $i-1$, i and $i+1$. In this way successive approximations are compared by considering elevations at given values of x .

Once the free surface profile at the end of one time step has been found, it can be used as the starting point

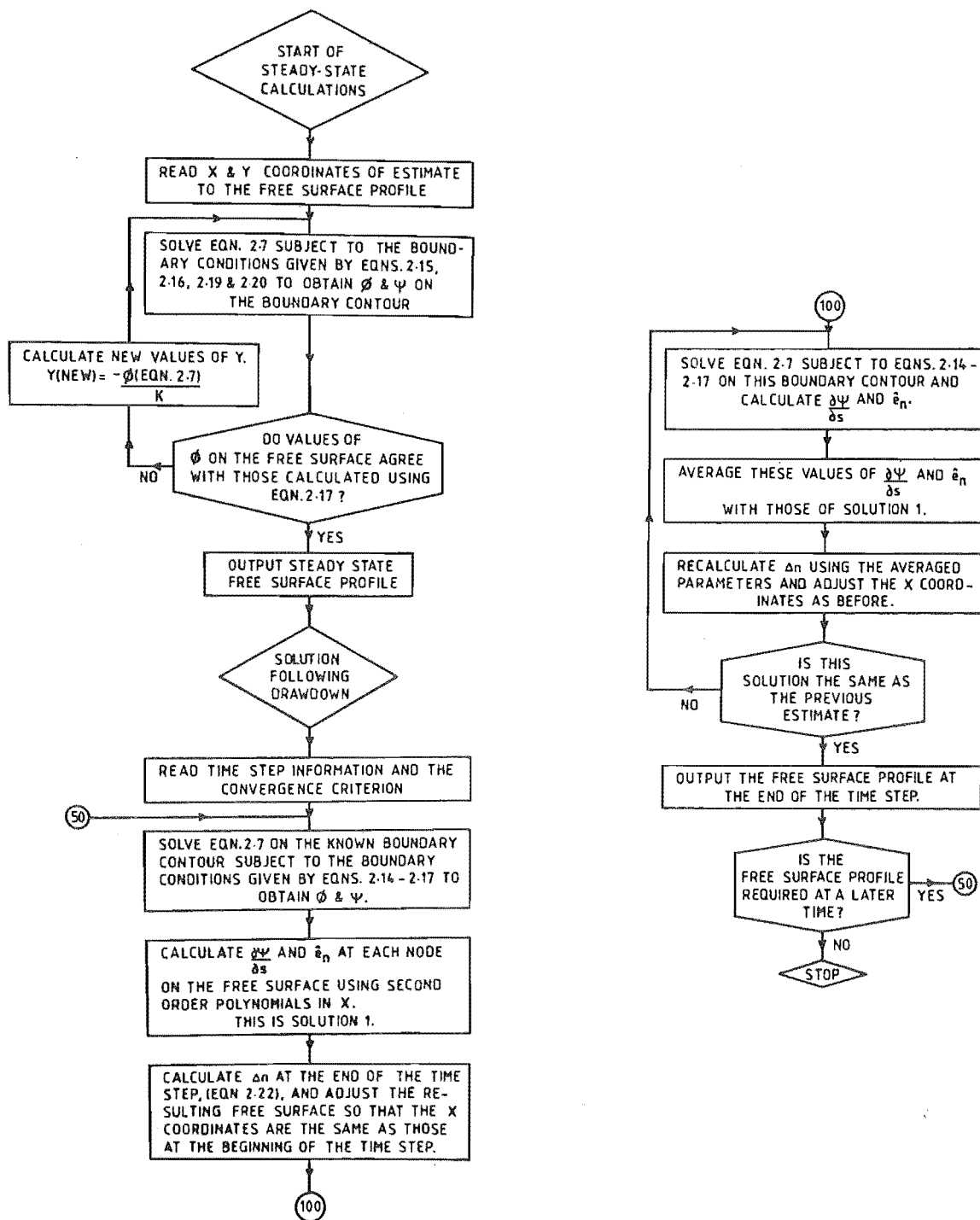


Fig. 3.2 Flow Chart for Calculation of Unsteady, Free Surface Profiles.

for another time step, and so the complete free surface time history can be obtained. A flow chart for this process is given in Fig. 3.2.

A typical steady-state nodal arrangement is shown in Fig. 3.3. In the initial stages following drawdown pore

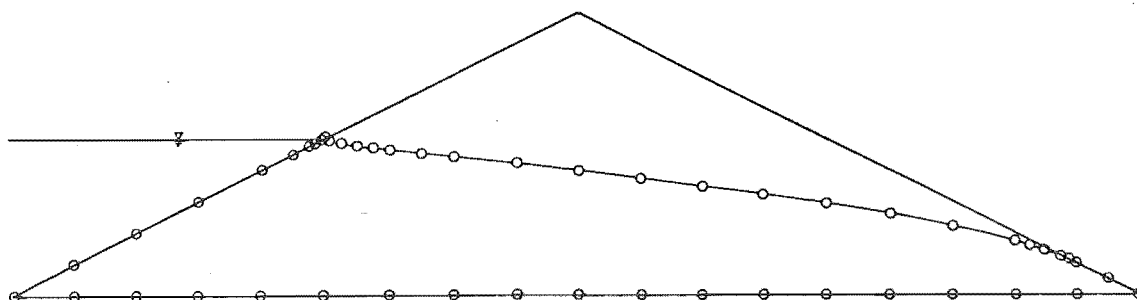


Fig. 3.3 Typical Steady-State Nodal Arrangement.

velocities are greatest where the free surface and the upstream face of the embankment intersect, and so a high concentration of nodes is required there. Thus the same nodal layout as for the steady-state case is used. As drawdown proceeds, velocities become smaller and the nodal spacing can be increased accordingly. A typical nodal arrangement used during the latter stages of drawdown is shown in Fig. 3.4.

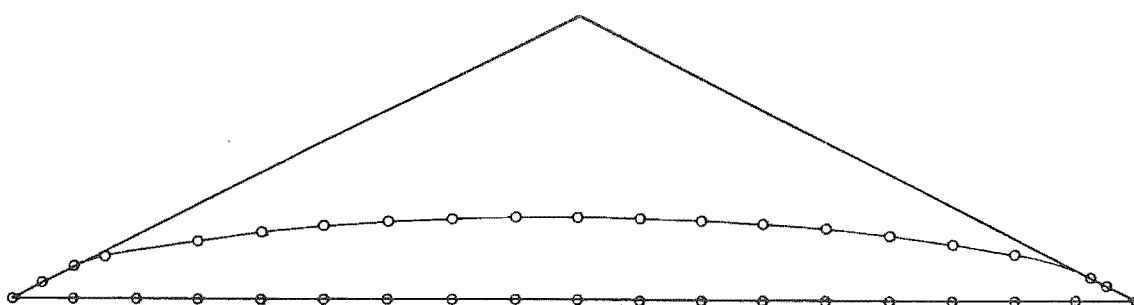


Fig. 3.4 Typical Nodal Arrangement Following Drawdown.

Typically dimensionless time step lengths are of the order $K\Delta t/\sigma L = 0.005$ in the initial stages of drawdown, but as time proceeds the free surface falls more slowly and dimensionless time steps of the order $K\Delta t/\sigma L = 0.1$ can be used.

3.5 EXPERIMENTAL SOLUTION

The analogy between gravity flow through a porous medium and viscous flow between parallel plates was developed by Hele-Shaw in 1897 and is well documented in texts like Polubarinova-Kochina (1962) and Harr (1962). The flow of oil between parallel perspex plates that are geometrically similar to the embankment being considered was observed in order to check the accuracy of one of the numerical solutions. The plates had base widths of 920 mm, 2:1 upstream and downstream face slopes and were spaced 3.0 mm apart. During steady flow conditions oil was recycled back to the upstream reservoir by pumping with a 600 watt electric motor, while instantaneous drawdown was simulated by suddenly draining the upstream reservoir. The subsequent free surface profiles were recorded photographically, and a ruler and stopwatch that appeared in each photograph were used to scale free surface coordinates as a function of time.

3.6 DUPUIT APPROXIMATION SOLUTION

By making the Dupuit approximation, which assumes that the piezometric head, h , does not vary in the vertical direction, the steady flow through the homogeneous, isotropic embankment shown in Fig. 3.1 is governed by the following equation;

$$\frac{\partial}{\partial x} \left[h \frac{\partial h}{\partial x} \right] = 0 \quad (3.23)$$

During steady flow the boundary conditions are assumed to be;

$$h(\beta L) = H_0 \quad (3.24)$$

$$h(L) = 0 \quad (3.25)$$

in which βL is the horizontal coordinate of the intersection of the upstream face of the embankment with the reservoir free surface. The solution of Eqns. 3.23-3.25 is given by;

$$h(x) = H_0 \sqrt{\frac{L-x}{L(1-\beta)}} \quad (3.26)$$

and the two-dimensional flow rate is;

$$q = \frac{KH_0^2}{2L(1-\beta)} \quad (3.27)$$

in which q is independent of x .

The unsteady solution following instantaneous draw-down at $t = 0$ is obtained from;

$$\frac{\partial}{\partial x} \left[h \frac{\partial h}{\partial x} \right] = \frac{\sigma}{K} \frac{\partial h}{\partial t} \quad (3.28)$$

$$h(x, t=0) = H_0 \sqrt{\frac{L-x}{L(1-\beta)}} \quad (3.29)$$

$$h(x=0, t) = 0 \quad (3.30)$$

$$h(x=L, t) = 0 \quad (3.31)$$

in which σ and K are the constant values of embankment porosity and permeability, respectively. Eqn. 3.29 is the initial condition requiring steady-state conditions to exist prior to drawdown, and Eqns. 3.30 and 3.31 are the appropriate boundary conditions. Eqn. 3.28 is non-linear and, hence is most easily solved by a numerical scheme. Stephenson (1978), for example, uses an explicit finite-difference technique that uses a first-order, forward-difference approximation to the time derivative on the right side of Eqn. 3.28 and a second-order, central-difference approximation to the spatial derivative on the left side of Eqn. 3.28. The resulting finite difference equation is given by;

$$h(x, t+\Delta t) = h(x, t) + \frac{K\Delta t}{2\sigma\Delta x^2} \left[h(x-\Delta x, t)^2 + h(x+\Delta x, t)^2 - 2h(x, t)^2 \right] \quad (3.32)$$

in which Δt is the time step length, Δx is the nodal spacing and all values of h at time t which appear on the right side of Eqn. 3.32 are known. A theoretical stability analysis of Eqn. 3.32 is not readily obtainable and so the maximum

permissible value of the time step length must be found by trial and error.

Prior to drawdown the steady flow through the embankment is governed by Eqn. 3.23, which is linear in h^2 . If the unsteady flow equation, Eqn. 3.32, is linearized by choosing h^2 as the dependent variable (Polubarinova-Kochina, 1962), then the solution to this problem will agree with the steady state solution at the instant drawdown occurs ($t=0$). Letting;

$$\mu = h^2 \quad (3.33)$$

then
$$\frac{\partial^2 \mu}{\partial x^2} = \frac{\sigma}{Kh} \frac{\partial \mu}{\partial t} \quad (3.34)$$

The linearized form of this equation is obtained by replacing h with the constant value H_0 on the right side of Eqn. 3.34 to give;

$$\frac{\partial^2 \mu}{\partial x^2} = \frac{\sigma}{KH_0} \frac{\partial \mu}{\partial t} \quad (3.35)$$

The initial condition becomes;

$$\mu(x, t=0) = \frac{H_0^2 (L-x)}{L(1-\beta)} \quad (3.36)$$

and the boundary conditions are;

$$\mu(x=0, t) = 0 \quad (3.37)$$

$$\mu(x=L, t) = 0 \quad (3.38)$$

For the case of 2:1 embankment side slopes;

$$\beta = \frac{2H_0}{L} \quad (3.39)$$

and the solution of Eqns. 3.35 - 3.38 is given by;

$$\mu(x,t) = \frac{2 H_0^2}{(1-2\varepsilon)} \sum_{n=1}^{\infty} \frac{e^{\frac{-\varepsilon (n\pi)^2 Kt}{\sigma L}} \sin \frac{n\pi x}{L}}{n\pi} \quad (3.40)$$

$$\text{or } h(x,t) = H_0 \sqrt{\frac{2}{(1-2\varepsilon)} \sum_{n=1}^{\infty} \frac{e^{\frac{-\varepsilon (n\pi)^2 Kt}{\sigma L}} \sin \frac{n\pi x}{L}}{n\pi}} \quad (3.41)$$

$$\text{in which } \varepsilon = \frac{H_0}{L}.$$

Chapter 4

EVALUATION OF THE TECHNIQUES GIVEN IN CHAPTER 34.1 INTRODUCTION

The numerical method given in Sec. 3.4 is used to obtain solutions for unsteady, two-dimensional flow through a homogeneous, isotropic embankment. The results from an experimental solution are included to check the accuracy of one of the numerical solutions and are used to show the limitations of the experimental approach. The numerical results are also compared with the simpler results that are obtained by making the Dupuit approximation.

4.2 SEEPAGE THROUGH A HOMOGENEOUS, ISOTROPIC EMBANKMENT

Unsteady seepage through a triangular embankment with 2:1 side slopes was computed numerically for three different upstream reservoir levels. The results for dimensionless reservoir depths of $H_0/L = 0.1667$, 0.1389 , and 0.1111 are given in Figs. 4.1, 4.2, and 4.3 respectively, while a comparison between the numerical and experimental models is given in Fig. 4.4. The main point of interest with the comparison is the variation in free surface elevation between the numerical and experimental solutions for steady flow. This is not unexpected, however, for several reasons. A boundary layer with an approximate thickness of one and a half plate spacings exists along the base of the experimental model, as shown in Appendix A. This boundary layer accounts for approximately sixty percent of the difference, while the remaining forty percent is believed to be due to surface tension and three-dimensional effects where the free surface intersects the upstream and downstream embankment faces. During steady flow the free surface is a streamline and, thus, it intersects the upstream face at right angles and approaches the downstream face tangentially. This condition is satisfied by the numerical solution but not by the experimental solution, which indicates that better accuracy is probably achieved with the numerical model.

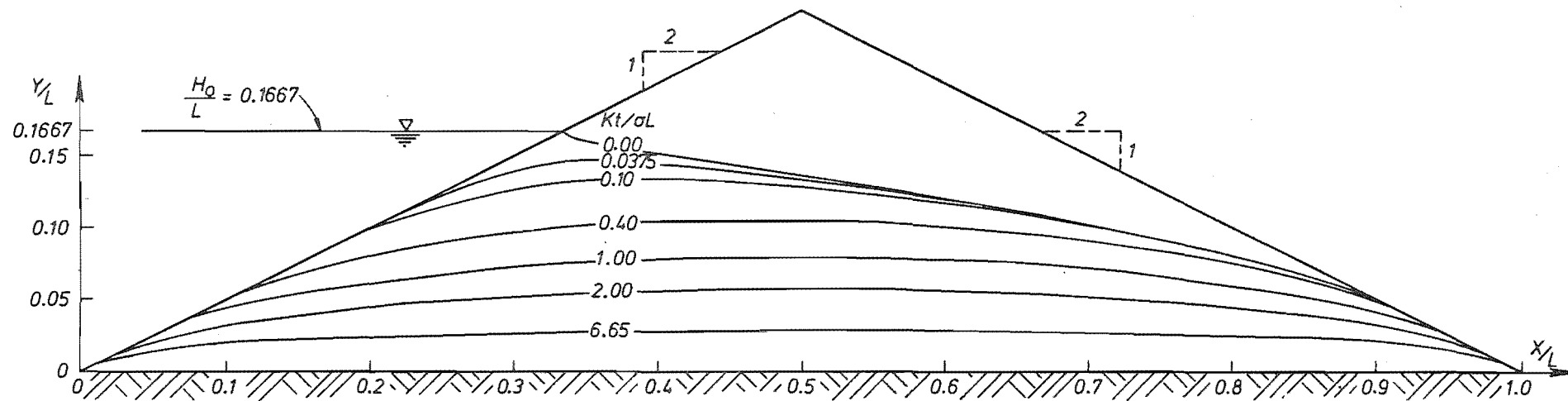


Fig. 4.1 Dimensionless free surface profiles for $\frac{H_0}{L} = 0.1667$.

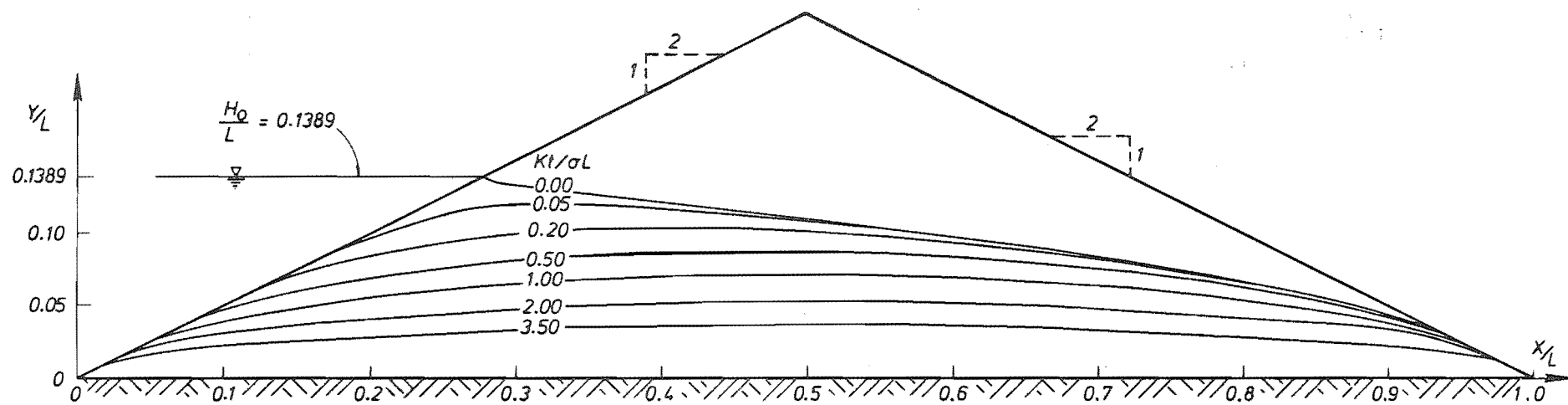


Fig. 4.2 Dimensionless free surface profiles for $\frac{H_0}{L} = 0.1389$.

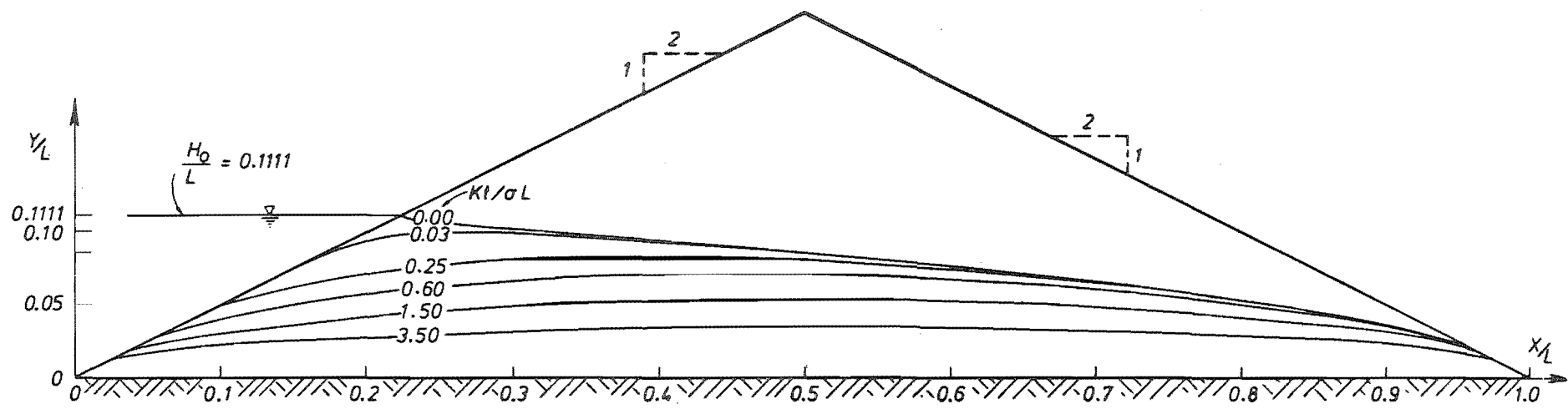


Fig. 4.3 Dimensionless free surface profiles for $\frac{H_0}{L} = 0.1111$.

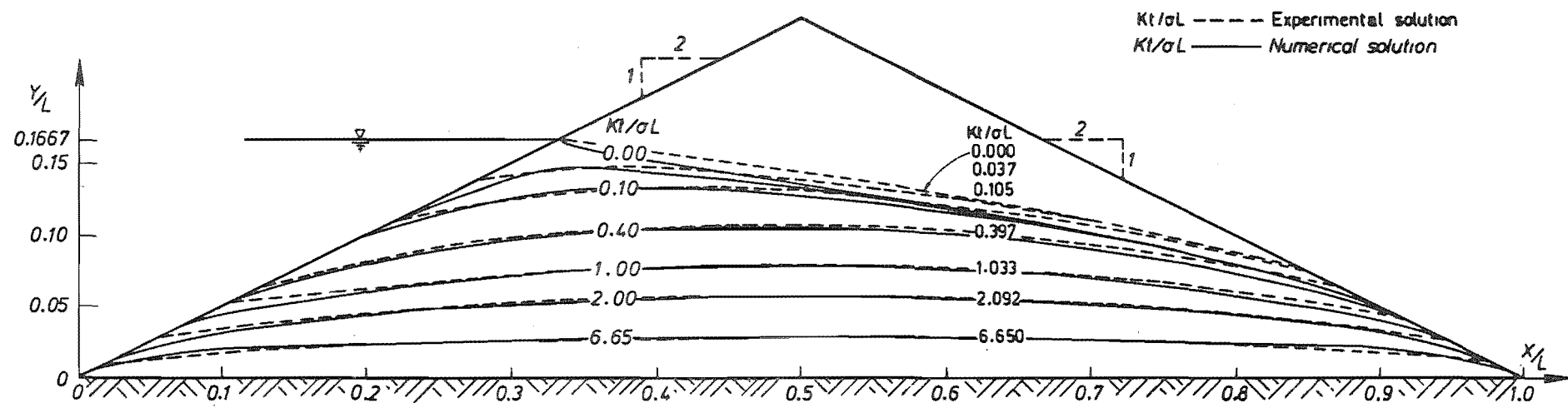


Fig. 4.4 Comparison between numerical and experimental solutions for $\frac{H_0}{L} = 0.1667$.

As drawdown proceeds, the difference between the numerical and experimental solutions decreases, which suggests that boundary layer and surface tension effects become relatively small in the experimental model as time increases.

Another major source of experimental error arises from oil viscosity variations (and hence permeability variations) that are caused by the pump supplying heat to the system. Viscosity is highly temperature-dependent and so temperature must be closely monitored throughout the experiment to ensure accurate results.

An excellent feature of the numerical formulation is that any small perturbation that is introduced into the solution is quickly damped out and has a minimal effect on surrounding nodes. This is extremely useful when dealing with a node at the intersection of the free surface and the upstream embankment face at $t=0$. Clearly, a parabolic free surface profile is not particularly realistic there, but once a solution at the end of the first time step has been calculated, the free surface can be manually smoothed in the vicinity of this node with little or no effect on subsequent calculations. As the free surface elevation falls, the values of ϕ and ψ calculated from Eqn. 3.7 vary less than at earlier times, and so if nodes are too closely spaced, small numerical errors in ψ and in the free surface elevation can result in poor polynomial fits to the true behaviour of these functions. Consequently changes in the free surface profile, calculated from Eqn. 3.22, will also be inaccurate. Redundant nodes, therefore, should be removed as drawdown proceeds. For these reasons the numerical solution does not lend itself to the generation of an entire free surface time-history.

Desai (1972) and Stephenson (1978) state that it is customary to assume instantaneous drawdown in unsteady seepage calculations and that this assumption is conservative. The results shown in Figs. 4.1 - 4.3 now allow a more precise

statement to be made in this regard. If t_0 is the time required for the reservoir to reach zero depth, these results show that a negligible movement of the free surface will have occurred by this time if

$$\frac{K t_0}{\sigma L} \leq 0.03 \quad (4.1)$$

For example, if an embankment has $K = 1 \times 10^{-5}$ m/s, $\sigma = 0.2$ and $L = 30$ m, Eqn. 4.1 gives a value of t_0 of 18,000 s or 5 hours. Similarly, a less permeable embankment with $K = 1 \times 10^{-6}$ m/s, $\sigma = 0.2$ and $L = 45$ m leads to the result $t_0 = 75$ hours. Thus it appears that the assumption of instantaneous drawdown is likely to be valid for a great many applications.

Comparisons between the numerical and linearized Dupuit solutions for dimensionless reservoir depths of $H_0/L = 0.1667$ and 0.1111 are given in Figs. 4.5 and 4.6, respectively. During steady flow conditions the agreement between the two solutions is reasonably good, especially in the case of smaller reservoir depths. This is to be expected however, because for small reservoir depths the streamlines are nearly horizontal and thus the equipotentials are almost vertical throughout most of the solution domain. During steady flow the free surface is a streamline and the numerical method calculates the two-dimensional flow rate through the embankment as part of the solution. The comparison between these values and those obtained from Eqn. 3.27 are given in dimensionless form in Table 4.1.

$\frac{H_0}{L}$	$\frac{q}{K H_0}$	
	Numerical Solution	Dupuit Solution
0.1111	0.0670	0.0714
0.1389	0.0906	0.0962
0.1667	0.1193	0.1250

Table 4.1 Comparison of steady-state flow rates for numerical and Dupuit solutions.

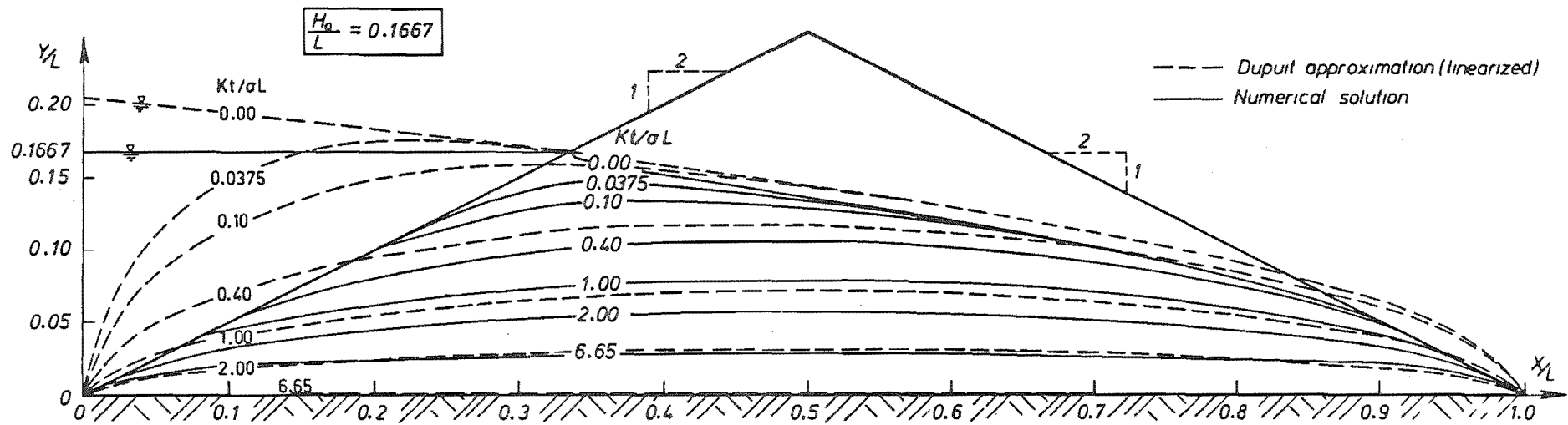


Fig. 4.5 Comparison between numerical and linearized Dupuit solution for $\frac{H_0}{L} = 0.1667$.

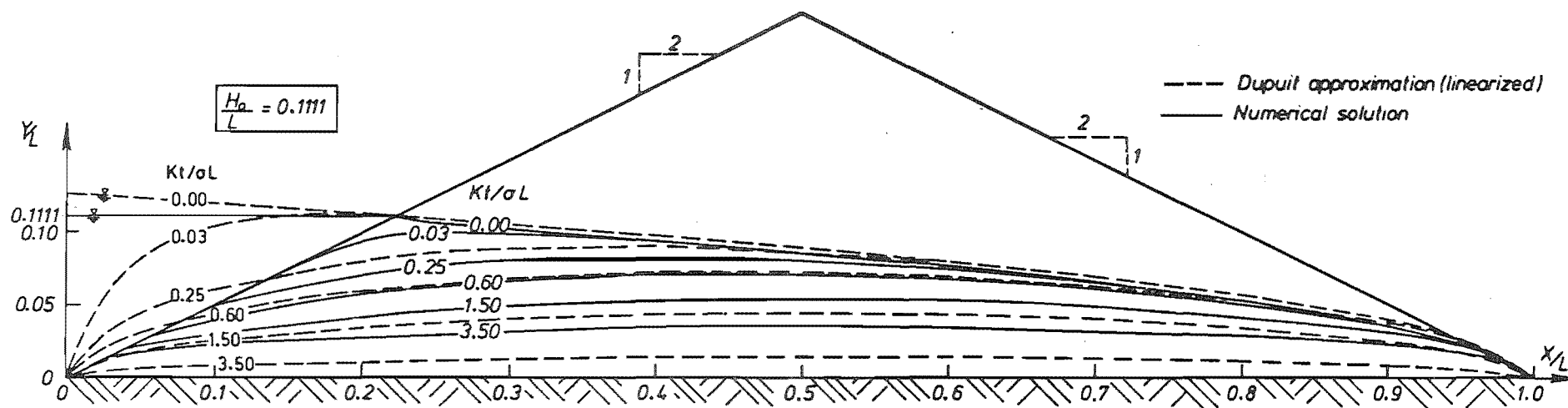


Fig. 4.6 Comparison between numerical and linearized Dupuit solution for $\frac{H_0}{L} = 0.1111$.

The closeness between the calculated flow rates is to be expected considering the good agreement that exists between the free surface coordinates and slopes, as shown in Figs. 4.5 and 4.6.

Once drawdown has occurred the two solutions are comparable for a limited period, but as time proceeds the linearized Dupuit solution tends to zero depth at a faster rate than the numerical solution (see Figs. 4.5 and 4.6). This apparent anomaly is to be expected, however, because of the assumptions made concerning the linearized Dupuit solution. Using the initial reservoir depth H_0 to linearize Eqn. 3.34 is a reasonable approximation and in the early stages following drawdown, but at later times when values of h are much smaller than H_0 , the approximation is less accurate. As a result of this, values of $\frac{\partial h}{\partial t}$ calculated from the linearized equation, Eqn. 3.35, are larger than those obtained from the non-linear equation, Eqn. 3.34. Thus the linearized Dupuit solution can be expected to approach zero depth faster than the true solution to the problem. Furthermore, the Dupuit solutions were obtained by assuming vertical velocities were negligible, but clearly such an assumption is unlikely to be valid following a sudden drawdown. Polubarinova-Kochina (1962) estimates the vertical velocity by considering the equation of continuity,

$$\frac{\partial u}{\partial x} + \frac{\partial v}{\partial y} = 0 \quad (4.2)$$

in which u and v are the horizontal and vertical velocity components. Because u has been assumed to be only a function of x , given by Darcy's law by

$$u = -K \frac{\partial h}{\partial x} \quad (4.3)$$

the integration of Eqn. 4.2 with respect to y gives;

$$v = - \int_0^y \frac{\partial u}{\partial x} dy = Ky \frac{\partial^2 h}{\partial x^2} \quad (4.4)$$

If h is given by Eqn. 3.41, then

$$u(x,t) = \frac{-K\epsilon \sum_{n=1}^{\infty} e^{\frac{-\epsilon(n\pi)^2 Kt}{\sigma L}} \cos \frac{n\pi x}{L}}{(1-2\epsilon) \sqrt{\frac{2}{(1-2\epsilon)} \sum_{n=1}^{\infty} \frac{e^{\frac{-\epsilon(n\pi)^2 Kt}{\sigma L}} \sin \frac{n\pi x}{L}}{n\pi}}} \quad (4.5)$$

and

$$v(x,y,t) = \frac{-Ky\epsilon}{2L} \sqrt{\frac{2}{(1-2\epsilon)}} \left[\frac{\left[\sum_{n=1}^{\infty} e^{\frac{-\epsilon(n\pi)^2 Kt}{\sigma L}} \cos \frac{n\pi x}{L} \right]^2}{2 \sum_{n=1}^{\infty} \frac{e^{\frac{-\epsilon(n\pi)^2 Kt}{\sigma L}} \sin \frac{n\pi x}{L}}{n\pi}} \right]^{3/2} + \frac{\sum_{n=1}^{\infty} n\pi e^{\frac{-\epsilon(n\pi)^2 Kt}{\sigma L}} \sin \frac{n\pi x}{L}}{\sqrt{\sum_{n=1}^{\infty} \frac{e^{\frac{-\epsilon(n\pi)^2 Kt}{\sigma L}} \sin \frac{n\pi x}{L}}{n\pi}}} \quad (4.6)$$

On the free surface $y = h$, therefore

$$v(x,y=h,t) = \frac{-K\epsilon^2}{(1-2\epsilon)} \left[\frac{\left[\sum_{n=1}^{\infty} e^{\frac{-\epsilon(n\pi)^2 Kt}{\sigma L}} \cos \frac{n\pi x}{L} \right]^2}{2 \sum_{n=1}^{\infty} \frac{e^{\frac{-\epsilon(n\pi)^2 Kt}{\sigma L}} \sin \frac{n\pi x}{L}}{n\pi}} \right] + \frac{\sum_{n=1}^{\infty} n\pi e^{\frac{-\epsilon(n\pi)^2 Kt}{\sigma L}} \sin \frac{n\pi x}{L}}{\sqrt{\sum_{n=1}^{\infty} \frac{e^{\frac{-\epsilon(n\pi)^2 Kt}{\sigma L}} \sin \frac{n\pi x}{L}}{n\pi}}} \quad (4.7)$$

in which $\epsilon = \frac{H_0}{L}$. Solutions for u and $v(y=h)$ throughout the solution domain for the case $\frac{H_0}{L} = 0.1667$ are shown in dimensionless form in Table 4.2.

$\frac{x}{L}$	Steady state		$\frac{Kt}{\sigma L} = 0.1$		$\frac{Kt}{\sigma L} = 2.0$	
	u	v(y=h)	u	v(y=h)	u	v(y=h)
0.05	0.1047	-0.0110	-0.8044	-0.7786	-0.1233	-0.0160
0.10	0.1076	-0.0116	-0.5013	-0.4864	-0.0845	-0.0086
0.20	0.1141	-0.0130	-0.1967	-0.3385	-0.0521	-0.0056
0.30	0.1220	-0.0149	-0.0175	-0.2127	-0.0323	-0.0050
0.40	0.1318	-0.0179	0.0815	-0.1058	-0.0156	-0.0049
0.50	0.1443	-0.0208	0.1303	-0.0491	0.0000	-0.0049
0.60	0.1614	-0.0260	0.1584	-0.0325	0.0156	-0.0049
0.70	0.1863	-0.0347	0.1859	-0.0358	0.0323	-0.0050
0.80	0.2282	-0.0521	0.2282	-0.0522	0.0521	-0.0056
0.90	0.3227	-0.1042	0.3227	-0.1042	0.0845	-0.0086
0.95	0.4564	-0.2083	0.4564	-0.2083	0.1233	-0.0160

Table 4.2 Comparison of horizontal and vertical velocities from linearized Dupuit solution.

During steady flow vertical velocities are very small over most of the solution domain, and the Dupuit approximation is applicable. However, once drawdown has occurred, vertical velocities are significant especially near $x=0$. At later times the free surface falls more slowly, and vertical velocities are again negligible.

The finite-difference technique given by Eqn. 3.32 was used to calculate solutions to the non-linear Dupuit equation, Eqn. 3.28. Stephenson (1978) used a dimensionless nodal spacing of $\frac{\Delta x}{L} = 0.1$ in his calculations, but because the free surface elevation changes rapidly near $x = 0$ following drawdown, a value of $\frac{\Delta x}{L} = 0.05$ was selected for this study. A dimensionless time step of $\frac{K\Delta t}{\sigma L} = 0.005$ was found to give stable solutions to these problems. Comparisons between these solutions and the numerical solutions (Eqn. 3.7) for dimensionless reservoir depths of $\frac{h_0}{L} = 0.1667$ and 0.1111 are given in Figs. 4.7 and 4.8, respectively. Although there is now good agreement between the solutions at later times, differences at earlier times (when vertical velocities are

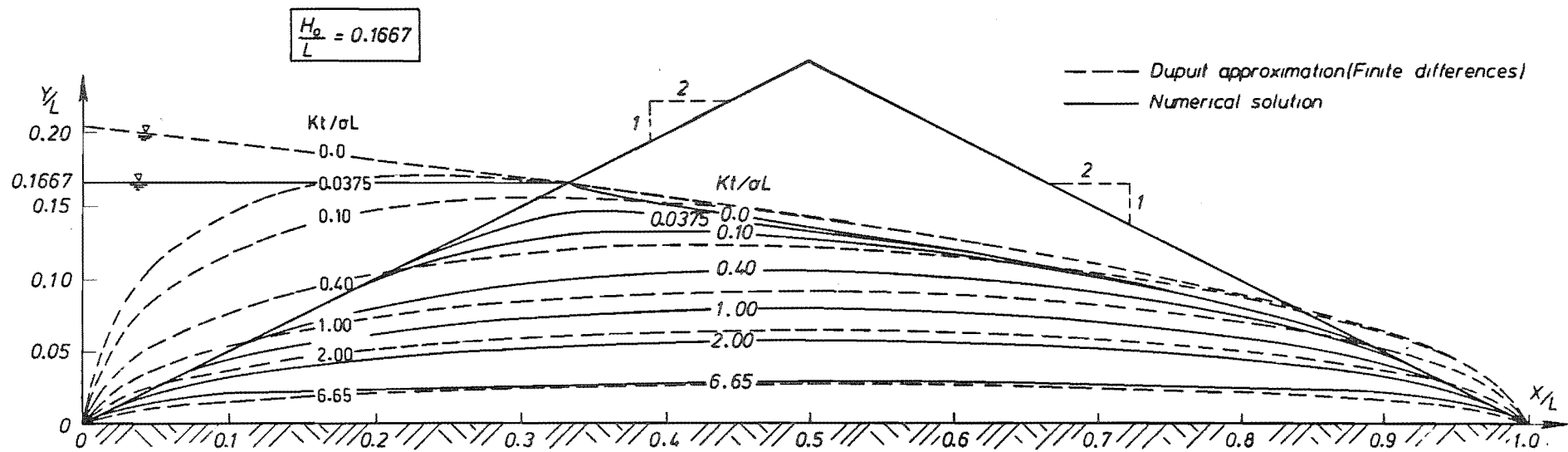


Fig. 4.7 Comparison between numerical and non-linear Dupuit solution for $\frac{H_0}{L} = 0.1667$.

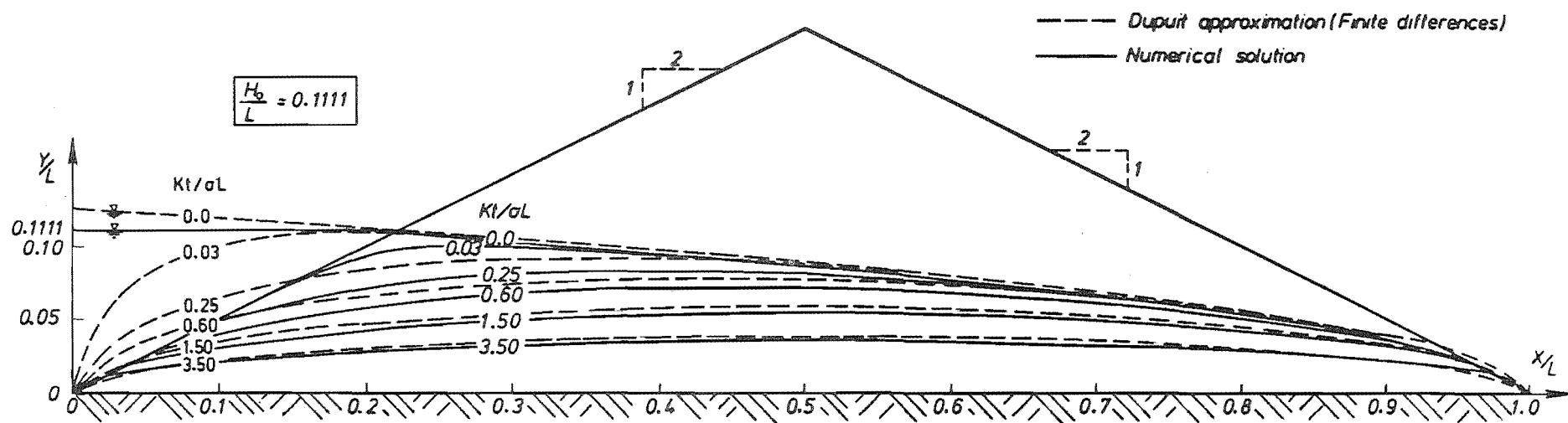


Fig. 4.8 Comparison between numerical and non-linear Dupuit solution for $\frac{H_0}{L} = 0.1111$.

large) are no less than those between the numerical and linearized Dupuit solutions shown in Figs. 4.5 and 4.6. Thus, it appears that the Dupuit approximation is not valid for this type of problem, especially immediately following drawdown.

h_0 for h

$\frac{\partial h}{\partial t}$ larger

error larger
for smaller h

Chapter 5

SOLUTIONS OF THE UNSTEADY DUPUIT EQUATION5.1 INTRODUCTION

The unsteady two-dimensional flow of groundwater through a region R with boundary contour Γ , as shown in Fig. 5.1, is governed by the Dupuit equation;

$$\nabla \cdot (T \nabla h) = S \frac{\partial h}{\partial t} + \sum_i Q_i \delta(x-x_i) \delta(y-y_i) \quad (5.1)$$

in which $T(x,y,t)$ = transmissivity,

S = storage coefficient,

$h(x,y,t)$ = piezometric head,

Q_i = flow rate in well i ,

x_i, y_i = coordinates of well i , and

t = time.

In a well-posed boundary-value problem either the piezometric head, or its normal derivative, must be known functions of time at all points on the boundary Γ , while the initial distribution of h within the solution domain at $t=0$ is also required.

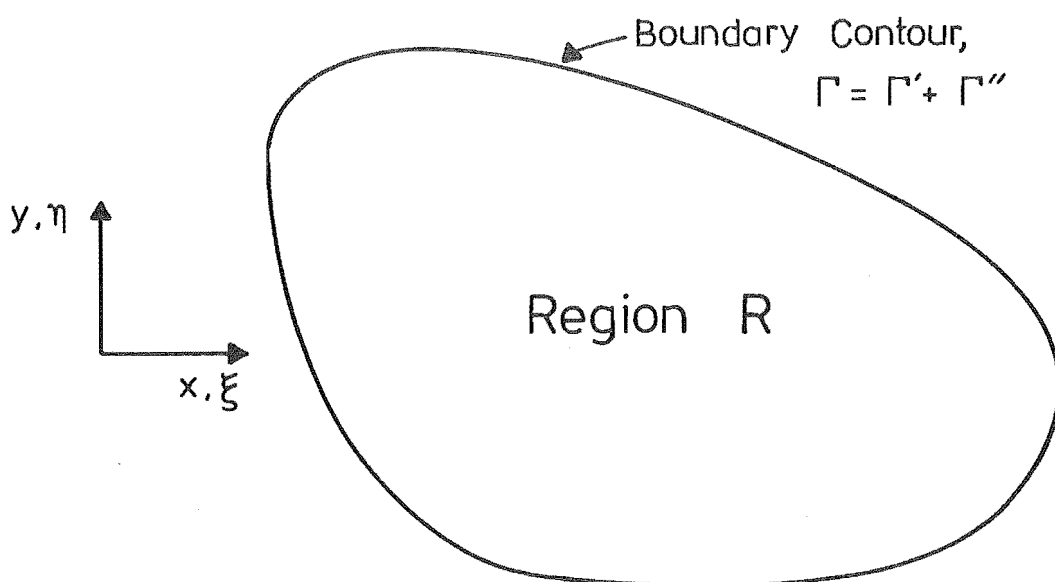


Fig. 5.1 Definition Diagram for Two-Dimensional Flow

For confined flows, Eqn 5.1 is linear. However, the transmissivity for unconfined flows is given by;

$$T(x,y,t) = K(x,y) h(x,y,t) \quad (5.2)$$

in which $K(x,y)$ = permeability, and so Eqn 5.1 is non-linear and, hence, difficult to solve. By assuming that a distribution for T calculated previously can be used for all times, Eqn 5.1 can be linearized and the principle of superposition used to write;

$$\bar{\nabla} \cdot (T \bar{\nabla} h) = S \frac{\partial h}{\partial t} + Q \delta(x-x_0) \delta(y-y_0) \quad (5.3)$$

$$h(x,y,t=0) = 0 \quad (5.4)$$

$$h(x,y,t) = f(x,y,t) \text{ for } x,y \text{ on } \Gamma' \in \Gamma \quad (5.5)$$

$$\frac{\partial h(x,y,t)}{\partial n} = g(x,y,t) \text{ for } x,y \text{ on } \Gamma'' \in \Gamma \quad (5.6)$$

in which, f and g are the known changes in piezometric head, and its normal derivative, around the boundary, respectively, h is the change in piezometric head caused by the changing boundary conditions together with pumping a flow rate Q from a well at (x_0, y_0) and $\frac{\partial h}{\partial n}$ is the normal derivative of h .

In this chapter an integral equation technique is used firstly to solve Eqns 5.3-5.6 for a homogeneous region in which there are no wells, and then to extend the method to solve problems that do include wells. This technique will then be generalized to solve problems for composite regions, in which the transmissivity is constant throughout each zone in the region, but varies from one zone to the next.

5.2 FORMULATION FOR A HOMOGENEOUS REGION THAT CONTAINS NO WELLS

For the case of a homogeneous region that contains no wells, Eqns 5.3-5.6 can be simplified and rewritten as;

$$a^2 \nabla_{x,y}^2 h = \frac{\partial h}{\partial t} \quad (a^2 \equiv T/S = \text{constant}, \quad x,y \text{ in } R) \quad (5.7)$$

$$h = 0 \text{ at } t = 0 \quad (5.8)$$

$$h = f \text{ for } x,y \text{ on } \Gamma' \in \Gamma \quad (5.9)$$

$$\frac{\partial h}{\partial n} = g \text{ for } x,y \text{ on } \Gamma'' \in \Gamma \quad (5.10)$$

(see Fig. 5.1).

The solution of Eqns 5.7-5.10 is based on the method used by Brebbia and Walker (1979). If (x,y,t) is replaced with (ξ,η,τ) in $h(x,y,t)$ and $u(x-\xi, y-\eta, t-\tau)$ is a fundamental solution of Eqn 5.7 with properties that will be defined later, then;

$$a^2 u \nabla_{\xi,\eta}^2 h - u \frac{\partial h}{\partial \tau} = 0 \quad (5.11)$$

But,

$$\begin{aligned} u \nabla^2 h &= \bar{\nabla} \cdot (u \bar{\nabla} h) - \bar{\nabla} u \cdot \bar{\nabla} h \\ &= \bar{\nabla} \cdot (u \bar{\nabla} h) - \bar{\nabla} \cdot (h \bar{\nabla} u) + h \nabla^2 u \end{aligned} \quad (5.12)$$

and

$$u \frac{\partial h}{\partial \tau} = \frac{\partial}{\partial \tau} (uh) - h \frac{\partial u}{\partial \tau} \quad (5.13)$$

Substituting Eqns 5.12 and 5.13 into Eqn 5.11 gives;

$$a^2 \left[\bar{\nabla} \cdot (u \bar{\nabla} h) - \bar{\nabla} \cdot (h \bar{\nabla} u) + h \nabla^2 u \right] - \frac{\partial (uh)}{\partial \tau} + h \frac{\partial u}{\partial \tau} = 0 \quad (5.14)$$

Integrating Eqn 5.14 over the region R and from $\tau=0$ to $\tau=t$ and using the divergence theorem gives;

$$\int_0^t \int_{\Gamma' + \Gamma''} a^2 \left(u \frac{\partial h}{\partial n} - h \frac{\partial u}{\partial n} \right) ds d\tau$$

$$\begin{aligned}
& + \int_0^t \int_R h(a^2 \nabla_{\xi, \eta}^2 u + \frac{\partial u}{\partial \tau}) d\xi d\eta d\tau \\
& - \int_R (uh)_{\tau=t} d\xi d\eta = 0
\end{aligned} \tag{5.15}$$

in which s = arc length measured along the boundary contour Γ .

Now define $u(x, y, t)$ so that it satisfies the following set of equations;

$$a^2 \nabla_{x, y}^2 u = \frac{\partial u}{\partial t} \quad \text{for } x, y \text{ in } R \tag{5.16}$$

$$u(x, y, 0) = \delta(x) \delta(y) \tag{5.17}$$

in which δ is the Dirac delta function. Thus $u(x-\xi, y-\eta, t-\tau)$ satisfies;

$$a^2 \nabla_{\xi, \eta}^2 u + \frac{\partial u}{\partial \tau} = 0 \quad \text{for } x, y \text{ and } \xi, \eta \text{ in } R \tag{5.18}$$

$$u(x-\xi, y-\eta, t-\tau) = \delta(x-\xi) \delta(y-\eta) \tag{5.19}$$

The solution of Eqns 5.18 and 5.19 is given by Carslaw and Jaeger (1959) as;

$$u(x-\xi, y-\eta, t-\tau) = u(r, t-\tau) = \frac{1}{4\pi a^2(t-\tau)} e^{\frac{-r^2}{4a^2(t-\tau)}} \tag{5.20}$$

$$\text{in which } r = \sqrt{(x-\xi)^2 + (y-\eta)^2}$$

Substituting Eqns 5.18 and 5.19 into Eqn 5.15 gives;

$$h(x, y, t) = \int_0^t \int_{\Gamma' + \Gamma''} a^2 \left(u \frac{\partial h}{\partial n} - h \frac{\partial u}{\partial n} \right) ds d\tau, \quad \text{for } x, y \text{ in } R \tag{5.21}$$

It will be shown later that;

$$\int_0^t u \, d\tau \sim \frac{-1}{4\pi a^2} \ln \left(\frac{r^2 e^\gamma}{4a^2 t} \right) \text{ as } r \rightarrow 0 \quad (5.22)$$

in which γ = Euler's constant = 0.5772156649...

$$\text{and } \int_0^t \frac{\partial u}{\partial n} \, d\tau \sim \frac{-\cos(r, n)}{2\pi a^2 r} \text{ as } r \rightarrow 0 \quad (5.23)$$

Thus, as the point (x, y) approaches a point on the boundary, methods similar to those used by Kellogg (1929) and Sternberg and Smith (1946) can be used to obtain the following integral equation from Eqn 5.21;

$$\frac{\theta}{2\pi} h(x, y, t) = \int_0^t \int_{\Gamma' + \Gamma''} a^2 \left(u \frac{\partial h}{\partial n} - h \frac{\partial u}{\partial n} \right) ds \, d\tau \quad (5.24)$$

in which θ = interior angle between the boundary tangents at (x, y) as shown in Fig. 5.2. At points where the boundary turns continuously $\theta = \pi$.

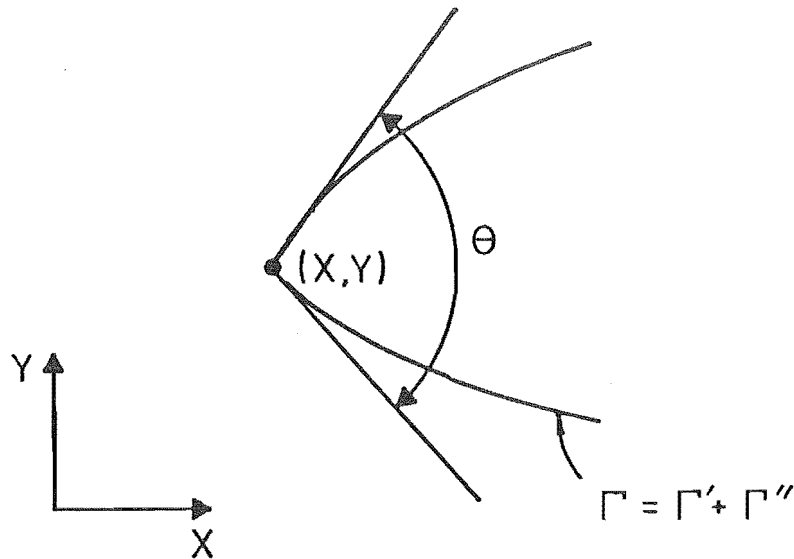


Fig. 5.2 Boundary Node Geometry

Eqn 5.24 can be solved by selecting a finite number of nodes on the boundary contour, Γ , and then calculating the

integrals numerically. The nodes should be closely spaced on portions of the boundary where h or $\frac{\partial h}{\partial n}$ change rapidly, and more sparsely spaced where h and $\frac{\partial h}{\partial n}$ vary less rapidly. Nodes will be numbered consecutively as the boundary is traversed in an anti-clockwise direction. A typical nodal arrangement is shown in Fig. 5.3.

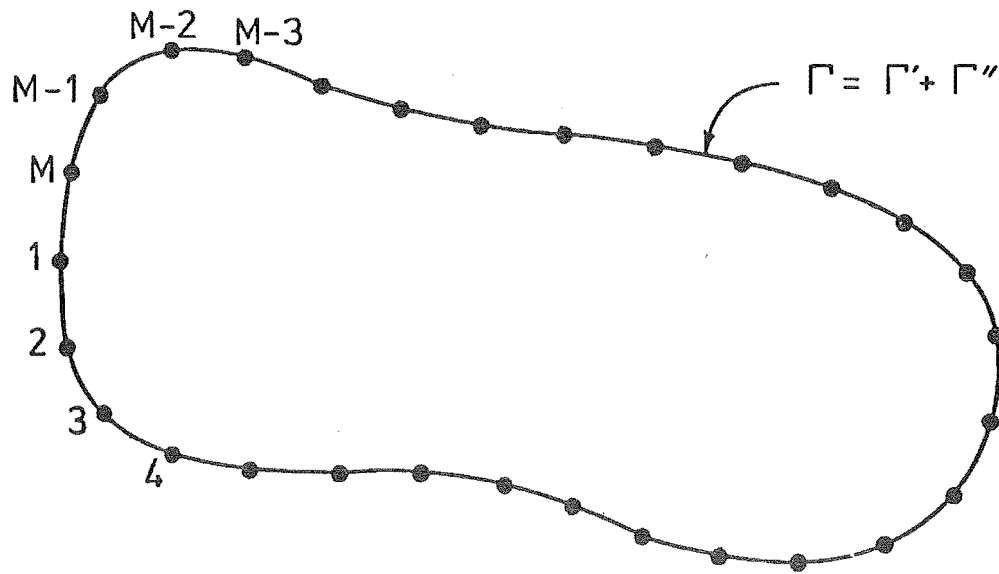


Fig. 5.3 Typical Nodal Arrangement for Homogeneous Region

An algebraic approximation to Eqn 5.24 can be written for each of M nodes, which gives M equations containing $2M$ unknowns (h and $\frac{\partial h}{\partial n}$ at each node). The remaining M equations required for a complete solution are obtained from the boundary conditions.

5.3 NUMERICAL SOLUTIONS

Method 1

The simplest way to integrate Eqn 5.24 numerically is to divide the time interval $(0, t)$ into N time steps and to assume that both h and $\frac{\partial h}{\partial n}$ remain constant at each node throughout each time step. The order of integration in Eqn 5.24 can be changed to give;

$$\begin{aligned}
\frac{\theta}{2\pi} h(x, y, t) = & \int_{\Gamma' + \Gamma''} a^2 \sum_{k=2}^N \left[\frac{\partial h^k}{\partial n} \int_{t_{k-1}}^{t_k} u(x-\xi, y-\eta, t-\tau) d\tau \right. \\
& \left. - h^k \int_{t_{k-1}}^{t_k} \frac{\partial u(x-\xi, y-\eta, t-\tau)}{\partial n} d\tau \right] ds \quad (5.25)
\end{aligned}$$

in which $t_N \equiv t$ and $t_1 \equiv 0$.

It can be shown that

$$\int_{t_{k-1}}^{t_k} u d\tau = \frac{1}{4\pi a^2} \left[E_1 \left[\frac{r^2}{4a^2(t_N - t_{k-1})} \right] - E_1 \left[\frac{r^2}{4a^2(t_N - t_k)} \right] \right] \quad (5.26)$$

$$\text{in which the exponential integral } E_1(x) \equiv \int_x^\infty \frac{e^{-t}}{t} dt \quad (5.27)$$

It can also be shown that

$$\int_{t_{k-1}}^{t_k} \frac{\partial u}{\partial n} d\tau = \frac{\cos(r, n)}{2\pi a^2 r} \left[e^{\frac{-r^2}{4a^2(t_N - t_k)}} - e^{\frac{-r^2}{4a^2(t_N - t_{k-1})}} \right] \quad (5.28)$$

in which (r, n) is the angle between r (the vector joining points (x, y) and (ξ, η)) and n the outward pointing normal to Γ at (ξ, η) . Thus Eqn 5.25 becomes;

$$\frac{\theta h^N(x, y, t_N)}{2\pi} = \frac{1}{4\pi} \sum_{k=2}^N \int_{\Gamma' + \Gamma''} \frac{\partial h^k}{\partial n} \left[E_1 \left[\frac{r^2}{4a^2(t_N - t_{k-1})} \right] \right]$$

$$\begin{aligned}
& - E_1 \left[\frac{r^2}{4a^2(t_N - t_k)} \right] \Bigg] ds + \frac{1}{2\pi} \sum_{k=2}^N \int_{\Gamma' + \Gamma''} h^k \frac{\cos(r, n)}{r} \\
& \left[e^{\frac{-r^2}{4a^2(t_N - t_{k-1})}} - e^{\frac{-r^2}{4a^2(t_N - t_k)}} \right] ds \quad (5.29)
\end{aligned}$$

in which the integrals are calculated in the sense of a Cauchy principal value.

It is necessary to examine the integrals in Eqn 5.29 so that any singularities in the integrands can be treated correctly. The first integral on the right hand side of Eqn 5.29 can be rewritten in the form

$$J_k = \int_{\Gamma' + \Gamma''} \frac{\partial h^k}{\partial n} G ds \quad (5.30)$$

$$\text{in which } G = E_1 \left[\frac{r^2}{4a^2(t_N - t_{k-1})} \right] - E_1 \left[\frac{r^2}{4a^2(t_N - t_k)} \right] \quad (5.31)$$

For $k < N$

$$\text{Since } E_1(x) \sim -\ln x - \gamma - \sum_{m=1}^{\infty} \frac{(-1)^m x^m}{mm!}, \text{ as } x \rightarrow 0 \quad (5.32)$$

in which γ = Euler's constant as defined in Eqn 5.22,

$$G \sim \ln \left(\frac{t_N - t_{k-1}}{t_N - t_k} \right) + O(r^2) \text{ as } r \rightarrow 0 \quad (5.33)$$

in which the order symbol, $O(r^2)$ indicates that the next term in the expansion is a constant multiplied by r^2 . Eqn 5.30 can be approximated by using the trapezium rule. (See Fig. 5.4).

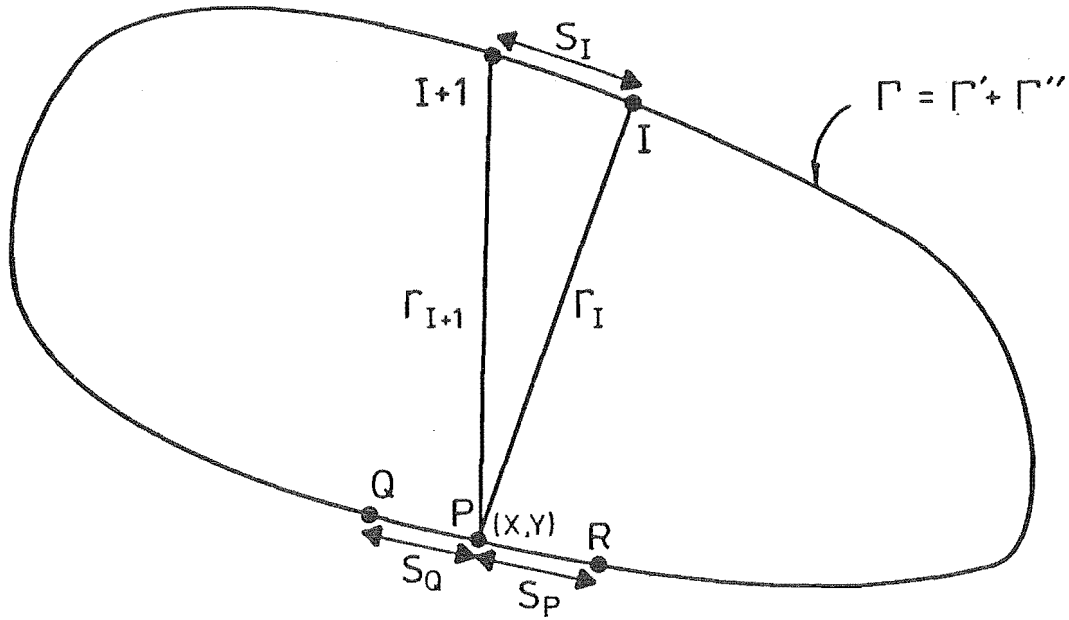


Fig. 5.4 Definition Diagram for Numerical Calculation of Eqn 5.30

$$\begin{aligned}
 & \int_I^{I+1} \frac{\partial h^k}{\partial n} G \, ds \\
 & \quad \begin{matrix} I \neq Q \\ I \neq P \end{matrix} \\
 & \approx \left[\frac{\partial h^k}{\partial n}(I) \left[E_1 \left[\frac{r_I^2}{4a^2(t_N - t_{k-1})} \right] - E_1 \left[\frac{r_I^2}{4a^2(t_N - t_k)} \right] \right] \right. \\
 & \quad \left. + \frac{\partial h^k}{\partial n}(I+1) \left[E_1 \left[\frac{r_{I+1}^2}{4a^2(t_N - t_{k-1})} \right] - E_1 \left[\frac{r_{I+1}^2}{4a^2(t_N - t_k)} \right] \right] \right] \frac{S_I}{2} \quad (5.34)
 \end{aligned}$$

in which r_I = length of line segment joining nodes P and I, S_I = length of line segment joining nodes I and I+1 and $\frac{\partial h^k}{\partial n}(I)$ = value of $\frac{\partial h}{\partial n}$ at node I at time t_k .

$$\begin{aligned}
\int_Q^R \frac{\partial h^k}{\partial n} G \, ds &\approx \frac{\partial h^k}{\partial n}(Q) \left[E_1 \left[\frac{r_Q^2}{4a^2(t_N - t_{k-1})} \right] - E_1 \left[\frac{r_Q^2}{4a^2(t_N - t_k)} \right] \right] \frac{S_Q}{2} \\
&+ \frac{\partial h^k}{\partial n}(R) \left[E_1 \left[\frac{r_R^2}{4a^2(t_N - t_{k-1})} \right] - E_1 \left[\frac{r_R^2}{4a^2(t_N - t_k)} \right] \right] \frac{S_P}{2} \\
&+ \frac{\partial h^k}{\partial n}(P) \ln \left[\frac{t_N - t_{k-1}}{t_N - t_k} \right] \frac{(S_Q + S_P)}{2}
\end{aligned} \tag{5.35}$$

For $k = N$

$$G = E_1 \left[\frac{r^2}{4a^2(t_N - t_{N-1})} \right] \sim -\ln \left(\frac{r^2 e^\gamma}{4a^2 \Delta t_N} \right) + O(r^2) \text{ as } r \rightarrow 0 \tag{5.36}$$

in which $\Delta t_N = t_N - t_{N-1}$

Clearly G becomes infinite as $r \rightarrow 0$, but using the method of "subtracting the singularity" as described by Scheid (1968), Eqn 5.30 can be rewritten as;

$$\begin{aligned}
J_N &= \int_{\Gamma' + \Gamma''} \left[\frac{\partial h^N}{\partial n} E_1 \left(\frac{r^2}{4a^2 \Delta t_N} \right) + \frac{\partial h^N(P)}{\partial n} \ln \left(\frac{r^2 e^\gamma}{4a^2 \Delta t_N} \right) \right] ds \\
&- \frac{\partial h^N(P)}{\partial n} \int_{\Gamma' + \Gamma''} \ln \left(\frac{r^2 e^\gamma}{4a^2 \Delta t_N} \right) ds
\end{aligned} \tag{5.37}$$

in which $\frac{\partial h^N(P)}{\partial n}$ = the value of $\frac{\partial h}{\partial n}$ at the singular point (x, y) at time t_N . The integrand in the first integral on the right hand side of Eqn 5.37 equals zero when $r = 0$, which enables the integral to be calculated numerically with the trapezium rule. (See Fig. 5.4).

$$\begin{aligned}
& \int_{\substack{I \\ I \neq Q \\ I \neq P}}^{I+1} \left[\frac{\partial h^N}{\partial n} E_1 \left(\frac{r^2}{4a^2 \Delta t_N} \right) + \frac{\partial h^N(P)}{\partial n} \ln \left(\frac{r^2 e^\gamma}{4a^2 \Delta t_N} \right) \right] ds \\
& \approx \left[\frac{\partial h^N(I)}{\partial n} E_1 \left(\frac{r_I^2}{4a^2 \Delta t_N} \right) + \frac{\partial h^N(I+1)}{\partial n} E_1 \left(\frac{r_{I+1}^2}{4a^2 \Delta t_N} \right) \right. \\
& \quad \left. + \frac{\partial h^N(P)}{\partial n} \left[\ln \left(\frac{r_I^2 e^\gamma}{4a^2 \Delta t_N} \right) + \ln \left(\frac{r_{I+1}^2 e^\gamma}{4a^2 \Delta t_N} \right) \right] \right] \frac{S_I}{2} \quad (5.38)
\end{aligned}$$

$$\begin{aligned}
\text{while } & \int_Q^R \left[\frac{\partial h^N}{\partial n} E_1 \left(\frac{r^2}{4a^2 \Delta t_N} \right) + \frac{\partial h^N(P)}{\partial n} \ln \left(\frac{r^2 e^\gamma}{4a^2 \Delta t_N} \right) \right] ds \\
& \approx \left[\frac{\partial h^N(Q)}{\partial n} E_1 \left(\frac{r_Q^2}{4a^2 \Delta t_N} \right) \right] \frac{S_Q}{2} + \left[\frac{\partial h^N(R)}{\partial n} E_1 \left(\frac{r_R^2}{4a^2 \Delta t_N} \right) \right] \frac{S_P}{2} \\
& \quad + \frac{\partial h^N(P)}{\partial n} \left[\ln \left(\frac{r_Q^2 e^\gamma}{4a^2 \Delta t_N} \right) \frac{S_Q}{2} + \ln \left(\frac{r_R^2 e^\gamma}{4a^2 \Delta t_N} \right) \frac{S_P}{2} \right] \quad (5.39)
\end{aligned}$$

The second integral on the right hand side of Eqn 5.37 can be evaluated as follows;

$$\begin{aligned}
& \int_{\Gamma' + \Gamma''} \ln \left(\frac{r^2 e^\gamma}{4a^2 \Delta t_N} \right) ds = \int_{\Gamma' + \Gamma''} \left[2 \ln r + \ln \left(\frac{e^\gamma}{4a^2 \Delta t_N} \right) \right] ds \\
& = 2 \int_{\Gamma' + \Gamma''} \ln r ds + L \ln \left(\frac{e^\gamma}{4a^2 \Delta t_N} \right) \quad (5.40)
\end{aligned}$$

in which $L = \text{length of } \Gamma' + \Gamma''$. The term $2 \int_{\Gamma' + \Gamma''} \ln r ds$ must be evaluated in part numerically and in part

analytically because of the singularity in $\ln r$ as $r \rightarrow 0$. The trapezium rule can be used over the entire boundary, except for segments QP and PR as shown in Fig. 5.4. For example;

$$\int_{\substack{I \\ I \neq Q \\ I \neq P}}^{I+1} \ln r \, ds \approx \ln \left(r_I r_{I+1} \right) \frac{S_I}{2} \quad (5.41)$$

If the boundary between nodes Q and P is approximated by a straight line, then;

$$\int_Q^P \ln r \, ds = \int_{r_Q}^0 - \ln r \, dr = r_Q (\ln r_Q - 1) \quad (5.42)$$

$$\text{and similarly } \int_P^R \ln r \, ds = r_R (\ln r_R - 1) \quad (5.43)$$

The second term on the right side of Eqn 5.29 can be written in the form;

$$I_k = \int_{\Gamma' + \Gamma''} h^k F \, ds \quad (5.44)$$

$$\text{in which } F = \frac{\cos(r, n)}{r} \left[e^{\frac{-r^2}{4a^2(t_N - t_{k-1})}} - e^{\frac{-r^2}{4a^2(t_N - t_k)}} \right] \quad (5.45)$$

For $k < N$

$$F \sim \frac{r \cos(r, n)}{4a^2} \frac{(t_k - t_{k-1})}{(t_N - t_k)(t_N - t_{k-1})} + O(r^3) \text{ as } r \rightarrow 0 \quad (5.46)$$

Thus the integral on the right hand side of Eqn 5.44 can be calculated approximately with the trapezium rule. (See Fig. 5.5).

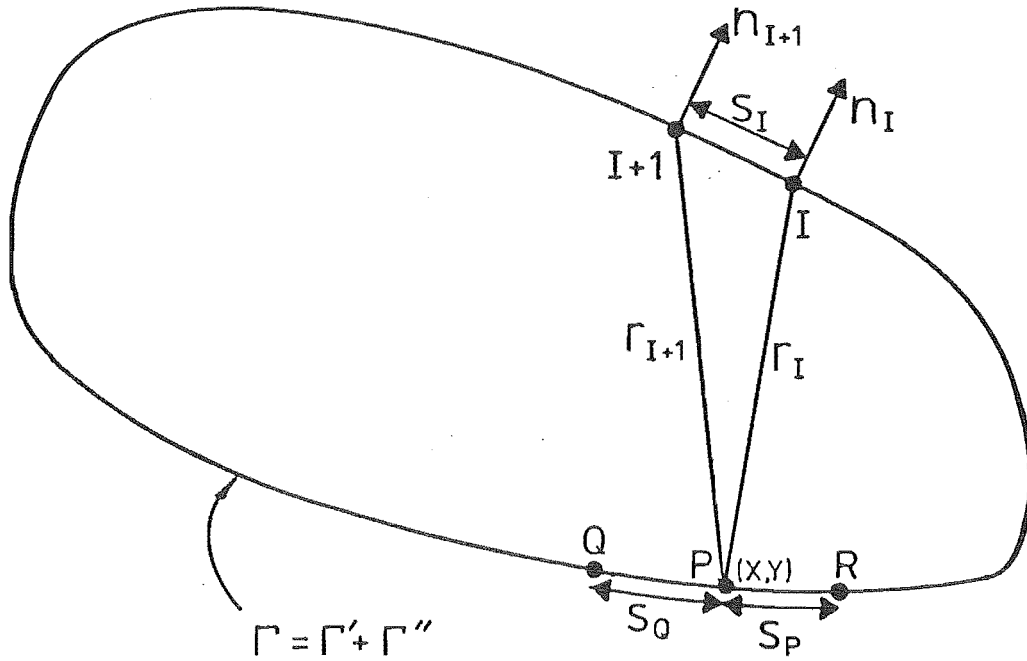


Fig. 5.5 Definition Diagram for Numerical Calculation of Eqn 5.44

$$\begin{aligned}
 & \int_{I}^{I+1} h^k F ds \\
 & \begin{matrix} I \\ I \neq Q \\ I \neq P \end{matrix} \\
 & \approx \left[h^k(I) \frac{\cos(r_I, n_I)}{r_I} \left[e^{\frac{-r_I^2}{4a^2(t_N - t_{k-1})}} - e^{\frac{-r_I^2}{4a^2(t_N - t_k)}} \right] \right. \\
 & \left. + h^k(I+1) \frac{\cos(r_{I+1}, n_{I+1})}{r_{I+1}} \left[e^{\frac{-r_{I+1}^2}{4a^2(t_N - t_{k-1})}} - e^{\frac{-r_{I+1}^2}{4a^2(t_N - t_k)}} \right] \right] \frac{s_I}{2}
 \end{aligned}
 \tag{5.47}$$

in which $h^k(I)$ = value of h at node I at time t_k , n_I = outward pointing normal to $\Gamma' + \Gamma''$ at node I , which is determined herein by fitting a second order polynomial through nodes $I-1$, I and $I+1$ and calculating the outward pointing normal to this curve at node I . For the boundary segment QPR the integral is given by;

$$\begin{aligned}
\int_Q^R h^k F \, ds \approx & \left[h^k(Q) \frac{\cos(r_Q, n_Q)}{r_Q} \left[e^{\frac{-r_Q^2}{4a^2(t_N - t_{k-1})}} - e^{\frac{-r_Q^2}{4a^2(t_N - t_k)}} \right] \right] \frac{S_Q}{2} \\
& + \left[h^k(R) \frac{\cos(r_R, n_R)}{r_R} \left[e^{\frac{-r_R^2}{4a^2(t_N - t_{k-1})}} - e^{\frac{-r_R^2}{4a^2(t_N - t_k)}} \right] \right] \frac{S_P}{2}
\end{aligned}
\tag{5.48}$$

For $k = N$

$$F = \frac{\cos(r, n)}{r} e^{\frac{-r^2}{4a^2 \Delta t_N}} \tag{5.49}$$

$$\text{Thus, as } r \rightarrow 0, F \sim \frac{\cos(r, n)}{r} + O(r). \tag{5.50}$$

As $r \rightarrow 0$, F becomes unbounded. Using the method of "subtracting the singularity" again Eqn 5.44 can be rewritten as;

$$\begin{aligned}
I_N = & \int_{\Gamma' + \Gamma''} \left[h^N \frac{\cos(r, n)}{r} e^{\frac{-r^2}{4a^2 \Delta t_N}} - h^N(P) \frac{\cos(r, n)}{r} \right] ds \\
& + h^N(P) \int_{\Gamma' + \Gamma''} \frac{\cos(r, n)}{r} \, ds
\end{aligned}
\tag{5.51}$$

in which $h^N(P)$ = the value of h at the singular point (x, y) at time t_N , and the integrand in the first integral is zero when $r = 0$. The first integral on the right hand side of Eqn 5.51 can be calculated approximately by the trapezium rule. (See Fig. 5.5).

$$\begin{aligned}
& \int_I^{I+1} \left[h^N \frac{\cos(r,n)}{r} e^{\frac{-r^2}{4a^2\Delta t_N}} - h^N(P) \frac{\cos(r,n)}{r} \right] ds \\
& \begin{matrix} I \neq Q \\ I \neq P \end{matrix} \\
& \approx \left[h^N(I) \frac{\cos(r_I, n_I)}{r_I} e^{\frac{-r_I^2}{4a^2\Delta t_N}} + h^N(I+1) \frac{\cos(r_{I+1}, n_{I+1})}{r_{I+1}} e^{\frac{-r_{I+1}^2}{4a^2\Delta t_N}} \right. \\
& \left. - h^N(P) \left[\frac{\cos(r_I, n_I)}{r_I} + \frac{\cos(r_{I+1}, n_{I+1})}{r_{I+1}} \right] \right] \frac{S_I}{2} \quad (5.52)
\end{aligned}$$

On the boundary segment QPR the corresponding result is;

$$\begin{aligned}
& \int_Q^R \left[h^N \frac{\cos(r,n)}{r} e^{\frac{-r^2}{4a^2\Delta t_N}} - h^N(P) \frac{\cos(r,n)}{r} \right] ds \\
& \approx \left[h^N(Q) \frac{\cos(r_Q, n_Q)}{r_Q} e^{\frac{-r_Q^2}{4a^2\Delta t_N}} \right] \frac{S_Q}{2} + \left[h^N(R) \frac{\cos(r_R, n_R)}{r_R} e^{\frac{-r_R^2}{4a^2\Delta t_N}} \right] \frac{S_P}{2} \\
& - h^N(P) \left[\frac{\cos(r_Q, n_Q)}{r_Q} \frac{S_Q}{2} + \frac{\cos(r_R, n_R)}{r_R} \frac{S_P}{2} \right] \quad (5.53)
\end{aligned}$$

The second integral on the right hand side of Eqn 5.51 can be calculated as follows; (See Fig. 5.6)

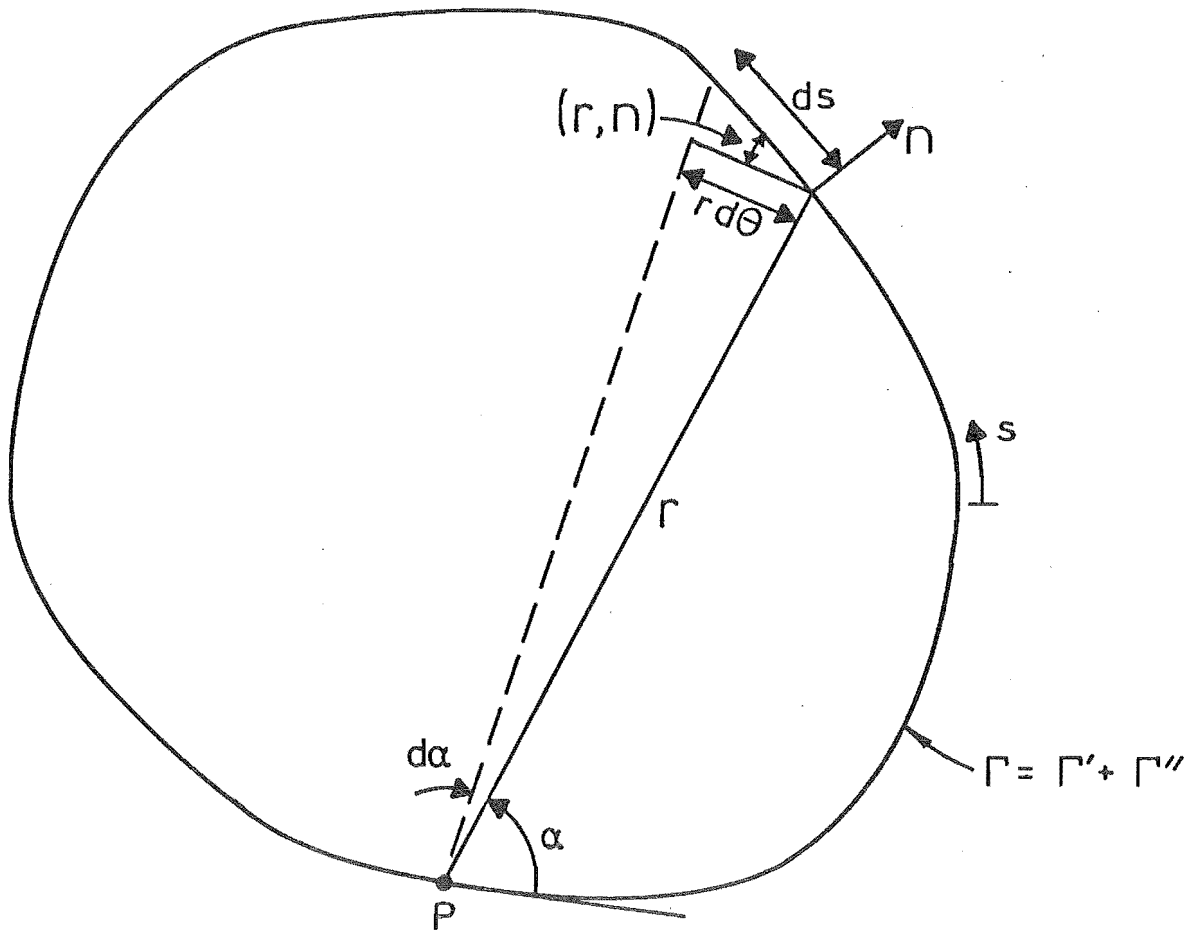


Fig. 5.6 Definition Diagram for Calculating $\int_{\Gamma' + \Gamma''} \frac{\cos(r, n)}{r} ds$

$$\cos(r, n) = r \frac{d\alpha}{ds} \quad (5.54)$$

$$\text{Hence } \frac{\cos(r, n)}{r} ds = d\alpha \quad (5.55)$$

$$\text{And so, } \int_{\Gamma' + \Gamma''} \frac{\cos(r, n)}{r} ds = \int_{\Gamma' + \Gamma''} d\alpha = \theta \quad (5.56)$$

in which θ = the interior angle between the boundary tangents at (x, y) as defined in Fig. 5.2.

Using the results from Eqns 5.30-5.56, Eqn 5.29 can be

expressed in its final form as;

$$\begin{aligned}
 & \int_{\Gamma' + \Gamma''} \left[\frac{\partial h^N}{\partial n} E_1 \left(\frac{r^2}{4a^2 \Delta t_N} \right) + \frac{\partial h^N}{\partial n}(P) \ln \left(\frac{r^2 e^Y}{4a^2 \Delta t_N} \right) \right] ds \\
 & + 2 \int_{\Gamma' + \Gamma''} \left[\frac{h^N \cos(r, n)}{r} e^{\frac{-r^2}{4a^2 \Delta t_N}} - \frac{h^N(P) \cos(r, n)}{r} \right] ds \\
 & - \frac{\partial h^N}{\partial n}(P) \left[2 \int_{\Gamma' + \Gamma''} \ln r \, ds + L \ln \left(\frac{e^Y}{4a^2 \Delta t_N} \right) \right] \\
 & = - \sum_{k=2}^{N-1} \int_{\Gamma' + \Gamma''} \left[\frac{\partial h^k}{\partial n} G + 2h^k F \right] ds \tag{5.57}
 \end{aligned}$$

in which G is as defined in Eqns 5.31 and 5.33

and F is as defined in Eqns 5.45 and 5.46.

The right hand side of Eqn 5.57 contains only known information from previous time steps, while the left hand side contains the unknown values of h and $\frac{\partial h}{\partial n}$ at time $t = t_N$. Eqn 5.57 is applied successively to each boundary node, and this together with the boundary conditions, gives a set of simultaneous equations which can be solved by Gauss Elimination to give the solution for h and $\frac{\partial h}{\partial n}$ at each boundary node. The first integral on the left hand side of Eqn 5.57 is calculated numerically by Eqns 5.38 and 5.39, and the second integral is numerically approximated by Eqns 5.52 and 5.53. The final term on the left hand side of Eqn 5.57 is approximated by Eqns 5.40-5.43, while the integral on the right hand side is calculated by the numerical schemes given in Eqns 5.34, 5.35, 5.47 and 5.48.

Method 2

A second, more accurate way to integrate Eqn 5.24, is to divide the time interval $(0, t)$ into N time steps as before, but to assume that both h and $\frac{\partial h}{\partial n}$ vary linearly with

time throughout each time step. Eqn 5.24 can be rewritten as;

$$\begin{aligned} \frac{\theta}{2\pi} h(x, y, t_N) = & \int_{\Gamma' + \Gamma''} a^2 \sum_{k=2}^N \left[\int_{t_{k-1}}^{t_k} (A_k + B_k \tau) u(r, t_N - \tau) d\tau \right. \\ & \left. - \int_{t_{k-1}}^{t_k} (C_k + D_k \tau) \frac{\partial u(r, t_N - \tau)}{\partial n} d\tau \right] \end{aligned} \quad (5.58)$$

$$\text{in which: } A_k = \left(\frac{\partial h^{k-1}}{\partial n} t_k - \frac{\partial h^k}{\partial n} t_{k-1} \right) / (t_k - t_{k-1})$$

$$B_k = \left(\frac{\partial h^k}{\partial n} - \frac{\partial h^{k-1}}{\partial n} \right) / (t_k - t_{k-1})$$

$$C_k = (h^{k-1} t_k - h^k t_{k-1}) / (t_k - t_{k-1})$$

$$D_k = (h^k - h^{k-1}) / (t_k - t_{k-1}) \quad (5.59)$$

and $u(r, t_N - \tau)$ is as defined in Eqn 5.20.

An integration by parts gives;

$$\begin{aligned} I &= \int_{t_{k-1}}^{t_k} (\alpha + \beta \tau) u(r, t_N - \tau) d\tau \\ &= \left[\frac{-(\alpha + \beta \tau)}{4\pi a^2} E_1 \left(\frac{r^2}{4a^2(t_N - \tau)} \right) \right]_{t_{k-1}}^{t_k} + \frac{\beta}{4\pi a^2} \int_{t_{k-1}}^{t_k} E_1 \left(\frac{r^2}{4a^2(t_N - \tau)} \right) d\tau \end{aligned} \quad (5.60)$$

in which α and β are constants.

$$\text{Thus, } 4\pi a^2 I = (\alpha + \beta t_{k-1}) E_1 \left(\frac{r^2}{4a^2(t_N - t_{k-1})} \right)$$

$$- (\alpha + \beta t_k) E_1 \left(\frac{r^2}{4a^2(t_N - t_k)} \right) + \beta I_1 \quad (5.61)$$

$$\text{in which } I_1 = \int_{t_{k-1}}^{t_k} \left[\int_{\frac{r^2}{4a^2(t_N - \tau)}}^{\infty} \frac{e^{-P}}{P} dP \right] d\tau \quad (5.62)$$

Interchanging the order of integration in Eqn. 5.62 gives;

$$\begin{aligned} I_1 &= \int_{\frac{r^2}{4a^2(t_N - t_k)}}^{\infty} \frac{e^{-P}}{P} \left[\int_{t_{k-1}}^{t_k} d\tau \right] dP \\ &+ \int_{\frac{r^2}{4a^2(t_N - t_{k-1})}}^{\frac{r^2}{4a^2(t_N - t_k)}} \frac{e^{-P}}{P} \left[\int_{t_{k-1}}^{t_N - \frac{r^2}{4a^2 P}} d\tau \right] dP \end{aligned} \quad (5.63)$$

Thus,

$$\begin{aligned} I_1 &= (t_k - t_{k-1}) E_1 \left(\frac{r^2}{4a^2(t_N - t_k)} \right) \\ &+ \int_{\frac{r^2}{4a^2(t_N - t_{k-1})}}^{\frac{r^2}{4a^2(t_N - t_k)}} \frac{e^{-P}}{P} \left[(t_N - t_{k-1}) - \frac{r^2}{4a^2 P} \right] dP \end{aligned} \quad (5.64)$$

$$\therefore I_1 = (t_k - t_{k-1}) E_1 \left(\frac{r^2}{4a^2(t_N - t_k)} \right)$$

$$\begin{aligned}
& + (t_N - t_{k-1}) \left[E_1 \left(\frac{r^2}{4a^2(t_N - t_{k-1})} \right) - E_1 \left(\frac{r^2}{4a^2(t_N - t_k)} \right) \right] \\
& - \frac{r^2}{4a^2} \int_{\frac{r^2}{4a^2(t_N - t_{k-1})}}^{\frac{r^2}{4a^2(t_N - t_k)}} \frac{e^{-P}}{P^2} dP
\end{aligned} \tag{5.65}$$

$$\begin{aligned}
\therefore I_1 &= (t_k - t_N) E_1 \left(\frac{r^2}{4a^2(t_N - t_k)} \right) + (t_N - t_{k-1}) E_1 \left(\frac{r^2}{4a^2(t_N - t_{k-1})} \right) \\
&+ (t_N - t_k) E_2 \left(\frac{r^2}{4a^2(t_N - t_k)} \right) - (t_N - t_{k-1}) E_2 \left(\frac{r^2}{4a^2(t_N - t_{k-1})} \right)
\end{aligned} \tag{5.66}$$

$$\text{in which } E_2(z) \equiv z \int_z^\infty \frac{e^{-P}}{P^2} dP = e^{-z} - z E_1(z) \tag{5.67}$$

$$\begin{aligned}
\text{Thus, } I_1 &= (t_N - t_k) e^{\frac{-r^2}{4a^2(t_N - t_k)}} - (t_N - t_{k-1}) e^{\frac{-r^2}{4a^2(t_N - t_{k-1})}} \\
&+ E_1 \left(\frac{r^2}{4a^2(t_N - t_k)} \right) \left(t_k - t_N - \frac{r^2}{4a^2} \right) \\
&- E_1 \left(\frac{r^2}{4a^2(t_N - t_{k-1})} \right) \left(t_{k-1} - t_N - \frac{r^2}{4a^2} \right)
\end{aligned} \tag{5.68}$$

Hence

$$\begin{aligned}
 4\pi a^2 I = & \beta \left[(t_N - t_k) e^{\frac{-r^2}{4a^2(t_N - t_k)}} - (t_N - t_{k-1}) e^{\frac{-r^2}{4a^2(t_N - t_{k-1})}} \right] \\
 & + \left(\alpha + \beta(t_N + \frac{r^2}{4a^2}) \right) \left[E_1 \left(\frac{r^2}{4a^2(t_N - t_{k-1})} \right) - E_1 \left(\frac{r^2}{4a^2(t_N - t_k)} \right) \right]
 \end{aligned} \quad (5.69)$$

Since the spacial coordinates are independent of time, differentiation of Eqn 5.60 gives;

$$4\pi a^2 \frac{\partial I}{\partial n} = 4\pi a^2 \int_{t_{k-1}}^{t_k} (\alpha + \beta\tau) \frac{\partial u(r, t_N - \tau)}{\partial n} d\tau \quad (5.70)$$

Thus Eqns 5.69 and 5.70 give;

$$\begin{aligned}
 & 4\pi a^2 \int_{t_{k-1}}^{t_k} (\alpha + \beta\tau) \frac{\partial u(r, t_N - \tau)}{\partial n} d\tau \\
 = & (\alpha + \beta t_N) \left[e^{\frac{-r^2}{4a^2(t_N - t_k)}} - e^{\frac{-r^2}{4a^2(t_N - t_{k-1})}} \right] \cdot \frac{2 \cos(r, n)}{r} \\
 & + \frac{\beta r \cos(r, n)}{2a^2} \left[E_1 \left(\frac{r^2}{4a^2(t_N - t_{k-1})} \right) - E_1 \left(\frac{r^2}{4a^2(t_N - t_k)} \right) \right]
 \end{aligned} \quad (5.71)$$

Substituting Eqns 5.69 and 5.71 into the right hand side of Eqn 5.58 gives;

$$\begin{aligned}
& \frac{\theta}{2\pi} h(x, y, t_N) \\
&= \frac{1}{4\pi} \sum_{k=2}^N \int_{\Gamma' + \Gamma''} B_k \left[(t_N - t_k) e^{\frac{-r^2}{4a^2(t_N - t_k)}} - (t_N - t_{k-1}) e^{\frac{-r^2}{4a^2(t_N - t_{k-1})}} \right] \\
&+ \left[A_k + B_k \left(t_N + \frac{r^2}{4a^2} \right) \right] \left[E_1 \left(\frac{r^2}{4a^2(t_N - t_{k-1})} \right) - E_1 \left(\frac{r^2}{4a^2(t_N - t_k)} \right) \right] \\
&- (C_k + D_k t_N) \left[e^{\frac{-r^2}{4a^2(t_N - t_k)}} - e^{\frac{-r^2}{4a^2(t_N - t_{k-1})}} \right] \frac{2 \cos(r, n)}{r} \\
&- \frac{D_k r \cos(r, n)}{2a^2} \left[E_1 \left(\frac{r^2}{4a^2(t_N - t_{k-1})} \right) - E_1 \left(\frac{r^2}{4a^2(t_N - t_k)} \right) \right] ds
\end{aligned} \tag{5.72}$$

in which A_k , B_k , C_k and D_k are as defined in Eqn 5.59, and the integrals are calculated in the sense of a Cauchy principal value. The integrals on the right hand side of Eqn 5.72 must be investigated so that any singularities in the integrand can be treated correctly. The first term can be written in the form;

$$J_k = \int_{\Gamma' + \Gamma''} B_k R_k ds \tag{5.73}$$

in which B_k is as defined in Eqn 5.59 and

$$R_k = (t_N - t_k) e^{\frac{-r^2}{4a^2(t_N - t_k)}} - (t_N - t_{k-1}) e^{\frac{-r^2}{4a^2(t_N - t_{k-1})}} \tag{5.74}$$

$$\text{For } k < N \quad R_k \sim (t_{k-1} - t_k) + O(r^2) \text{ as } r \rightarrow 0 \quad (5.75)$$

$$\begin{aligned} \text{For } k = N \quad R_N &= -(t_N - t_{N-1}) e^{\frac{-r^2}{4a^2(t_N - t_{N-1})}} \\ &\sim -\Delta t_N + O(r^2) \text{ as } r \rightarrow 0 \end{aligned} \quad (5.76)$$

The second integral on the right hand side of Eqn 5.72 can be expressed as;

$$K_k = \int_{\Gamma' + \Gamma''} \left[A_k + B_k \left(t_N + \frac{r^2}{4a^2} \right) \right] T_k \, ds \quad (5.77)$$

in which A_k and B_k are as defined in Eqn 5.59 and

$$T_k = E_1 \left(\frac{r^2}{4a^2(t_N - t_{k-1})} \right) - E_1 \left(\frac{r^2}{4a^2(t_N - t_k)} \right) \quad (5.78)$$

For $k < N$ Because of the behaviour of $E_1(x)$ as $x \rightarrow 0$,

$$T_k \sim \ln \left(\frac{t_N - t_{k-1}}{t_N - t_k} \right) + O(r^2) \text{ as } r \rightarrow 0 \quad (5.79)$$

For $k = N$

$$T_N = E_1 \left(\frac{r^2}{4a^2 \Delta t_N} \right) \sim -\ln \left(\frac{r^2 e^\gamma}{4a^2 \Delta t_N} \right) + O(r^2) \text{ as } r \rightarrow 0 \quad (5.80)$$

Because T_N becomes infinite as r tends to zero, the method of "subtracting the singularity" can be used to rewrite Eqn 5.77 as;

$$K_N = \int_{\Gamma' + \Gamma''} \left[A_N + B_N \left(t_N + \frac{r^2}{4a^2} \right) \right] E_1 \left(\frac{r^2}{4a^2 \Delta t_N} \right)$$

$$\begin{aligned}
& + \left[A_N(p) + B_N(p) t_N \right] \ln \left(\frac{r^2 e^\gamma}{4a^2 \Delta t_N} \right) \bigg] ds \\
& - \left[A_N(p) + B_N(p) t_N \right] \int_{\Gamma' + \Gamma''} \ln \left(\frac{r^2 e^\gamma}{4a^2 \Delta t_N} \right) ds \quad (5.81)
\end{aligned}$$

in which the integrand in the first integral on the right hand side must be set to zero when $r = 0$, and the second integral is calculated according to Eqns 5.40-5.43. The third integral on the right hand side of Eqn 5.72 can be expressed in the form;

$$L_k = \int_{\Gamma' + \Gamma''} (C_k + D_k t_N) U_k ds \quad (5.82)$$

in which C_k and D_k are defined in Eqn 5.59 and

$$U_k = \left[e^{\frac{-r^2}{4a^2(t_N - t_k)}} - e^{\frac{-r^2}{4a^2(t_N - t_{k-1})}} \right] \frac{2 \cos(r, n)}{r} \quad (5.83)$$

For $k < N$

$$U_k \sim \frac{r \cos(r, n)}{2a^2} \frac{(t_k - t_{k-1})}{(t_N - t_k)(t_N - t_{k-1})} + O(r^3) \text{ as } r \rightarrow 0 \quad (5.84)$$

For $k = N$

$$\begin{aligned}
U_N &= \frac{-2 \cos(r, n)}{r} e^{\frac{-r^2}{4a^2 \Delta t_N}} \\
&\sim \frac{-2 \cos(r, n)}{r} + O(r) \text{ as } r \rightarrow 0 \quad (5.85)
\end{aligned}$$

Because U_N becomes infinite as r tends to zero Eqn 5.82 can be written as;

$$\begin{aligned}
L_N = & \int_{\Gamma' + \Gamma''} \left[-2(C_N + D_N t_N) \frac{\cos(r, n)}{r} e^{\frac{-r^2}{4a^2 \Delta t_N}} \right. \\
& + 2(C_N(p) + D_N(p) t_N) \frac{\cos(r, n)}{r} \left. \right] ds \\
& - 2(C_N(p) + D_N(p) t_N) \int_{\Gamma' + \Gamma''} \frac{\cos(r, n)}{r} ds \quad (5.86)
\end{aligned}$$

in which the integrand in the first integral must be set to zero when $r = 0$, and the second integral is calculated according to Eqn 5.56.

The final integral on the right hand side of Eqn 5.72 can be written in the form;

$$M_k = \int_{\Gamma' + \Gamma''} D_k V_k ds \quad (5.87)$$

in which D_k is as defined in Eqn 5.59 and

$$V_k = \frac{r \cos(r, n)}{2a^2} \left[E_1 \left(\frac{r^2}{4a^2(t_N - t_{k-1})} \right) - E_1 \left(\frac{r^2}{4a^2(t_N - t_k)} \right) \right] \quad (5.88)$$

For $k < N$

$$V_k \sim \frac{r \cos(r, n)}{2a^2} \ln \left(\frac{t_N - t_{k-1}}{t_N - t_k} \right) + O(r^2) \text{ as } r \rightarrow 0 \quad (5.89)$$

For $k = N$

$$\begin{aligned}
V_N = & \frac{r \cos(r, n)}{2a^2} E_1 \left(\frac{r^2}{4a^2 \Delta t_N} \right) \sim \frac{r \cos(r, n)}{2a^2} \ln \left(\frac{r^2 e^\gamma}{4a^2 \Delta t_N} \right) + O(r^2) \\
& \text{as } r \rightarrow 0 \quad (5.90)
\end{aligned}$$

Thus $V_N \rightarrow 0$ as $r \rightarrow 0$ (5.91)

The results from Eqns 5.73-5.91, together with the definitions of Eqn 5.59, enable Eqn 5.72 to be written in its final form as;

$$\begin{aligned}
 & \int_{\Gamma' + \Gamma''} \left[\frac{\partial h}{\partial n} G^N + \frac{\partial h^N}{\partial n}(P) G^N(P) + h^N F^N + h^N(P) F^N(P) \right] ds \\
 & - \frac{\partial h^N}{\partial n}(P) \int_{\Gamma' + \Gamma''} \ln \left(\frac{r^2 e^\gamma}{4a^2 \Delta t_N} \right) ds \\
 & = - \int_{\Gamma' + \Gamma''} \left[\frac{\partial h^{N-1}}{\partial n} G^{N-1} + \frac{\partial h^{N-1}}{\partial n}(p) G^{N-1}(p) + h^{N-1} F^{N-1} \right] ds \\
 & - \sum_{k=2}^{N-1} \int_{\Gamma' + \Gamma''} \left[\frac{\partial h^k}{\partial n} G^k + \frac{\partial h^{k-1}}{\partial n} G^{k-1} + \frac{\partial h^k}{\partial n}(p) G^k(p) \right. \\
 & \left. + \frac{\partial h^{k-1}}{\partial n}(p) G^{k-1}(p) + h^k F^k + h^{k-1} F^{k-1} \right] ds \quad (5.92)
 \end{aligned}$$

in which, for $r \neq 0$

$$G^N = E_1 \left(\frac{r^2}{4a^2 \Delta t_N} \right) \left[1 + \frac{r^2}{4a^2 \Delta t_N} \right] - e^{\frac{-r^2}{4a^2 \Delta t_N}}$$

$$G^{N-1} = - E_1 \left(\frac{r^2}{4a^2 \Delta t_N} \right) \left[\frac{r^2}{4a^2 \Delta t_N} \right] + e^{\frac{-r^2}{4a^2 \Delta t_N}}$$

$$G^N(p) = \ln \left(\frac{r^2 e^\gamma}{4a^2 \Delta t_N} \right)$$

$$G^{N-1}(p) = 0$$

$$F^N = \frac{2 \cos(r, n)}{r} e^{\frac{-r^2}{4a^2 \Delta t_N}} - \frac{r \cos(r, n)}{2a^2 \Delta t_N} E_1 \left(\frac{r^2}{4a^2 \Delta t_N} \right)$$

$$F^{N-1} = \frac{r \cos(r, n)}{2a^2 \Delta t_N} E_1 \left[\frac{r^2}{4a^2 \Delta t_N} \right]$$

$$F^N(p) = \frac{-2 \cos(r, n)}{r}$$

$$G^k = \left[E_1 \left[\frac{r^2}{4a^2 (t_N - t_{k-1})} \right] - E_1 \left[\frac{r^2}{4a^2 (t_N - t_k)} \right] \right] \left[\frac{(t_N - t_{k-1} + \frac{r^2}{4a^2})}{(t_k - t_{k-1})} \right] \\ + \frac{(t_N - t_k)}{(t_k - t_{k-1})} e^{\frac{-r^2}{4a^2 (t_N - t_k)}} - \frac{(t_N - t_{k-1})}{(t_k - t_{k-1})} e^{\frac{-r^2}{4a^2 (t_N - t_{k-1})}}$$

$$G^{k-1} = \left[E_1 \left[\frac{r^2}{4a^2 (t_N - t_{k-1})} \right] - E_1 \left[\frac{r^2}{4a^2 (t_N - t_k)} \right] \right] \left[\frac{(t_k - t_N - \frac{r^2}{4a^2})}{(t_k - t_{k-1})} \right] \\ + \frac{(t_N - t_{k-1})}{(t_k - t_{k-1})} e^{\frac{-r^2}{4a^2 (t_N - t_{k-1})}} - \frac{(t_N - t_k)}{(t_k - t_{k-1})} e^{\frac{-r^2}{4a^2 (t_N - t_k)}}$$

$$G^k(p) = 0$$

$$G^{k-1}(p) = 0$$

$$F^k = 2 \frac{(t_N - t_{k-1})}{(t_k - t_{k-1})} \frac{\cos(r, n)}{r} \left[e^{\frac{-r^2}{4a^2 (t_N - t_{k-1})}} - e^{\frac{-r^2}{4a^2 (t_N - t_k)}} \right]$$

$$- \frac{r \cos(r, n)}{2a^2 (t_k - t_{k-1})} \left[E_1 \left[\frac{r^2}{4a^2 (t_N - t_{k-1})} \right] - E_1 \left[\frac{r^2}{4a^2 (t_N - t_k)} \right] \right]$$

$$F^{k-1} = -2 \frac{(t_N - t_k)}{(t_k - t_{k-1})} \frac{\cos(r, n)}{r} \left[e^{\frac{-r^2}{4a^2 (t_N - t_{k-1})}} - e^{\frac{-r^2}{4a^2 (t_N - t_k)}} \right]$$

$$+ \frac{r \cos(r, n)}{2a^2 (t_k - t_{k-1})} \left[E_1 \left[\frac{r^2}{4a^2 (t_N - t_{k-1})} \right] - E_1 \left[\frac{r^2}{4a^2 (t_N - t_k)} \right] \right] \quad (5.93)$$

for $r = 0$

$$G^{N-1}(p) = 1$$

$$G^N(p) = -1$$

$$G^N = G^{N-1} = F^N = F^{N-1} = F^N(p) = 0$$

$$G^{k-1}(p) = \ln \left(\frac{t_N - t_{k-1}}{t_N - t_k} \right) \left(\frac{t_k - t_N}{t_k - t_{k-1}} \right) + 1$$

$$G^k(p) = \ln \left(\frac{t_N - t_{k-1}}{t_N - t_k} \right) \left(\frac{t_N - t_{k-1}}{t_k - t_{k-1}} \right) - 1$$

$$G^k = G^{k-1} = F^k = F^{k-1} = 0 \quad (5.94)$$

The second integral on the left hand side of Eqn 5.92 is calculated according to Eqns 5.40-5.43.

By applying Eqn 5.92 to each node successively and using a quadrature formula such as the trapezium rule, a set of simultaneous equations is obtained which can be solved (subject to the given boundary conditions) for h and $\frac{\partial h}{\partial n}$ at each node.

5.4 INCLUSION OF WELLS IN A HOMOGENEOUS REGION

For a homogeneous region that contains a well at the point (x_0, y_0) , Eqns 5.3-5.6 can be rewritten as;

$$a^2 \nabla_{x,y}^2 h = \frac{\partial h}{\partial t} + \frac{Q}{S} \delta(x-x_0) \delta(y-y_0),$$

$$(a^2 \equiv \frac{T}{S} = \text{constant}, x, y \text{ in } R) \quad (5.95)$$

$$h = 0 \text{ at } t = 0 \quad (5.96)$$

$$h = f \text{ for } x, y \text{ on } \Gamma' \in \Gamma \quad (5.97)$$

$$\frac{\partial h}{\partial n} = g \text{ for } x, y \text{ on } \Gamma'' \in \Gamma \quad (5.98)$$

Eqns 5.95-5.98 can be solved by using a method similar to that used in Sec. 5.2. If (x,y,t) is replaced with (ξ,η,τ) in $h(x,y,t)$ and $u(x-\xi,y-\eta,t-\tau)$ is a fundamental solution with properties that will be defined later, then

$$a^2 u \nabla_{\xi,\eta}^2 h - u \frac{\partial h}{\partial \tau} - \frac{Q}{S} \delta(\xi-x_0) \delta(\eta-y_0) u = 0 \quad (5.99)$$

$$\text{But } u \nabla^2 h = \bar{\nabla} \cdot (u \bar{\nabla} h) - \bar{\nabla} \cdot (h \bar{\nabla} u) + h \nabla^2 u \quad (5.100)$$

$$\text{and } u \frac{\partial h}{\partial \tau} = \frac{\partial}{\partial \tau} (uh) - h \frac{\partial u}{\partial \tau} \quad (5.101)$$

Substituting Eqns 5.100 and 5.101 into Eqn 5.99 gives;

$$\begin{aligned} a^2 \left[\bar{\nabla} \cdot (u \bar{\nabla} h) - \bar{\nabla} \cdot (h \bar{\nabla} u) + h \nabla^2 u \right] - \frac{\partial (uh)}{\partial \tau} + h \frac{\partial u}{\partial \tau} \\ - \frac{Q}{S} \delta(\xi-x_0) \delta(\eta-y_0) u = 0 \end{aligned} \quad (5.102)$$

If Eqn 5.102 is integrated over the region R and from $\tau = 0$ to $\tau = t$ and the divergence theorem is used;

$$\begin{aligned} \int_0^t \int_{\Gamma' + \Gamma''} a^2 \left(u \frac{\partial h}{\partial n} - h \frac{\partial u}{\partial n} \right) ds d\tau + \int_0^t \int_R h \left(a^2 \nabla_{\xi,\eta}^2 u + \frac{\partial u}{\partial \tau} \right) d\xi d\eta d\tau \\ - \int_R (uh)_{\tau=t} d\xi d\eta - \int_0^t \int_R \frac{Q}{S} \delta(\xi-x_0) \delta(\eta-y_0) u d\xi d\eta d\tau = 0 \end{aligned} \quad (5.103)$$

Now define $u(x,y,t)$ so that it satisfies the following set of equations;

$$a^2 \nabla_{x,y}^2 u = \frac{\partial u}{\partial t} \quad \text{for } x,y \text{ in } R \quad (5.104)$$

$$u(x,y,0) = \delta(x) \delta(y) \quad (5.105)$$

The solution for $u(x-\xi,y-\eta,t-\tau)$ is given by

$$u(x-\xi, y-\eta, t-\tau) = u(r, t-\tau) = \frac{1}{4\pi a^2(t-\tau)} e^{\frac{-r^2}{4a^2(t-\tau)}} \quad (5.106)$$

(See Eqns 5.18-5.20).

Thus,

$$\begin{aligned} & \int_0^t \int_{\Gamma' + \Gamma''} a^2 \left(u \frac{\partial h}{\partial n} - h \frac{\partial u}{\partial n} \right) ds d\tau - h(x, y, t) \\ & - \int_0^t \frac{Q}{S} u(x-x_0, y-y_0, t-\tau) d\tau = 0 \end{aligned} \quad (5.107)$$

and so,

$$\begin{aligned} h(x, y, t) &= \int_0^t \int_{\Gamma' + \Gamma''} a^2 \left(u \frac{\partial h}{\partial n} - h \frac{\partial u}{\partial n} \right) ds d\tau \\ &- \int_0^t \frac{Q}{S} u(x-x_0, y-y_0, t-\tau) d\tau \end{aligned} \quad (5.108)$$

If $Q = 0$ for $t < 0$ and constant for $t > 0$ then,

$$\begin{aligned} \int_0^t Qu(x-x_0, y-y_0, t-\tau) d\tau &= \frac{Q}{4\pi T} \int_0^t \frac{1}{(t-\tau)} e^{\frac{-r^2}{4a^2(t-\tau)}} d\tau \\ &= \frac{Q}{4\pi T} E_1 \left(\frac{r^2}{4a^2 t} \right) \end{aligned} \quad (5.109)$$

Thus the final result is:

$$\begin{aligned} h(x, y, t) &= \int_0^t \int_{\Gamma' + \Gamma''} a^2 \left(u \frac{\partial h}{\partial n} - h \frac{\partial u}{\partial n} \right) ds d\tau - \frac{Q}{4\pi T} E_1 \left(\frac{r^2}{4a^2 t} \right) \\ &\text{for } x, y \text{ in } R \end{aligned} \quad (5.110)$$

and,

$$\frac{\theta h(x,y,t)}{2\pi} = \int_0^t \int_{\Gamma'+\Gamma''} a^2 \left(u \frac{\partial h}{\partial n} - h \frac{\partial u}{\partial n} \right) ds d\tau - \frac{Q}{4\pi T} E_1 \left(\frac{r^2}{4a^2 t} \right) \quad \text{for } x,y \text{ on } \Gamma'+\Gamma'' \quad (5.111)$$

in which θ is defined in Fig. 5.2. The integrals on the right sides of Eqns 5.110 and 5.111 are calculated numerically by using either of the methods given in Sec. 5.3.

5.5 CALCULATION OF h AT INTERNAL POINTS

The solution for h at any point (x,y) contained in the region R at time $t = t_N$ is given by Eqn 5.110. Once h and $\frac{\partial h}{\partial n}$ have been determined at all boundary nodes by the methods given in Sec. 5.3, h at any internal point can be calculated directly by numerically integrating the right hand side of Eqn 5.110. The integration is greatly simplified because there are no singularities in the integrand. For the purposes of this study h and $\frac{\partial h}{\partial n}$ will be assumed to vary linearly between successive time steps. Thus,

$$h(x,y,t_N) =$$

$$\begin{aligned} & \frac{1}{4\pi} \sum_{k=2}^N \int_{\Gamma'+\Gamma''} \frac{\partial h}{\partial n}^k \left(\frac{(t_N - t_k)}{(t_k - t_{k-1})} e^{\frac{-r^2}{4a^2(t_N - t_k)}} - \frac{(t_N - t_{k-1})}{(t_k - t_{k-1})} e^{\frac{-r^2}{4a^2(t_N - t_{k-1})}} \right. \\ & + \left. \left[\frac{(t_N - t_{k-1} + \frac{r^2}{4a^2})}{(t_k - t_{k-1})} \right] \left[E_1 \left(\frac{r^2}{4a^2(t_N - t_{k-1})} \right) - E_1 \left(\frac{r^2}{4a^2(t_N - t_k)} \right) \right] \right) \\ & + \frac{\partial h}{\partial n}^{k-1} \left(\frac{(t_N - t_{k-1})}{(t_k - t_{k-1})} e^{\frac{-r^2}{4a^2(t_N - t_{k-1})}} - \frac{(t_N - t_k)}{(t_k - t_{k-1})} e^{\frac{-r^2}{4a^2(t_N - t_k)}} \right. \\ & - \left. \left[\frac{(t_N - t_k + \frac{r^2}{4a^2})}{(t_k - t_{k-1})} \right] \left[E_1 \left(\frac{r^2}{4a^2(t_N - t_{k-1})} \right) - E_1 \left(\frac{r^2}{4a^2(t_N - t_k)} \right) \right] \right) \end{aligned}$$

$$\begin{aligned}
& + h^k \left[2 \frac{(t_N - t_{k-1})}{(t_k - t_{k-1})} \frac{\cos(r, n)}{r} \left[e^{\frac{-r^2}{4a^2(t_N - t_{k-1})}} - e^{\frac{-r^2}{4a^2(t_N - t_k)}} \right] \right. \\
& - \frac{r \cos(r, n)}{2a^2(t_k - t_{k-1})} \left[E_1 \left(\frac{r^2}{4a^2(t_N - t_{k-1})} \right) - E_1 \left(\frac{r^2}{4a^2(t_N - t_k)} \right) \right] \Bigg] \\
& + h^{k-1} \left[-2 \frac{(t_N - t_k)}{(t_k - t_{k-1})} \frac{\cos(r, n)}{r} \left[e^{\frac{-r^2}{4a^2(t_N - t_{k-1})}} - e^{\frac{-r^2}{4a^2(t_N - t_k)}} \right] \right. \\
& + \frac{r \cos(r, n)}{2a^2(t_k - t_{k-1})} \left[E_1 \left(\frac{r^2}{4a^2(t_N - t_{k-1})} \right) - E_1 \left(\frac{r^2}{4a^2(t_N - t_k)} \right) \right] \Bigg] ds \\
& - \frac{Q}{4\pi T} E_1 \left(\frac{r^2}{4a^2 t_N} \right)
\end{aligned} \tag{5.112}$$

in which the contour integral is evaluated by a quadrature formula such as the trapezium rule.

5.6 COMPOSITE REGIONS

The region of analysis, R , may consist of a number of zones such that T and S are constant within each zone but vary from one zone to the next. A typical type of problem is shown in Fig. 5.7.

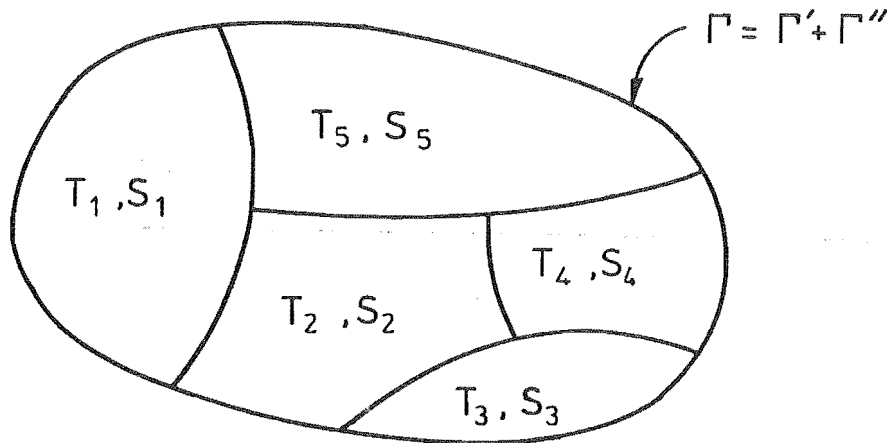


Fig. 5.7 Typical Composite Region

point are antiparallel.

The flow of groundwater within any one zone can be analysed by the methods given in the preceding sections, while the compatibility conditions of Eqns 5.113 and 5.114 are required for the overall solution.

The boundary of each zone is approximated by a finite number of nodes, which should be closely spaced where h and $\frac{\partial h}{\partial n}$ change rapidly and more sparsely spaced where h and $\frac{\partial h}{\partial n}$ vary slowly. The nodes will be numbered consecutively as the boundary is traversed in an anticlockwise direction. Thus, the region shown in Fig. 5.7 can be approximated as depicted in Fig. 5.8.

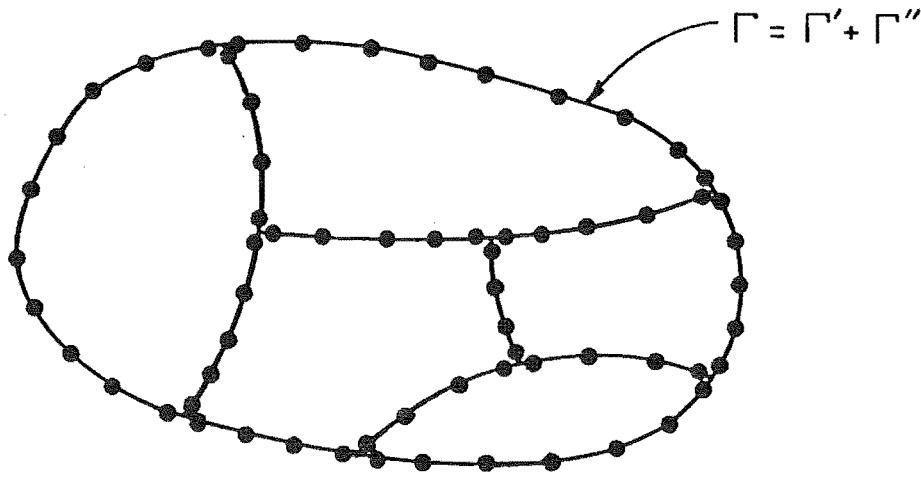


Fig. 5.8 Typical Nodal Arrangement for Composite Region

The boundary conditions on the external contour Γ are the same as those given in Eqns 5.9 and 5.10, which state that either h or $\frac{\partial h}{\partial n}$ at any point are prescribed functions of time. At a point on the boundary between zones i and j , h must have the same value and continuity of flow must be preserved. Thus;

$$h_i = h_j \quad (5.113)$$

$$\text{and} \quad T_i \left(\frac{\partial h}{\partial n} \right)_i = -T_j \left(\frac{\partial h}{\partial n} \right)_j \quad (5.114)$$

The negative sign appears on the right hand side of Eqn 5.114 because the outward pointing normals to zones i and j at any

Chapter 6

COMPARISONS BETWEEN THE NUMERICAL TECHNIQUES OF CHAPTER 56.1 INTRODUCTION

The techniques developed in Chapter 5 will be used to solve a variety of mixed boundary-value problems using the Fortran computer programs listed in Appendix B. The results will be compared with known analytical solutions and in selected cases comparisons with the finite-difference method will also be made.

Results can be expressed most simply by introducing the following dimensionless variables;

$$\begin{aligned} h' &= \frac{h}{L} \\ x' &= \frac{x}{L} \\ y' &= \frac{y}{L} \\ t' &= \frac{tT_1}{L^2 S_1} \\ Q' &= \frac{Q}{T_1 L} \end{aligned} \tag{6.1}$$

in which L is a characteristic length in the problem. The subscripts denote the values of T and S in zone 1 of a composite region, but can be ignored if the region is homogeneous.

Although solutions will be obtained for a number of boundary contour shapes, two of the most commonly used will be the square and the quarter circle because analytical solutions for flows in these regions are readily calculated. The nodal arrangements selected for these two shapes are shown in Figs. 6.1 and 6.2, respectively. Because the boundary conditions on either side of a sharp corner may be different and because there is a discontinuity in geometry

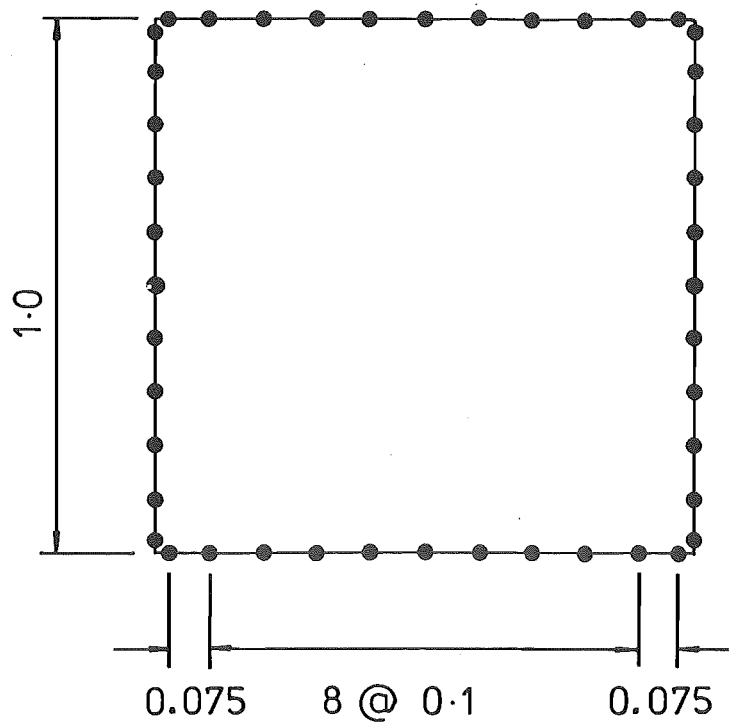


Fig. 6.1 Nodal Arrangement for Square Region

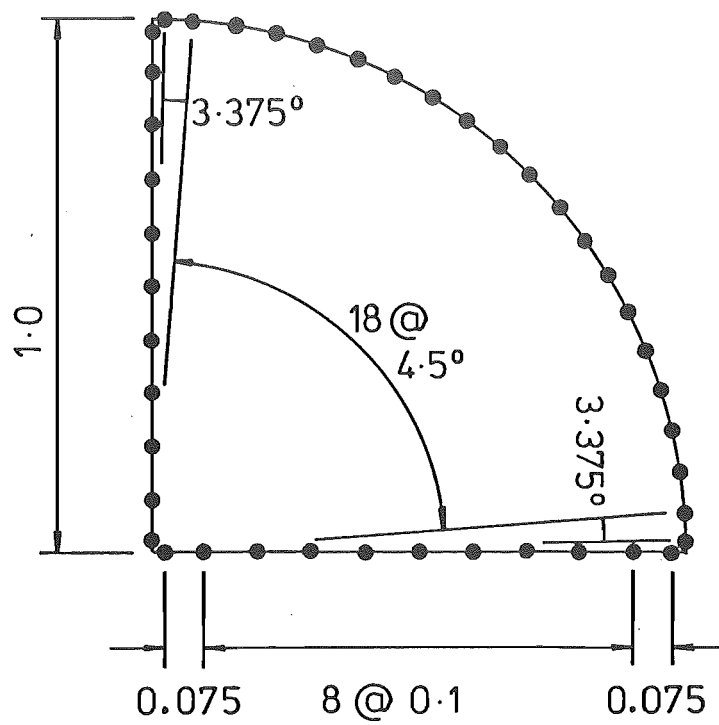


Fig. 6.2 Nodal Arrangement for Quarter Circle

there, nodes are placed adjacent to, rather than exactly at the corners, as shown in Figs 6.1 and 6.2. Experience has shown that the distance between a sharp corner and the adjacent nodes should be approximately one quarter of the usual nodal spacing. The contribution that these "corner nodes" make to the numerical integrals is calculated by assuming that values of h and $\frac{\partial h}{\partial n}$ on the boundary contour between such a node and the sharp corner are constant and equal to the values at the node.

6.2 FLOWS IN HOMOGENEOUS REGIONS THAT CONTAIN NO WELLS

Suppose that three sides of the square region shown in Fig. 6.3 are impermeable and that $h'=0$ everywhere within the region at $t'=0$, Carslaw and Jaeger (1959) give the exact solution as;

$$h'(x', t') = 1 - 2 \sum_{n=0}^{\infty} \frac{(-1)^n e^{-\alpha_n^2 t'}}{\alpha_n} \cos \alpha_n x' \quad (6.2)$$

$$\text{and } \frac{\partial h'}{\partial n}(x'=1.0, t') = 2 \sum_{n=0}^{\infty} e^{-\alpha_n^2 t'} \quad (6.3)$$

in which $\alpha_n = (2n+1)\frac{\pi}{2}$. Numerically calculated values of h' , both on the boundary contour and at selected points within the flow region itself, are compared with Eqn 6.2 in Figs 6.3 and 6.4, respectively. The 15 values of t' used in the these numerical calculations have been labelled TS1 and are listed in Table 6.1. The comparison between the numerical and analytical values of $\frac{\partial h'}{\partial n}$ at $x'=1.0$ is shown in Fig. 6.5. (Due to its magnitude, the value of $\frac{\partial h'}{\partial n}$ calculated at $x'=1.0$ at the end of the first time step using Method 2 has been omitted from Fig. 6.5. The omitted value is $\frac{\partial h'}{\partial n}(t'=0.001) = 42.5467$.)

Because $\frac{\partial h'}{\partial n}$ at $x'=1.0$ is infinite at $t'=0$ (Eqn 6.3), there are inherent problems in using Method 2 of Chapter 5, in which h' and $\frac{\partial h'}{\partial n}$ are assumed to vary linearly with time over each time step. When calculating values of h' and $\frac{\partial h'}{\partial n}$ at the end of the first time step, values of h' and $\frac{\partial h'}{\partial n}$ at $t'=0$ are required, as described by Eqn 5.92.

time step number	t'			
	TS1	TS2	TS3	TS4
1	0	0	0	0
2	0.001	0.05	0.1	0.0005
3	0.005	0.1	0.2	0.001
4	0.01	0.2	0.3	0.005
5	0.02	0.3	0.5	0.01
6	0.05	0.4	0.7	0.02
7	0.1	0.5	0.8	0.03
8	0.2	0.6	0.9	0.05
9	0.3	0.7	1.0	0.075
10	0.4	0.8	1.1	0.1
11	0.5	1.0	1.2	0.15
12	0.6	1.5	1.3	0.2
13	0.7	2.0	1.5	0.3
14	0.8	3.0	1.7	0.4
15	1.0	4.0	1.8	0.5
16		5.0	1.9	0.6
17			2.0	

Table 6.1 Incremental time schemes used in the numerical calculations.

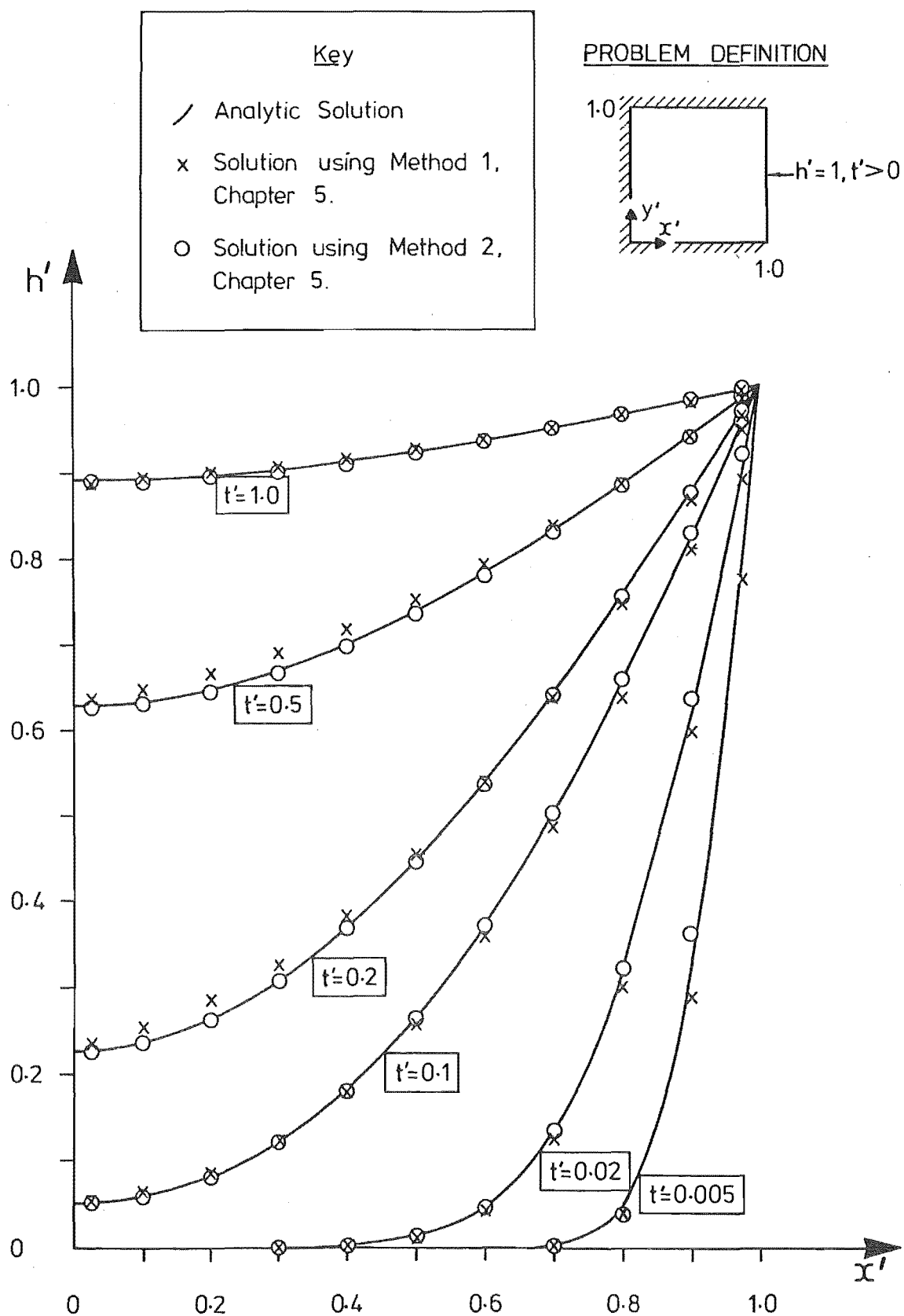


Fig. 6.3 Distribution of h' on $y'=0$ following instantaneous unit rise in h' at $x'=1.0$.

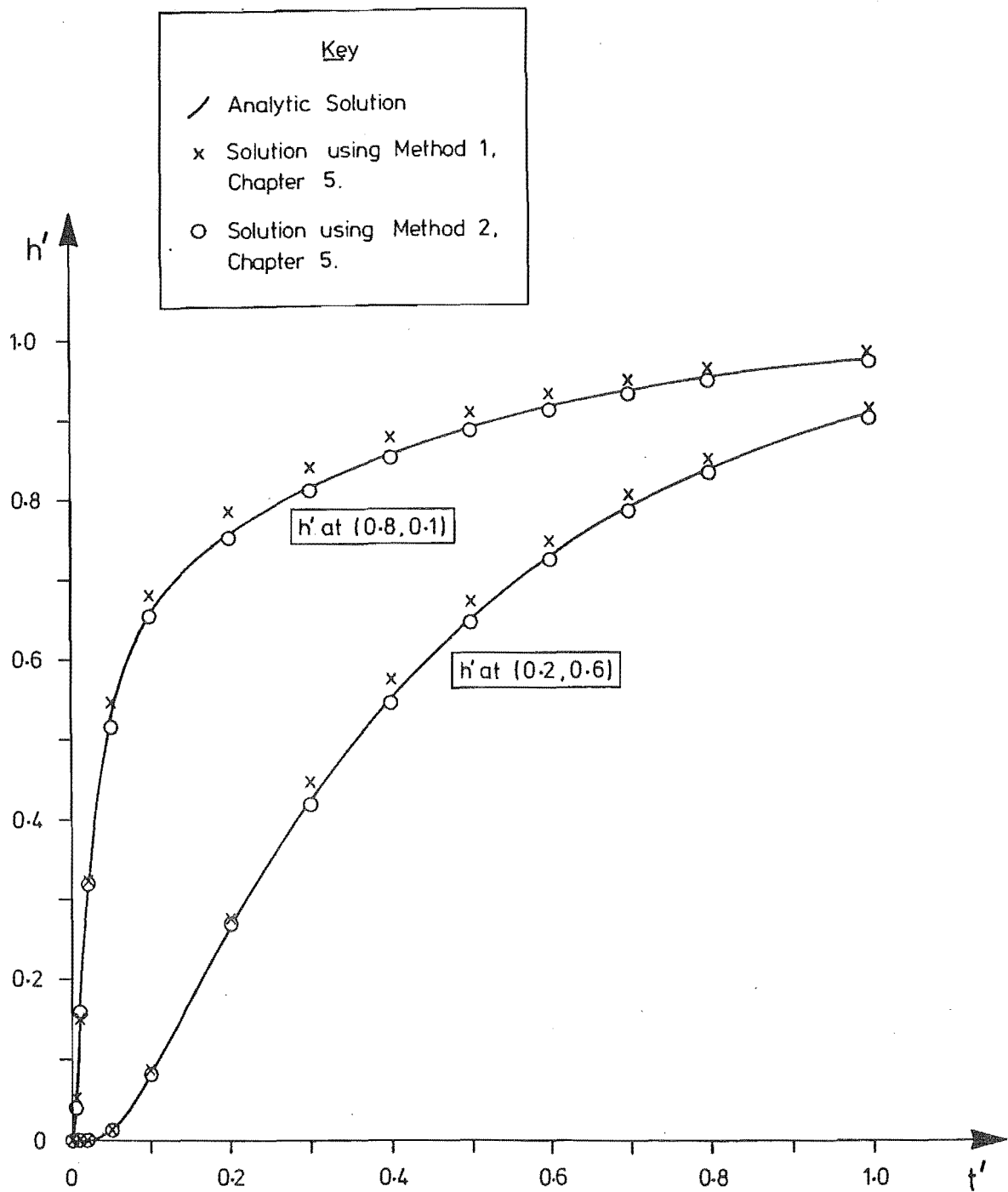


Fig. 6.4 Variation of h' with time at two internal points for the problem shown in Fig. 6.3.

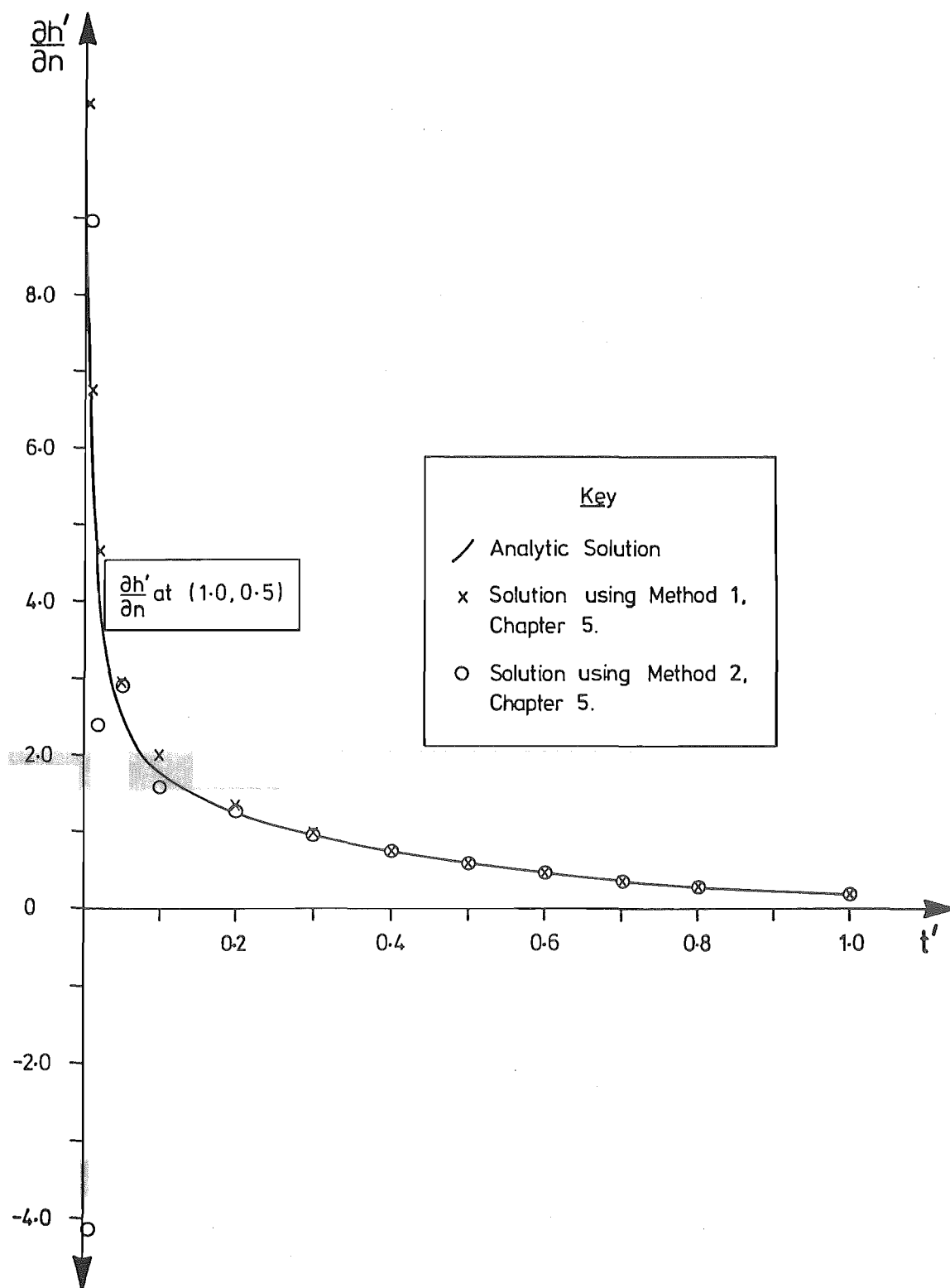


Fig. 6.5 Variation of $\frac{\partial h'}{\partial n}$ with time at (1.0, 0.5) for the problem shown in Fig. 6.3.

The text following '*' should read as follows;

and, thus,
increasing the number of time steps, the computational cost
rises rapidly. It should be noted that the computational time
required by Method 1 is approximately eighty percent of that
required by Method 2 when the same time steps are used for
both sets of calculations.

Consequently, the large instability in $\frac{\partial h'}{\partial n}$ at $x'=1.0$ (Fig. 6.5), and the minor instability in h' , that occur near $x'=1.0$ (Fig. 6.3), are to be expected initially. However an excellent feature of this method is that despite the initial instability, the numerical solution closely approximates the analytical solution after only a few time steps. Also, numerically calculated values of h' within the flow region are in good agreement with Eqn 6.2, even at the end of the first time step.

The problem associated with the infinite value of $\frac{\partial h'}{\partial n}$ at $t'=0$ does not arise with Method 1 of Chapter 5 because values of h' and $\frac{\partial h'}{\partial n}$ at $t'=0$ are not required for the solution at the end of the first time step, as stated in Eqn 5.57. However, because Method 1 assumes that h' and $\frac{\partial h'}{\partial n}$ are constant throughout each time step, time steps must be closely spaced to ensure accurate results. Immediately following the instantaneous rise in h' time steps are closely spaced, but as time proceeds and the step length increases, there is a loss in accuracy. Although the results can be improved by decreasing the time step length*, the computational cost becomes prohibitive. It should be noted that the computational time required by Method 1 is approximately eighty percent of that required by Method 2.

The instability that occurs with Method 2 following instantaneous changes in h' is not really considered a problem for groundwater flows because changes in h' are never instantaneous in real situations. If the instantaneous rise at $x'=1.0$ is replaced with;

$$h'(x'=1.0, t') = 1 - e^{-\epsilon t'}, \quad t' > 0 \quad (6.4)$$

in which ϵ is a positive constant, very rapid changes can be modelled by choosing a sufficiently large value of ϵ . More gradual changes in h' are modelled by substituting a smaller value of ϵ in the right side of Eqn 6.4. The exact solution to this problem, calculated from Eqn 6.2 using the Duhamel superposition integral, (Hildebrand 1976) is;

$$h'(x', t') = 1 - e^{-\epsilon t'} - 2\epsilon \sum_{n=0}^{\infty} \frac{(-1)^n \cos \alpha_n x'}{\alpha_n (\alpha_n^2 - \epsilon)} \left[e^{-\epsilon t'} - e^{-\alpha_n^2 t'} \right] \quad (6.5)$$

$$\text{and, } \frac{\partial h'}{\partial n}(x'=1.0, t') = 2\epsilon \sum_{n=0}^{\infty} \frac{e^{-\epsilon t'} - e^{-\alpha_n^2 t'}}{\alpha_n^2 - \epsilon} \quad (6.6)$$

in which $\alpha_n = (2n+1)\frac{\pi}{2}$. The right side of Eqn 6.6 is equal to zero at $t'=0$ for all values of ϵ except for $\epsilon=\alpha_n^2$. Consequently there is no discontinuity in $\frac{\partial h'}{\partial n}$ and the problems experienced with Method 2 at $t'=0$ are eliminated. An instantaneous rise in h' at $x'=1.0$ is closely approximated by substituting a value of $\epsilon=500$ in the right side of Eqn 6.4. The numerical and analytical values of h' on the boundary contour are compared for this case in Fig. 6.6, while the solutions at points within the flow region are shown in Fig. 6.7. The solutions for $\frac{\partial h'}{\partial n}$ at $x'=1.0$ are compared in Fig. 6.8. There is now excellent agreement between the analytical solutions and those obtained using Method 2, and there is no evidence of any numerical instability. There is virtually no difference between the solutions obtained using Method 1 for an instantaneous rise in h' and for $h'(x'=1.0) = 1 - e^{-500t'}$. This is to be expected because the two analytical solutions are almost identical except for different values of $\frac{\partial h'}{\partial n}$ at $x'=1.0$ at $t'=0$, which do not appear in the numerical calculations. The accuracy is limited by the length of the time step as outlined previously.

More gradual changes in h' at $x'=1.0$ can be modelled by substituting a value of $\epsilon=1$ in the right side of Eqn 6.4. Because h' varies more slowly than in the previous examples, larger time steps were chosen and are labelled TS2 in Table 6.1. Solutions for h' around the boundary contour and at selected points within the flow region are shown in Figs 6.9 and 6.10, respectively, and solutions for $\frac{\partial h'}{\partial n}$ at $x'=1.0$ in Fig. 6.11. The solutions obtained using Method 2 are in

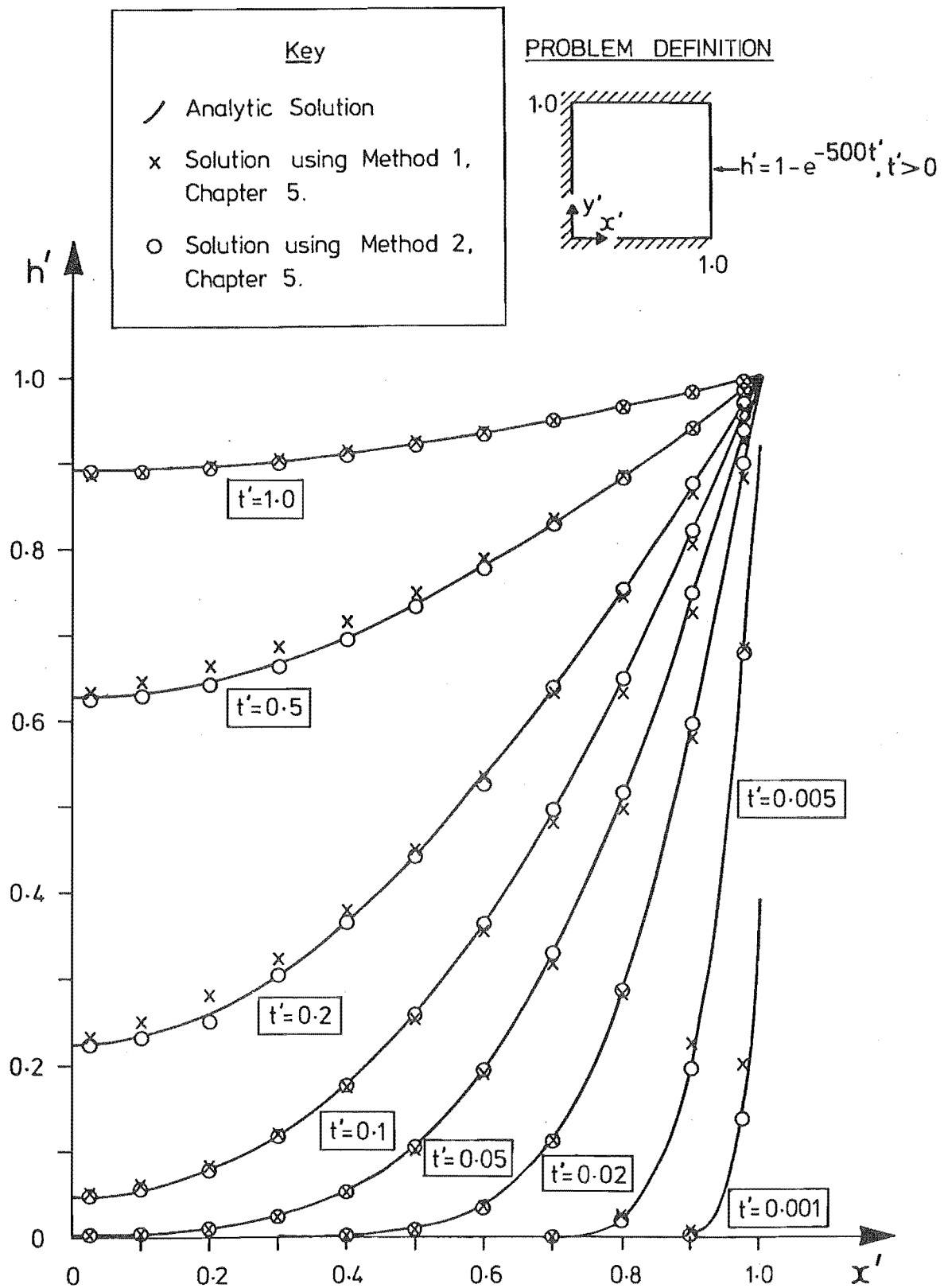


Fig. 6.6 Distribution of h' on $y'=0$ when $h'(x'=1.0, t') = 1 - e^{-500t'}$, $t' > 0$.

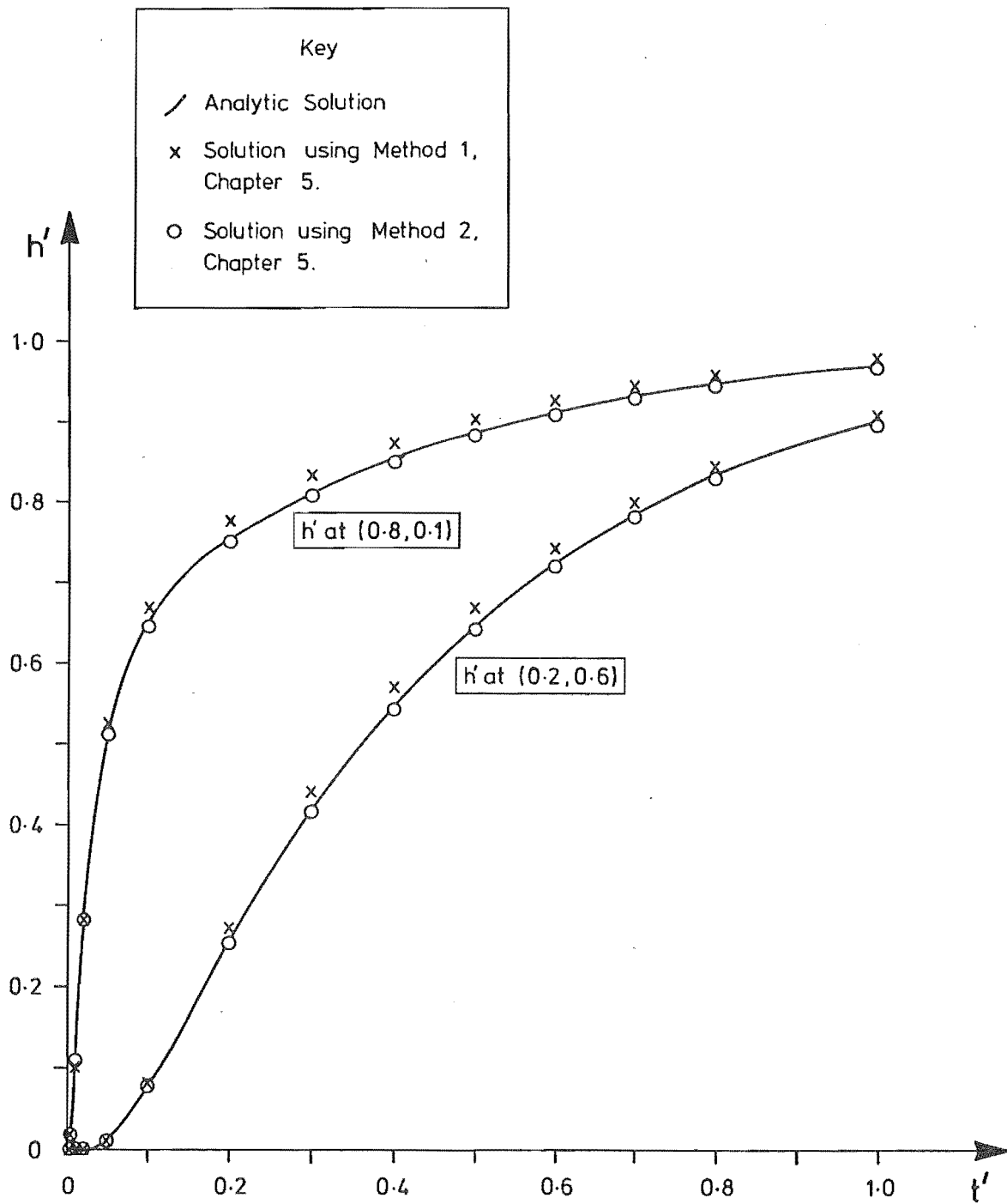


Fig. 6.7 Variation of h' with time at two internal points for the problem shown in Fig. 6.6.

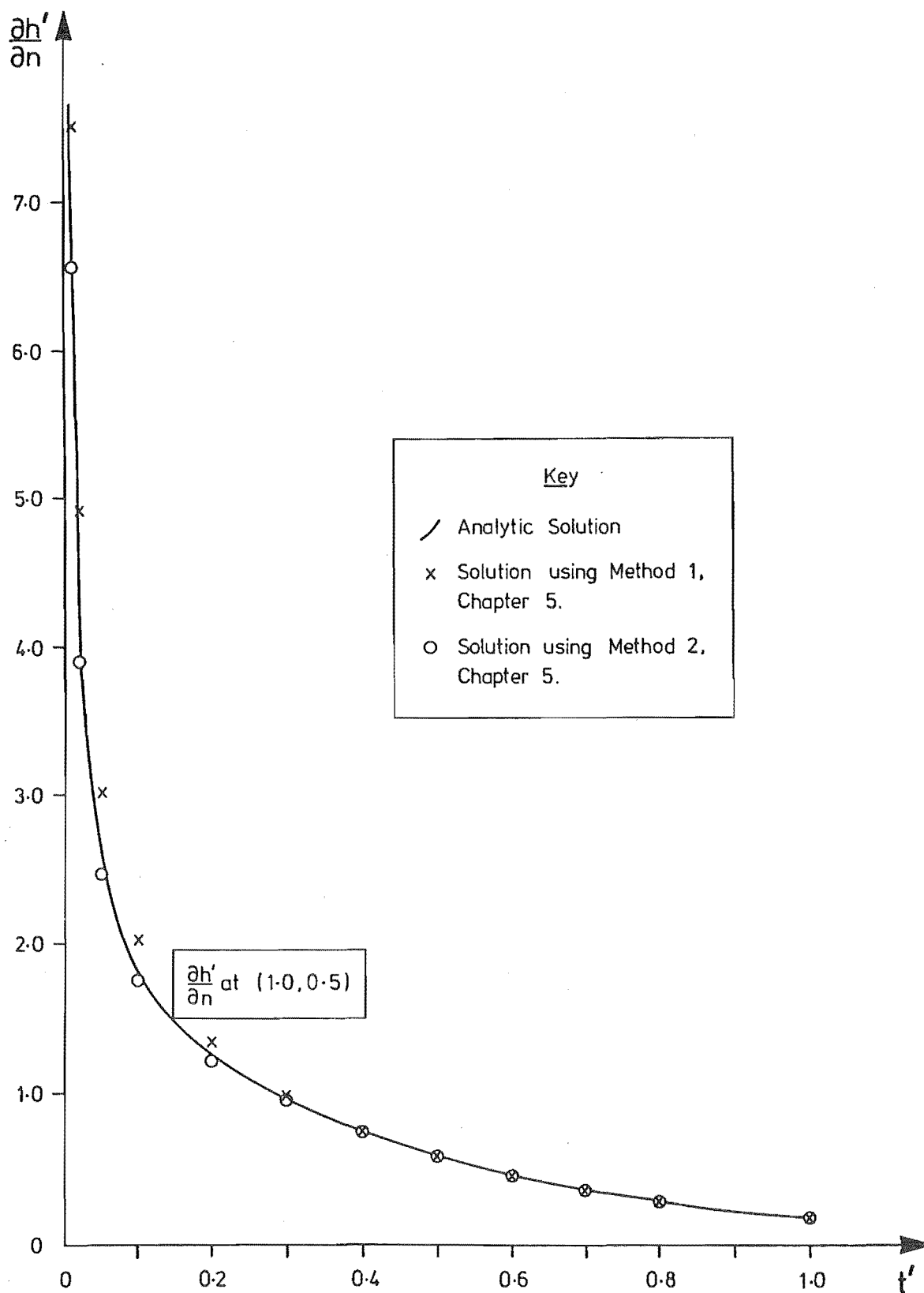


Fig. 6.8 Variation of $\frac{\partial h'}{\partial n}$ with time at (1.0, 0.5) for the problem shown in Fig. 6.6.

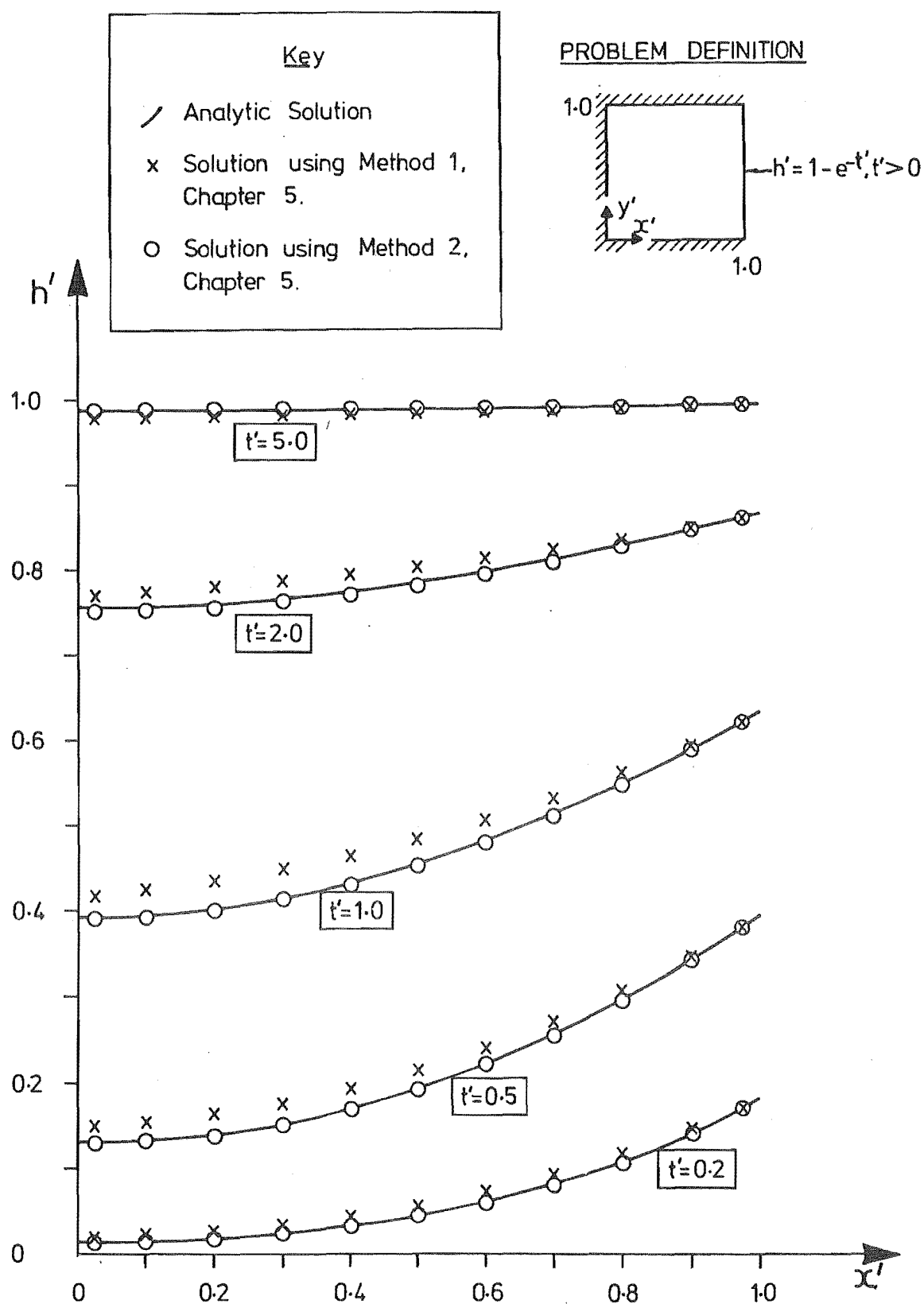


Fig. 6.9 Distribution of h' on $y'=0$ when $h'(x'=1.0, t') = 1 - e^{-t'}$, $t' > 0$.

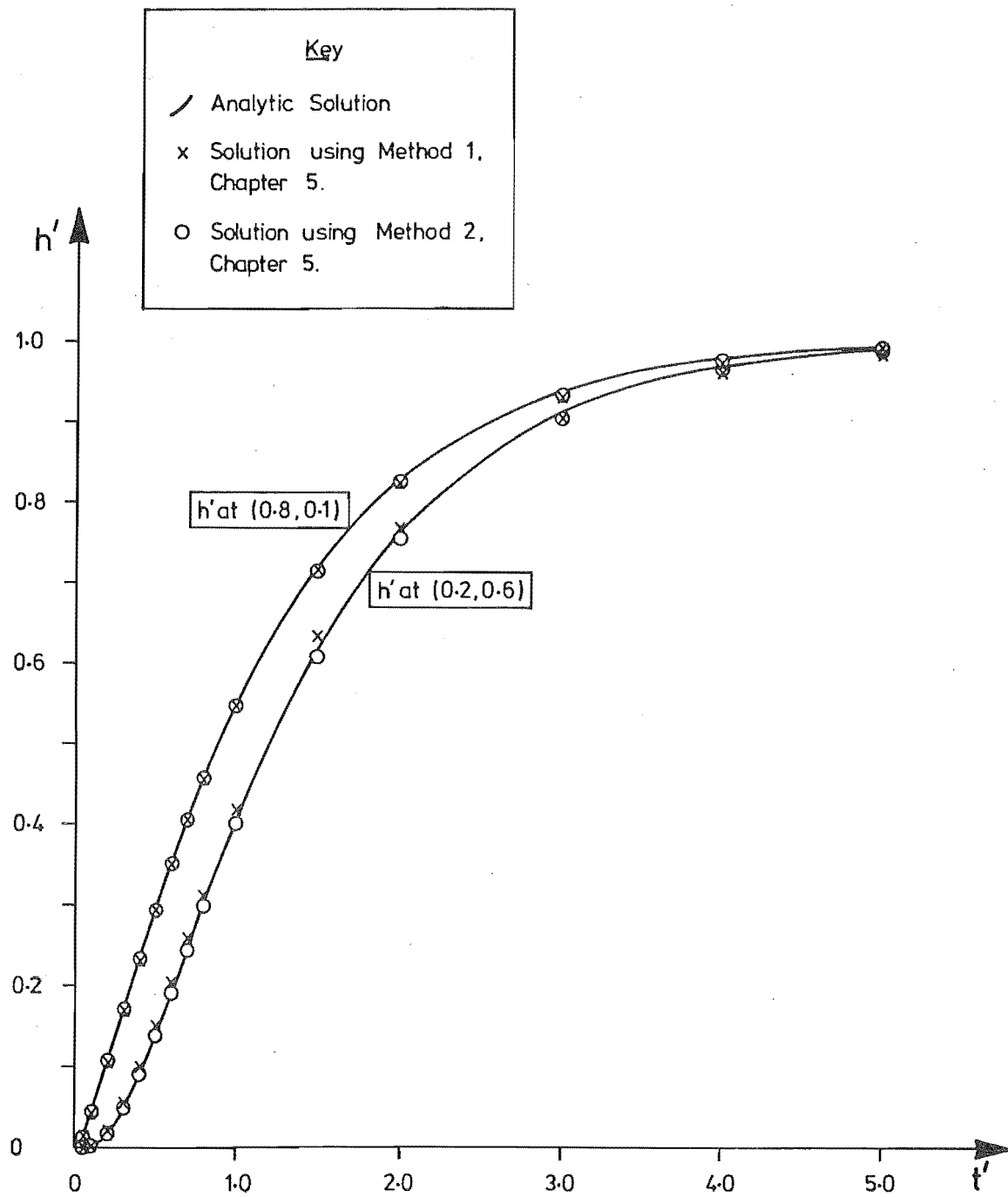


Fig. 6.10 Variation of h' with time at two internal points for the problem shown in Fig. 6.9.

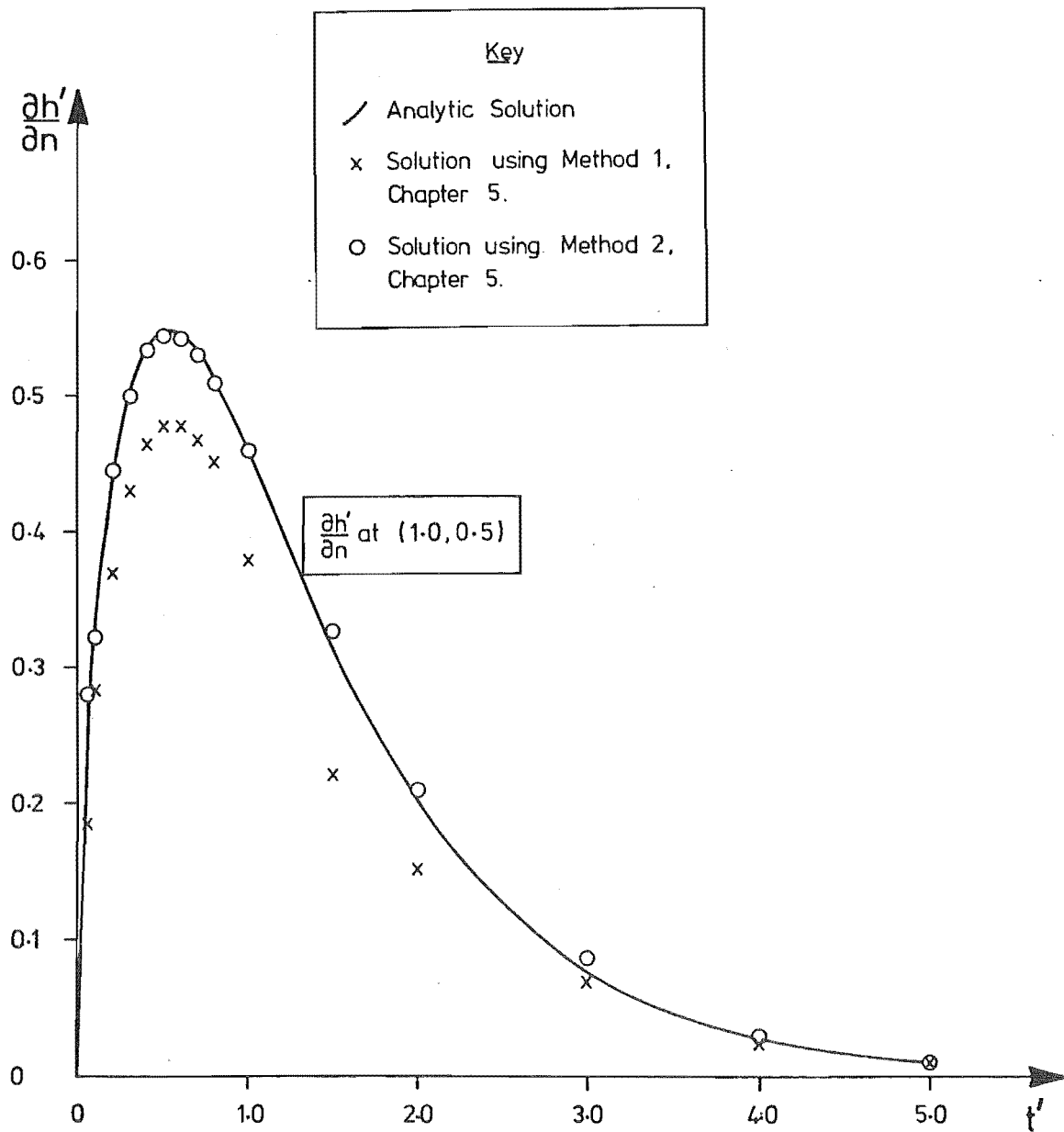


Fig. 6.11 Variation of $\frac{\partial h'}{\partial n}$ with time at (1.0, 0.5) for the problem shown in Fig. 6.9.

excellent agreement with the analytical solutions, while those obtained using Method 1 are somewhat less accurate due to the large time steps used.

The three cases examined so far all have steady-state solutions which are approached as t' becomes infinite. However, if the boundary condition at $x'=1.0$ is a periodic function of time, flow within the square region is oscillatory. For example, when the boundary condition at $x'=1.0$ is;

$$h'(x'=1.0, t') = \sin \frac{\pi t'}{2}, \quad t' > 0 \quad (6.7)$$

the exact solution calculated from Eqn 6.2 using the Duhamel superposition integral (Hildebrand, 1976) is;

$$h'(x', t') = \sin \frac{\pi t'}{2} - \pi \sum_{n=0}^{\infty} \frac{(-1)^n}{\alpha_n} \cos \alpha_n x' \left(\frac{\alpha_n^2 (\cos \frac{\pi t'}{2} - e^{-\alpha_n^2 t'}) + \frac{\pi}{2} \sin \frac{\pi t'}{2}}{\alpha_n^4 + \frac{\pi^2}{4}} \right) \quad (6.8)$$

and

$$\frac{\partial h'}{\partial n}(x'=1.0, t') = \pi \sum_{n=0}^{\infty} \frac{\alpha_n^2 (\cos \frac{\pi t'}{2} - e^{-\alpha_n^2 t'}) + \frac{\pi}{2} \sin \frac{\pi t'}{2}}{\alpha_n^4 + \frac{\pi^2}{4}} \quad (6.9)$$

in which $\alpha_n = (2n+1)\frac{\pi}{2}$. The time steps chosen for this problem, labelled TS3, are given in Table 6.1. Because of the relatively large time steps selected, numerical calculations have been attempted only with Method 2, the more accurate of the schemes developed in Chapter 5. Also, since no discontinuity in h' or $\frac{\partial h'}{\partial n}$ occurs at $t'=0$ (see Eqns 6.8 and 6.9), Method 2 will be stable. Values of h' on the boundary contour and at selected points within the flow region are compared with Eqn 6.8 in Figs 6.12 and 6.13, respectively, while the solution for $\frac{\partial h'}{\partial n}$ at $x'=1.0$ is compared with Eqn 6.9 in Fig. 6.14. Once again all the

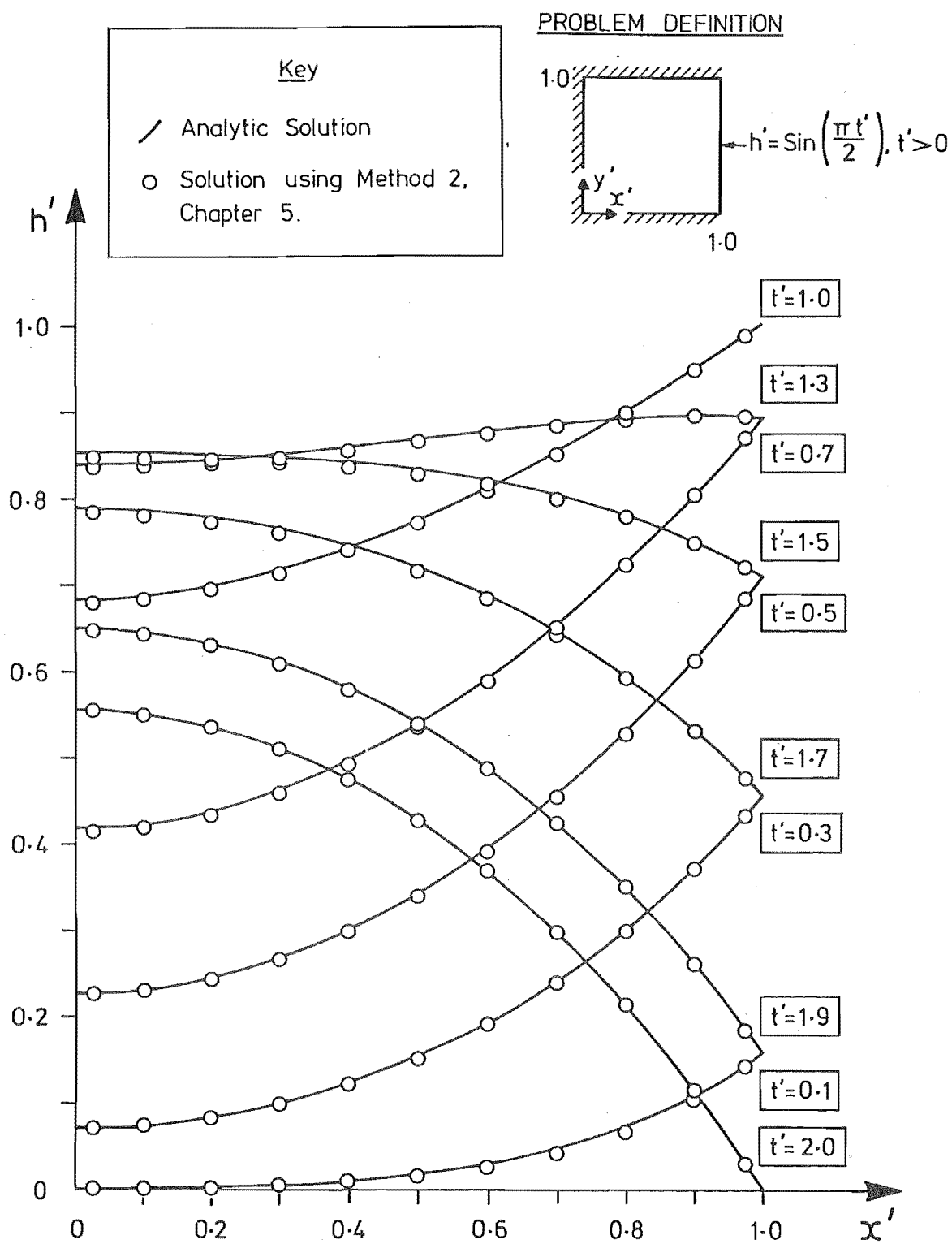


Fig. 6.12 Distribution of h' on $y'=0$ when $h'(x'=1.0, t') = \sin\left(\frac{\pi t'}{2}\right), t' > 0$.

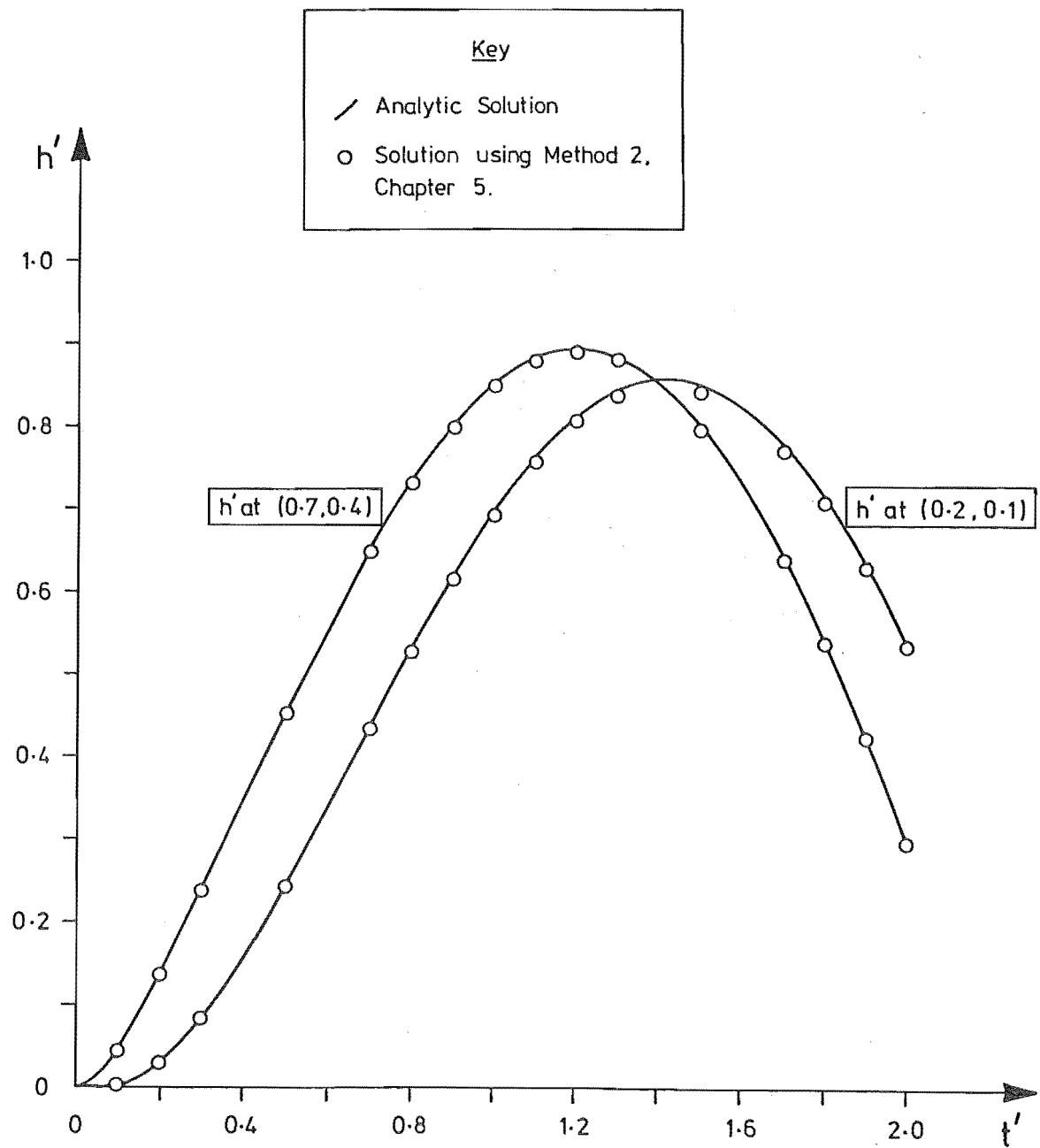


Fig. 6.13 Variation of h' with time at two internal points for the problem shown in Fig. 6.12.

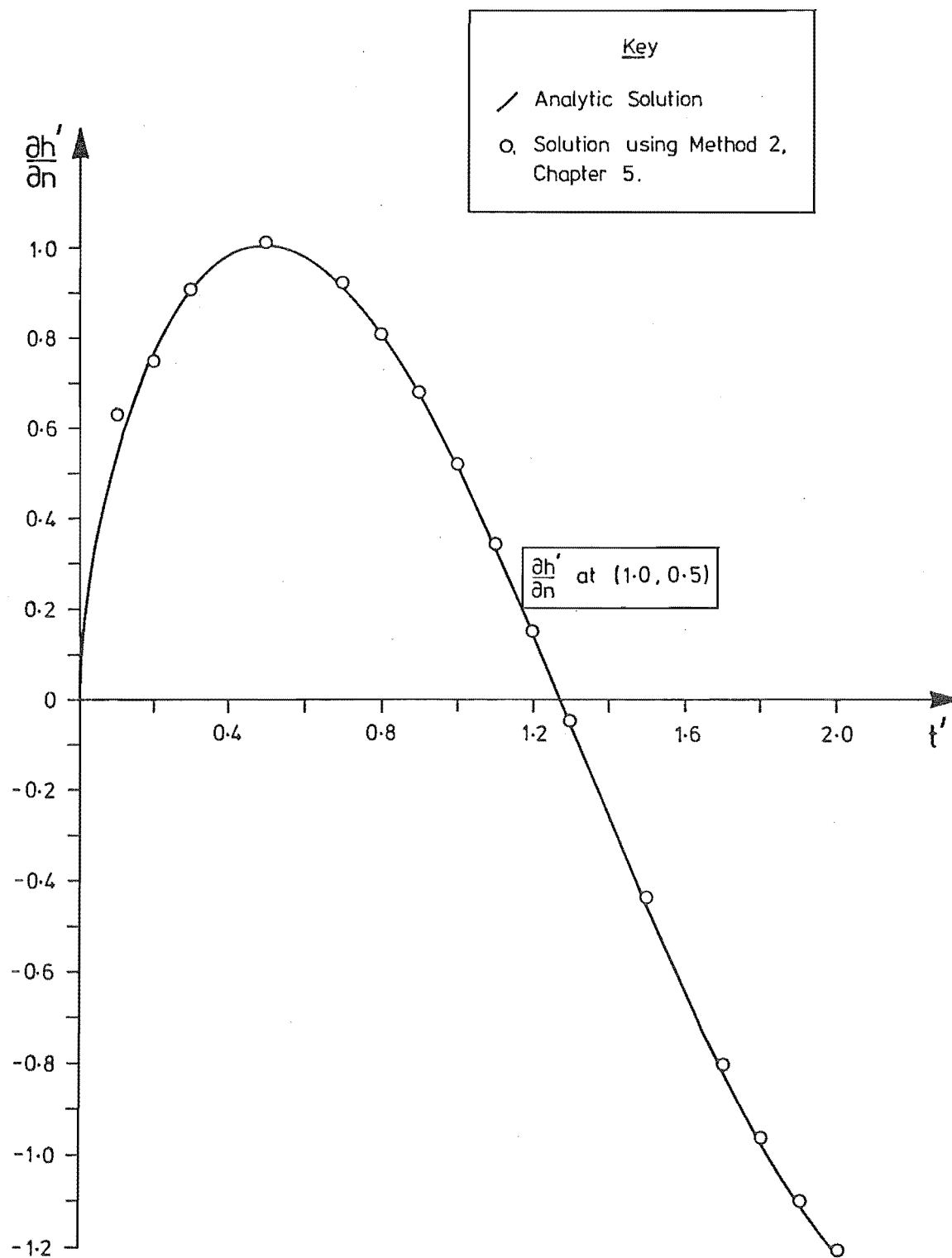


Fig. 6.14 Variation of $\frac{\partial h'}{\partial n}$ with time at (1.0,0.5) for the problem shown in Fig. 6.12.

results are in excellent agreement.

Solutions for two of the flows through the square region have been calculated using a finite-difference technique developed by Hunt (1983, at press) and the results compared with those obtained using Method 2. The finite-difference scheme uses a second-order approximation to the boundary conditions, a first-order backward-difference approximation to the time derivative, and solves the resulting set of simultaneous equations by Gauss-Seidel iteration. A finite-difference grid with a dimensionless nodal spacing of 0.1 was selected. Thus, the square region consisted of 121 nodes, and the time steps chosen for the finite-difference calculations were the same as those used for Method 2. The cases studied are the near instantaneous rise in h' , when a value of $\epsilon=500$ is substituted in the right side of Eqn 6.4, and the more gradual rise that occurs when $\epsilon=1.0$. Results from these two cases are compared with the results from Method 2 in Figs 6.15 and 6.16, respectively. Although the finite-difference solutions are obtained in only about one ninth of the computational time required by Method 2, the superior accuracy of Method 2 is apparent. The accuracy of the finite-difference solutions can be improved by using a finer grid spacing and more time steps, but, in doing so, the computational cost is increased and the amount of data preparation becomes excessive.

The solutions obtained thus far for flows through the square region are all functions of only one Cartesian coordinate. Flows through the quarter circle will be examined in order to verify the accuracy of the numerical techniques when applied to problems whose solutions are functions of two Cartesian coordinates. If the two radial boundaries of the quarter circle shown in Fig. 6.17 are impermeable, and if there is an instantaneous unit rise in h' on the circumferential boundary at $t'=0$, Carslaw and Jaeger (1959) show that;

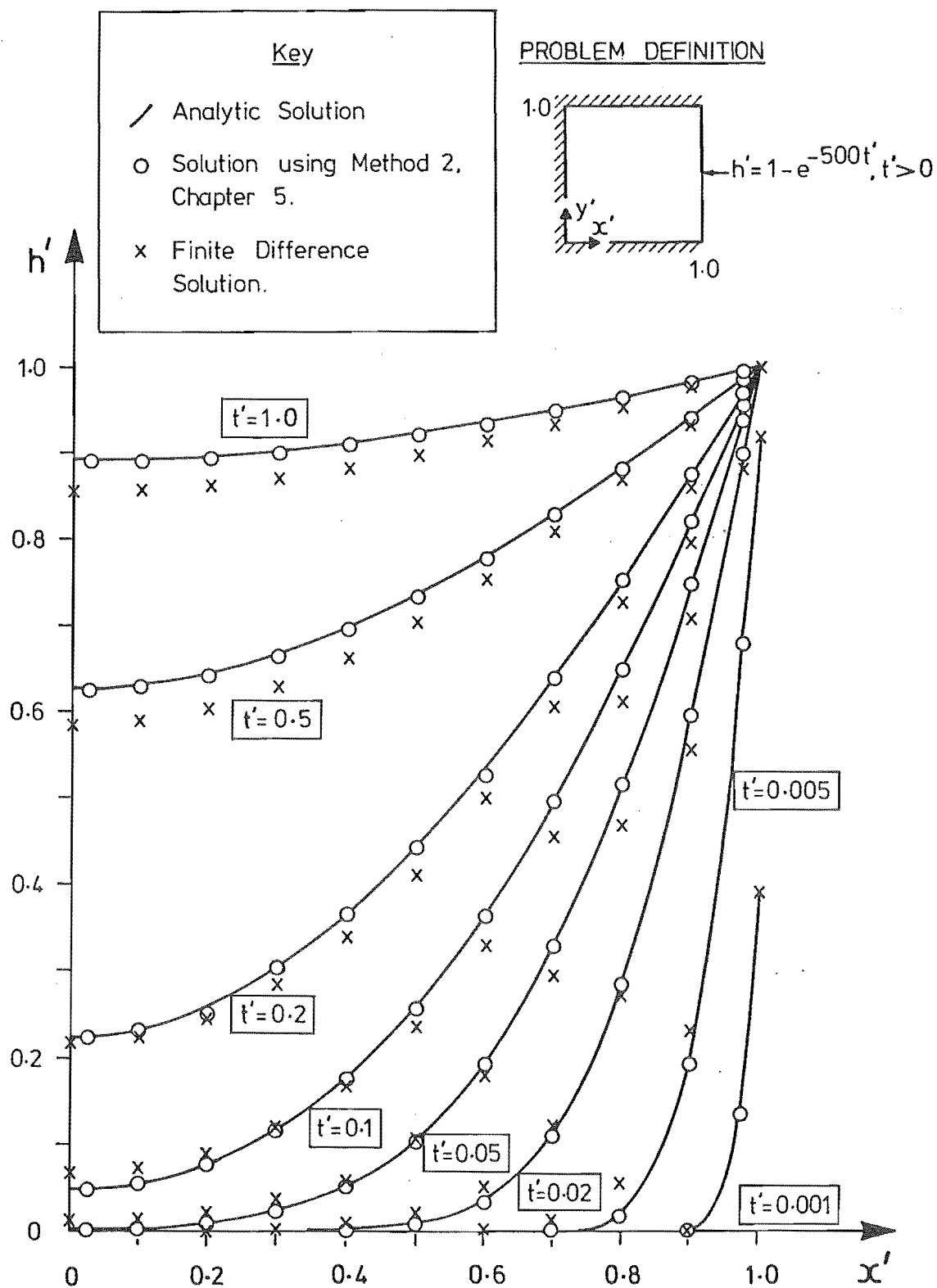


Fig. 6.15 Comparison between Method 2 and Finite-Difference solutions when $h'(x'=1.0, t') = 1 - e^{-500t'}, t' > 0$

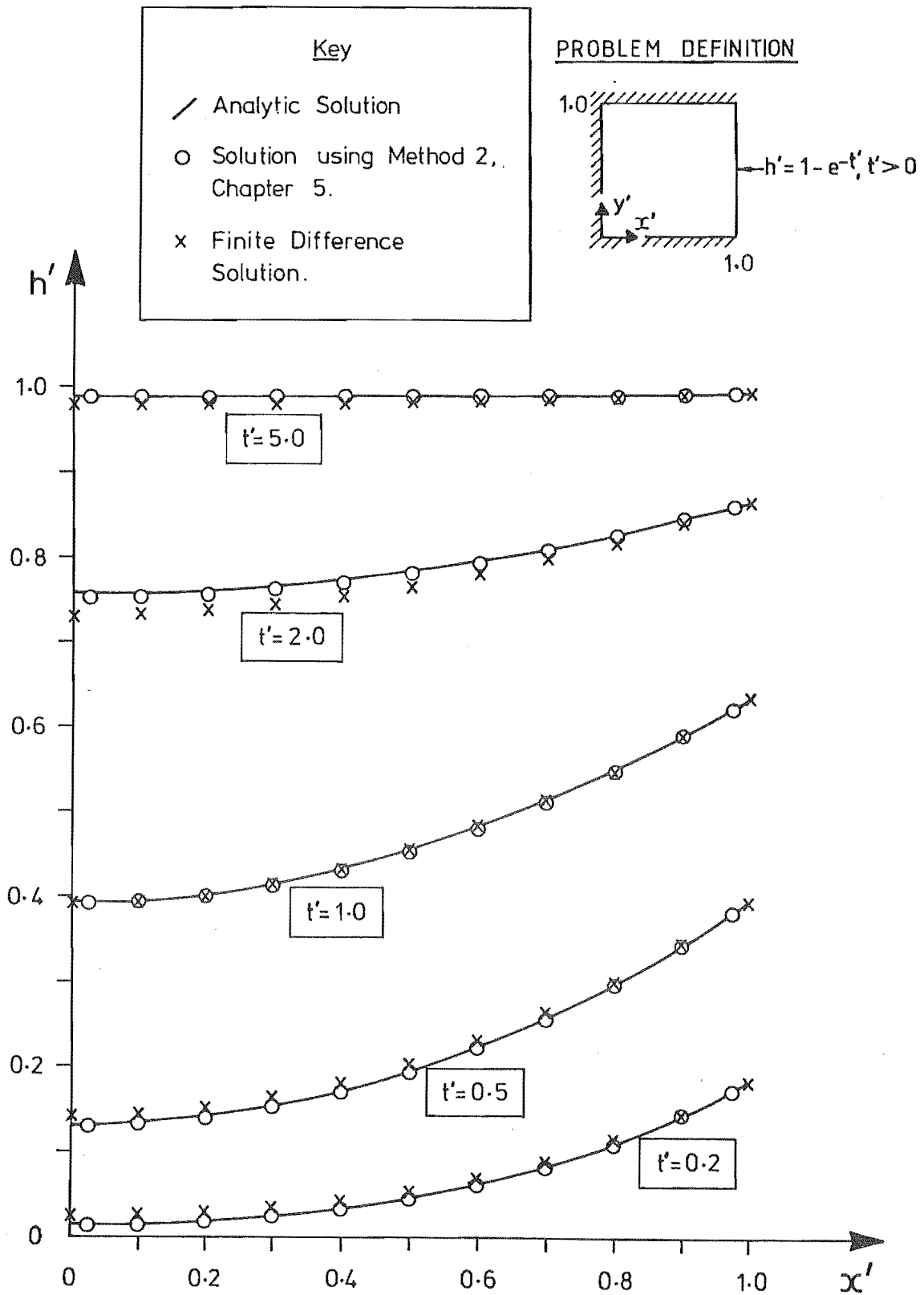


Fig. 6.16 Comparison between Method 2 and Finite-Difference solutions when $h'(x'=1.0, t') = 1 - e^{-t'}, t' > 0$.

$$h'(r', t') = 1 - 2 \sum_{n=1}^{\infty} \frac{J_0(\beta_n r')}{\beta_n J_1(\beta_n)} e^{-\beta_n^2 t'} \quad (6.10)$$

$$\text{and, } \frac{\partial h'}{\partial n}(r'=1.0, t') = 2 \sum_{n=1}^{\infty} e^{-\beta_n^2 t'} \quad (6.11)$$

in which $r' = \sqrt{x'^2 + y'^2}$, $J_p(x)$ is the Bessel function of the first kind of order p , and β_n are the positive roots of $J_0(\beta)=0$. Solutions to the instantaneous rise problem, using time steps TS4 in Table 6.1, are given in Figs 6.17-6.19. The solutions obtained on the boundary contour using Method 2 (Figs 6.17 and 6.19) are unstable because the value of $\frac{\partial h'}{\partial n}$ at $r'=1.0$ is infinite at $t'=0$. (Because of the large scatter in values of $\frac{\partial h'}{\partial n}$ at $r'=1.0$ calculated at the end of the first three time steps using Method 2, they have been omitted from Fig. 6.19. The omitted values are $\frac{\partial h'}{\partial n}(t'=0.0005) = 62.4055$, $\frac{\partial h'}{\partial n}(t'=0.001) = -10.3894$ and $\frac{\partial h'}{\partial n}(t'=0.005) = 19.2942$.) Despite this instability, values of h' within the flow region (Fig. 6.18) are in good agreement. The accuracy achieved with Method 1 is again limited by the length of time step used, this being particularly evident at points within the flow region (Fig. 6.18).

If the circumferential boundary condition is;

$$h'(r'=1.0, t') = 1 - e^{-\epsilon t'}, \quad t' > 0 \quad (6.12)$$

in which ϵ is a positive constant, then the exact solution obtained from Eqn 6.10 using the Duhamel superposition integral is given by;

$$h'(r', t') = 1 - e^{-\epsilon t'} - 2\epsilon \sum_{n=1}^{\infty} \frac{J_0(\beta_n r')}{\beta_n (\beta_n^2 - \epsilon) J_1(\beta_n)} \left[e^{-\epsilon t'} - e^{-\beta_n^2 t'} \right] \quad (6.13)$$

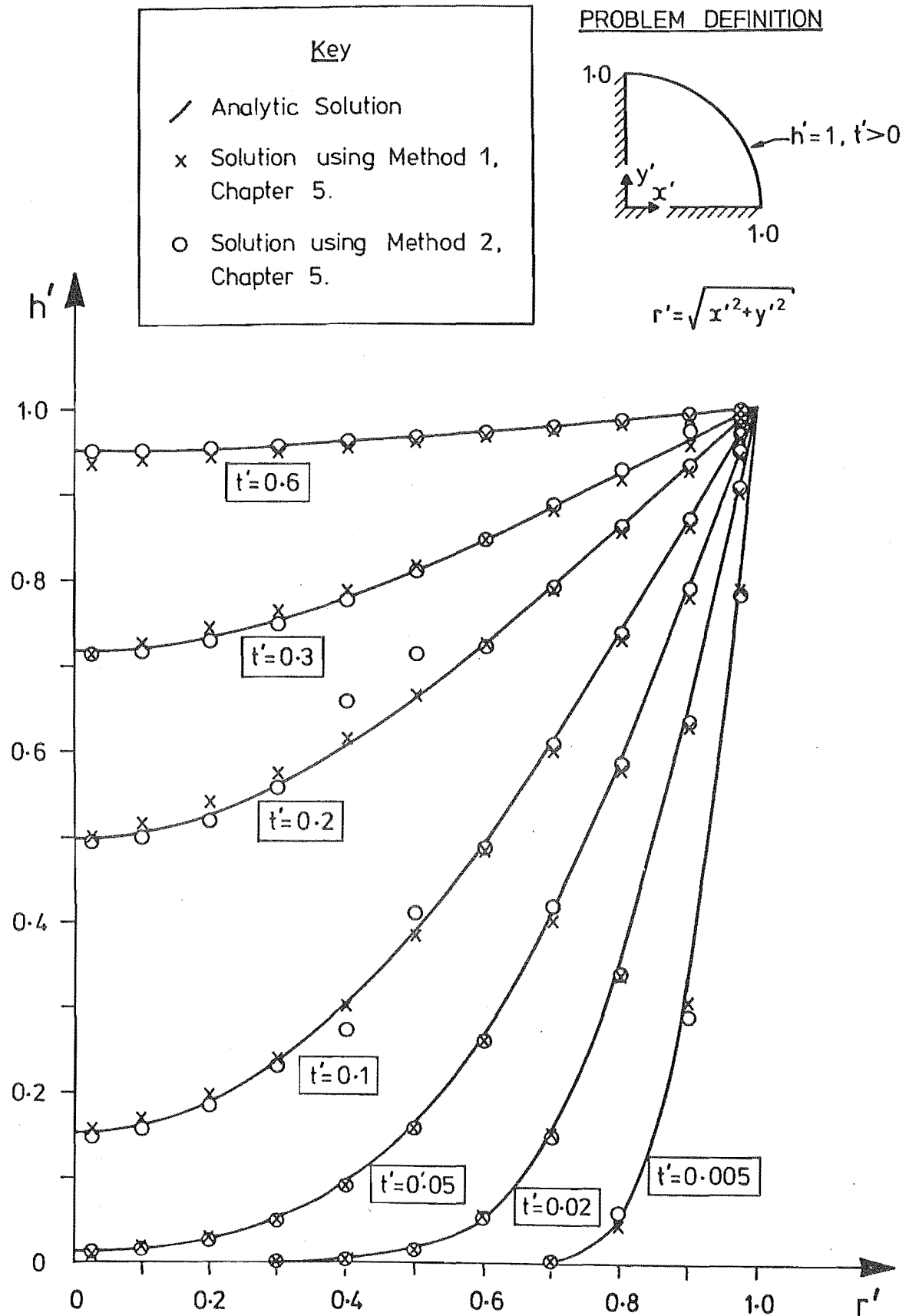


Fig. 6.17 Distribution of h' on the radial boundaries following instantaneous rise in h' at $r'=1.0$.

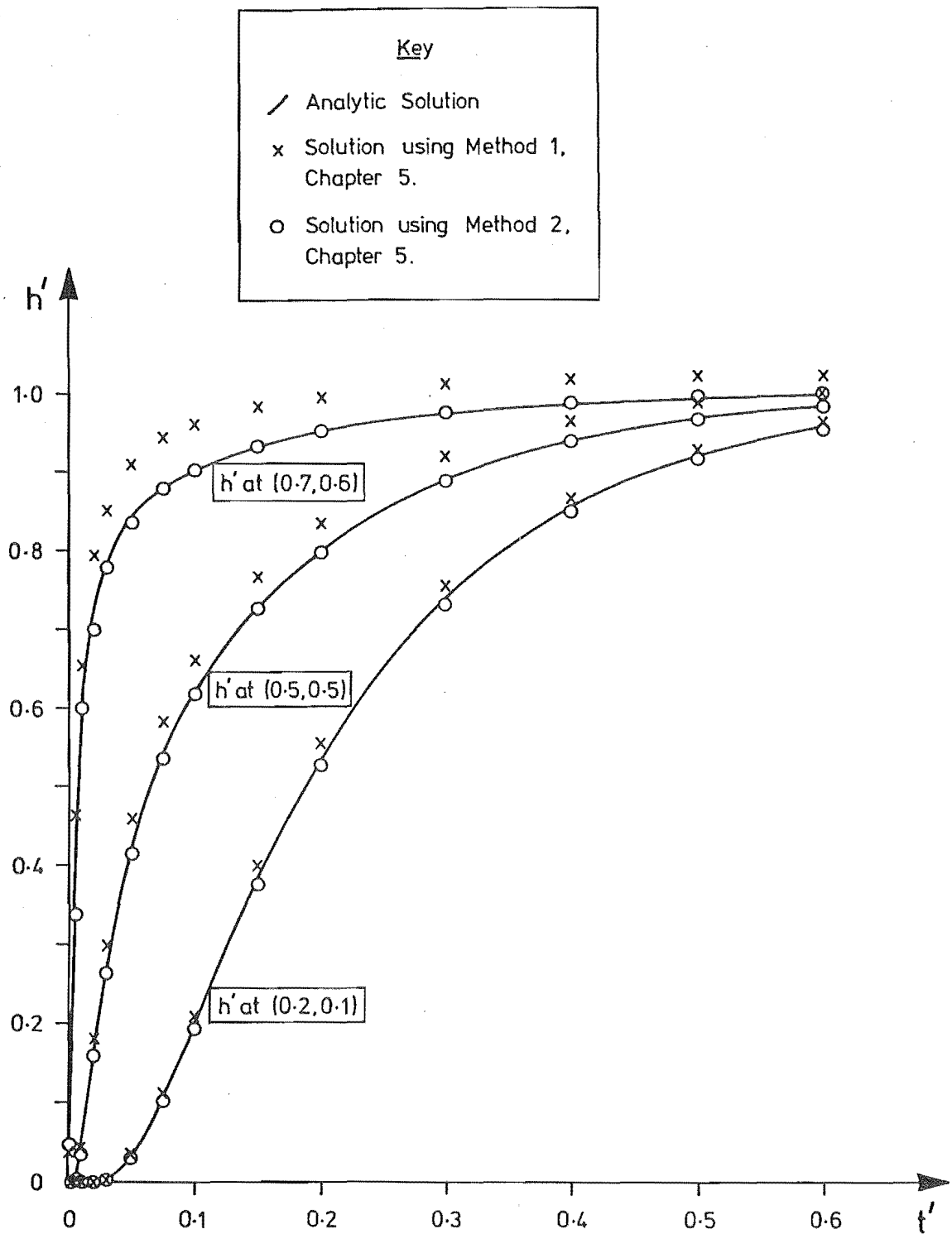


Fig. 6.18 Variation of h' with time at three internal points for the problem shown in Fig. 6.17.

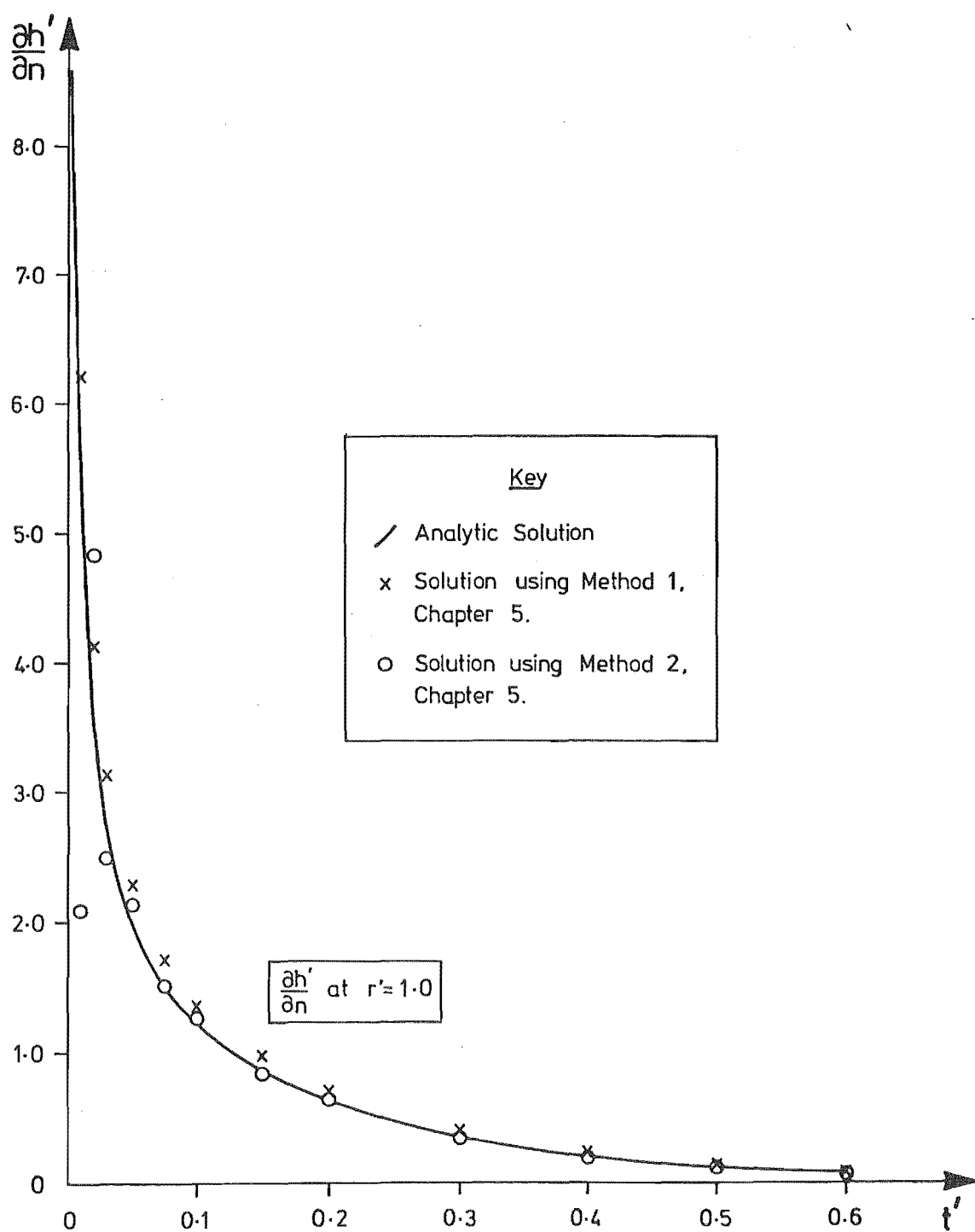


Fig. 6.19 Variation of $\frac{\partial h'}{\partial n}$ with time on the circumferential boundary for the problem shown in Fig. 6.17.

$$\text{and, } \frac{\partial h'}{\partial n} (r'=1.0, t') = 2\epsilon \sum_{n=1}^{\infty} \frac{e^{-\epsilon t'} - e^{-\beta_n^2 t'}}{\beta_n^2 - \epsilon} \quad (6.14)$$

The value of $\frac{\partial h'}{\partial n}$ at $r'=1.0$ is equal to zero at $t'=0$, provided $\beta_n^2 \neq \epsilon$, so there is no discontinuity in $\frac{\partial h'}{\partial n}$ at $t'=0$.

An instantaneous rise in h' is closely approximated by substituting a value of $\epsilon=500$ in the right side of Eqn 6.12. The solutions to this problem are compared in Figs 6.20-6.22. There is now excellent agreement between the analytical solutions and those obtained using Method 2, while the accuracy attained using Method 1 is limited by the time step lengths.

Less rapid changes in h' are achieved if a value of $\epsilon=1.0$ is substituted in the right side of Eqn 6.12. The solutions to this problem, obtained using time steps TS2 (Table 6.1), are compared in Figs 6.23-6.25. As has been the case in all problems where $\frac{\partial h'}{\partial n}$ at $r'=1.0$ is equal to zero at $t'=0$, the superior accuracy of Method 2 over Method 1 is strongly evident.

Applying the Duhamel superposition integral to Eqn 6.10 when the circumferential boundary condition is given by;

$$h'(r'=1.0, t') = \sin \frac{\pi t'}{2}, \quad t' > 0 \quad (6.15)$$

yields,

$$h'(r', t') = \sin \frac{\pi t'}{2} - \pi \sum_{n=1}^{\infty} \frac{J_0(\beta_n r')}{\beta_n (\beta_n^4 + \frac{\pi^2}{4}) J_1(\beta_n)} \left(\alpha_n^2 \left(\cos \frac{\pi t'}{2} - e^{-\beta_n^2 t'} \right) + \frac{\pi \sin \frac{\pi t'}{2}}{2} \right) \quad (6.16)$$

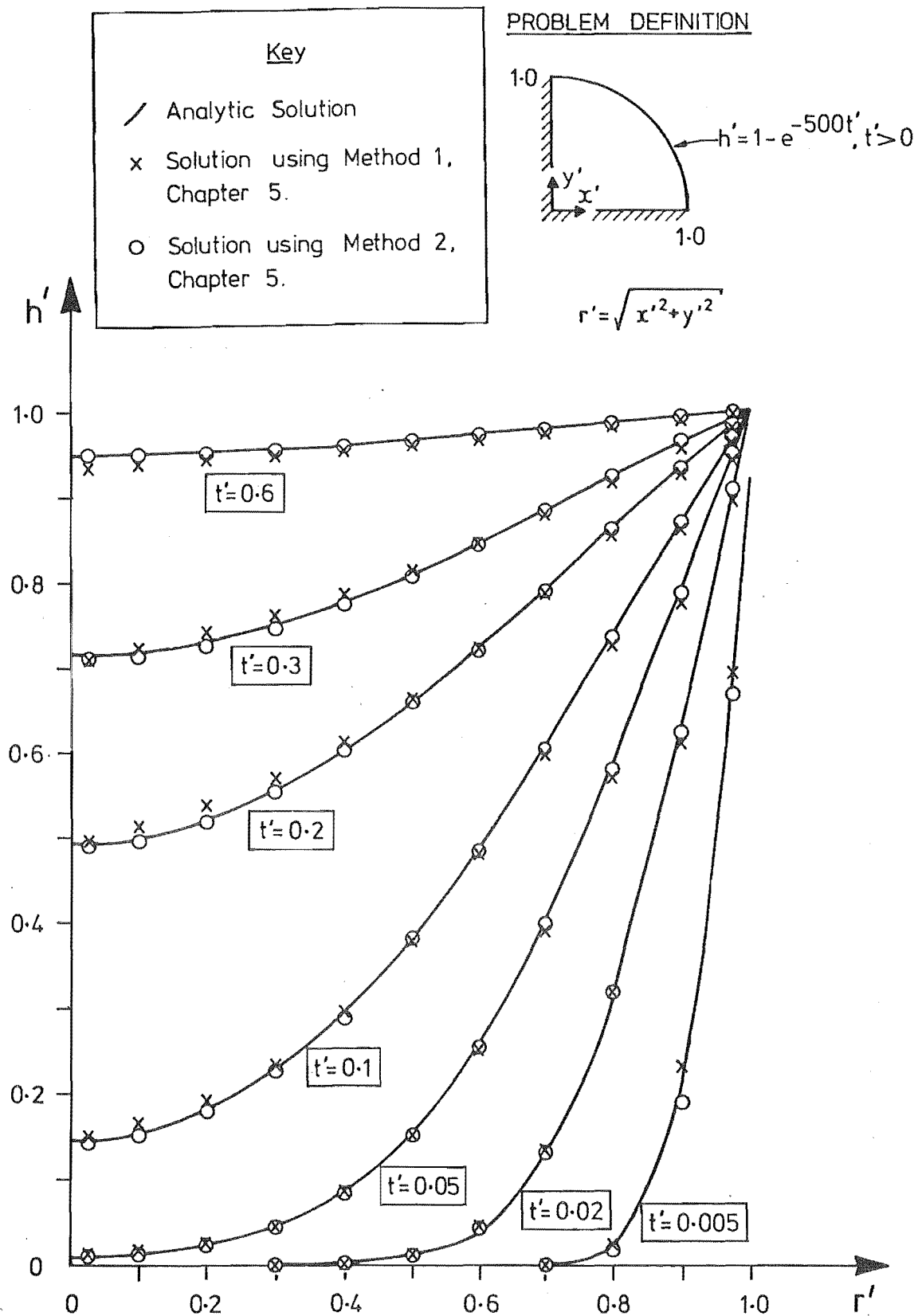


Fig. 6.20 Distribution of h' on the radial boundary when $h'(r'=1.0, t') = 1 - e^{-500t'}, t' > 0$.

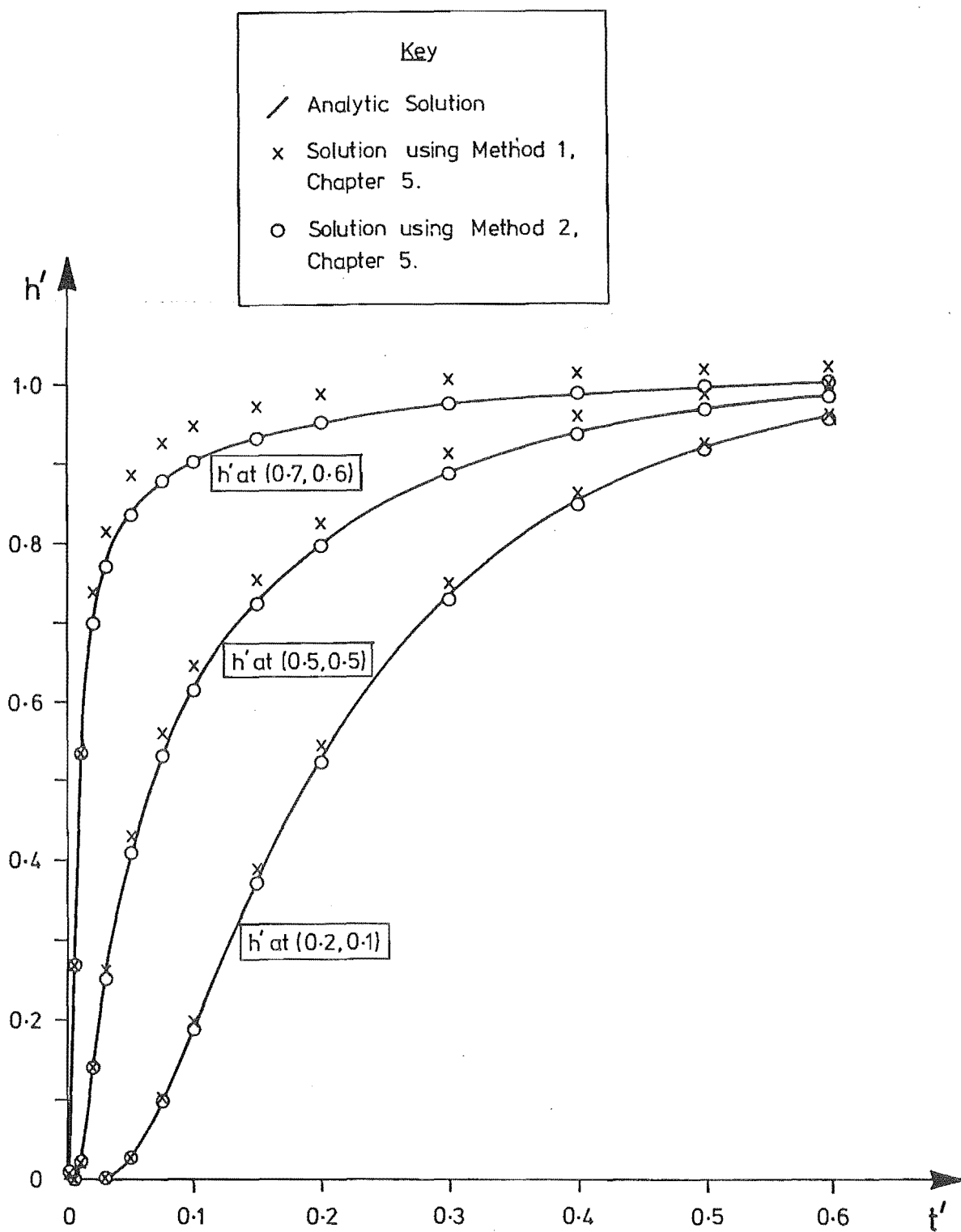


Fig. 6.21 Variation of h' with time at three internal points for the problem shown in Fig. 6.20.

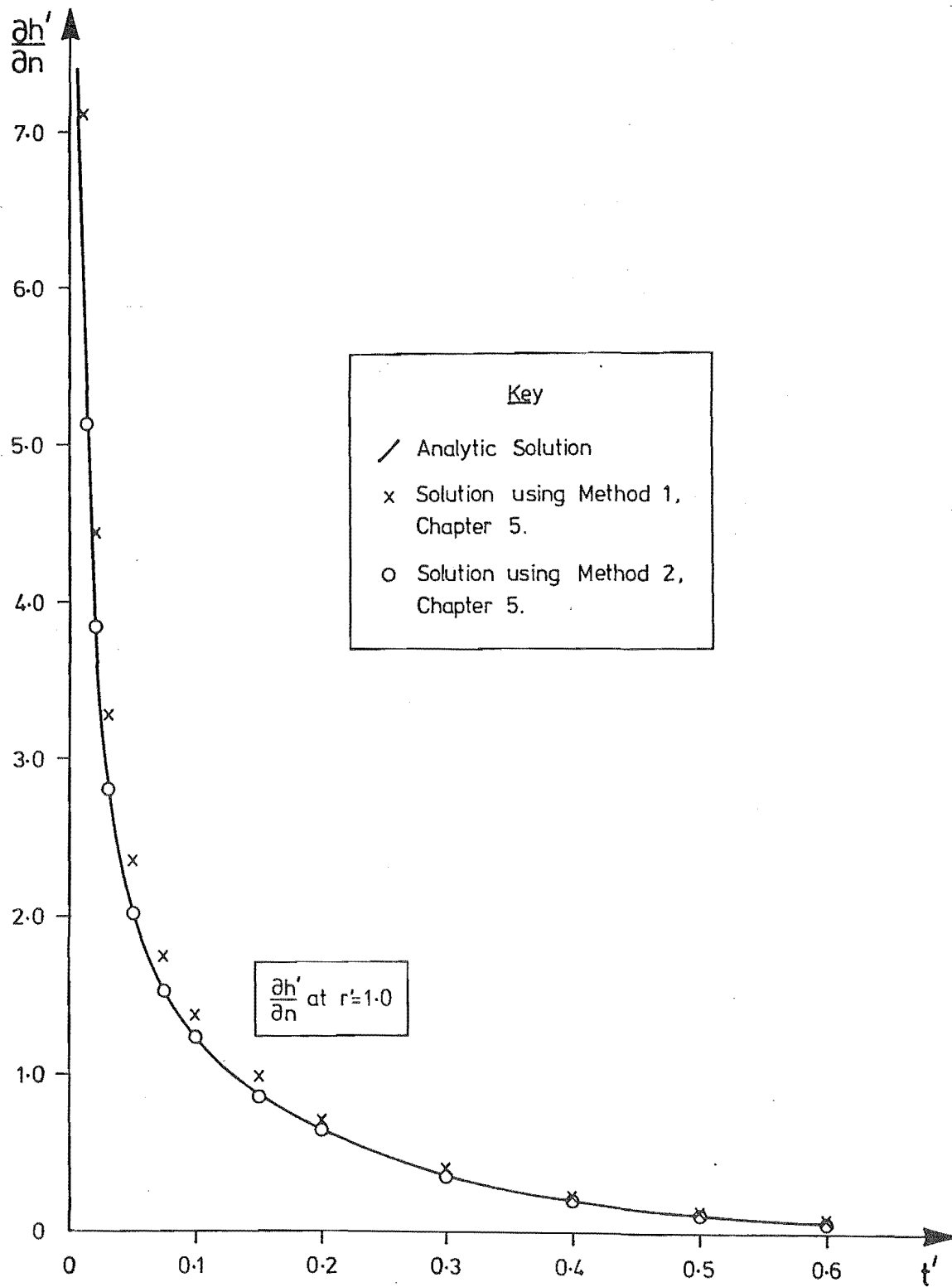


Fig. 6.22 Variation of $\frac{\partial h'}{\partial n}$ with time on the circumferential boundary for the problem shown in Fig. 6.20.

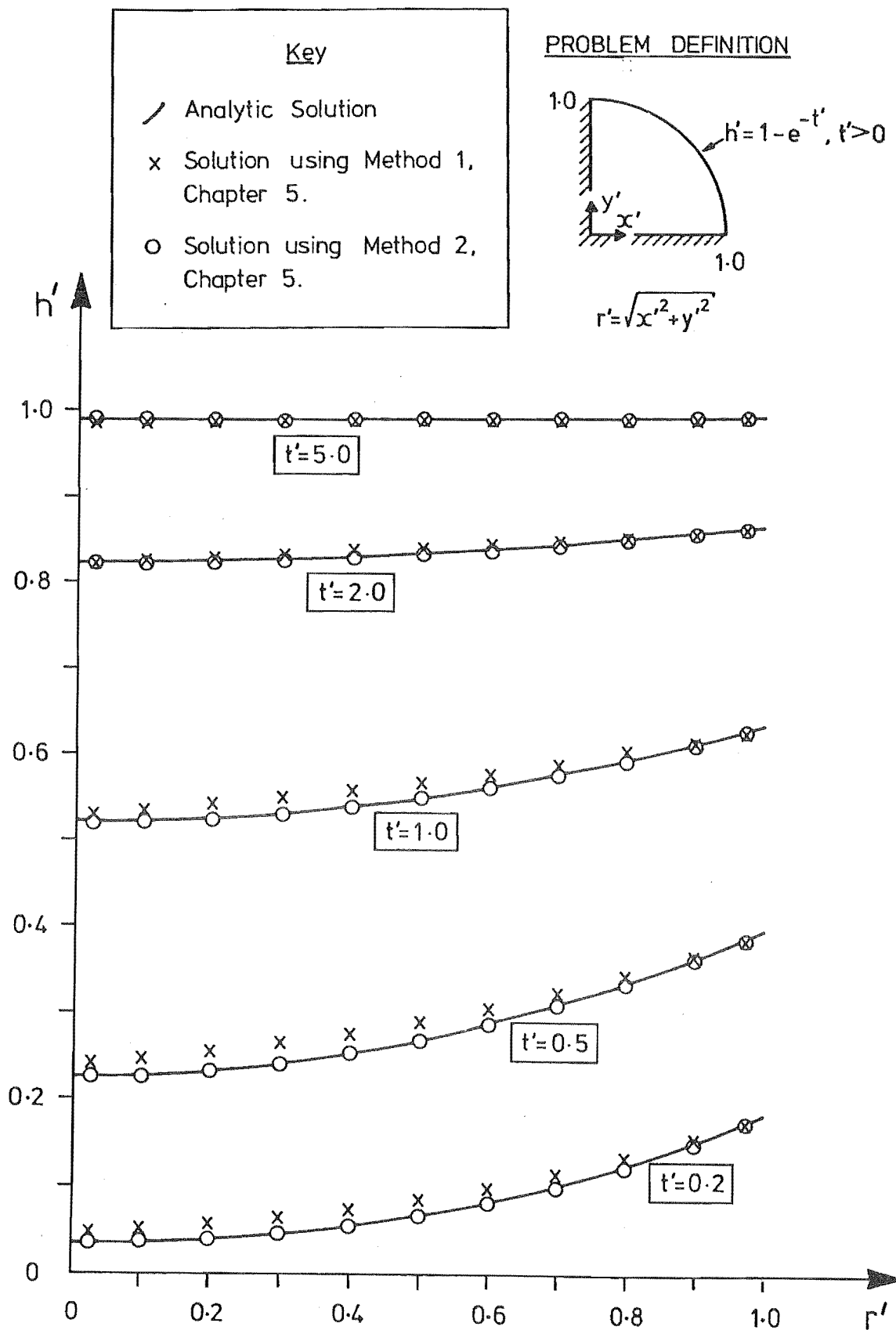


Fig. 6.23 Distribution of h' on the radial boundary when $h'(r'=1.0, t') = 1 - e^{-t'}$, $t' > 0$.

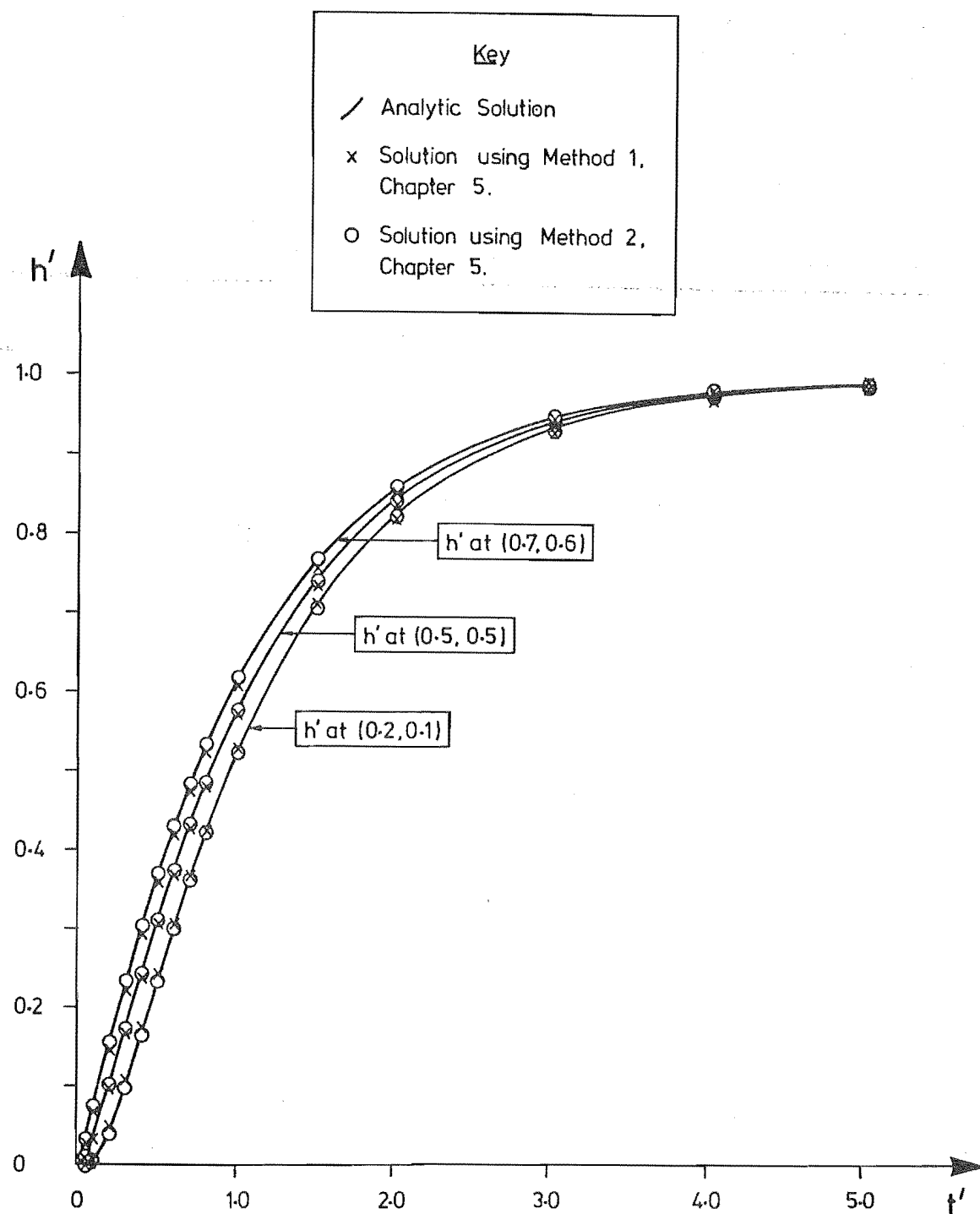


Fig. 6.24 Variation of h' with time at three internal points for the problem shown in Fig. 6.23.

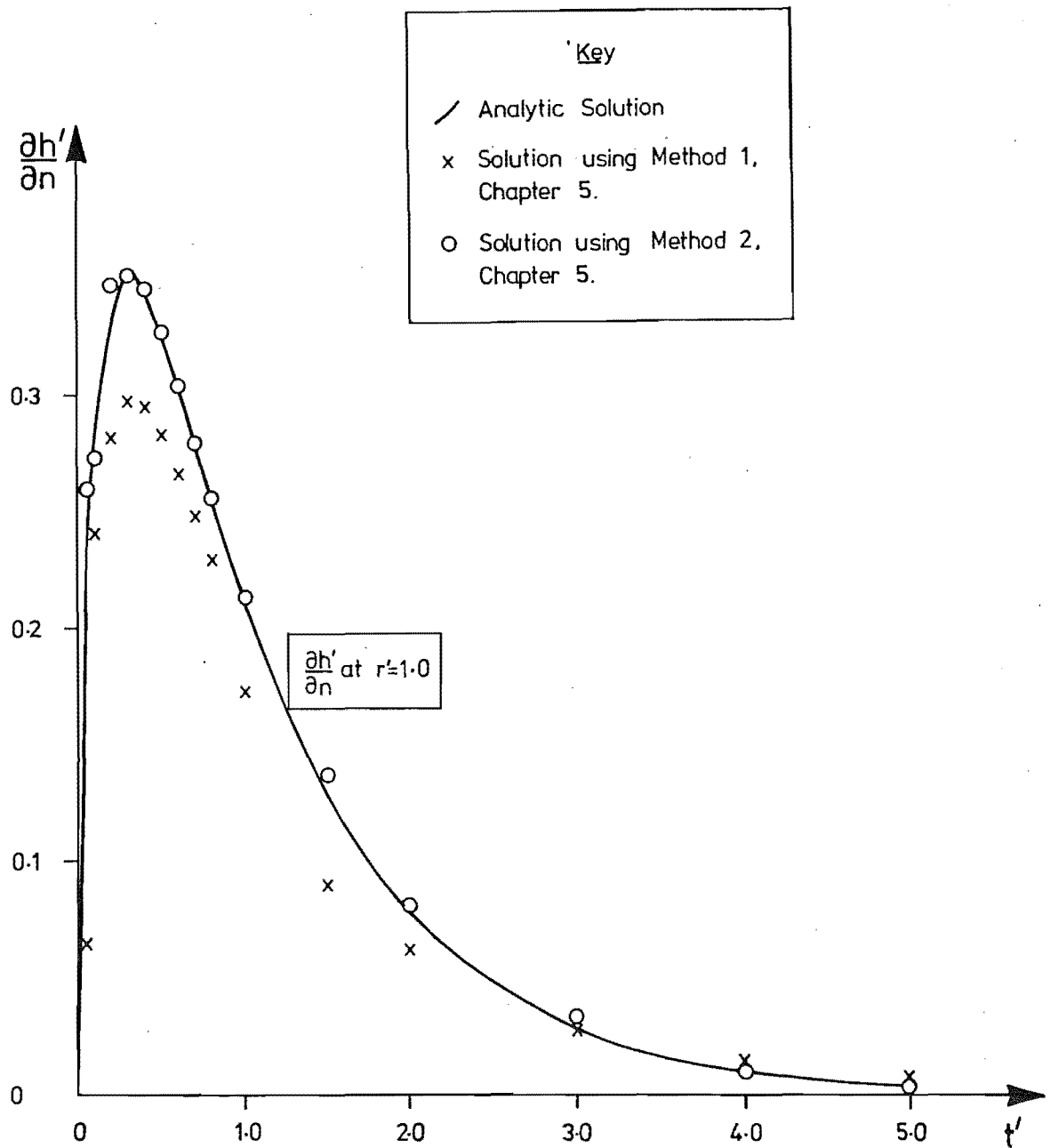


Fig. 6.25 Variation of $\frac{\partial h'}{\partial n}$ with time on the circumferential boundary for the problem shown in Fig. 6.23.

$$\text{and, } \frac{\partial h'}{\partial n} (r'=1.0, t') = \frac{\pi \sum_{n=1}^{\infty} \frac{\beta_n^2 (\cos \frac{\pi t'}{2} - e^{-\beta_n^2 t'}) + \frac{\pi}{2} \sin \frac{\pi t'}{2}}{\beta_n^4 + \frac{\pi^2}{4}}}{(6.17)}$$

Because there is no discontinuity in h' or $\frac{\partial h'}{\partial n}$ at $t'=0$, and because the time steps chosen (TS3, Table 6.1) are large, calculations have been attempted with Method 2 only. Values of h' on the radial boundary and at selected points within the flow region are compared with Eqn 6.16 in Figs 6.26 and 6.27, respectively, while the solution for $\frac{\partial h'}{\partial n}$ at $r'=1.0$ is compared with Eqn 6.17 in Fig. 6.28. The slight discrepancy in $\frac{\partial h'}{\partial n}$ at the end of the first time step is solely due to the length of the first time step. If the step length near $t'=0$ is decreased then there is a significant increase in the accuracy of $\frac{\partial h'}{\partial n}$ as shown in Fig. 6.28. There is also a slight improvement in an already accurate solution for h' on the boundary contour, as shown in Fig. 6.26.

6.3 FLOWS IN HOMOGENEOUS REGIONS THAT INCLUDE WELLS

Three sides of the square region described previously are again assumed to be impermeable. Suppose that the fourth side of the square ($x'=1.0$) is maintained at zero head throughout the pumping of a constant dimensionless flow rate, Q' , from a well located at (x'_0, y'_0) . If pumping starts at $t'=0$ the analytic solution, calculated using a double Fourier series, is given by;

$$h'(x', y', t') = \sum_{n=0}^{\infty} \sum_{m=0}^{\infty} \frac{\gamma_n Q' \cos n\pi y'_0 \cos(2m+1) \frac{\pi x'_0}{2}}{\pi^2 \left[\left[\frac{2m+1}{2} \right]^2 + n^2 \right]} \cos n\pi y' \cos(2m+1) \frac{\pi x'}{2} \left[e^{-\pi^2 \left[\left[\frac{2m+1}{2} \right]^2 + n^2 \right] t'} - 1 \right] \quad (6.18)$$

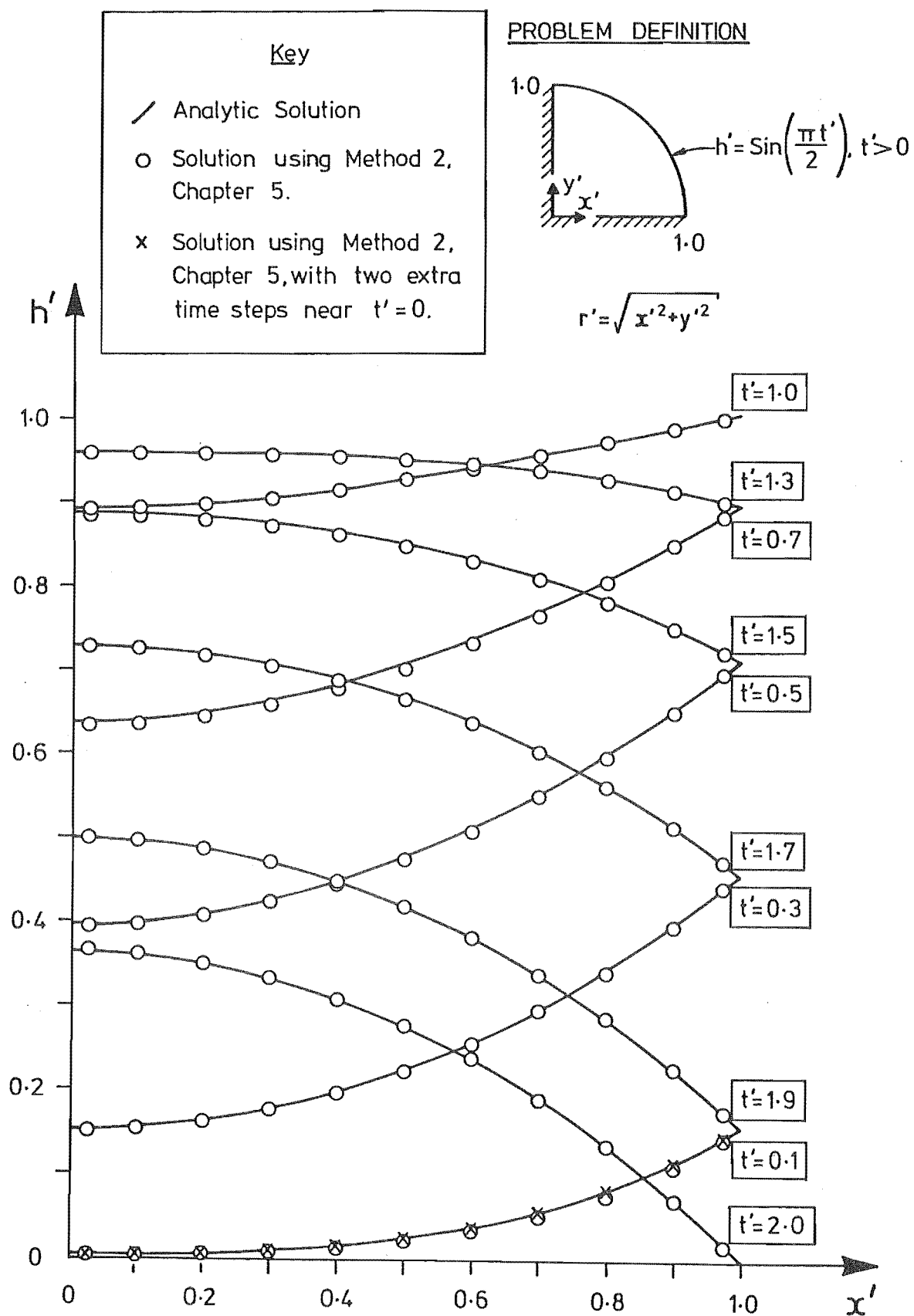


Fig. 6.26 Distribution of h' on the radial boundary when $h'(r'=1.0, t') = \sin\left(\frac{\pi t'}{2}\right), t' > 0$.

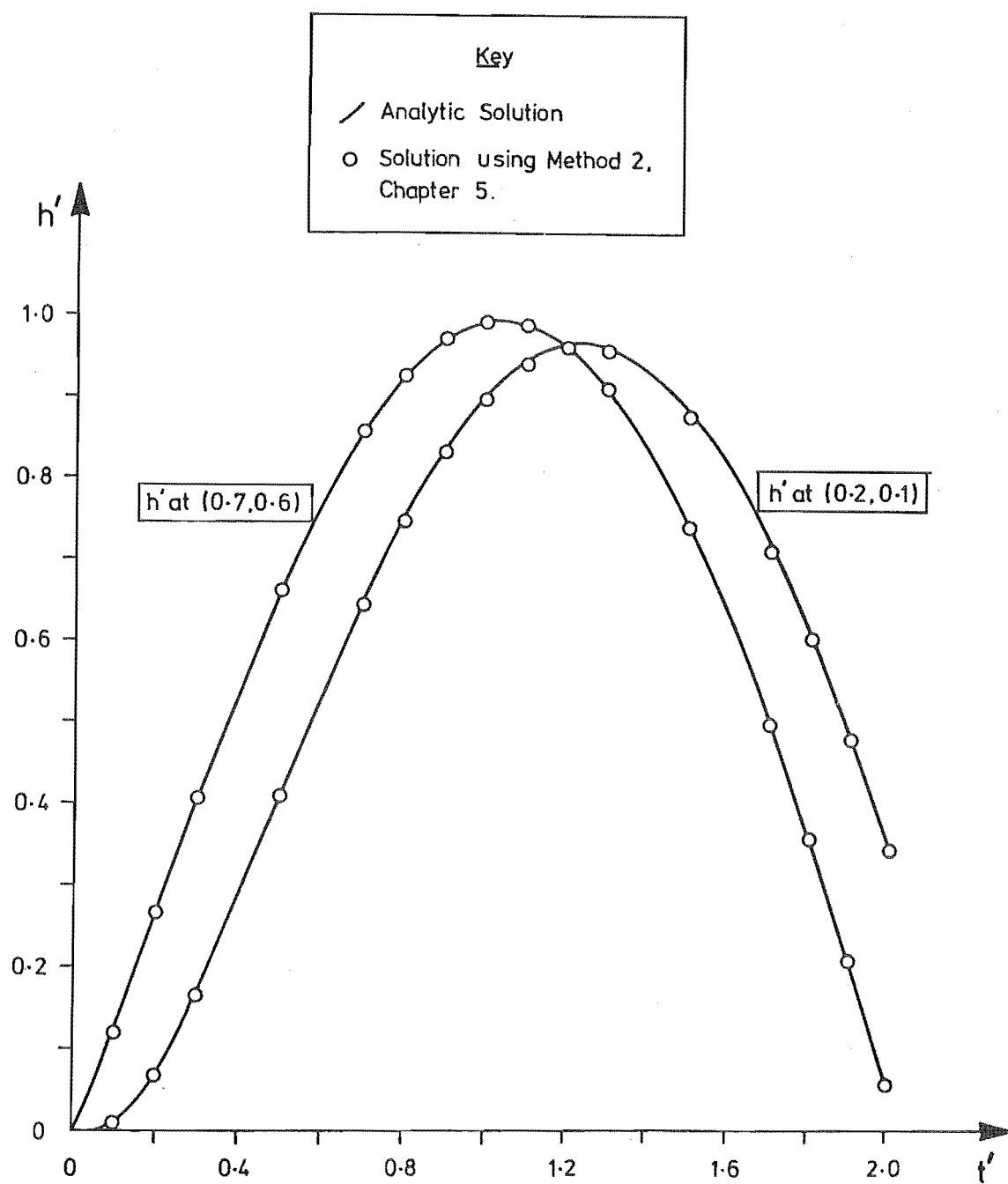


Fig. 6.27 Variation of h' with time at two internal points for the problem shown in Fig. 6.26.

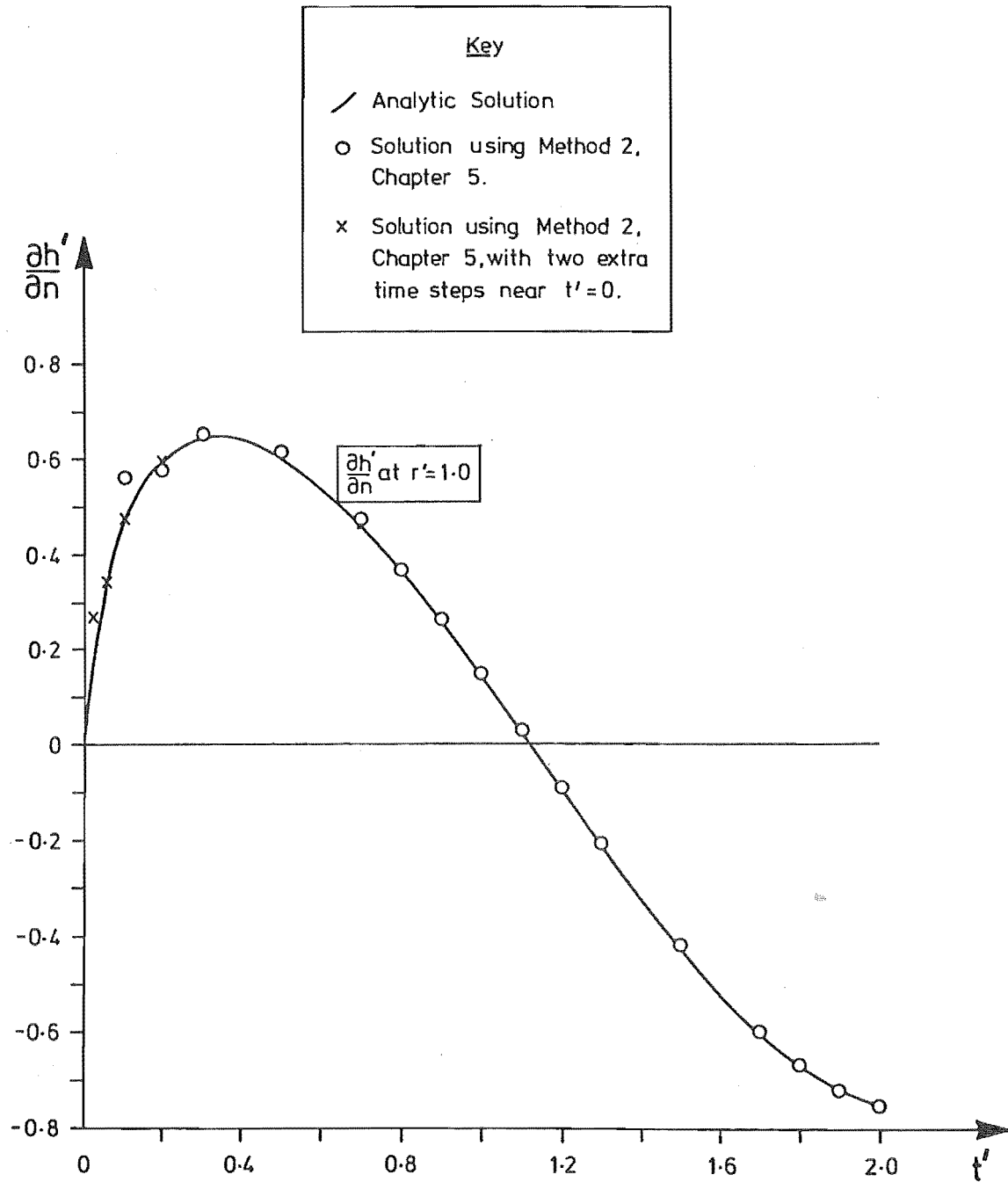


Fig. 6.28 Variation of $\frac{\partial h'}{\partial n}$ with time on the circumferential boundary for the problem shown on Fig. 6.26.

and,

$$\frac{\partial h'}{\partial n}(x'=1.0, y', t') =$$

$$\sum_{n=0}^{\infty} \sum_{m=0}^{\infty} \frac{(-1)^{m+1} (2m+1) \frac{\pi}{2} \gamma_n Q' \cos n\pi y'_0 \cos(2m+1) \frac{\pi x'_0}{2}}{\pi^2 \left[\left[\frac{2m+1}{2} \right]^2 + n^2 \right]} \cos n\pi y' \left(e^{-\pi^2 \left[\left[\frac{2m+1}{2} \right]^2 + n^2 \right] t'} - 1 \right) \quad (6.19)$$

in which $\gamma_n=2$ if $n=0$ or 4 if $n \geq 1$. Suppose that an analytical solution can be found for flow in the square when there are no wells and when $h'(x'=1.0, y', t') = F(y', t')$, in which F is a specified function. The superposition of this solution and the right side of Eqn 6.18 yields the solution for this given boundary condition when there is a well at (x'_0, y'_0) . For example, if the boundary condition at $x'=1.0$ is given by $h'=1-e^{-\varepsilon t'}$, in which ε is a positive constant, and if there is a well at (x'_0, y'_0) the exact solution for h' is obtained by summing the right sides of Eqns 6.5 and 6.18. The values of $\frac{\partial h'}{\partial n}$ at $x'=1.0$ are calculated by adding the right sides of Eqns 6.6 and 6.19. Thus;

$$h'(x', y', t') = 1 - e^{-\varepsilon t'} - 2\varepsilon \sum_{n=0}^{\infty} \frac{(-1)^n \cos \alpha_n x'}{\alpha_n (\alpha_n^2 - \varepsilon)} \left(e^{-\varepsilon t'} - e^{-\alpha_n^2 t'} \right) + \sum_{n=0}^{\infty} \sum_{m=0}^{\infty} \frac{\gamma_n Q' \cos n\pi y'_0 \cos(2m+1) \frac{\pi x'_0}{2} \cos n\pi y' \cos(2m+1) \frac{\pi x'}{2}}{\pi^2 \left[\left[\frac{2m+1}{2} \right]^2 + n^2 \right]} \left(e^{-\pi^2 \left[\left[\frac{2m+1}{2} \right]^2 + n^2 \right] t'} - 1 \right) \quad (6.20)$$

and,

$$\begin{aligned} \frac{\partial h'}{\partial n}(x'=1.0, y', t') = & 2\epsilon \sum_{n=0}^{\infty} \frac{e^{-\epsilon t'} - e^{-\alpha_n^2 t'}}{\alpha_n^2 - \epsilon} + \\ & \sum_{n=0}^{\infty} \sum_{m=0}^{\infty} \frac{(-1)^{m+1} (2m+1) \frac{\pi}{2} \gamma_n Q' \cos n\pi y'_0 \cos(2m+1) \frac{\pi x'_0}{2} \cos n\pi y'}{\pi^2 \left[\left[\frac{2m+1}{2} \right]^2 + n^2 \right]} \\ & \left[e^{-\pi^2 \left[\left[\frac{2m+1}{2} \right]^2 + n^2 \right] t'} - 1 \right] \end{aligned} \quad (6.21)$$

in which $\alpha_n = (2n+1) \frac{\pi}{2}$ and $\gamma_n = 2$ if $n=0$, or 4 if $n \geq 1$.

Consider the case when $\epsilon=1.0$ and there is a well of strength $\frac{Q'}{4\pi} = 0.1$ located at $(0.5, 0.5)$, as shown in Fig. 6.29. The solutions for h' on the boundary contour, calculated using Methods 1 and 2 and time steps TS2, are compared with Eqn 6.20 in Fig. 6.29. Values of h' within the flow region are compared with Eqn 6.20 in Fig. 6.30, while the numerical and analytical solutions for $\frac{\partial h'}{\partial n}$ at $(1.0, 0.2)$ are shown in Fig. 6.31. Although the results obtained using Method 1 are in good agreement with the analytical solution as the steady state solution is approached (and changes in h' and $\frac{\partial h'}{\partial n}$ are small), those obtained with Method 2 are accurate at all times. The finite-difference solution, calculated using time steps TS2 and a dimensionless nodal spacing of 0.1 is compared with the solution obtained using Method 2 in Fig. 6.32. The accuracy achieved with finite-differences, while comparable to that of Method 1, is significantly poorer than that achieved with Method 2. For this problem the finite-difference solution requires only about one ninth of the computational time needed for Method 2. However, the finite-difference solution also requires a significantly greater amount of data preparation.

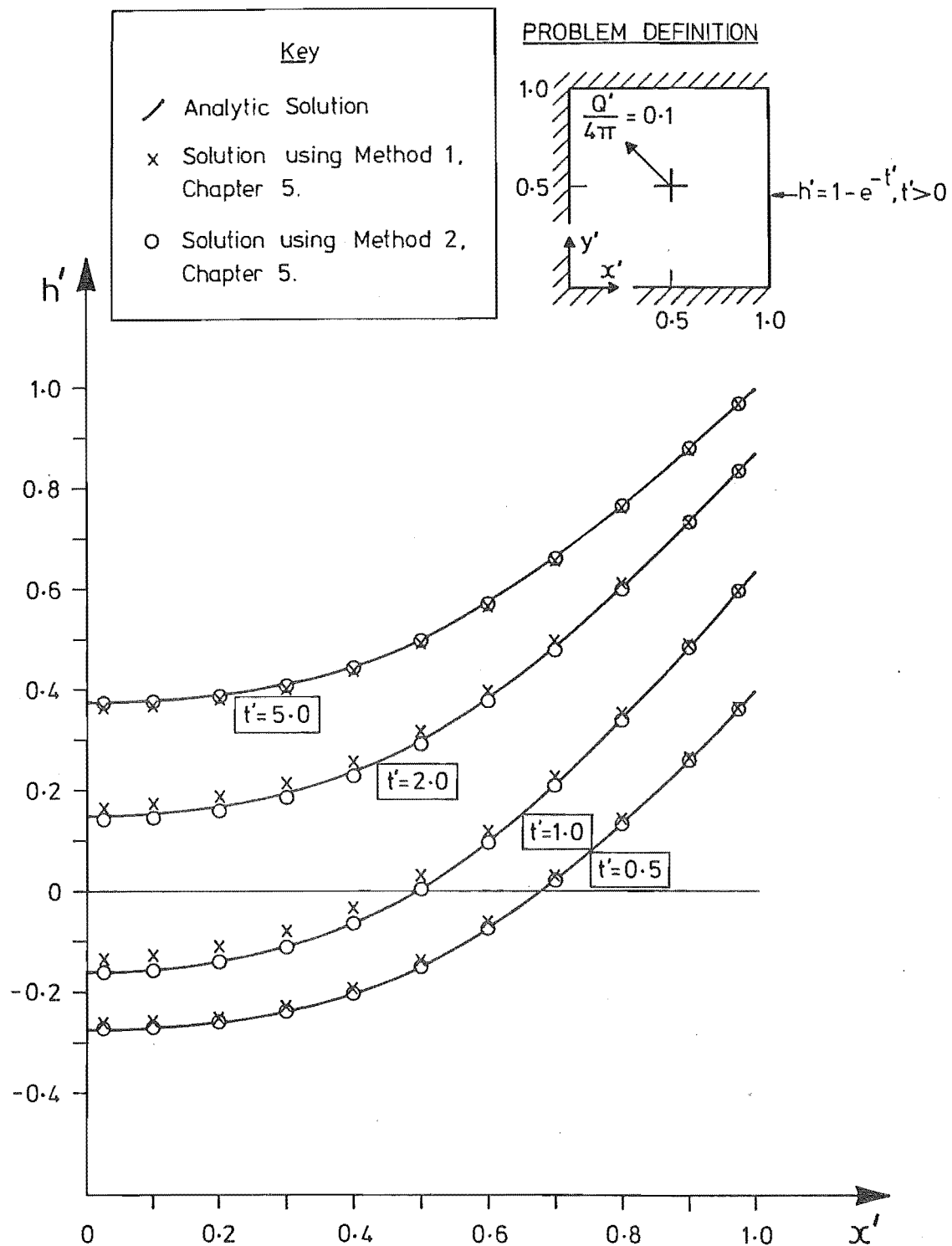


Fig. 6.29 Distribution of h' on $y'=0$ when $h'(x'=1.0, t') = 1 - e^{-t'}$, $t' > 0$ and there is a well of strength $\frac{Q'}{4\pi} = 0.1$ at $(0.5, 0.5)$.

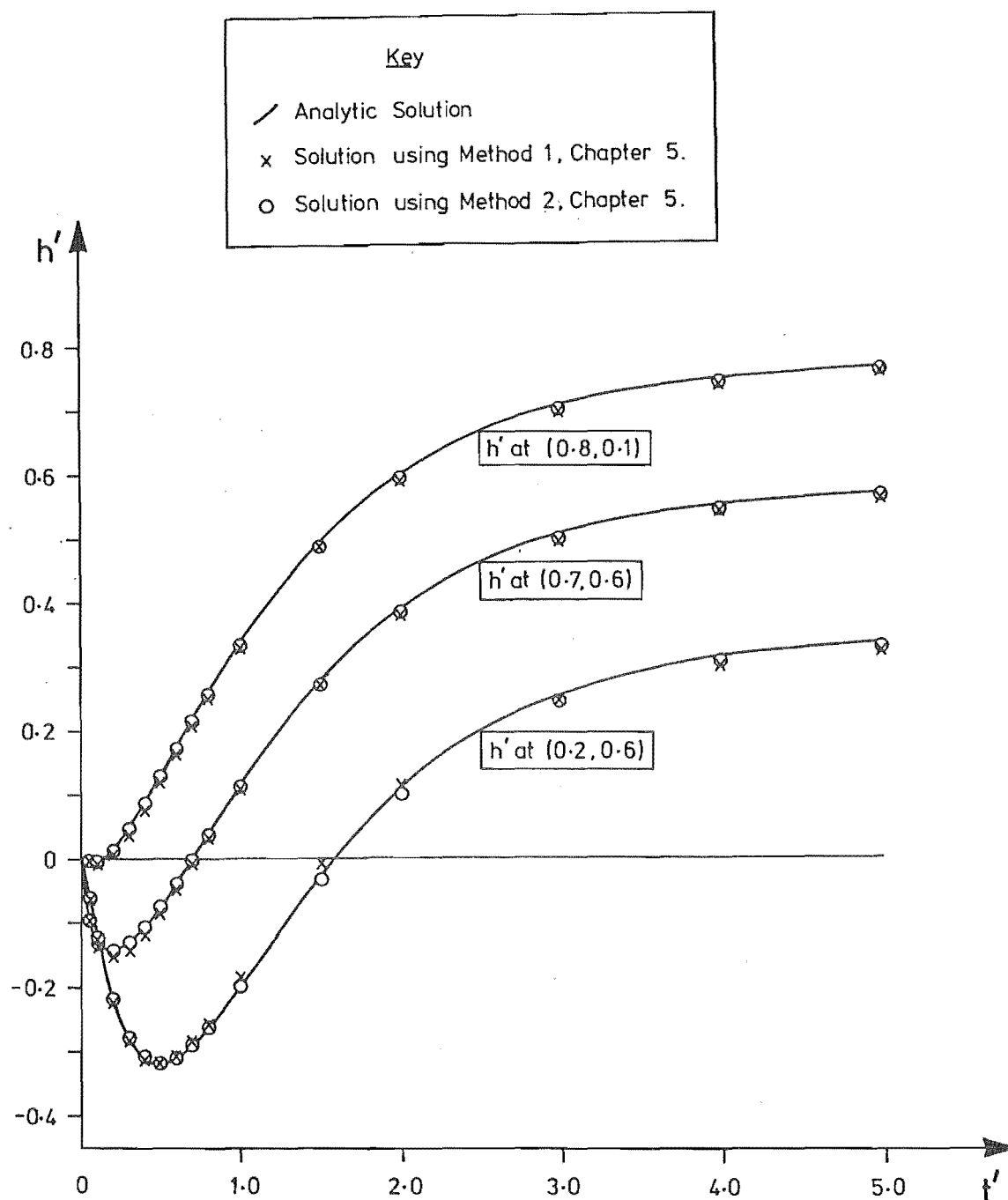


Fig. 6.30 Variation of h' with time at three internal points for the problem shown in Fig. 6.29.

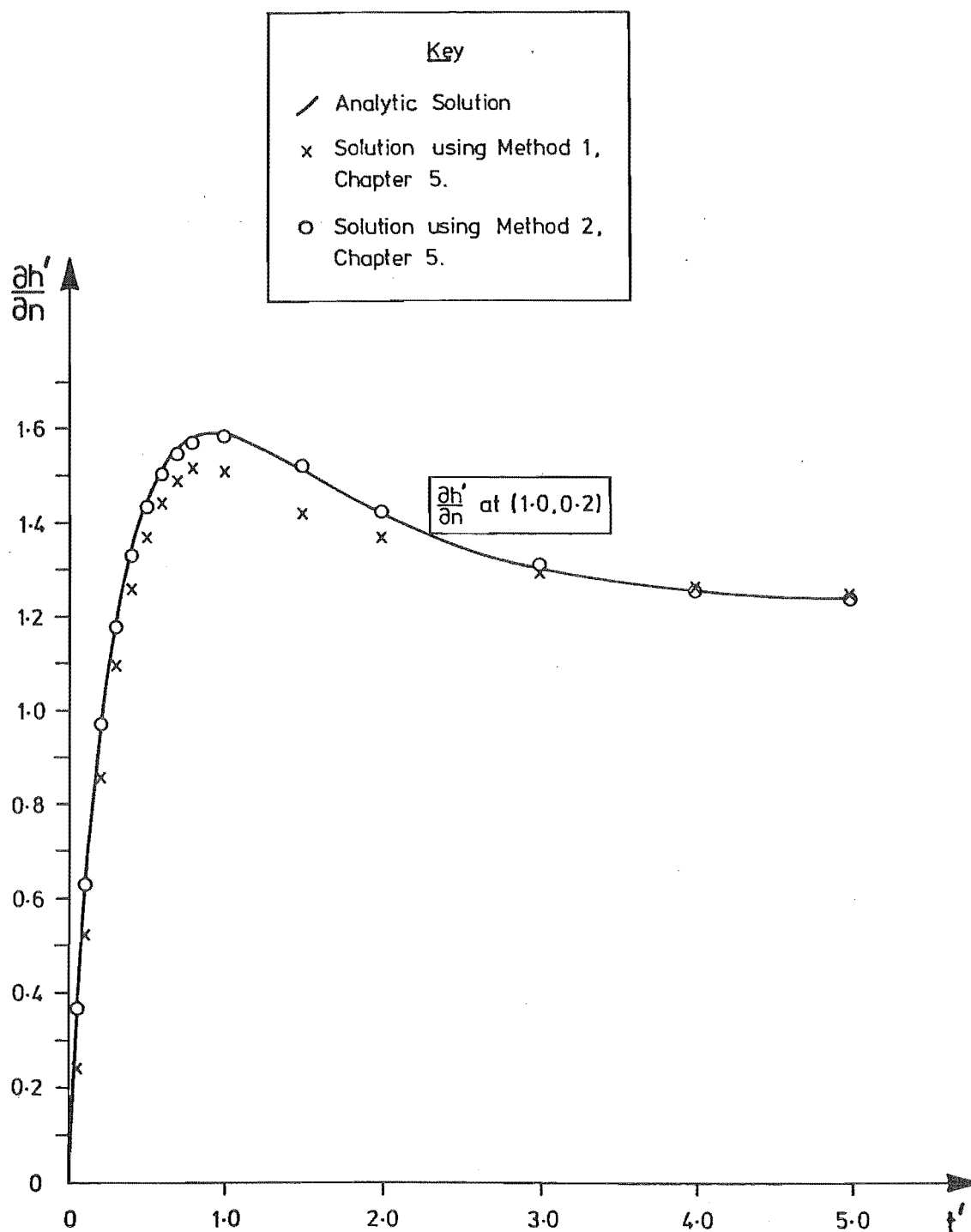


Fig. 6.31 Variation of $\frac{\partial h'}{\partial n}$ with time at (1.0, 0.2) for the problem shown in Fig. 6.29.

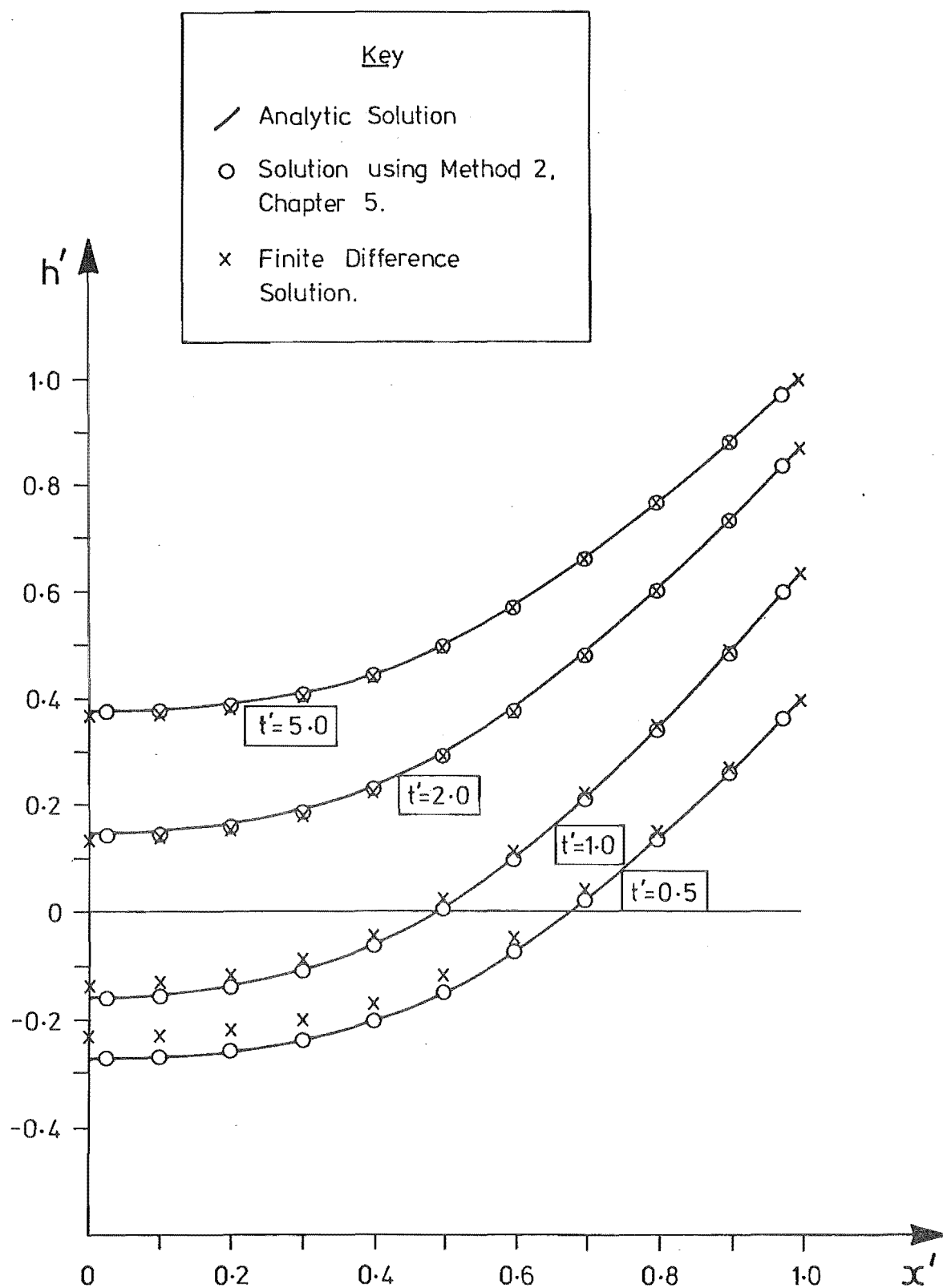


Fig. 6.32 Comparison between Method 2 and Finite-Difference Solutions on $y'=0$ for the problem shown in Fig. 6.29.

As a second example suppose that $\epsilon=500$ and the well at $(0.5, 0.5)$ pumps a flow rate of $\frac{Q'}{4\pi} = 0.1$, as shown in Fig. 6.33. Because the rise in h' is essentially instantaneous when $\epsilon=500$, time steps TS1 have been used in the numerical calculations. Values of h' on the boundary contour and at several points within the flow region are compared in Figs 6.33 and 6.34, respectively, while the solutions for $\frac{\partial h'}{\partial n}$ at $(1.0, 0.2)$, are shown in Fig. 6.35.

The two examples studied in this section both have solutions which are symmetrical about $y'=0.5$. However, if the head at $x'=1.0$ is given by $h'=1-e^{-t'}$ and there is a well of strength $\frac{Q'}{4\pi} = 0.1$ at $(0.25, 0.25)$ the solution given by Eqn 6.20 is asymmetric. The numerical solutions to this problem were calculated using time steps TS2. Values of h' along two sides of the square, namely $y'=0$ and $x'=0$, are compared to Eqn 6.20 in Figs 6.36 and 6.37, respectively. The solutions for h' at three points within the flow region are given in Fig. 6.38 and the solutions for $\frac{\partial h'}{\partial n}$ at $(1.0, 0.2)$ and $(1.0, 0.8)$ are given in Fig. 6.39. The agreement between the Method 2 and exact solutions is once again satisfactory, while the solution obtained with Method 1 is again limited by the length of the time steps. In the two previous examples finite-difference solutions were calculated using a nodal spacing of 0.1. Because the well in this problem would not coincide with a node at this spacing, a spacing of 0.05 was selected. This resulted in a total of 441 nodes. Fig. 6.40 shows the comparison between the finite-difference solution on $y'=1.0$ and the solution obtained using Method 2. Although the finite-difference solution is nearly as accurate as Method 2, it should be realised that the computational times are approximately equal and that the finite-difference solution requires about ten times the data preparation of Method 2.

Consider the flow of groundwater in the semi-infinite homogeneous region $x'>0$ and $y'>0$. If there are wells of strength Q' at (x'_0, y'_0) and (y'_0, x'_0) and if the initial and boundary conditions are given by;

PROBLEM DEFINITION

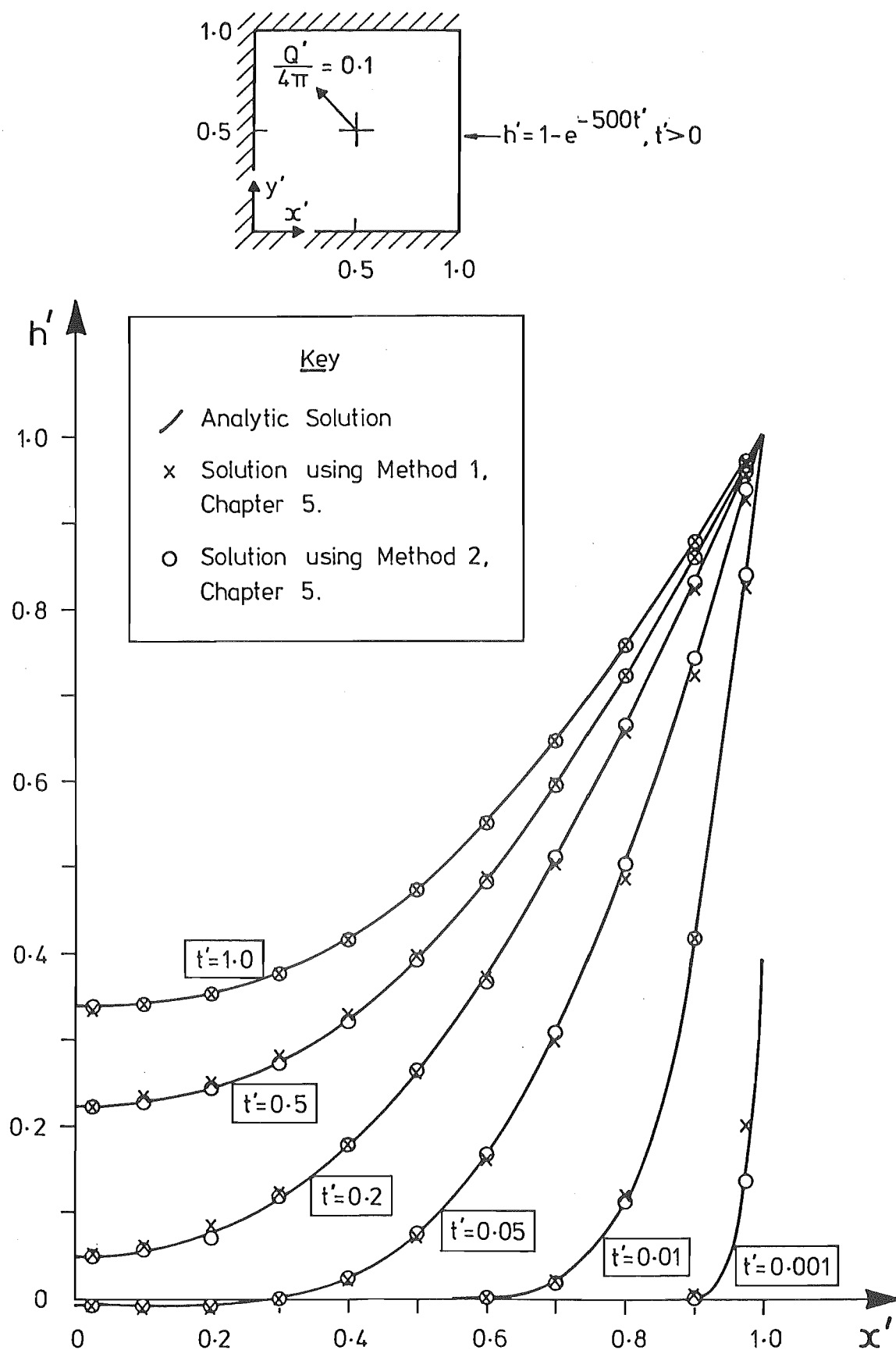


Fig. 6.33 Distribution of h' on $y'=0$ when $h'(x'=1.0, t') = 1 - e^{-500t'}$, $t' > 0$ and there is a well of strength $\frac{Q'}{4\pi} = 0.1$ at $(0.5, 0.5)$.

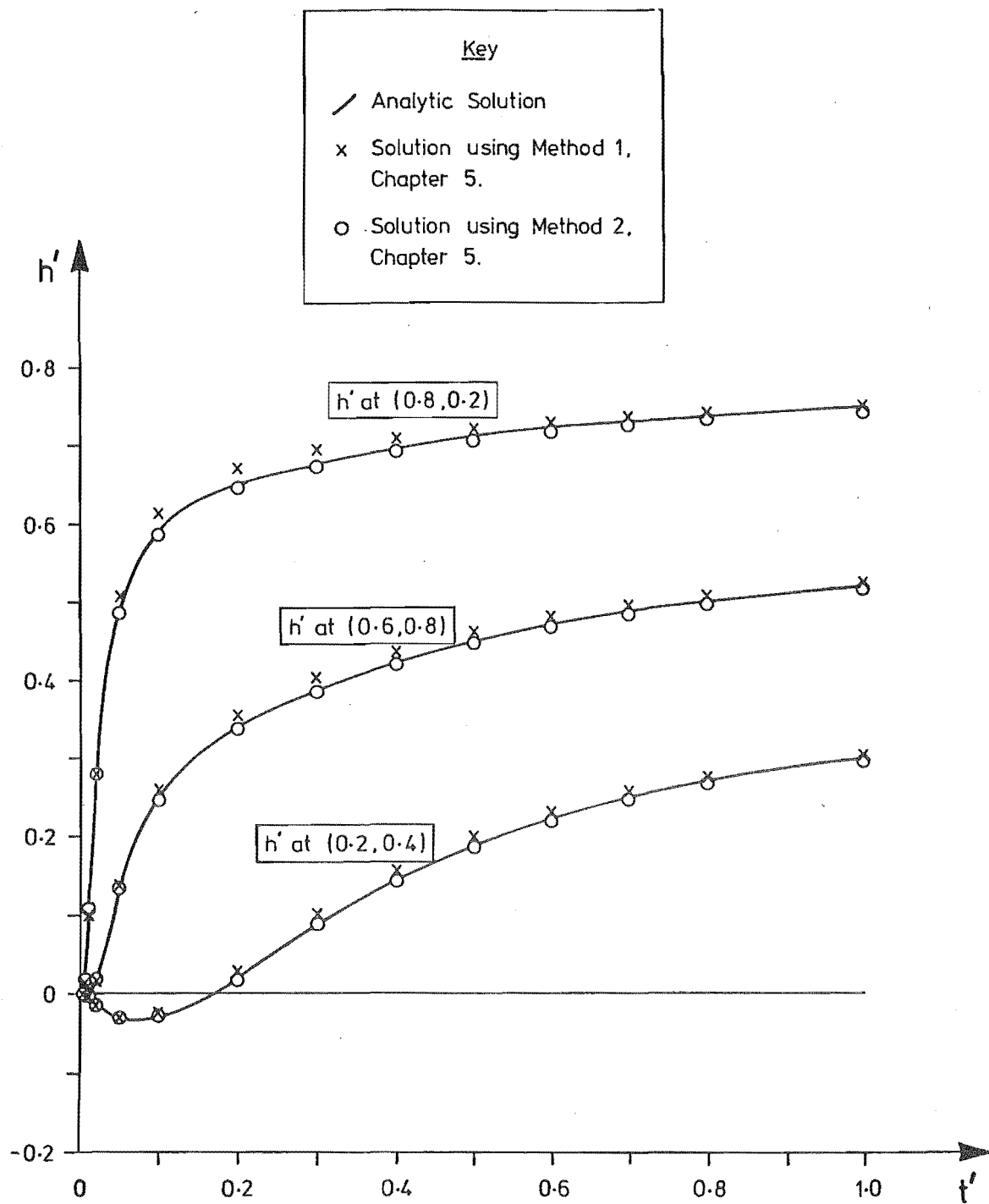


Fig. 6.34 Variation of h' with time at three internal points for the problem shown in Fig. 6.33.

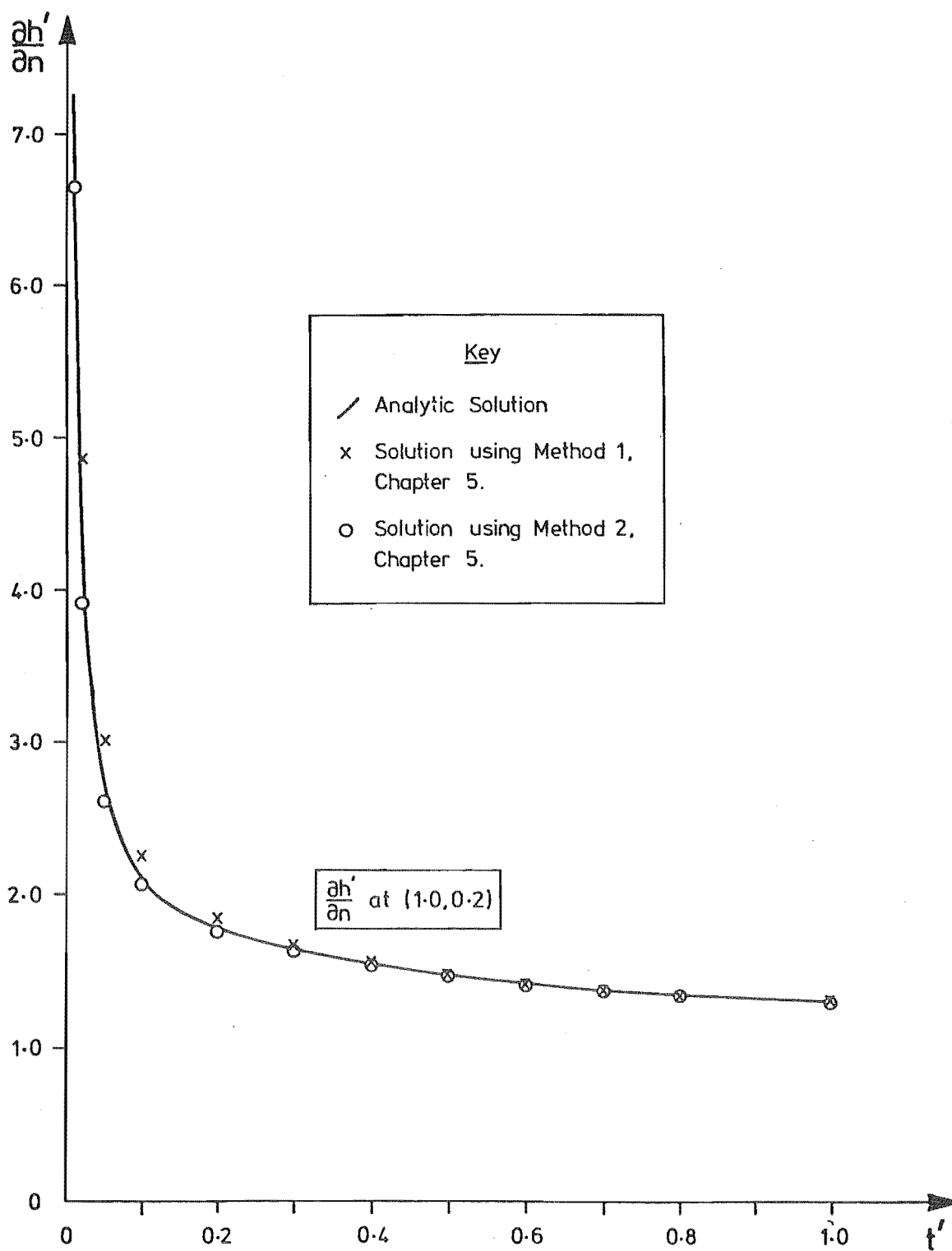


Fig. 6.35 Variation of $\frac{\partial h'}{\partial n}$ with time at (1.0, 0.2) for the problem shown in Fig. 6.33.

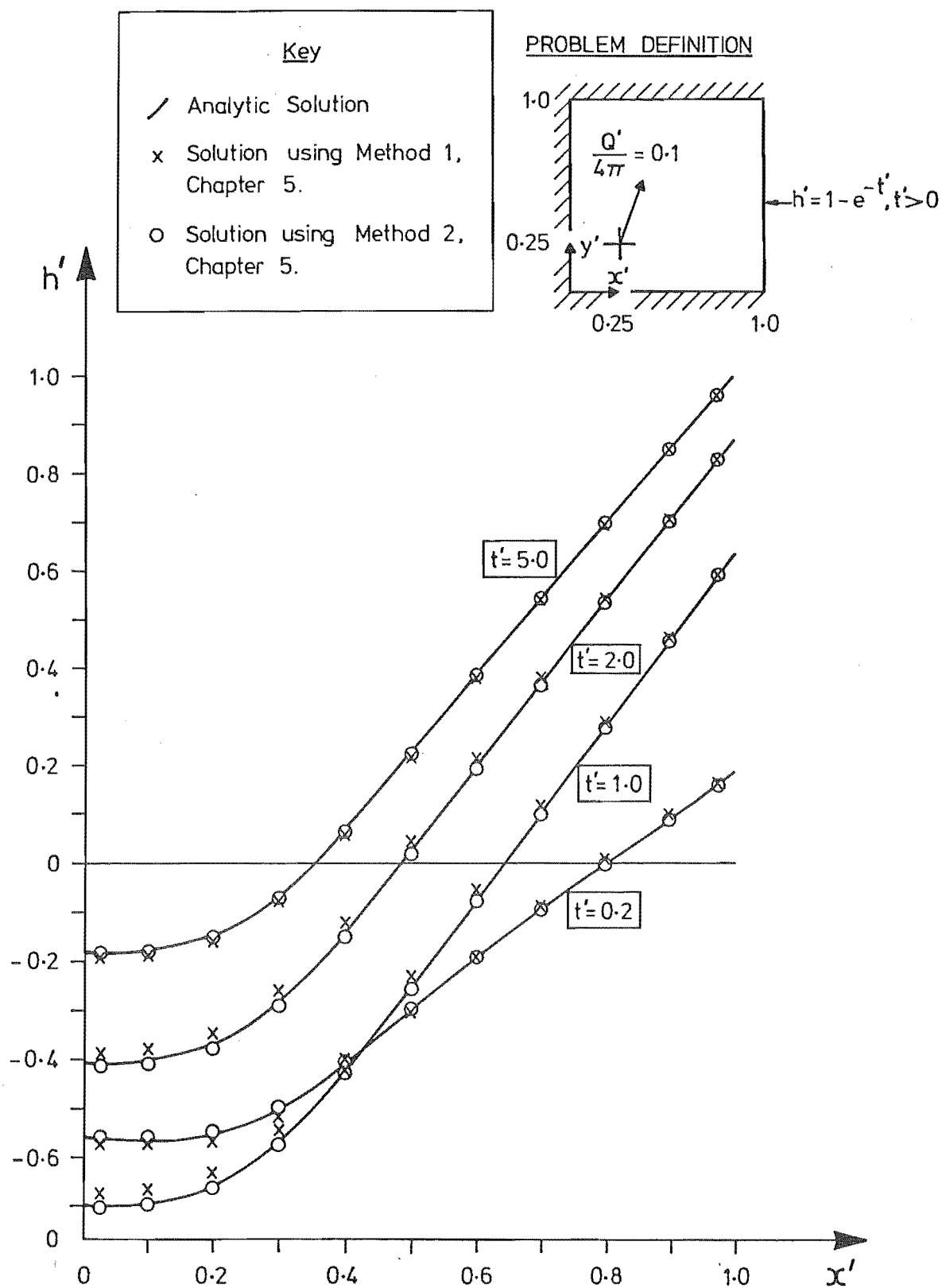


Fig. 6.36 Distribution of h' on $y'=0$ when $h'(x'=1.0, t') = 1 - e^{-t'}$, $t' > 0$ and there is a well of strength $\frac{Q'}{4\pi} = 0.1$ at $(0.25, 0.25)$.

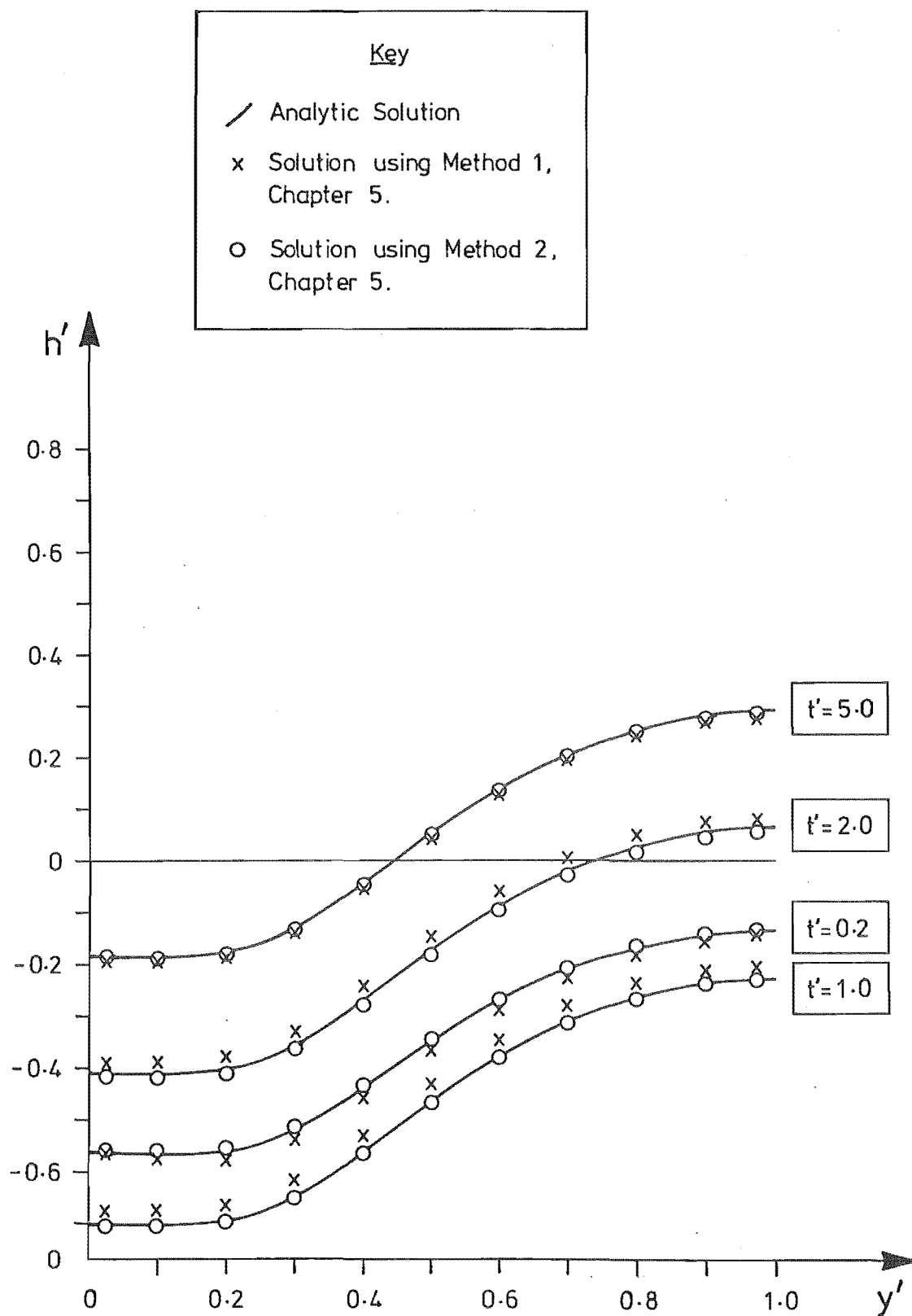


Fig. 6.37 Distribution of h' on $x'=0$ for the problem shown in Fig. 6.36.

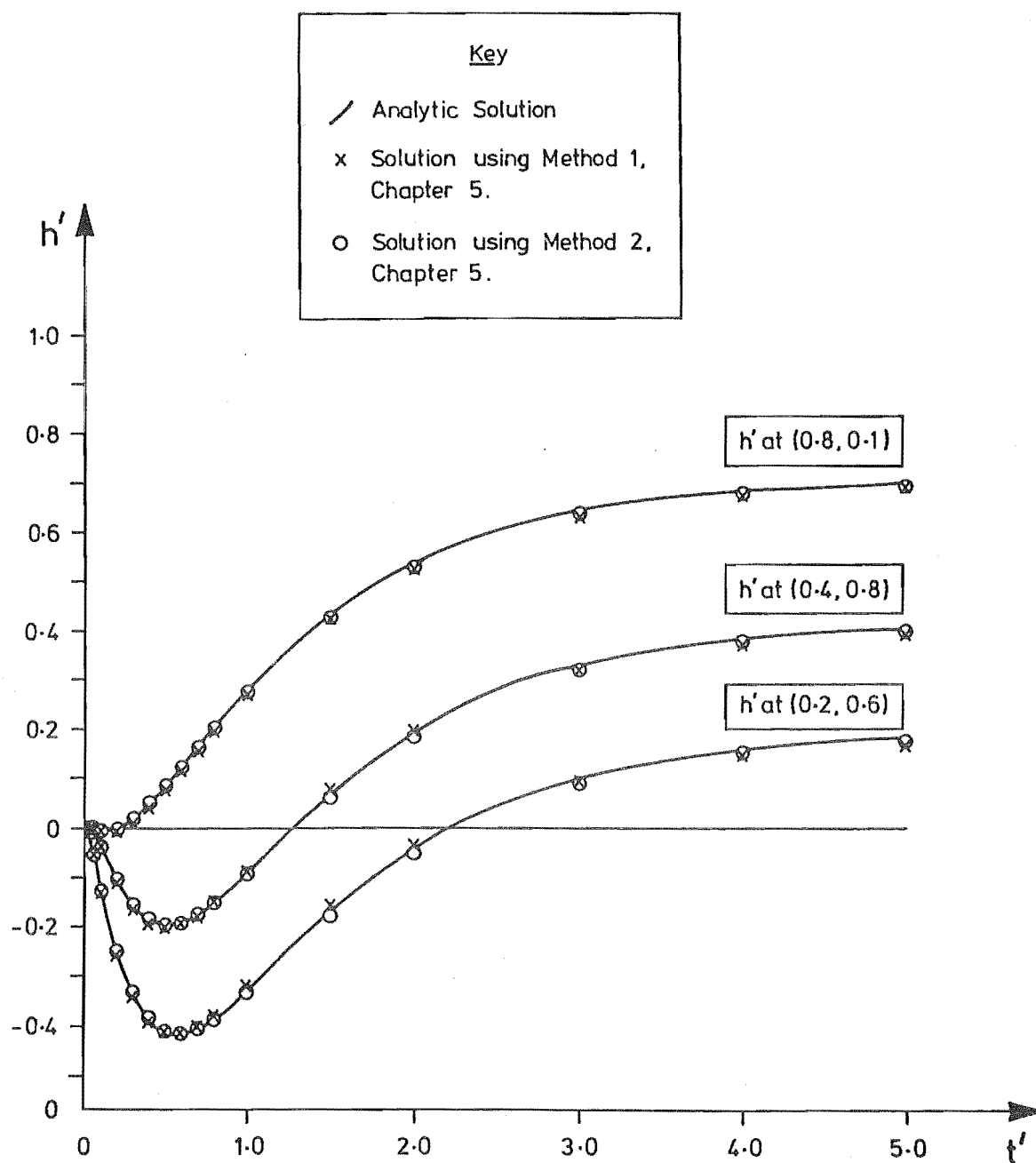


Fig. 6.38 Variation of h' with time at three internal points for the problem shown in Fig. 6.36.

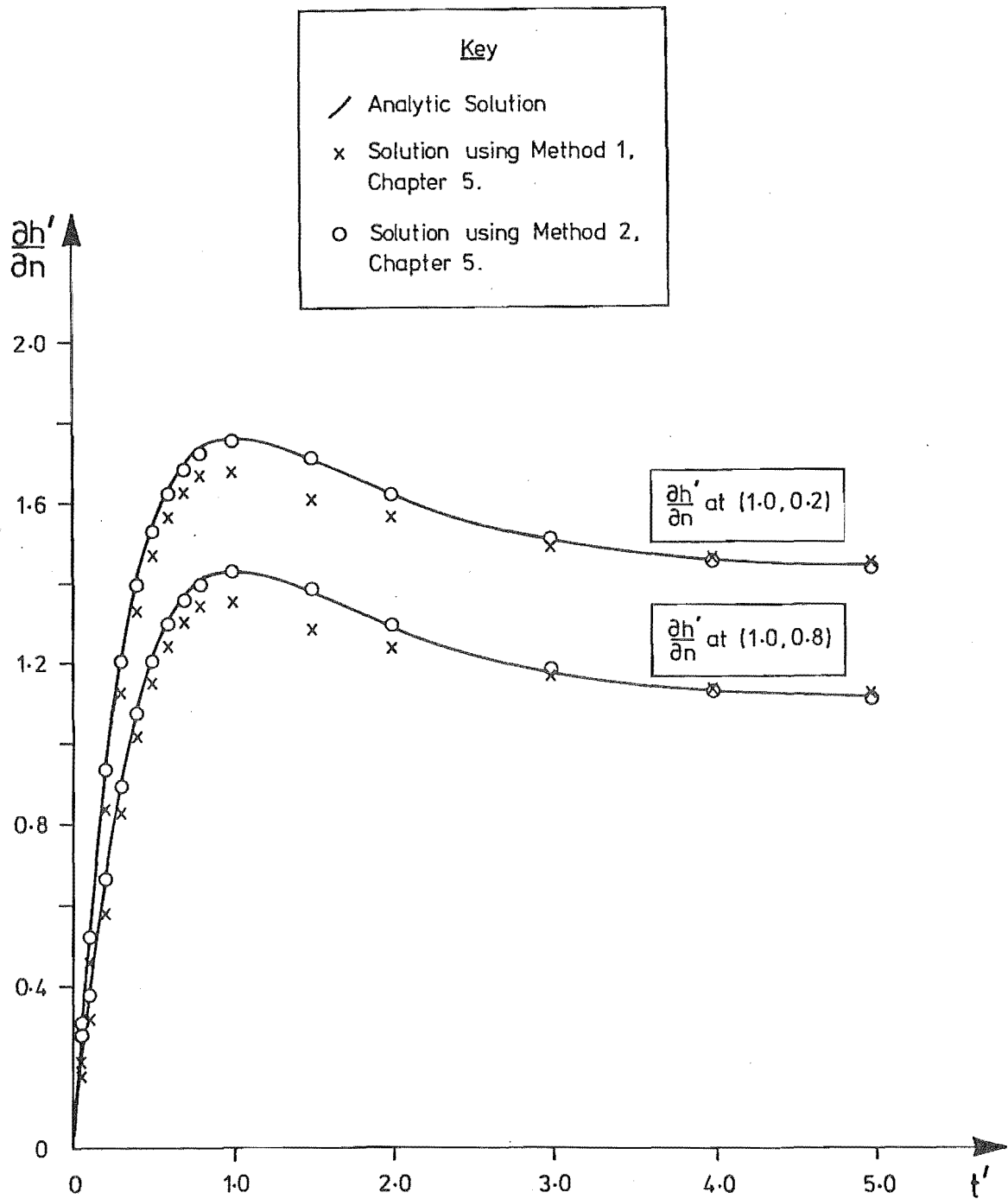


Fig. 6.39 Variation of $\frac{\partial h'}{\partial n}$ with time at two points on $x'=1.0$ for the problem shown in Fig. 6.36.

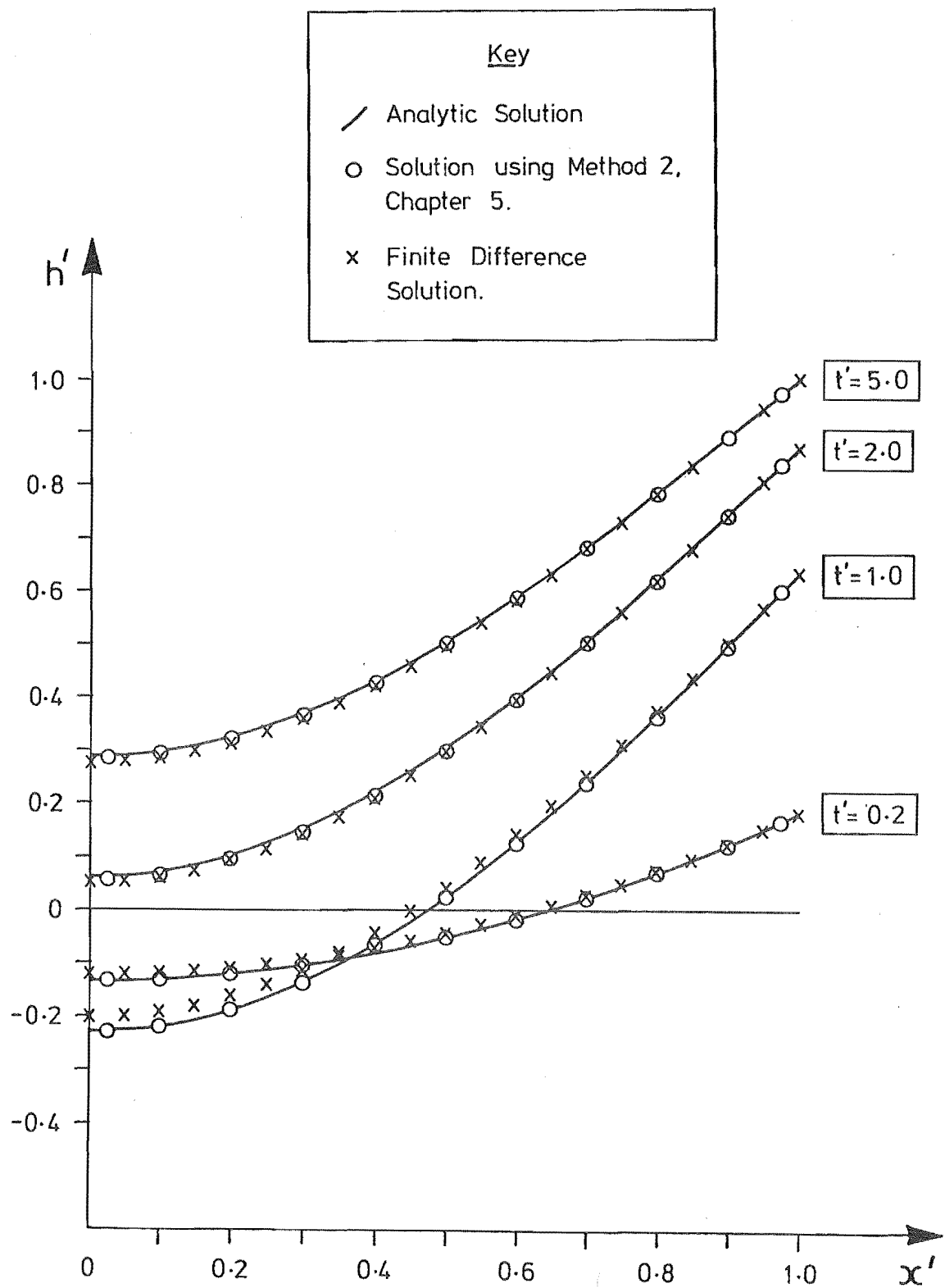


Fig. 6.40 Comparison between Method 2 and Finite-Difference solutions on $y'=1.0$ for the problem shown in Fig. 6.36.

$$h'(x', y', t'=0) = 0$$

$$h'(x'=0, y', t') = \operatorname{erfc} \left(\frac{y'}{2\sqrt{t'}} \right) \quad (6.22)$$

$$h'(x', y'=0, t') = \operatorname{erfc} \left(\frac{x'}{2\sqrt{t'}} \right)$$

then it can be shown that

$$\begin{aligned} h'(x', y', t') &= \operatorname{erfc} \left(\frac{x'}{2\sqrt{t'}} \right) \operatorname{erfc} \left(\frac{y'}{2\sqrt{t'}} \right) \\ &+ \frac{Q'}{4\pi} \left[E_1 \left[\frac{(x'+y'_0)^2 + (y'-x'_0)^2}{4t'} \right] + E_1 \left[\frac{(x'+x'_0)^2 + (y'-y'_0)^2}{4t'} \right] \right. \\ &+ E_1 \left[\frac{(x'-y'_0)^2 + (y'+x'_0)^2}{4t'} \right] + E_1 \left[\frac{(x'-x'_0)^2 + (y'+y'_0)^2}{4t'} \right] \\ &- E_1 \left[\frac{(x'-x'_0)^2 + (y'-y'_0)^2}{4t'} \right] - E_1 \left[\frac{(x'-y'_0)^2 + (y'-x'_0)^2}{4t'} \right] \\ &\left. - E_1 \left[\frac{(x'+x'_0)^2 + (y'+y'_0)^2}{4t'} \right] - E_1 \left[\frac{(x'+y'_0)^2 + (y'+x'_0)^2}{4t'} \right] \right] \quad (6.23) \end{aligned}$$

in which $\operatorname{erfc}(x)$ is the complementary error function.

Because of the symmetrical nature of Eqn 6.23 there is no flow across the line $y'=x'$.

Consider flow through the region shown in Fig. 6.41, which encloses the well at (x'_0, y'_0) . If the line $y'=x'$ is an impermeable boundary and if h' on the rest of the boundary contour is given by Eqn 6.23, then the solution for h' within this region is also given by Eqn 6.23. Numerical solutions were attempted for the case when a well of strength $\frac{Q'}{4\pi} = 0.1$ was located at $(0.7, 0.4)$. Time steps TS2 were selected for this problem. The solution obtained using Method 2 required 51 boundary nodes, spaced on average 0.047 apart, while the finite-difference solution used a nodal spacing of 0.04 which resulted in a total of 243 nodes. Values of h' along the impermeable boundary $y'=x'$ are compared with Eqn 6.23 in Fig. 6.41. The solution calculated using Method 2 is in good agreement at all times, but the finite-difference solution is quite inaccurate. The finite-difference solution takes only one fifth of the computational time and uses one tenth the computer storage of Method 2, but it also requires five times the data preparation. Fig. 6.42 shows the comparison between the analytical values of h' at three points within the flow region and those obtained using Method 2. The solutions for $\frac{\partial h'}{\partial n}$ at five points on the boundary contour are compared in Fig. 6.43. In all cases the agreement is very good.

6.4 FLOW IN COMPOSITE REGIONS

Consider the semi-infinite region $-1 < x' < 1$, of which $-1 < x' < 0$ is one homogeneous zone, and $0 < x' < 1$ another. Let T_1 and S_1 denote the transmissivity and storage coefficient, respectively, of the zone $-1 < x' < 0$, and T_2 and S_2 the corresponding quantities of the zone $0 < x' < 1$. Suppose the dimensionless head at $x' = -1.0$ is raised instantaneously to unity at $t' = 0$ while the head at $x' = 1.0$ is maintained at zero. If $T_1 = 4T_2$ and $S_1 = S_2$, Carslaw and Jaeger (1959) show that; for $-1 < x' < 0$,

$$h'(x', t') = \frac{1 - 0.25x'}{1.25} - \frac{1}{2.5\pi} \sum_{n=1}^{\infty} \frac{(-1)^n}{n} \sin n\pi x' e^{-n^2 \pi^2 t'}$$

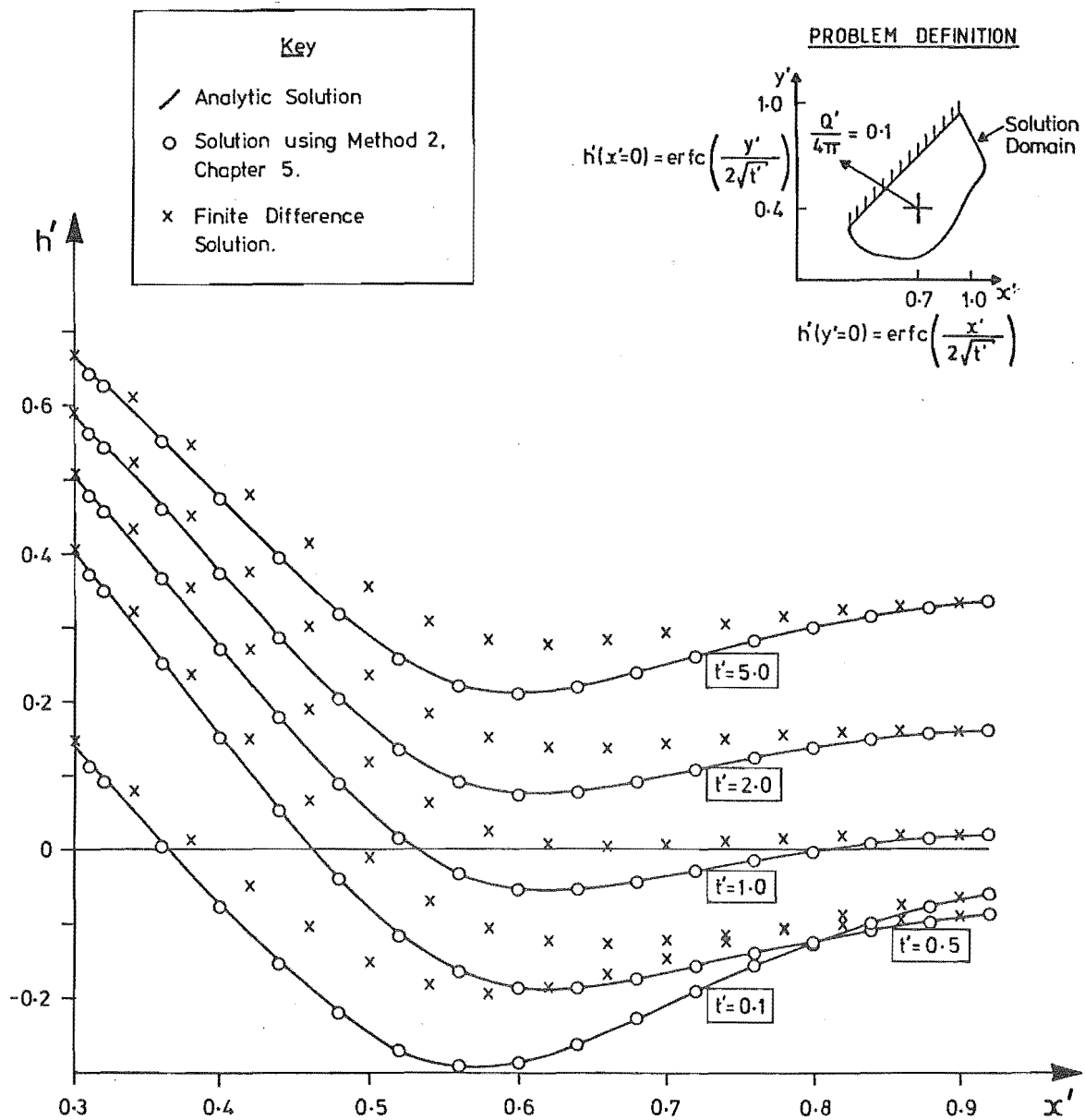


Fig. 6.41 Distribution of h' on $y'=x'$ when $\frac{\partial h'}{\partial n}(x'=y') = 0$ and h' on the permeable portion of the boundary is given by Eqn 6.23.

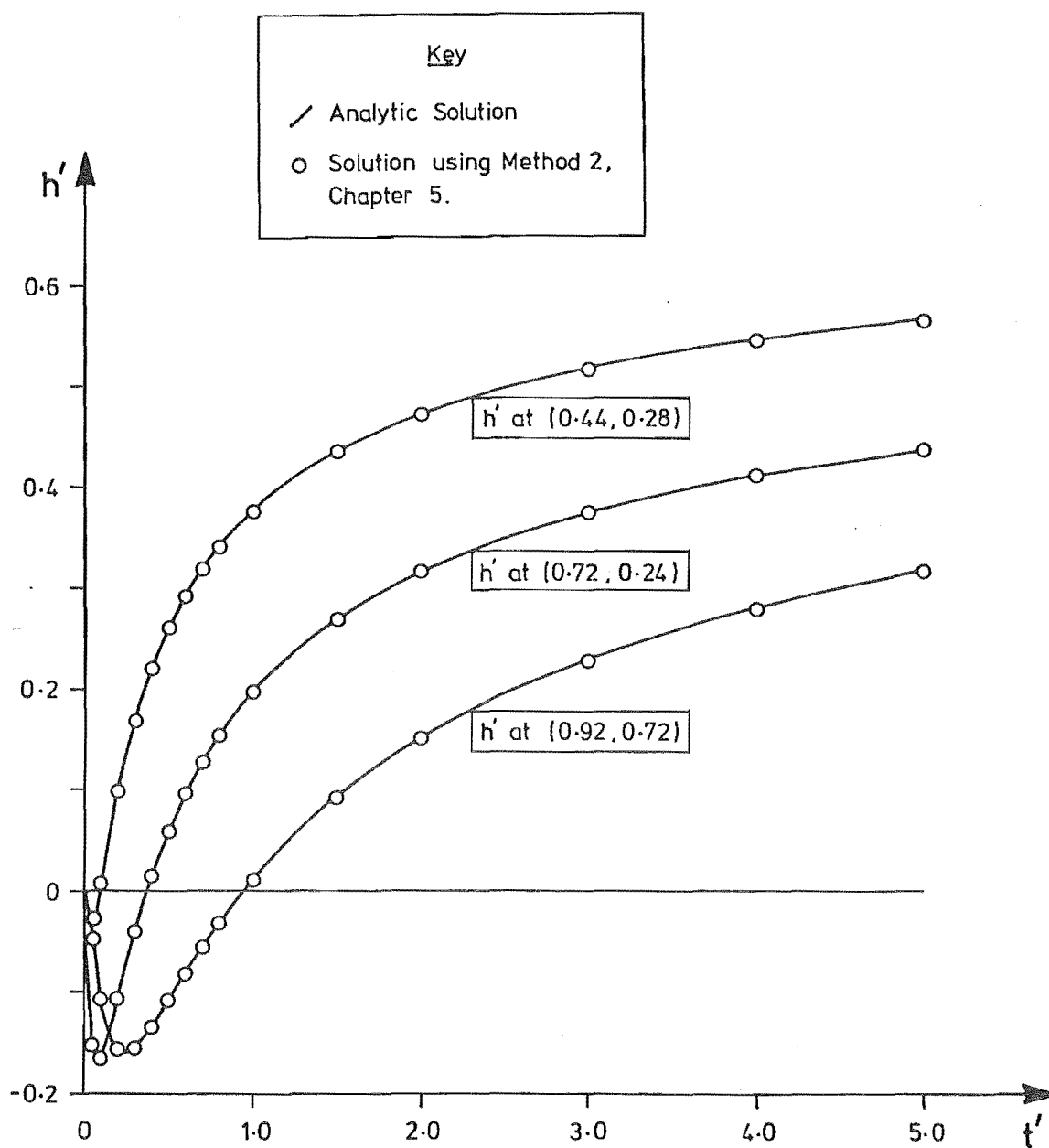


Fig. 6.42 Variation of h' with time at three internal points for the problem shown in Fig. 6.41.

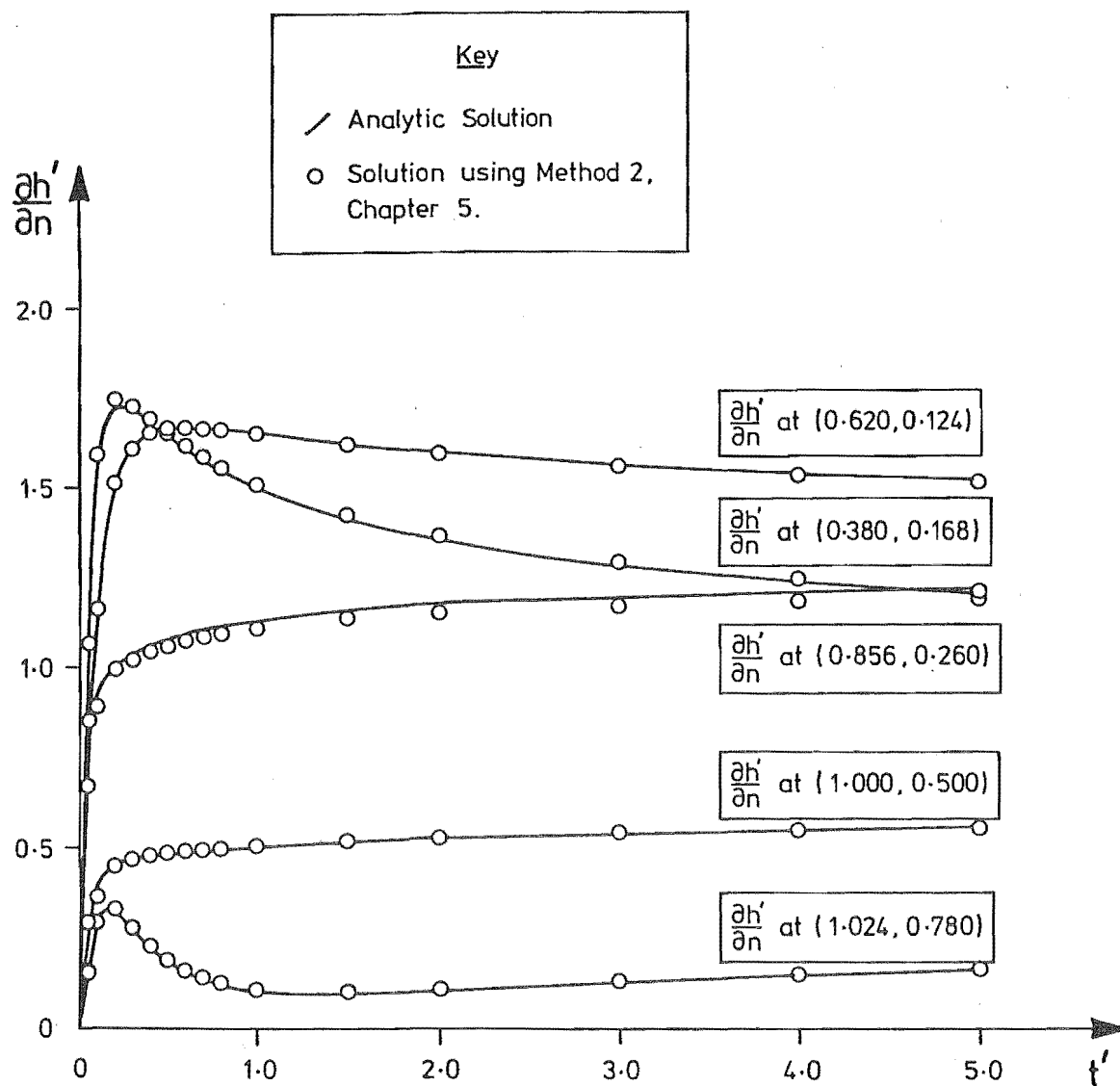


Fig. 6.43 Variation of $\frac{\partial h'}{\partial n}$ with time at various points on the boundary contour for the problem shown in Fig. 6.41.

$$- 2 \sum_{n=1}^{\infty} \frac{\sin^2 2\beta_n \sin \beta_n (1+x')}{\beta_n (\sin^2 2\beta_n + \sin^2 \beta_n)} e^{-\beta_n^2 t'} \quad (6.24)$$

and for $0 < x' < 1$

$$h'(x', t') = \frac{1-x'}{1.25} - \frac{1}{1.25\pi} \sum_{n=1}^{\infty} \frac{(-1)^n}{n} \sin 2n\pi x' e^{-n^2 \pi^2 t'} \\ - 2 \sum_{n=1}^{\infty} \frac{\sin \beta_n \sin 2\beta_n \sin 2\beta_n (1-x')}{\beta_n (\sin^2 2\beta_n + \sin^2 \beta_n)} e^{-\beta_n^2 t'} \quad (6.25)$$

in which β_n are the roots of $\cot \beta + \frac{1}{2} \cot 2\beta = 0$ and t' is defined in Eqn 6.1. Because the value of $\frac{\partial h'}{\partial n}$ at $x' = -1.0$ is infinite at $t' = 0$, the solution calculated at $x' = -1.0$ using Method 2 will be unstable. So that Method 2 can be used, consider flow in the two zoned square region shown in Fig. 6.44 when $h'(x' = -1.0) = 1.0$ and $h'(x' = 1.0) = 0$, for $t > 0$. Because the solution to this problem is a function of only one spatial dimension, x' , two sides of the square region, $y' = 0$ and $y' = 1.0$ can be considered impermeable. The boundary condition at $x' = -0.5$ is given by Eqn 6.24 and at $x' = 0.5$ by Eqn 6.25. The solutions to this problem calculated using Methods 1 and 2 were obtained using time steps TS2 and spacing boundary nodes for each zone 0.1 apart and 0.025 from sharp corners. This resulted in a total of 34 nodes for each zone, 11 of which were common to both. Numerically calculated values of h' on the impermeable boundary and at two points within each zone are compared with Eqns 6.24 or 6.25 in Figs 6.44 and 6.45, respectively. The solutions for $\frac{\partial h'}{\partial n}$ at $x' = \pm 0.5$, and on the interzonal boundary at $x' = 0$, are shown in Fig. 6.46. The solutions for h' and $\frac{\partial h'}{\partial n}$ on the boundary contour obtained using Method 1 converge towards the exact solution as time proceeds, but are a little inaccurate at earlier times. However there is satisfactory agreement in the solution for h' at internal points. There are no accuracy problems with Method 2, and all results are in good agreement.

PROBLEM DEFINITION

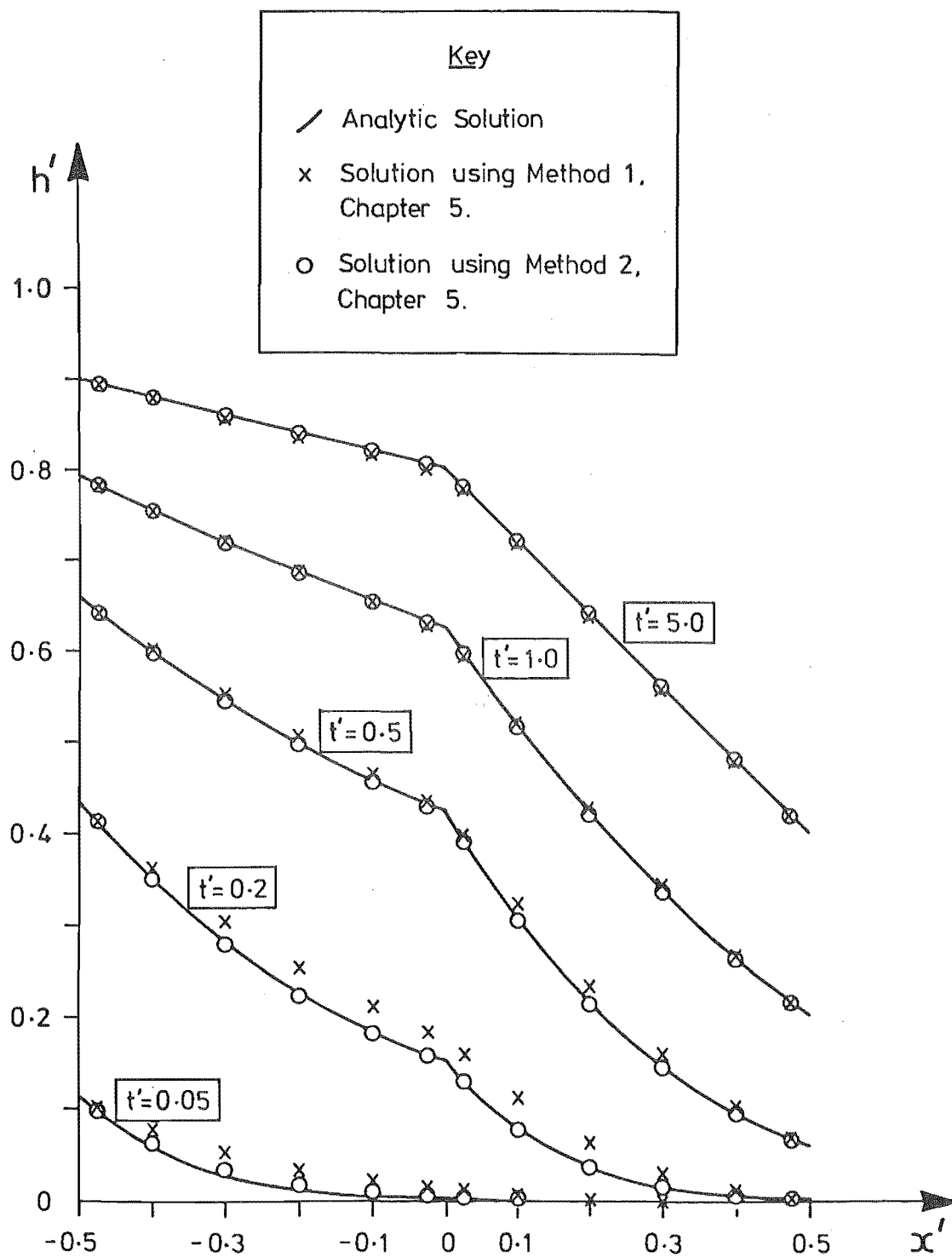
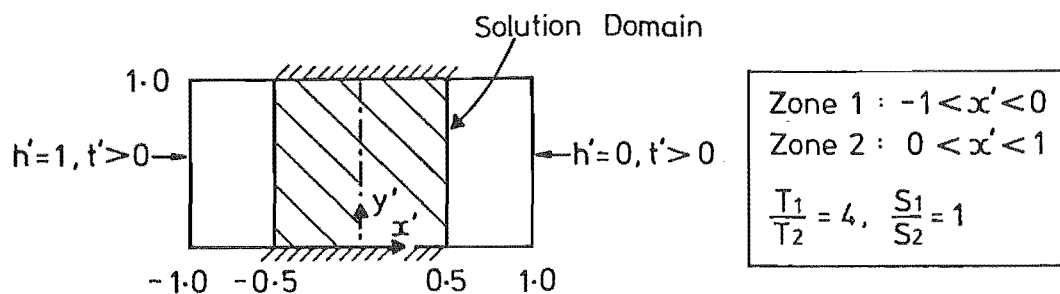


Fig. 6.44 Distribution of h' on $y'=0$ when $h'(x'=-1.0) = 1.0$ and $h'(x'=1.0) = 0$.

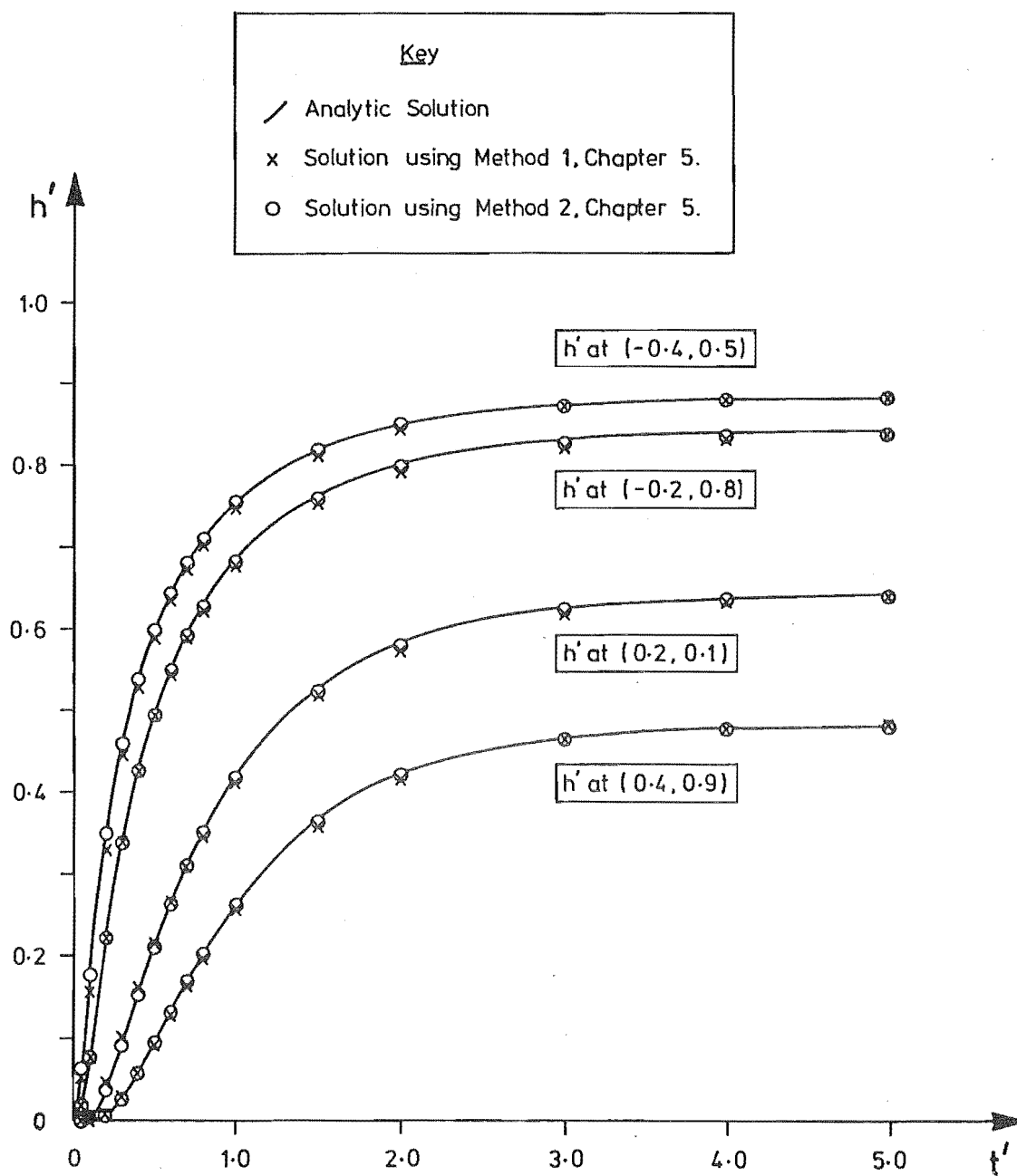


Fig. 6.45 Variation of h' with time at two points within each zone for the problem shown in Fig. 6.44.

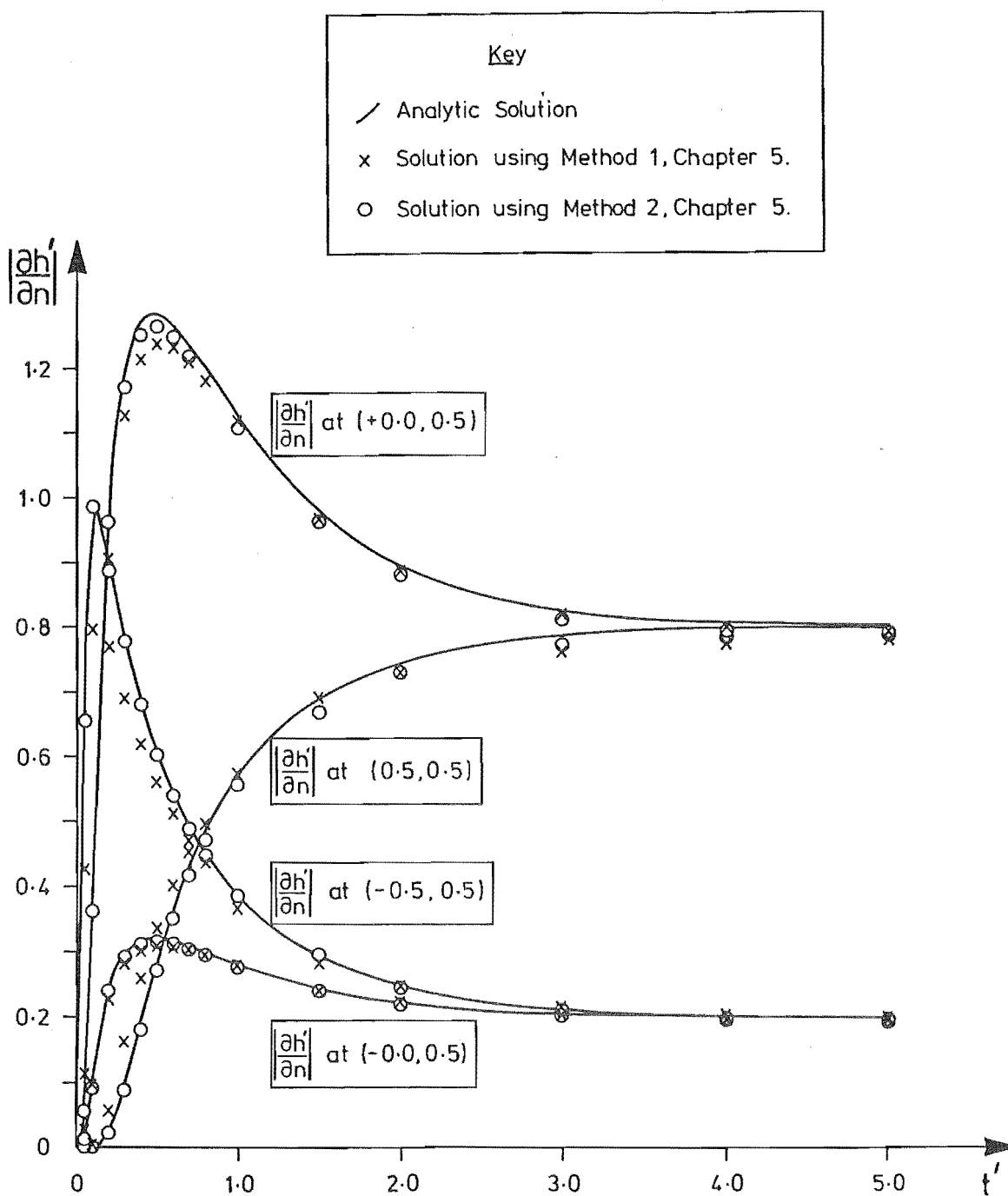


Fig. 6.46 Variation of $\frac{\partial h'}{\partial n}$ with time at $x' = -0.5$, $x' = 0.5$ and $x' = 0$ for the problem shown in Fig. 6.44.

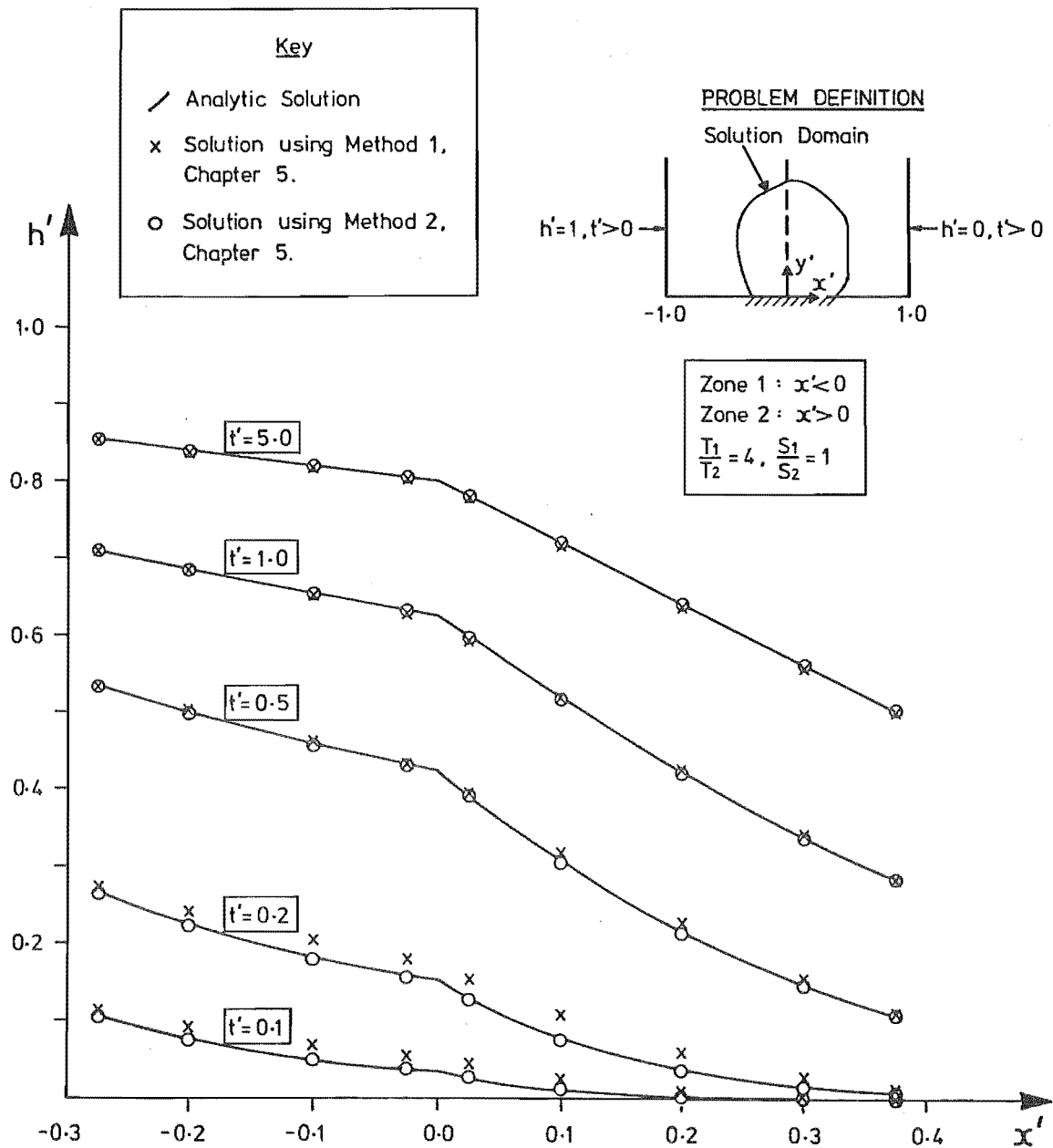


Fig. 6.47 Distribution of h' on $y'=0$ when $h'(x'=-1.0) = 1.0$, $h'(x'=1.0) = 0$ and the boundary contour is irregular.

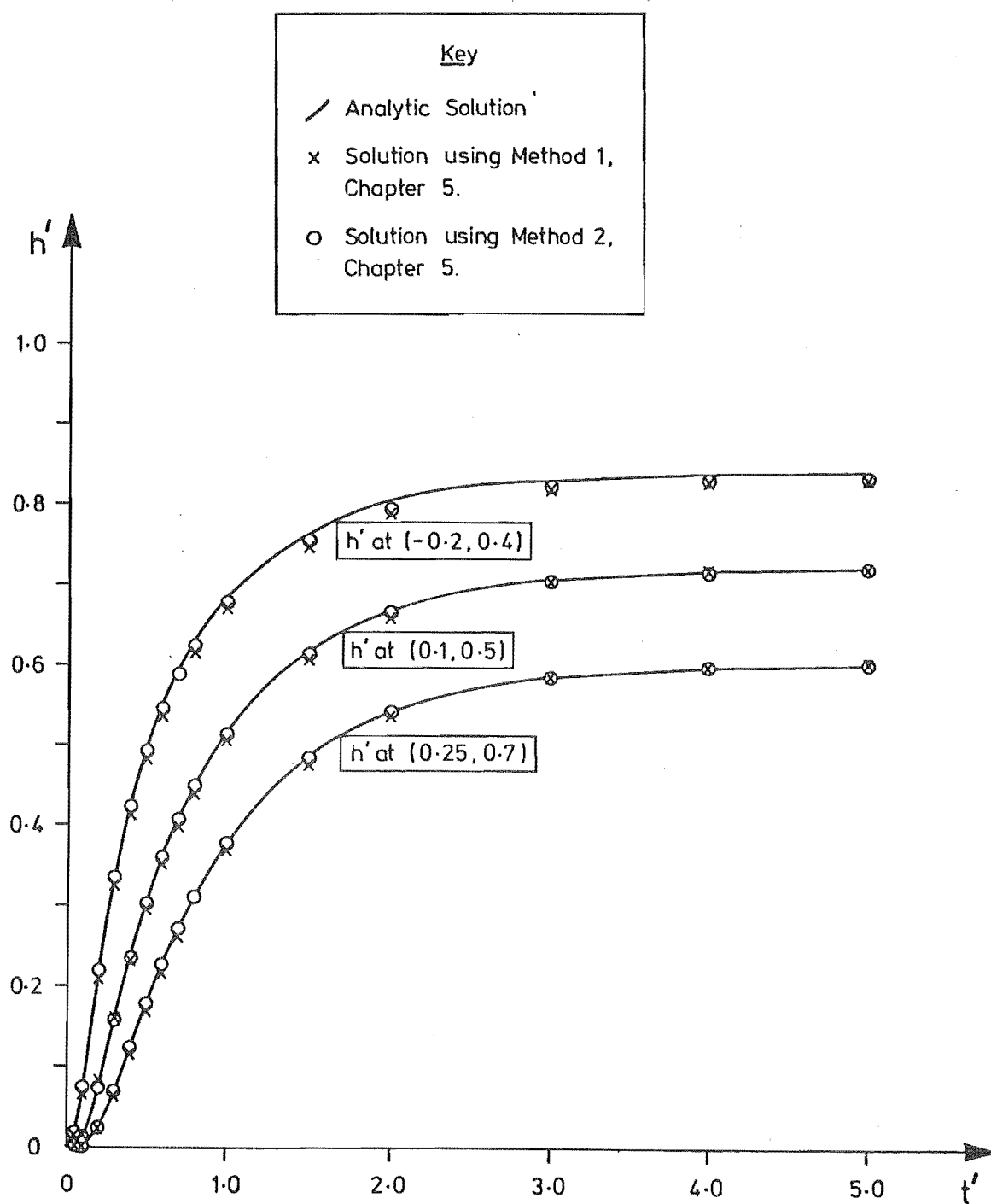


Fig. 6.48 Variation of h' with time at three internal points for the problem shown in Fig. 6.47.

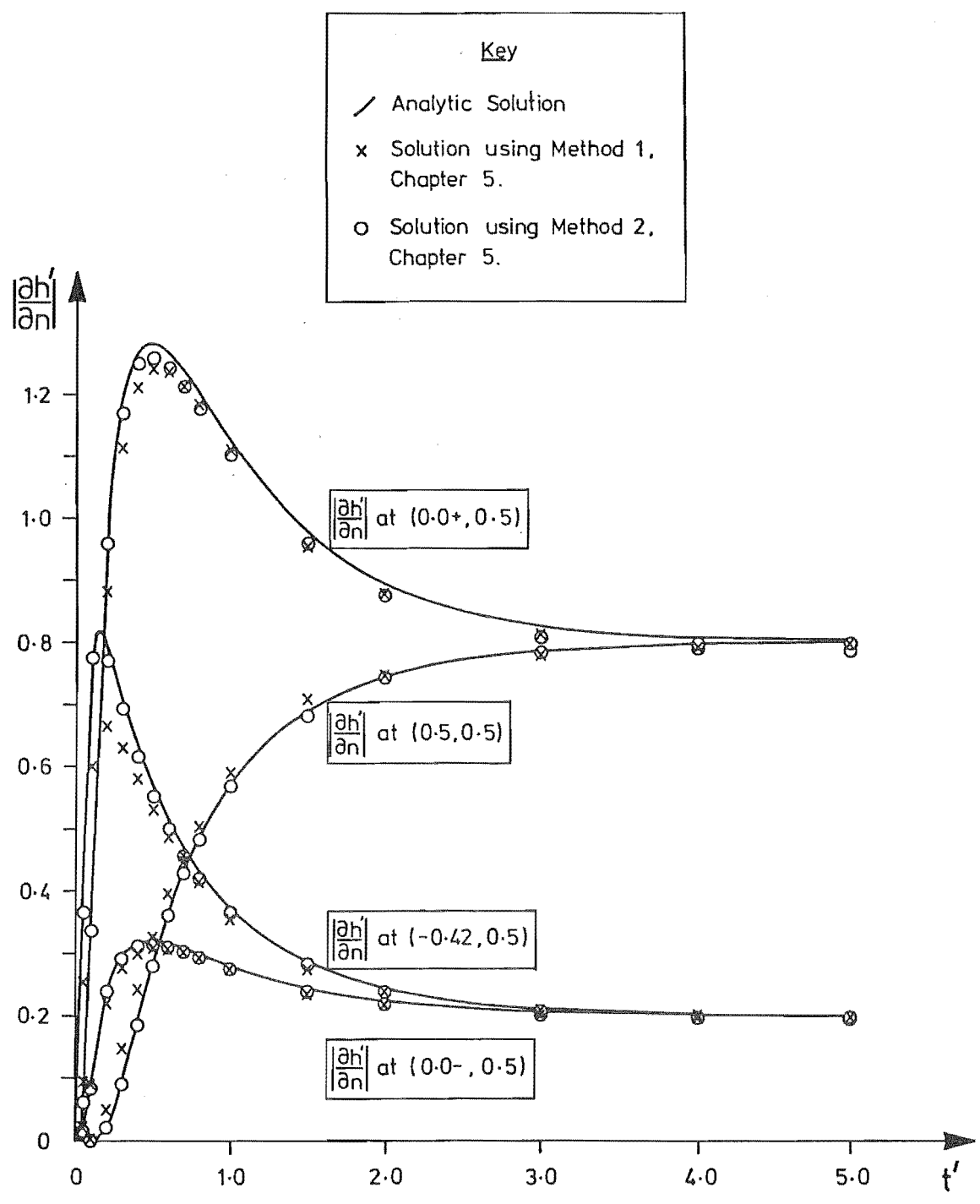


Fig. 6.49 Variation of $\frac{\partial h'}{\partial n}$ with time on the boundary contour for the problem shown in Fig. 6.47.

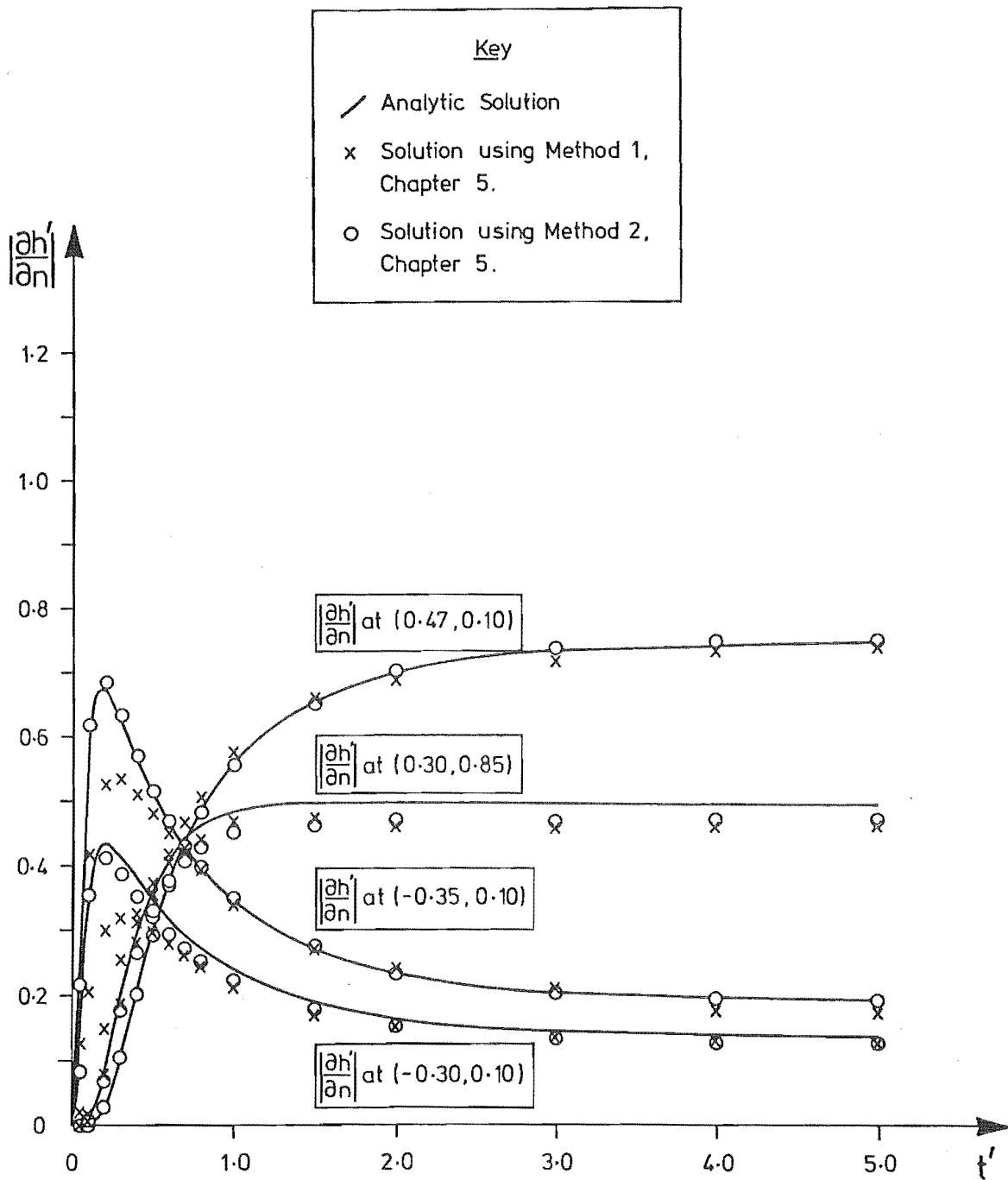


Fig. 6.50 Variation of $\frac{\partial h'}{\partial n}$ with time on the boundary contour for the problem shown in Fig. 6.47.

Consider flow through the unsymmetrical two zoned region shown in Fig. 6.47 when $h'(x'=-1.0) = 1.0$ and $h'(x'=1.0) = 0$, for $t > 0$. The horizontal portion of the external boundary ($y'=0$) is impermeable, while the boundary condition on the remainder of the boundary is given by Eqn 6.24 or 6.25, depending on whether x' is positive or negative. Numerical solutions to this problem were obtained by approximating zone 1 with 26 boundary nodes, zone 2 with 30 boundary nodes, and using time steps TS2. Values of h' along the impermeable boundary and at points within the solution domain are compared with Eqns 6.24 or 6.25 in Figs 6.47 and 6.48, respectively. The comparison between the numerical and analytical solutions for $\frac{\partial h'}{\partial n}$ around each zone are shown in Figs 6.49 and 6.50. Method 2 provides good results but the accuracy achieved with Method 1 is limited by the length of time step selected. The slight discrepancy between the numerical and analytical solutions for $\frac{\partial h'}{\partial n}$ at (0.30, 0.85) shown in Fig. 6.50, is due to the boundary contour curvature in the vicinity not being closely approximated by a second-order polynomial, as assumed in the numerical calculations.

Because there are very few analytical solutions for flows in composite regions, a homogeneous region can be divided into two or more separate zones and analysed as a composite region. For example, when h' on the fourth side of the homogeneous square region shown in Fig. 6.9 is given by $h'(x'=1.0, t') = 1 - e^{-t}$, $t > 0$ and the other three sides are impermeable, h' within the square region is given by Eqn 6.5. An alternative numerical solution to that calculated in Section 6.2 could be obtained by splitting the square into two zones, as shown in Fig. 6.51. Such a solution, using both Methods 1 and 2, has been calculated by spacing boundary nodes 0.1 apart and 0.025 from sharp corners, and by using time steps TS2. Numerical and analytical values of h' on the impermeable boundary are compared in Fig. 6.51, and values of h' within each zone are compared in Fig. 6.52. The solutions for $\frac{\partial h'}{\partial n}$ at $x'=1.0$, and at the interzonal boundary ($x'=0.5$), are compared in Fig. 6.53. As was the case previously, the solution obtained using Method 2 is in good

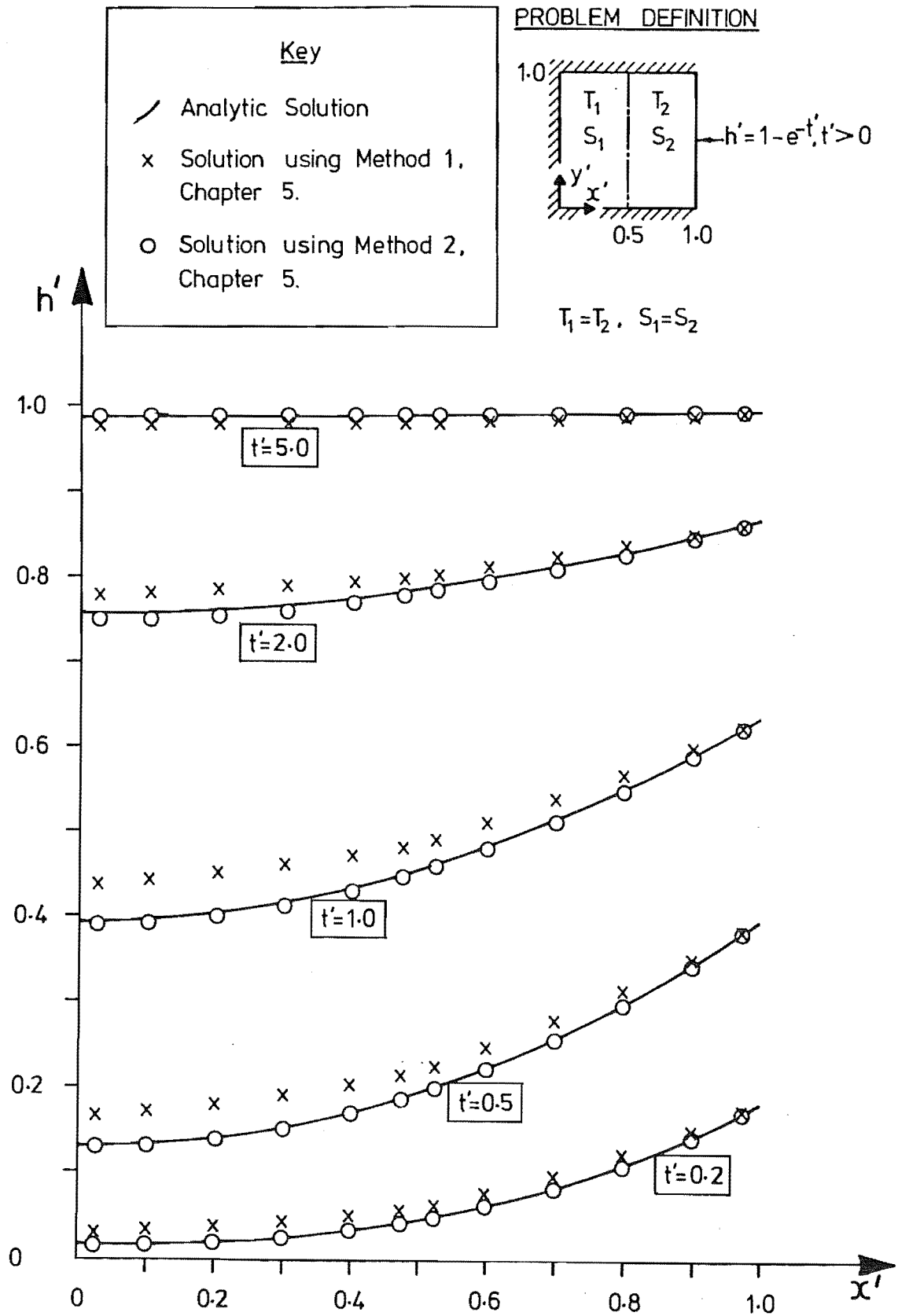


Fig. 6.51 Distribution of h' on $y'=0$ when $h'(x'=1.0, t') = 1 - e^{-t'}$, $t' > 0$ and the solution domain consists of two zones.

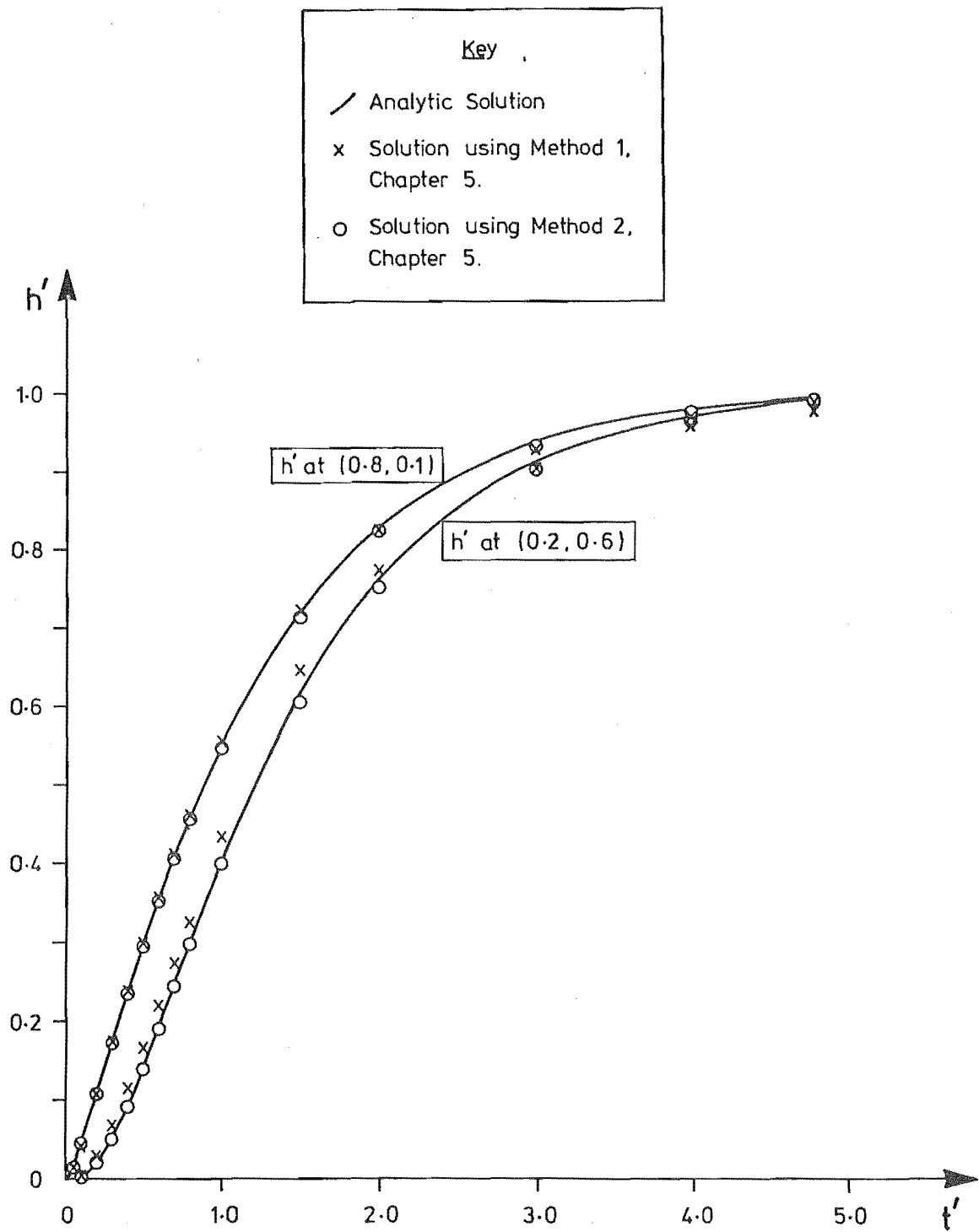


Fig. 6.52 Variation of h' with time at one point within each zone for the problem shown in Fig. 6.51.

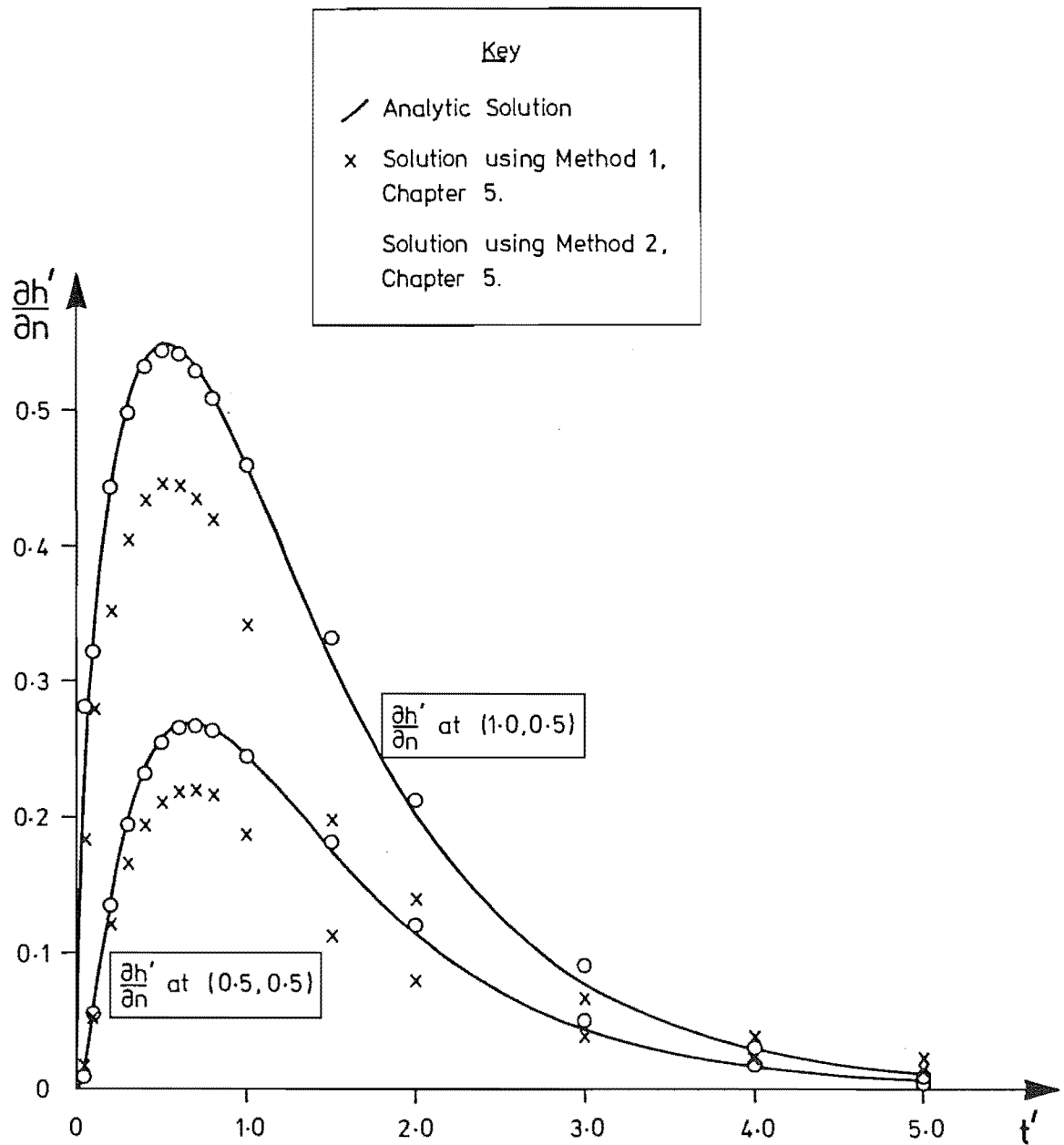


Fig. 6.53 Variation of $\frac{\partial h'}{\partial n}$ with time at (0.5, 0.5) and (1.0, 0.5) for the problem shown in Fig. 6.51.

agreement with the analytical solution; while the accuracy achieved with Method 1 is somewhat less.

As a second example, suppose that an abstraction well of strength $\frac{Q'}{4\pi} = 0.1$ is introduced into the square region at $(0.25, 0.25)$ at $t'=0$. If the boundary conditions are unchanged from the previous example then the exact solution for h' is given by Eqn 6.20. Numerical solutions have been attempted by splitting the square region into the two zones shown in Fig. 6.54. A nodal spacing of 0.1 with nodes placed 0.025 from sharp corners gives a total of 34 nodes in each zone, 11 of which are common to both. Time steps TS2 were used in the calculations. The solutions for h' on the impermeable and interzonal boundaries are compared with Eqn 6.20 in Figs 6.54-6.56, and 6.57, respectively, while values of h' within each zone are shown in Fig. 6.58. Figs 6.59 and 6.60 show the comparison between the numerical and analytical solutions for $\frac{\partial h'}{\partial n}$ at $x'=0.5$ and $x'=1.0$, respectively. The superior accuracy of Method 2 over Method 1 is quite apparent, especially in the solution for $\frac{\partial h'}{\partial n}$.

PROBLEM DEFINITION

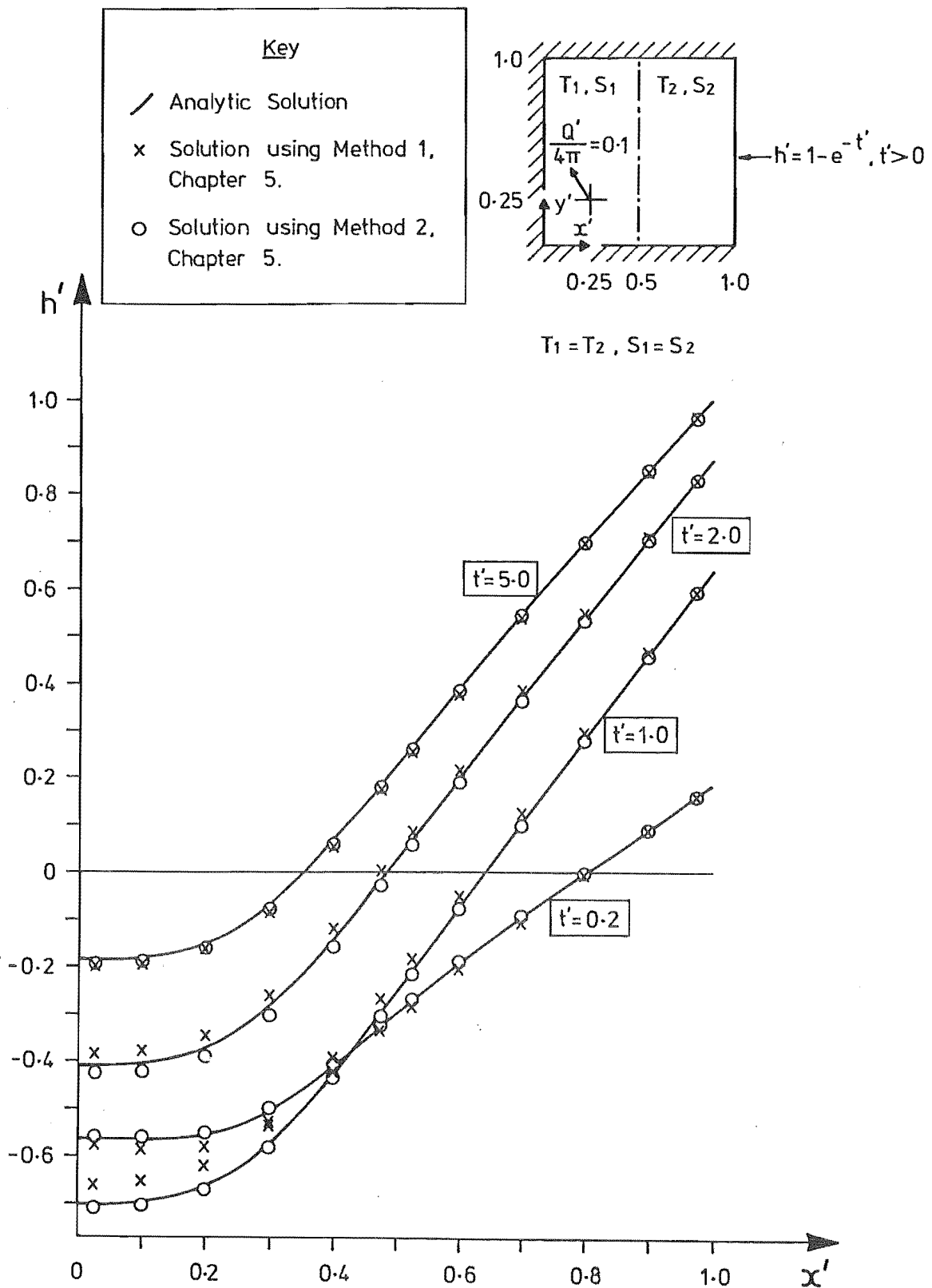


Fig. 6.54 Distribution of h' on $y'=0$ when $h'(x'=1.0, t') = 1 - e^{-t'}$, $t' > 0$ and there is a well of strength $\frac{Q'}{4\pi} = 0.1$. (The solution domain consists of two zones.)

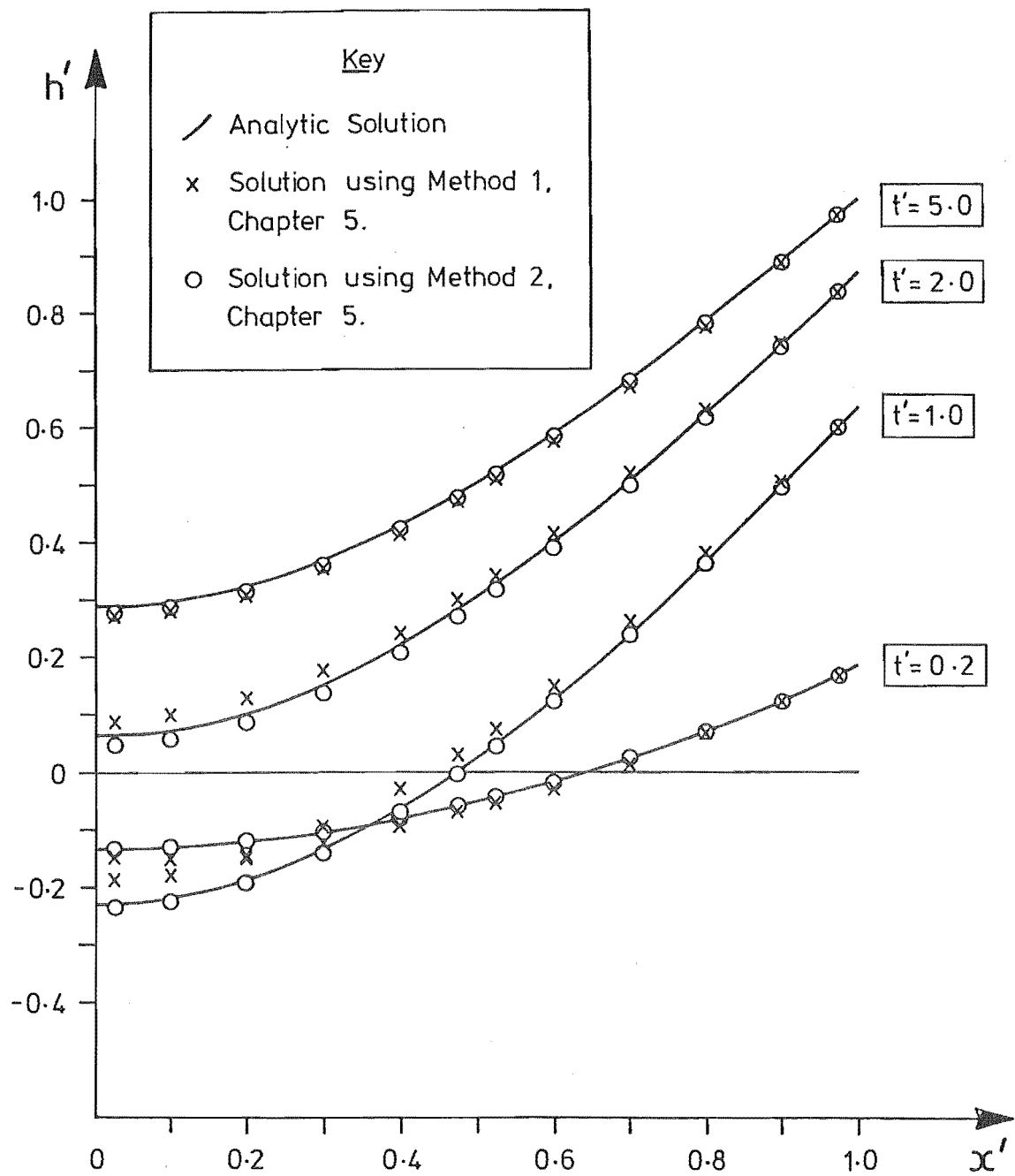


Fig. 6.55 Distribution of h' on $y'=1.0$ for the problem shown in Fig. 6.54.

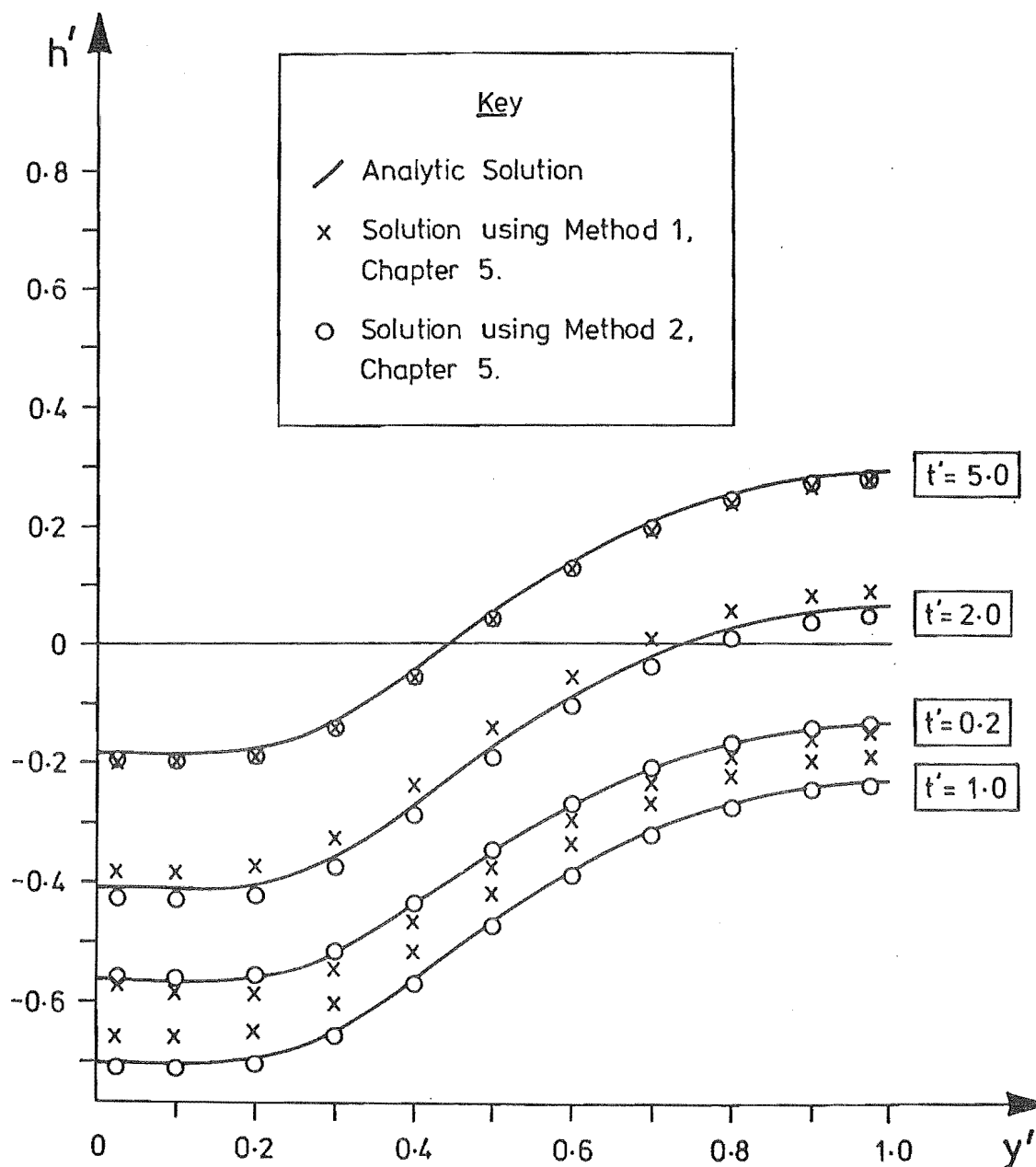


Fig. 6.56 Distribution of h' on $x'=0$ for the problem shown in Fig. 6.54.

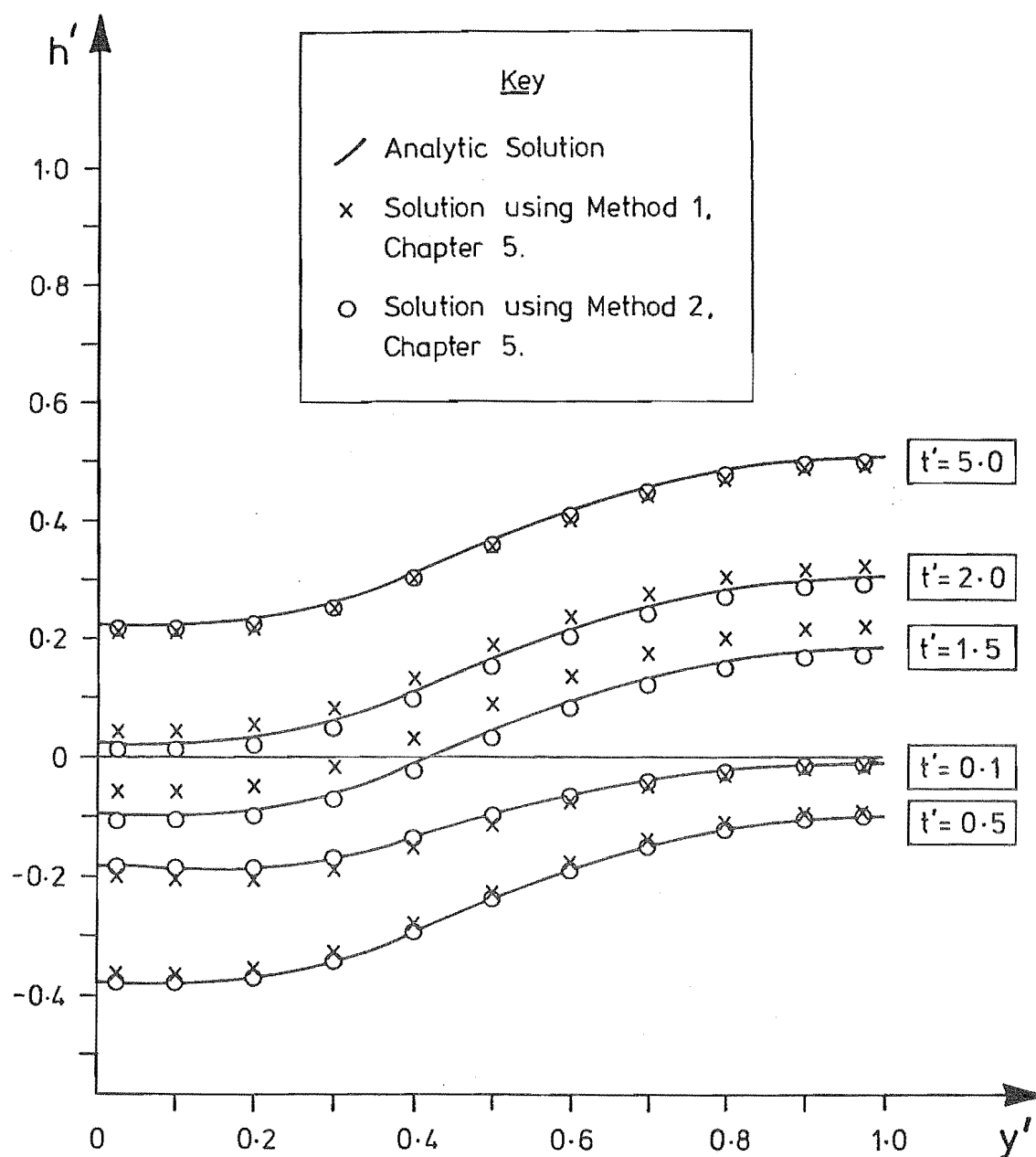


Fig. 6.57 Distribution of h' on $x'=0.5$ for the problem shown in Fig. 6.54.

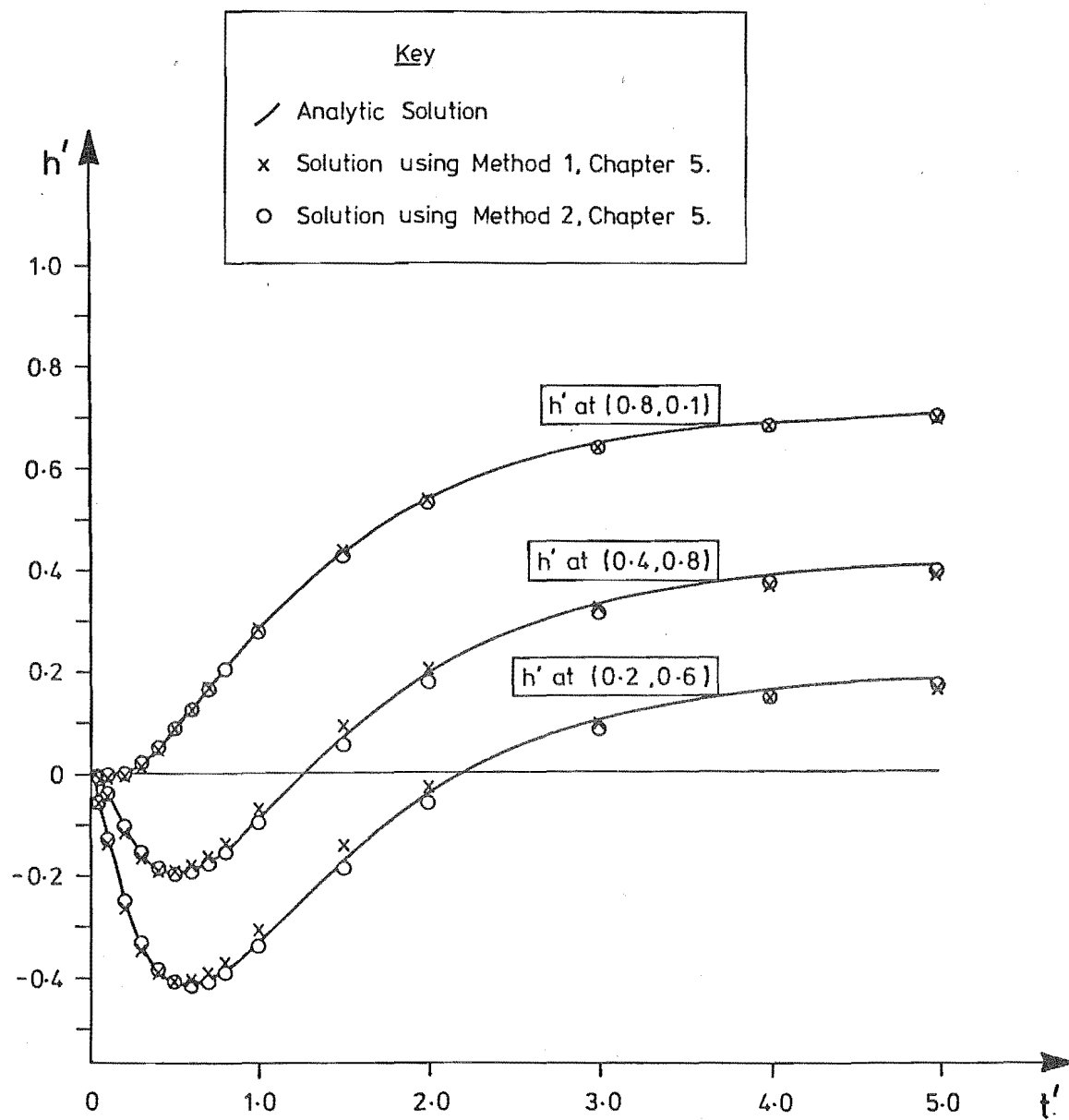


Fig. 6.58 Variation of h' with time at three internal points for the problem shown in Fig. 6.54.

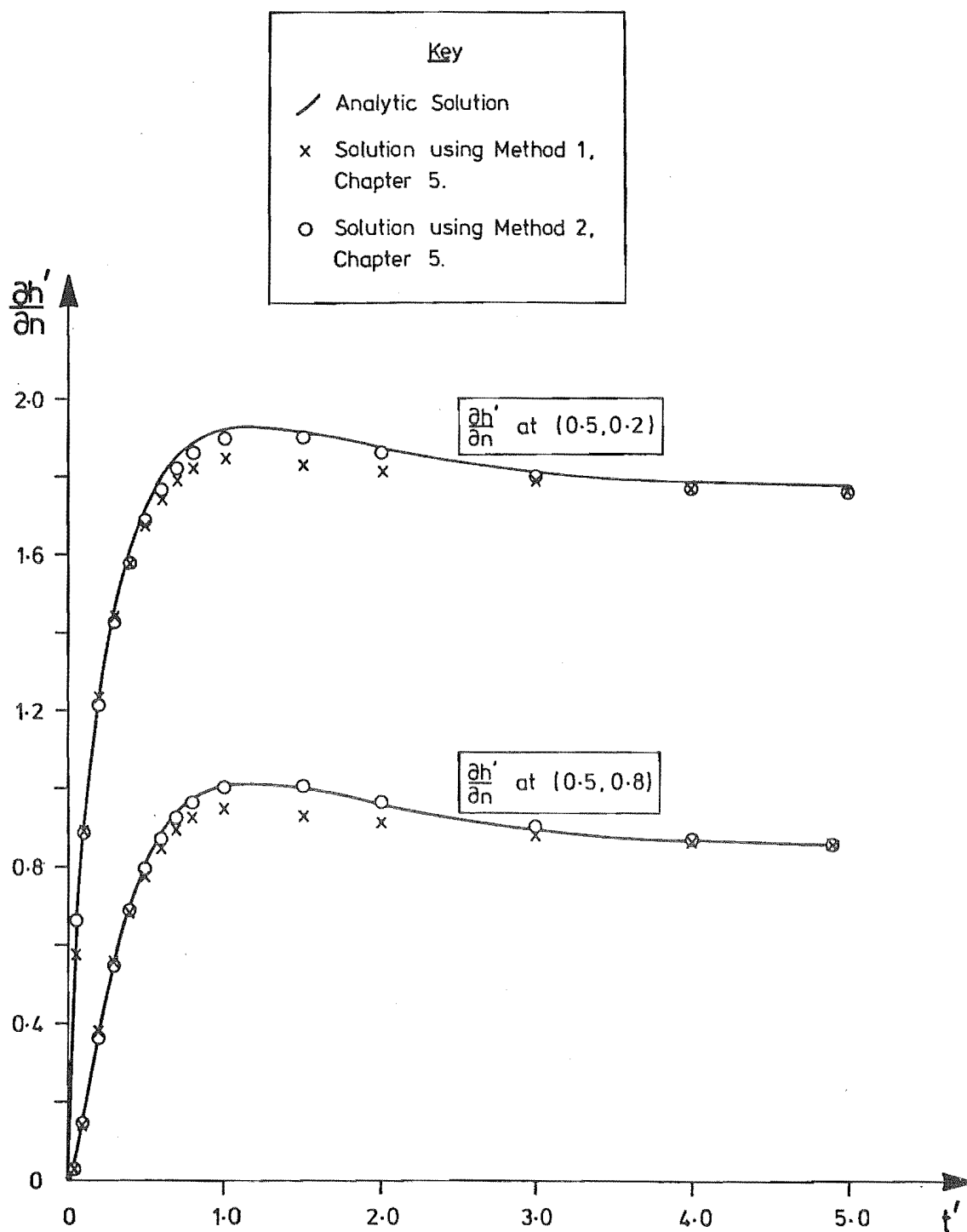


Fig. 6.59 Variation of $\frac{\partial h'}{\partial n}$ with time at (0.5, 0.2) and (0.5, 0.8) for the problem shown in Fig. 6.54.

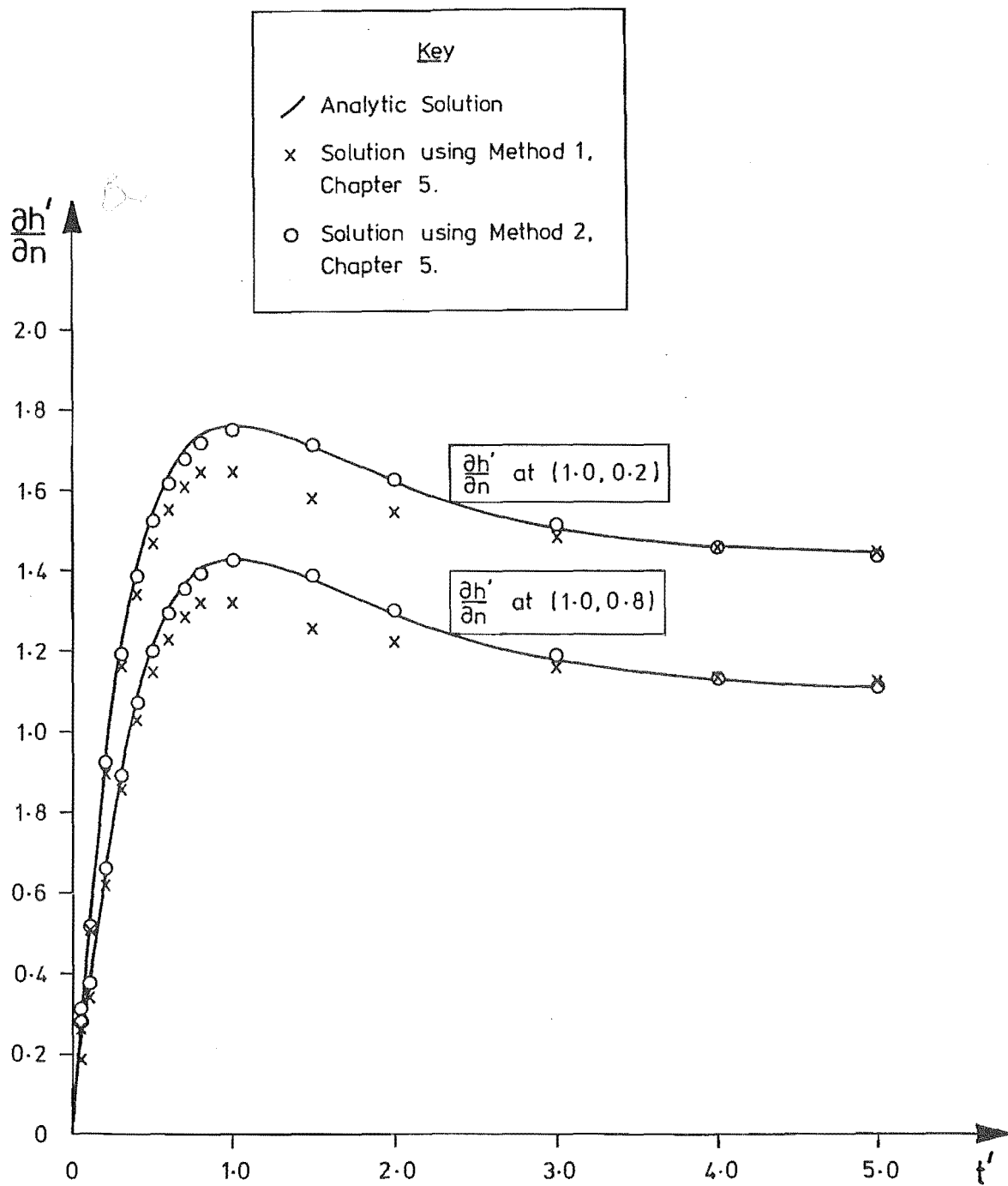


Fig. 6.60 Variation of $\frac{\partial h'}{\partial n}$ with time at $(1.0, 0.2)$ and $(1.0, 0.8)$ for the problem shown in Fig. 6.54.

Chapter 7

CONCLUSIONS7.1 SUMMARY

The integral equation techniques presented here have been found to be satisfactory for solving unsteady, two-dimensional groundwater flow problems, and in all cases the accuracy achieved is superior to that obtained by finite-difference methods. The other principal advantage of the integral equation techniques is that only boundary data is required to generate a solution. Consequently, large savings in data preparation time can be achieved, although this advantage is negated to some extent because of the relatively large computational times required. However, it is felt that as computer efficiency is continuing to improve, and manpower is at a premium, the advantages far outweigh the disadvantages.

7.2 UNSTEADY SEEPAGE THROUGH EMBANKMENTS

The integral equation formulation of Hunt and Isaacs (1981) is well suited to solving problems of unsteady, two-dimensional, free-surface flows. The comparison between one of these numerical solutions and an experimental solution, shown in Fig. 4.4, verifies the accuracy of the solutions. Comparisons between the numerical results and both the linear and non-linear Dupuit solutions (Fig. 4.5 - 4.8) show that the traditional approach of making the Dupuit approximation is not particularly satisfactory for analysing unsteady flows through embankments, even though the Dupuit solutions can be obtained in several orders of magnitude less computer time.

7.3 THE UNSTEADY DUPUIT EQUATION

The use of time-dependent fundamental solutions has led to accurate integral equation formulations for solving the unsteady Dupuit equation in both homogeneous and zoned regions. Of the two formulations presented, that in which

the piezometric head and its normal derivative are assumed to vary linearly with time over each time step has proved more accurate. Comparisons between Method 2 of Chapter 5 and finite-difference solutions have demonstrated the superior accuracy of the integral equation formulation. It should be noted that, although the integral equation techniques of Chapter 5 can be applied to flows in composite regions, the advantage of reduced data preparation decreases as the number of zones increases.

Bibliography

- Abramowitz, M. and Stegun, I.A. (Eds.) "Handbook of Mathematical Functions", Dover Publications, Inc., New York, 1972.
- Albrecht, J. and Collaty, L. (Eds.) "Numerical Treatment of Integral Equations", Birkhäuser Verlag, Basel, 1980.
- Anderssen, R.S., de Hoog, F.R. and Lukas, M.A. "The Application and Numerical Solution of Integral Equations", Sythoff and Noordhoff, Netherlands, 1980.
- Banerjee, P.K. and Butterfield, R. "Developments in Boundary Element Methods - 1", Applied Science Publishers Ltd., London, 1979.
- Banerjee, P.K., Butterfield, R. and Tomlin, G.R. "Boundary Element Methods for Two-Dimensional Problems of Transient Groundwater Flow", International Journal for Numerical and Analytical Methods in Geomechanics, Vol. 5, pp. 15-31, 1981.
- Bear, J. "Hydraulics of Groundwater", McGraw-Hill Inc., New York, 1979.
- Brebbia, C.A. (Ed.) "New Developments in Boundary Element Methods", Proceedings of the Second International Seminar on Recent Advances in Boundary Element Methods, held at University of Southampton, March 1980, C.M.L. Publications, Southampton, 1980.
- Brebbia, C.A. (Ed.) "Boundary Element Methods", Proceedings of the Third International Seminar at Irvine, California, July 1981, Springer-Verlag, Berlin, 1981.
- Brebbia, C.A. and Walker, S. "Boundary Element Techniques in Engineering", Newnes-Butterworths, London, 1979.

- Brebbia, C.A. and Wrobel, L.C. "Steady and Unsteady Potential Problems using the Boundary Element Method", in Recent Advances in Numerical Methods in Fluids, Taylor, C. (Ed.), Pineridge Press, Swansea, 1979.
- Carrier, G.F., Krook, M. and Pearson, C.E. "Functions of a Complex Variable: Theory and Technique", McGraw-Hill Inc., New York, 1966.
- Carslaw, H.S. and Jaeger, J.C. "Conduction of Heat in Solids, 2nd Edition", Clarendon Press, Oxford, 1959.
- Chang, Y.P., Kang, C.S. and Chen, D.J. "The Use of Fundamental Green's Functions for the Solution of Problems of Heat Conduction in Anisotropic Media", International Journal of Heat and Mass Transfer, Vol. 16, pp. 1905-1918, 1973.
- Cruse, T.A. and Rizzo, F.J. "A Direct Formulation and Numerical Solution of the General Elastodynamic Problem I", Journal of Mathematical Analysis and Applications, 22, pp. 244-259, 1968a.
- Cruse, T.A. and Rizzo, F.J. "A Direct Formulation and Numerical Solution of the General Elastodynamic Problem II", Journal of Mathematical Analysis and Applications, 22, pp. 341-355, 1968b.
- Delves, L.M. and Freeman, T.L. "Analysis of Global Expansion Methods: Weakly Asymptotically Diagonal Systems", Academic Press, London, 1981.
- Desai, C.S. "Seepage Analysis of Earth Banks Under Draw-down", Journal of the Soil Mechanics and Foundations Division, A.S.C.E., Vol. 98, No. SM11, pp. 1143-1162, November, 1972.
- Desai, C.S. "Drawdown Analysis of Slopes by Numerical Method", Journal of the Geotechnical Division, A.S.C.E., Vol. 103, No. GT7, pp. 667-676, July, 1977.

- Desai, C.S. and Li, G.C. "A Residual Flow Procedure and Application for Free Surface Flow in Porous Media", *Advances in Water Resources*, Vol. 6, pp. 27-35, March, 1983.
- Desai, C.S. and Li, G.C. "Stress and Seepage Analysis of Earth Dams", *Journal of Geotechnical Engineering*, A.S.C.E., Vol. 109, No. 7, pp. 946-960, July, 1983.
- Dubois, M. and Buysse, M. "Transient Heat Transfer Analysis by the Boundary Integral Equation Method", in *New Developments in Boundary Element Methods*, Brebbia, C. (Ed.), C.M.L. Publications, Southampton, 1980.
- France, P.W., Parekh, C.J., Peters, J.C., and Taylor, C. "Numerical Analysis of Free Surface Seepage Problems", *Journal of the Irrigation and Drainage Division*, A.S.C.E., Vol. 97, No. IR1, pp. 165-179, March, 1971.
- Giesing, J.P. "Extension of the Douglas Neumann Program to Problems of Lifting Infinite Cascades, Douglas Aircraft Company Report LB31653, 1964.
- Giesing, J.P. "Potential Flow About Two-Dimensional Airfoils", Douglas Aircraft Company Report LB31946, 1966.
- Goldberg, M.A. (Ed.) "Solution Methods for Integral Equations: Theory and Applications", Plenum Press, New York, 1979.
- Harr, M.E. "Groundwater and Seepage", McGraw-Hill Book Company, Inc., New York, 1962.
- Herdman, T.L., Stech, H.W. and Rankine, S.M.III. "Integral and Functional Differential Equations", Dekker, New York, 1981.
- Hess, J.L. and Smith, A.M.O. "Calculation of Non-Lifting Potential Flow About Arbitrary Three-Dimensional Bodies", Douglas Aircraft Company Report ES40622, 1962.

- Hess, J.L. and Smith, A.M.O. "Calculation of Potential Flow About Arbitrary Bodies", in Progress in Aeronautical Sciences, Vol. 8, Kuchemann, K. (Ed.), Pergamon Press, 1967.
- Hildebrand, F.B. "Advanced Calculus for Applications, 2nd Edition", Prentice-Hall, Inc., New Jersey, 1976.
- Hunt, B. "Mathematical Analysis of Groundwater Resources", Butterworth Publishing Co., London, 1983 (at press).
- Hunt, B. and Isaacs, L.T. "Integral Equation Formulation for Groundwater Flow", Journal of the Hydraulics Division, A.S.C.E., Vol. 107, No. HY10, pp. 1197-1209, October, 1981.
- Jaswon, M.A. "Integral Equation Methods in Potential Theory I.", Proceedings of the Royal Society (A), Vol. 275, pp. 23-32, 1963.
- Jaswon, M.A. and Symm, G.T. "Integral Equation Methods in Potential Theory and Elastostatics", Academic Press, London, 1977.
- Kellogg, O.D. "Foundations of Potential Theory", Verlag von Julius Springer, Berlin, 1929.
- Lafe, O.E., Liggett, J.A. and Liu, P.L.F. "BIEM Solutions to Combinations of Leaky, Layered, Confined, Unconfined, Nonisotropic Aquifers", Water Resources Research, Vol. 17, No. 5, pp. 1431-1444, October, 1981.
- Lennon, G.P., Liu, P.L.F. and Liggett, J.A. "Boundary Integral Equation Solution to Axisymmetric Potential Flows; 1. Basic Formulation; 2. Recharge and Well Problems in Porous Media", Water Resources Research, Vol. 15, No. 5, pp. 1102-1115, October, 1979.
- Lennon, G.P., Liu, P.L.F. and Liggett, J.A. "Boundary Integral Solutions to Three-Dimensional Unconfined Darcy's Flow", Water Resources Research, Vol. 16, No. 4, pp. 651-658, August, 1980.

- Liggett, J.A. "Location of Free Surface in Porous Media", Journal of the Hydraulics Division, A.S.C.E., Vol. 103, No. HY4, pp. 353-365, April, 1977.
- Liggett, J.A. and Liu, P.L.F. "Unsteady Free Surface Flow Through a Zoned Dam Using Boundary Integration", Proceedings of the Symposium on Application of Computer Methods in Engineering, pp. 357-365, 1979a.
- Liggett, J.A. and Liu, P.L.F. "Unsteady Flow in Confined Aquifers: A Comparison of Two Boundary Integral Methods", Water Resources Research, Vol. 15, No. 4, pp. 861-866, August, 1979b.
- Liu, P.L.F. and Liggett, J.A. "An Efficient Method of Two-Dimensional Steady Groundwater Problems", Water Resources Research, Vol. 14, No. 3, pp. 385-390, June, 1978.
- Liu, P.L.F. and Liggett, J.A. "Boundary Solutions to Two Problems in Porous Media", Journal of the Hydraulics Division, A.S.C.E., Vol. 105, No. HY3, pp. 171-183, March, 1979.
- Liu, P.L.F., Cheng, A.H.D., Liggett, J.A. and Lee, J.H. "Boundary Integral Solution to Moving Interface Between Two Fluids in Porous Media", Water Resources Research, Vol. 17, No. 5, pp. 1445-1452, October, 1981.
- MacDonald, D.A. "On the Method of the Local Potential as Applied to the Solution of the Equations of Diffusion", International Journal of Heat and Mass Transfer, Vol. 17, pp. 393-400, 1974.
- Massonnet, C.E. "Numerical Use of Integral Procedures in Stress Analysis", Zienkiewicz, O.C. and Holister, G.S. (Eds.), John Wiley and Sons, Inc., New York, 1965.

- Muskhelishvili, N.I. "Singular Integral Equations (Translated from Russian by Radok, J.R.M. and Noordhoof, N.V.)", Groningen, Holland, 1946.
- Norrie, D.H. and de Vries, G. "An Introduction to Finite Element Analysis", Academic Press, New York, 1978.
- Polubarinova-Kochina, P.Ya. "Theory of Groundwater Movement (Translated from Russian by Roger de Wiest, J.M.)", Princeton University Press, New Jersey, 1962.
- Rizzo, F.J. and Shippy, D.J. "A Method of Solution for Certain Problems of Transient Heat Conduction", A.I.A.A. Journal, Vol. 8, No. 11, pp. 2004-2009, 1970.
- Scheid, F.J. "Theory and Problems of Numerical Analysis: Schaum's Outline Series". McGraw-Hill Book Company, Inc., New York, 1968.
- Schwabik, S., Tvardy, M. and Vejvoda, O. "Differential and Integral Equations: Boundary Value Problems and Adjoints", D. Reidel Publishing Co., 1979.
- Schapery, R.A. "Approximate Methods of Transform Inversion for Viscoelastic Stress Analysis", Proceedings of the 4th U.S. National Congress on Applied Mechanics, Vol. 2, pp. 1075-1085, 1962.
- Shaw, R.P. "An Integral Equation Approach to Diffusion", International Journal of Heat and Mass Transfer, Vol. 17, pp. 693-699, 1974.
- Smith, A.M.O. and Pierce, J. "Exact Solution of the Neumann Problem. Calculations of Non-Circulatory Plane and Axially Symmetric Flow about or within Arbitrary Boundaries", Douglas Aircraft Company Report ES26988, 1958.
- Stephenson, D. "Drawdown in Embankments", Geotechnique, Vol. 28, No. 3, pp. 273-280, 1978.

Sternberg, W.J. and Smith, T.L. "The Theory of Potential and Spherical Harmonics", Toronto University Press, Toronto, 1946.

Symm, G.T. "Integral Equation Methods in Potential Theory. II", Proceedings of the Royal Society (A), Vol. 275, pp. 33-46, 1963.

Wrobel, L.C. and Brebbia, C.A. "The Boundary Element Method for Steady State and Transient Heat Conduction", Proceedings of International Conference on Numerical Methods in Thermal Problems, Pineridge Press, Swansea, 1979a.

Wrobel, L.C. and Brebbia, C.A. "Boundary Elements for Fluid Flow", Advances in Water Resources, Vol. 2, No. 2, June 1979b.

Wrobel, L.C. and Brebbia, C.A. "Boundary Elements in Thermal Problems", in Numerical Methods in Heat Transfer, Lewis, R.W. (Ed.), Wiley, Chichester, 1981a.

Wrobel, L.C. and Brebbia, C.A. "A Formulation of the Boundary Element Method for Axisymmetric Transient Heat Conduction", International Journal of Heat and Mass Transfer, Vol. 24, No. 5, pp. 843-850, 1981b.

Appendix A

Estimation of Boundary Layer Thickness for the
Hele-Shaw Experiment

Assume that fully-developed flow exists between two parallel flat plates that extend to infinity in the directions parallel and perpendicular to the base of the model. In this case the Navier-Stokes equations reduce to;

$$-g \frac{\partial h}{\partial x} + \nu \left(\frac{\partial^2 u}{\partial y^2} + \frac{\partial^2 u}{\partial z^2} \right) = 0 \quad (\text{A.1})$$

in which g = gravitational acceleration, ν = kinematic viscosity of the fluid, h = piezometric head, u = velocity, x = coordinate parallel to the base of the model, y = coordinate normal to the base of the model and z = coordinate normal to the plates. Assume, in the spirit of boundary layer analysis, that $h = h(x)$ only. Because the flow is fully-developed, u and the partial derivatives of u are not functions of x , which means that $\partial h / \partial x$ is a constant in Eqn. A.1. Thus the well known Hele-Shaw solution outlined in texts like Polubarinova-Kochina (1962) and Harr (1962) gives:

$$u_{\infty}(z) = \lim_{y \rightarrow \infty} u(y, z) = \frac{-gB^2}{8\nu} \frac{\partial h}{\partial x} \left[1 - \left(\frac{z}{B/2} \right)^2 \right] \quad (\text{A.2})$$

in which B = plate spacing. Hence set

$$u'(y, z) \equiv u_{\infty}(z) - u(y, z) \quad (\text{A.3})$$

and use Eqns. A.2 and A.3 to eliminate $u(y, z)$ from Eqn. A.1, to obtain;

$$\frac{\partial^2 u'}{\partial y^2} + \frac{\partial^2 u'}{\partial z^2} = 0 \quad (\text{A.4})$$

The solution of Eqn. A.4 subject to the following boundary conditions;

$$u'(y, z = \pm B/2) = 0 \quad (A.5)$$

$$u'(y = \infty, z) = 0 \quad (A.6)$$

$$u'(y = 0, z) = \frac{-gB^2}{8\nu} \frac{\partial h}{\partial x} \left[1 - \left(\frac{z}{B/2} \right)^2 \right] \quad (A.7)$$

can be solved by the method of separation of variables to give;

$$u'(y, z) = \sum_{n=1}^{\infty} \frac{-4gB^2}{\nu \pi^3 (2n-1)^3} (-1)^{n+1} \frac{\partial h}{\partial x} \cos \left[(2n-1) \frac{\pi z}{B} \right] e^{-(2n-1) \frac{\pi y}{B}} \quad (A.8)$$

Evaluating both sides of Eqn. A.2 at $z = 0$ allows the constant value of $\frac{\partial h}{\partial x}$ to be eliminated from Eqn. A.8 to obtain;

$$\frac{u_{\infty}(z) - u(y, z)}{u_{\infty}(z=0)} = \frac{32}{\pi^3} \sum_{n=1}^{\infty} \frac{(-1)^{n+1}}{(2n-1)^3} \cos \left[(2n-1) \frac{\pi z}{B} \right] e^{-(2n-1) \frac{\pi y}{B}} \quad (A.9)$$

If the boundary layer thickness is defined in the usual manner by;

$$\frac{u_{\infty}(z=0) - u(y=\delta, z=0)}{u_{\infty}(z=0)} = 0.01 \quad (A.10)$$

in which δ is the boundary layer thickness, then the solutions of Eqns. A.9 and A.10 give;

$$\frac{\delta}{B} = 1.476 \quad (A.11)$$

Appendix B

Fortran Computer Programs Derived from1 and 2 of Chapter 5

The following Fortran listing can be used to solve mixed boundary value problems of groundwater flow. The user has the option of using either Method 1, in which h and $\frac{\partial h}{\partial n}$ are assumed to ^{be constant} ~~vary linearly~~ over each time step, or Method 2, in which h and $\frac{\partial h}{\partial n}$ are assumed to vary linearly with time over each time step. The listing for Method 2 is given in full, while the listing for Method 1 is obtained by removing lines 34200 - 43800 inclusive, and replacing them with the program segment that appears in Fig. B.1.

Problems may be formulated in either dimensional or dimensionless variables. If dimensionless variables are used the transmissivity and storage coefficient for zone 1 should both be set equal to unity and transmissivities and storage coefficients in other zones scaled accordingly.

```

C***** 00000100
C*      * 00000200
C* INTRODUCTION.      * 00000300
C* =====      * 00000400
C*      * 00000500
C* THIS PROGRAM USES A BOUNDARY INTEGRAL EQUATION FORMULATION TO SOLVE * 00000600
C* UNSTEADY GROUNDWATER FLOW PROBLEMS.      * 00000700
C* VALUES OF H OR DH/DN MUST BE SPECIFIED, AS FUNCTIONS OF TIME AT      * 00000800
C* EACH NODE ON THE BOUNDARY OF THE SOLUTION DOMAIN.      * 00000900
C* THE SOLUTION DOMAIN MAY CONTAIN ANY NUMBER OF REGIONS; EACH OF      * 00001000
C* WHICH MUST HAVE CONSTANT TRANSMISSIVITY AND STORAGE COEFFICIENT.      * 00001100
C* EACH REGION IS DEFINED BY A SERIES OF NODES AROUND ITS BOUNDARY.      * 00001200
C* EACH REGION MAY CONTAIN ANY NUMBER OF WELLS OF ANY STRENGTH.      * 00001300
C* THIS PROGRAM CALCULATES THE SOLUTION FOR BOTH H AND DH/DN AROUND      * 00001400
C* THE BOUNDARY OF EACH REGION, AND H AT ANY NUMBER OF POINTS WITHIN      * 00001500
C* THE REGION.      * 00001600
C* THE BOUNDARY NODES OF EACH REGION MUST BE NUMBERED CONSECUTIVELY      * 00001700
C* WHEN GOING AROUND THE BOUNDARY IN AN ANTI-CLOCKWISE DIRECTION.      * 00001800
C* (NODES ON BOUNDARIES BETWEEN REGIONS WILL HAVE TWO NUMBERS; ONE      * 00001900
C* FOR EACH REGION.)      * 00002000
C*      * 00002100
C*      * 00002200
C*      * 00002300
C*      * 00002400
C* EXPLANATION OF SYMBOLS USED.      * 00002500
C* =====      * 00002600
C*      * 00002700
C* NZ = NUMBER OF REGIONS IN THE SOLUTION DOMAIN.      * 00002800
C*      * 00002900
C* TRANS(K),STOR(K),NNZ(K) = TRANSMISSIVITY,STORAGE COEFFICIENT AND      * 00003000
C*      THE NUMBER OF NODES IN REGION K; FOR K=1,NZ.      * 00003100
C*      * 00003200
C* NCP(I,K) = NUMBER OF NODES COMMON TO REGIONS I AND K FOR I=1,NZ-1      * 00003300
C*      AND K=I+1,NZ.      * 00003400
C* X(I,K),Y(I,K) = COORDINATES OF BOUNDARY NODE I IN REGION K, FOR      * 00003500
C*      K=1,NZ AND I=1,NNZ(K).      * 00003600
C* NW(K) = NUMBER OF WELLS IN REGION K, FOR K=1,NZ.      * 00003700
C*      * 00003800
C* Q(I,K) = FLOW RATE IN WELL I IN REGION K, FOR K=1,NZ AND I=1,NW(K).      * 00003900
C* (NOTE THAT Q IS POSITIVE FOR AN ABSTRACTION WELL.)      * 00004000
C*      * 00004100
C* X(NNZ(K)+J,K),Y(NNZ(K)+J,K) = COORDINATES OF WELL J IN REGION K,      * 00004200
C*      FOR K=1,NZ AND J=1,NW(K).      * 00004300
C* NP(K) = NUMBER OF INTERNAL POINTS IN REGION K AT WHICH H IS      * 00004400
C*      REQUIRED, FOR K=1,NZ.      * 00004500
C* X(NNZ(K)+NW(K)+I,K),Y(NNZ(K)+NW(K)+I,K) = COORDINATES OF INTERNAL      * 00004600
C*      POINT I IN REGION K, FOR K=1,NZ AND I=1,NP(K).      * 00004700
C*      * 00004800
C* N = NUMBER OF TIME STEPS USED.      * 00004900
C* T(L) = TIME AT THE LTH TIME STEP, FOR L=1,N. (NOTE THAT T(1)=0.)      * 00005000
C*      * 00005100
C* ID(I,K) = NODE IDENTIFICATION NUMBER FOR BOUNDARY NODE I IN REGION K      * 00005200
C*      ,FOR K=1,NZ AND I=1,NNZ(K).      * 00005300
C* ID(I,K) = 1 IF H IS KNOWN.      * 00005400
C* ID(I,K) = 2 IF DH/DN IS KNOWN.      * 00005500
C* ID(I,K) = 3 IF BOTH H AND DH/DN ARE KNOWN.      * 00005600
C* ID(I,K) = 4 IF NODE IS COMMON TO TWO REGIONS.      * 00005700
C* JD(I,K) = 1 IF BOUNDARY DOES NOT TURN CONTINUOUSLY AT NODE I IN      * 00005800
C*      REGION K.      * 00005900
C* XC(I,K),YC(I,K) = COORDINATES OF SHARP CORNER BETWEEN NODES I AND      * 00006000
C*      I+1.      * 00006100
C* NCOMM(I,J) = THE FIRST NODE IN REGION I ON THE BOUNDARY WITH REGION      * 00006200
C*      J, FOR I=1,NZ AND J=1,NZ.      * 00006300
C* F(I,K) = KNOWN VALUE OF H AT NODE I IN REGION K.      * 00006400
C* G(I,K) = KNOWN VALUE OF DH/DN AT NODE I IN REGION K.      * 00006500
C*      * 00006600
C***** 00006700
C*      DIMENSION TRANS(5),NNZ(100),NCP(100,5),X(100,5),Y(100,5),ID(100,5) 00006800
C*      C,XC(100,5),YC(100,5),F(100,5),G(100,5),JD(100,5),EHATN(100,5) 00006900
C*      C,RN(100,100,5),S(100,5),TOTS(5),SLOG(100,5),NCOMM(5,5),A(200,200) 00007000
C*      C,NW(5),Q(5,5),RNP(5,100,5),NP(5),STOR(5),U(200,20),DSM(100,5) 00007100
C*      C,DSP(100,5),HW(100,5),HWP(5,20,5),H(100,5),DHDN(100,5),B(200), 00007200
C*      CHIP(5,30,5) 00007300
C*      COMMON/BLOCK1/R(100,100,5),T(20),ASQUAR(5),A0,A1,A2,A3,A4,A5,B1,B2 00007400
C*      C,B3,B4,B5,B6,B7,B8 00007500
C*      A0=-0.57721566 00007600
C*      A1=0.99999193 00007700
C*      A2=-0.249991055 00007800
C*      A3=0.05519968 00007900
C*      A4=-0.00976004 00008000
C*      A5=0.00107857 00008100
C*      B1=8.5733287401 00008200
C*      B2=18.0590169730 00008300
C*      B3=8.6347608925 00008400
C*      B4=0.2677737343 00008500
C*      B5=9.5733223454 00008600
C*      B6=25.6329561486 00008700
C*      B7=21.0996530827 00008800
C*      B8=3.9584969228 00008900

```

```

C
C
C INPUT BOUNDARY NODE DATA FOR EACH ZONE.
C
C
      READ(5,10)NZ
10  FORMAT(I10)
      READ(5,11)(TRANS(I),STOR(I),NNZ(I),I=1,NZ)
11  FORMAT(2F10.5,I10)
      IF(NZ.EQ.1) GO TO 12
      DO 13 I=1,NZ-1
13  READ(5,10)(NCP(I,J),J=I+1,NZ)
12  DO 14 J=1,NZ
14  READ(5,20)(X(I,J),Y(I,J),ID(I,J),JD(I,J),XC(I,J),YC(I,J),I=1,
      CNNZ(J))
20  FORMAT(2F10.5,2I10,2F10.5)
      DO 16 I=1,NZ
      DO 16 J=1,NZ
      IF(I.EQ.J) GO TO 16
      READ(5,10)NCOMM(I,J)
16  CONTINUE
      DO 65 I=1,NZ
      ASQUAR(I)=TRANS(I)/STOR(I)
      M=M+NNZ(I)
      WRITE(6,62)I,TRANS(I),STOR(I)
62  FORMAT(1H1,'INPUT DATA FOR ZONE',X,I1,X,'WHICH HAS A TRANSMISSIVIT
      CY OF',F10.5,X,'AND A STORAGE COEFFICIENT OF',X,F10.5)
      WRITE(6,61)
61  FORMAT(1H0,4X,'I',6X,'X(I)',9X,'Y(I)',5X,'ID(I)',5X,'H(I)',8X,
      C'DH/DN(I)')
      WRITE(6,63)(J,X(J,I),Y(J,I),ID(J,I),F(J,I),G(J,I),J=1,NNZ(I))
63  FORMAT(1H0,3X,I3,3X,F8.5,5X,F8.5,5X,I1,5X,F8.5,5X,F9.5)
      IF(NZ.EQ.1) GO TO 65
      IF(I.EQ.NZ) GO TO 65
      WRITE(6,66)(NCP(I,J),I,J,J=I+1,NZ)
66  FORMAT(1H0,'THERE ARE',X,I2,X,'COMMON NODES BETWEEN ZONES',X,I1,X,
      C'AND',X,I1)
65  CONTINUE
      MM=M+M
      DO 67 I=1,NZ
      DO 67 J=1,NZ
      IF(I.EQ.J) GO TO 67
      WRITE(6,68)I,J,NCOMM(I,J)
68  FORMAT(1H0,'THE FIRST NODE IN ZONE',X,I2,X,'ON THE BOUNDARY WITH
      C ZONE',X,I2,X,'IS',X,I3)
67  CONTINUE
C
C
C CALCULATION OF GEOMETRICAL PROPERTIES.
C
C
      DO 100 J=1,NZ
      DO 100 I=1,NNZ(J)
      K=I-1
      L=I+1
      IF(I.EQ.1)K=NNZ(J)
      IF(I.EQ.NNZ(J))L=1
      XI=X(I,J)
      XK=X(K,J)
      XL=X(L,J)
      YI=Y(I,J)
      YK=Y(K,J)
      YL=Y(L,J)
      IF(JD(I,J).EQ.0.AND.JD(K,J).EQ.0) GO TO 110
      IF(JD(I,J).EQ.1) GO TO 111
      XK=XC(K,J)
      YK=YC(K,J)
      GO TO 110
111 XL=XC(I,J)
      YL=YC(I,J)
110 IF(ABS(XL-XK).LT.0.0001) GO TO 102
      IF(ABS(XL-XI).LT.0.0001) GO TO 105
      IF(ABS(XK-XI).LT.0.0001) GO TO 105
      DP=XL-XI
      DM=XI-XK
      QU=DP/DM
      IF(QU.LT.0) GO TO 105
      DEL1=(YI-YK)/DM
      DEL2=(YL-YI)/DP
      DEL3=(DEL2-DEL1)/(XL-XK)
      DYDX=DEL1+DEL3*DM
      EHATN(I,J)=1.5707963+ATAN(DYDX)
      IF(XL.GT.XK)EHATN(I,J)=-1.5707963+ATAN(DYDX)
      GO TO 100

```

102	IF (YL.GT.YK) GO TO 104	00017400
	EHATN(I,J)=3.14159265	00017500
	GO TO 100	00017600
104	EHATN(I,J)=0.0	00017700
	GO TO 100	00017800
105	IF (YI.EQ.YK) GO TO 106	00017900
	IF (YI.EQ.YL) GO TO 107	00018000
	DYDX=(YL-YK)/(XL-XK)	00018100
	EHATN(I,J)=1.5707963+ATAN(DYDX)	00018200
	IF (DYDX.LT.0.0.AND.YL.LT.YK) EHATN(I,J)=-1.5707963+ATAN(DYDX)	00018300
	IF (DYDX.GT.0.0.AND.YL.GT.YK) EHATN(I,J)=-1.5707963+ATAN(DYDX)	00018400
	GO TO 100	00018500
106	IF (YL.GT.YI) EHATN(I,J)=-1.5707963	00018600
	IF (YL.LT.YI) EHATN(I,J)=+1.5707963	00018700
	GO TO 100	00018800
107	IF (YK.GT.YI) EHATN(I,J)=-1.5707963	00018900
	IF (YK.LT.YI) EHATN(I,J)=+1.5707963	00019000
100	CONTINUE	00019100
	DO 200 K=1,NZ	00019200
	DO 200 I=1,NNZ(K)	00019300
	DO 200 J=1,NNZ(K)	00019400
	IF (I.EQ.J) GO TO 200	00019500
	DYR=Y(J,K)-Y(I,K)	00019600
	DXR=X(J,K)-X(I,K)	00019700
	R(I,J,K)=SQRT(DYR**2+DXR**2)	00019800
	IF (DXR.EQ.0.0) GO TO 201	00019900
	DRDX=DYR/DXR	00020000
	ALPHA=ATAN(DRDX)	00020100
	IF (X(J,K).LT.X(I,K)) ALPHA=3.14159265+ATAN(DRDX)	00020200
	GO TO 202	00020300
201	IF (DYR.GT.0.0) GO TO 203	00020400
	ALPHA=-1.5707963	00020500
	GO TO 202	00020600
203	ALPHA=1.5707963	00020700
202	RN(I,J,K)=ALPHA-EHATN(J,K)	00020800
200	CONTINUE	00020900
	DO 300 J=1,NZ	00021000
	DO 300 I=1,NNZ(J)	00021100
	IP=I+1	00021200
	IF (I.EQ.NNZ(J)) IP=1	00021300
	S(I,J)=R(I,IP,J)	00021400
	IF (JD(I,J).EQ.0) GO TO 300	00021500
	XCOR1=(XC(I,J)-X(I,J))**2	00021600
	YCOR1=(YC(I,J)-Y(I,J))**2	00021700
	XCOR2=(XC(I,J)-X(IP,J))**2	00021800
	YCOR2=(YC(I,J)-Y(IP,J))**2	00021900
	DSM(I,J)=SQRT(XCOR1+YCOR1)	00022000
	DSP(I,J)=SQRT(XCOR2+YCOR2)	00022100
	S(I,J)=DSM(I,J)+DSP(I,J)	00022200
300	TOTS(J)=TOTS(J)+S(I,J)	00022300
	DO 400 K=1,NZ	00022400
	DO 400 I=1,NNZ(K)	00022500
	DO 400 J=1,NNZ(K)	00022600
	JM=J-1	00022700
	IF (J.EQ.1) JM=NNZ(K)	00022800
	IF (JD(JM,K).EQ.1) GO TO 403	00022900
	IF (J.EQ.I) GO TO 401	00023000
	IF (JM.EQ.I) GO TO 402	00023100
	SLOG(I,K)=SLOG(I,K)+0.5*S(JM,K)*ALOG(R(I,J,K)*R(I,JM,K))	00023200
	GO TO 400	00023300
401	SLOG(I,K)=SLOG(I,K)+R(I,JM,K)*(ALOG(R(I,JM,K))-1.0)	00023400
	GO TO 400	00023500
402	SLOG(I,K)=SLOG(I,K)+R(I,J,K)*(ALOG(R(I,J,K))-1.0)	00023600
	GO TO 400	00023700
403	XCOR1=(XC(JM,K)-X(JM,K))**2	00023800
	YCOR1=(YC(JM,K)-Y(JM,K))**2	00023900
	XCOR2=(XC(JM,K)-X(J,K))**2	00024000
	YCOR2=(YC(JM,K)-Y(J,K))**2	00024100
	RP1=SQRT(XCOR1+YCOR1)	00024200
	RP2=SQRT(XCOR2+YCOR2)	00024300
	IF (I.EQ.JM) GO TO 404	00024400
	IF (I.EQ.J) GO TO 405	00024500
	XCOR3=(XC(JM,K)-X(I,K))**2	00024600
	YCOR3=(YC(JM,K)-Y(I,K))**2	00024700
	RP3=SQRT(XCOR3+YCOR3)	00024800
	SLOG(I,K)=SLOG(I,K)+0.5*RP1*ALOG(R(I,JM,K)*RP3)	00024900
	C+0.5*RP2*ALOG(RP3*R(I,J,K))	00025000
	GO TO 400	00025100
404	SLOG(I,K)=SLOG(I,K)+RP1*(ALOG(RP1)-1.0)+0.5*RP2*ALOG(RP1*R(I,J,K))	00025200
	GO TO 400	00025300
405	SLOG(I,K)=SLOG(I,K)+RP2*(ALOG(RP2)-1.0)+0.5*RP1*ALOG	00025400
	C(RP2*R(I,JM,K))	00025500
400	CONTINUE	00025600

C		00025700
C		00025800
C	INPUT TIME DATA.	00025900
C		00026000
C		00026100
	READ(5,10)N	00026200
	READ(5,30)(T(I),I=1,N)	00026300
	30 FORMAT(F10.5)	00026400
C		00026500
C		00026600
C	INPUT WELL DATA.	00026700
C		00026800
C		00026900
	DO 760 K=1,NZ	00027000
	READ(5,10)NW(K)	00027100
	IF(NW(K).EQ.0) GO TO 760	00027200
	READ(5,9)(X(NNZ(K)+I,K),Y(NNZ(K)+I,K),Q(I,K),I=1,NW(K))	00027300
	9 FORMAT(3F10.5)	00027400
760	CONTINUE	00027500
	WRITE(6,710)	00027600
710	FORMAT(1H1,'**** WELL DATA ****')	00027700
	DO 770 K=1,NZ	00027800
	WRITE(6,720)NW(K),K	00027900
720	FORMAT(1H0,'THERE ARE',X,I2,X,'WELLS IN ZONE',X,I2,X,'AS FOLLOWS')	00028000
	IF(NW(K).EQ.0) GO TO 770	00028100
	WRITE(6,730)	00028200
730	FORMAT(1H0,4X,'I',6X,'X(I)',8X,'Y(I)',8X,'Q(I)')	00028300
	WRITE(6,740)(I,X(NNZ(K)+I,K),Y(NNZ(K)+I,K),Q(I,K),I=1,NW(K))	00028400
740	FORMAT(1H0,3X,I3,3X,F8.5,4X,F8.5,4X,F8.5)	00028500
770	CONTINUE	00028600
	DO 750 K=1,NZ	00028700
	IF(NW(K).EQ.0) GO TO 750	00028800
	DO 751 I=1,NW(K)	00028900
	DO 751 J=1,NNZ(K)	00029000
	DYR=Y(J,K)-Y(NNZ(K)+I,K)	00029100
	DXR=X(J,K)-X(NNZ(K)+I,K)	00029200
	R(NNZ(K)+I,J,K)=SQRT(DXR**2+DYR**2)	00029300
751	CONTINUE	00029400
750	CONTINUE	00029500
C		00029600
C		00029700
C	INPUT INTERNAL POINT DATA.	00029800
C		00029900
C		00030000
	DO 665 K=1,NZ	00030100
	READ(5,10) NP(K)	00030200
	IF(NP(K).EQ.0) GO TO 665	00030300
	READ(5,8)(X(NNZ(K)+NW(K)+I,K),Y(NNZ(K)+NW(K)+I,K),I=1,NP(K))	00030400
	8 FORMAT(2F10.5)	00030500
665	CONTINUE	00030600
	DO 666 K=1,NZ	00030700
	WRITE(6,660)NP(K),K	00030800
660	FORMAT(1H1,'THERE ARE',X,I2,X,'INTERNAL POINTS OF INTEREST IN	00030900
	C ZONE',X,I2)	00031000
	IF(NP(K).EQ.0) GO TO 666	00031100
	WRITE(6,670)	00031200
670	FORMAT(1H0,4X,'I',6X,'X(I)',8X,'Y(I)')	00031300
	WRITE(6,680)(I,X(NNZ(K)+NW(K)+I,K),Y(NNZ(K)+NW(K)+I,K),I=1,NP(K))	00031400
680	FORMAT(1H0,3X,I3,3X,F8.5,4X,F8.5)	00031500
666	CONTINUE	00031600
	DO 690 K=1,NZ	00031700
	IF(NP(K).EQ.0) GO TO 690	00031800
	DO 699 I=1,NP(K)	00031900
	DO 699 J=1,NNZ(K)+NW(K)	00032000
	DYR=Y(J,K)-Y(NNZ(K)+NW(K)+I,K)	00032100
	DXR=X(J,K)-X(NNZ(K)+NW(K)+I,K)	00032200
	R(NNZ(K)+NW(K)+I,J,K)=SQRT(DXR**2+DYR**2)	00032300
	IF(J.GT.NNZ(K)) GO TO 699	00032400
	IF(DXR.EQ.0) GO TO 691	00032500
	DRDX=DYR/DXR	00032600
	ALPHA=ATAN(DRDX)	00032700
	IF(X(J,K).LT.X(NNZ(K)+NW(K)+I,K)) ALPHA=3.14159265+ATAN(DRDX)	00032800
	GO TO 692	00032900
691	IF(DYR.GT.0.0) GO TO 693	00033000
	ALPHA=-1.5707963	00033100
	GO TO 692	00033200
693	ALPHA=1.5707963	00033300
692	RNP(I,J,K)=ALPHA-EHATN(J,K)	00033400
699	CONTINUE	00033500
690	CONTINUE	00033600


```

C
C
C SET UP MATRICES TO SOLVE A*(H,DH/DN)=B
C
C
DO 600 L=2,N
  ICYC=0
  ICYCIC=0
  DO 700 K=1,NZ
    DO 800 I=1,NNZ(K)
    DO 800 J=1,NNZ(K)
    JM=J-1
    IF (J.EQ.1) JM=NNZ(K)
    VAL=R(I,J,K)**2/(4.0*ASQUAR(K)*(T(L)-T(L-1)))
    DS=S(J,K)+S(JM,K)
    IF (JD(J,K).EQ.1) DS=S(JM,K)+DSM(J,K)*2.0
    IF (JD(JM,K).EQ.1) DS=S(J,K)+DSP(JM,K)*2.0
    IF (I.EQ.J) GO TO 802
    A(I+ICYC,I+ICYCIC)=A(I+ICYC,I+ICYCIC)-COS(RN(I,J,K))*DS/R(I,J,K)
    A(I+ICYC,J+ICYCIC)=COS(RN(I,J,K))*DS*((EXP(-VAL)/R(I,J,K))
    C-(R(I,J,K)*EONE(I,J,K,L-1,L)/(4.0*ASQUAR(K)*(T(L)-T(L-1))))
    A(I+ICYC,I+ICYCIC+NNZ(K))=A(I+ICYC,I+ICYCIC+NNZ(K))+0.5*ALOG
    C(VAL*1.7810723)*DS
    A(I+ICYC,J+ICYCIC+NNZ(K))=(EONE(I,J,K,L-1,L)*(1+VAL)-EXP(-VAL))
    C*DS/2.0
    GO TO 800
802 A(I+ICYC,I+ICYCIC+NNZ(K))=A(I+ICYC,I+ICYCIC+NNZ(K))
    C-2.0*SLOG(I,K)-TOTS(K)*ALOG(0.4452681/(ASQUAR(K)*(T(L)-T(L-1))))
    C-DS/2.0
800 CONTINUE
    ICYC=ICYC+NNZ(K)
    ICYCIC=ICYCIC+2*NNZ(K)
700 CONTINUE
    ICYC=0
    ICYCIC=0
    IF (L.EQ.2) GO TO 55
    DO 2220 K=1,NZ
    DO 2200 KT=2,L-1
    DELT1=T(KT)-T(KT-1)
    DELT2=T(L)-T(KT)
    DELT3=T(L)-T(KT-1)
    DO 2200 I=1,NNZ(K)
    DO 2200 J=1,NNZ(K)
    JM=J-1
    IF (J.EQ.1) JM=NNZ(K)
    DS=0.5*(S(J,K)+S(JM,K))
    IF (JD(J,K).EQ.1) DS=0.5*S(JM,K)+DSM(J,K)
    IF (JD(JM,K).EQ.1) DS=0.5*S(J,K)+DSP(JM,K)
    IF (I.EQ.J) GO TO 2150
    COSR=2.0*COS(RN(I,J,K))/R(I,J,K)
    RCOS=R(I,J,K)*COS(RN(I,J,K))/(2.0*ASQUAR(K))
    VAL1=EXP(-(R(I,J,K)**2/(4.0*ASQUAR(K)*DELT2)))
    VAL2=EXP(-(R(I,J,K)**2/(4.0*ASQUAR(K)*DELT3)))
    VAL3=EONE(I,J,K,KT,L)
    VAL4=EONE(I,J,K,KT-1,L)
    DELE=VAL4-VAL3
    DELEX=VAL2-VAL1
    B(I+ICYC)=B(I+ICYC)
    C-(U(J+ICYCIC+NNZ(K),KT)*DELE*(DELT3+R(I,J,K)**2/(4.0*ASQUAR(K))))
    C/DELT1)*DS
    C-(U(J+ICYCIC+NNZ(K),KT)*(DELT2*VAL1-DELT3*VAL2)/DELT1)*DS
    C+(U(J+ICYCIC+NNZ(K),KT-1)*DELE*(DELT2+R(I,J,K)**2/(4.0*ASQUAR(K))))
    C/DELT1)*DS

```

```

00033700
00033800
00033900
00034000
00034100
00034200
00034300
00034400
00034500
00034600
00034700
00034800
00034900
00035000
00035100
00035200
00035300
00035400
00035500
00035600
00035700
00035800
00035900
00036000
00036100
00036200
00036300
00036400
00036500
00036600
00036700
00036800
00036900
00037000
00037100
00037200
00037300
00037400
00037500
00037600
00037700
00037800
00037900
00038000
00038100
00038200
00038300
00038400
00038500
00038600
00038700
00038800
00038900
00039000
00039100
00039200
00039300
00039400
00039500
00039600
00039700
00039800
00039900

```

C-(U(J+ICYCIC+NNZ(K),KT-1)*(DELT3*VAL2*VAL1)/DELT1)*DS	000400000
C-(U(J+ICYCIC,KT)*DELT3*COSR*DELEX*DS/DELT1)	000401000
C+(U(J+ICYCIC,KT)*RCOS*DELE*DS/DELT1)	000402000
C+(U(J+ICYCIC,KT-1)*DELT2*COSR*DELEX*DS/DELT1)	000403000
C-(U(J+ICYCIC,KT-1)*RCOS*DELE*DS/DELT1)	000404000
GO TO 2200	000405000
2150 B(I+ICYC)=B(I+ICYC)	000406000
C-(U(J+ICYCIC+NNZ(K),KT)*((DELT3/DELT1)*ALOG(DELT3/DELT2))-1.0))	000407000
C*DS	000408000
C+(U(J+ICYCIC+NNZ(K),KT-1)*((DELT2/DELT1)*ALOG(DELT3/DELT2))-1.0	000409000
C))*DS	000410000
2200 CONTINUE	000411000
ICYC=ICYC+NNZ(K)	000412000
ICYCIC=ICYCIC+2*NNZ(K)	000413000
2220 CONTINUE	000414000
ICYC=0	000415000
ICYCIC=0	000416000
55 CONTINUE	000417000
DO 2250 K=1,NZ	000418000
DO 2240 I=1,NNZ(K)	000419000
DO 2240 J=1,NNZ(K)	000420000
JM=J-1	000421000
IF(J.EQ.1) JM=NNZ(K)	000422000
DS=0.5*(S(J,K)+S(JM,K))	000423000
IF(JD(J,K).EQ.1) DS=0.5*S(JM,K)+DSM(J,K)	000424000
IF(JD(JM,K).EQ.1) DS=0.5*S(J,K)+DSP(JM,K)	000425000
IF(I.EQ.J) GO TO 2160	000426000
DELT=T(L)-T(L-1)	000427000
RCOS=R(I,J,K)*COS(RN(I,J,K))/(2.0*ASQUAR(K))	000428000
VAL=R(I,J,K)**2/(4.0*ASQUAR(K)*DELT)	000429000
B(I+ICYC)=B(I+ICYC)	000430000
C+(U(J+ICYCIC+NNZ(K),L-1)*((VAL*EONE(I,J,K,L-1,L))-EXP(-VAL)))*DS	000431000
C-(U(J+ICYCIC,L-1)*RCOS*EONE(I,J,K,L-1,L)*DS/DELT)	000432000
GO TO 2240	000433000
2160 B(I+ICYC)=B(I+ICYC)-U(J+ICYCIC+NNZ(K),L-1)*DS	000434000
2240 CONTINUE	000435000
ICYC=ICYC+NNZ(K)	000436000
ICYCIC=ICYCIC+2*NNZ(K)	000437000
2250 CONTINUE	000438000
ICYC=0	000439000
ICYCIC=0	000440000
DO 2500 K=1,NZ	000441000
IF(NW(K).EQ.0) GO TO 2500	000442000
DO 2501 I=1,NW(K)	000443000
DO 2501 J=1,NNZ(K)	000444000
HW(J,K)=HW(J,K)-Q(I,K)*EONE(I+NNZ(K),J,K,1,L)/(TRANS(K)*12.566371)	000445000
2501 CONTINUE	000446000
2500 CONTINUE	000447000
DO 2550 K=1,NZ	000448000
IF(NP(K).EQ.0) GO TO 2550	000449000
IF(NW(K).EQ.0) GO TO 2550	000450000
DO 2555 I=1,NW(K)	000451000
DO 2555 J=1,NP(K)	000452000
HWP(J,L,K)=HWP(J,L,K)-Q(I,K)*EONE(J+NNZ(K)+NW(K),I+NNZ(K),K,1,L)	000453000
C/(TRANS(K)*12.566371)	000454000
2555 CONTINUE	000455000
2550 CONTINUE	000456000
DO 2551 K=1,NZ	000457000
DO 2552 I=1,NNZ(K)	000458000
2552 B(I+ICYC)=B(I+ICYC)-HW(I,K)*12.566371	000459000
ICYC=ICYC+NNZ(K)	000460000
2551 CONTINUE	000461000
ICYC=0	000462000

C		00046300
C		00046400
C	INPUT BOUNDARY CONDITIONS.	00046500
C		00046600
C		00046700
	DO 1150 K=1,NZ	00046800
	DO 1100 I=1,NNZ(K)	00046900
	IF (ID(I,K).EQ.1) F(I,K)=SIN(1.5707963*T(L))	00047000
	G(I,K)=0.0	00047100
	IF (ID(I,K).EQ.4) GO TO 1100	00047200
	IC=IC+1	00047300
	IF (ID(I,K).EQ.3) GO TO 1101	00047400
	IF (ID(I,K).EQ.2) GO TO 1102	00047500
	A(M+IC,I+ICYCIC)=1.0	00047600
	B(M+IC)=F(I,K)	00047700
	GO TO 1100	00047800
1101	DO 2001 I1=1,MM	00047900
2001	A(I+ICYC,I1)=0.0	00048000
	A(I+ICYC,I+ICYCIC)=1.0	00048100
	A(M+IC,I+ICYCIC+NNZ(K))=1.0	00048200
	B(I+ICYC)=F(I,K)	00048300
	B(M+IC)=G(I,K)	00048400
	GO TO 1100	00048500
1102	A(M+IC,I+ICYCIC+NNZ(K))=1.0	00048600
	B(M+IC)=G(I,K)	00048700
1100	CONTINUE	00048800
	ICYC=ICYC+NNZ(K)	00048900
	ICYCIC=ICYCIC+2*NNZ(K)	00049000
1150	CONTINUE	00049100
	ICYC=0	00049200
	ICYCIC=0	00049300
	IF (NZ.EQ.1) GO TO 1160	00049400
	DO 1160 K=1,NZ-1	00049500
	DO 1170 J=K+1,NZ	00049600
	ICYC=ICYC+2*NNZ(J-1)	00049700
	IF (NCP(K,J).EQ.0) GO TO 1170	00049800
	DO 1180 I=1,NCP(K,J)	00049900
	IC=IC+1	00050000
	N1=I-1+NCOMM(K,J)	00050100
	IF (N1.GT.NNZ(K)) N1=N1-NNZ(K)	00050200
	N2=NCOMM(J,K)+NCP(K,J)-I	00050300
	IF (N2.GT.NNZ(J)) N2=N2-NNZ(J)	00050400
	A(M+IC,ICYCIC+N1)=1.0	00050500
	A(M+IC,ICYC+N2)=-1.0	00050600
	IC=IC+1	00050700
	A(M+IC,ICYCIC+NNZ(K)+N1)=TRANS(K)	00050800
	A(M+IC,ICYC+NNZ(J)+N2)=TRANS(J)	00050900
1180	CONTINUE	00051000
1170	CONTINUE	00051100
	ICYCIC=ICYCIC+2*NNZ(K)	00051200
	ICYC=ICYCIC	00051300
1160	CONTINUE	00051400
	ICYC=0	00051500
	ICYCIC=0	00051600
	IC=0	00051700

C		00051800
C		00051900
C	SOLVE A*(H,DH/DN)=B.	00052000
C		00052100
C		00052200
	DO 5000 I=1,MM-1	00052300
	IP=I+1	00052400
	MAX=I	00052500
	DO 1000 J=IP,MM	00052600
	IF (ABS(A(J,I)).GT.ABS(A(MAX,I))) MAX=J	00052700
1000	CONTINUE	00052800
	DO 2000 J=1,MM	00052900
	TEMP=A(MAX,J)	00053000
	A(MAX,J)=A(I,J)	00053100
2000	A(I,J)=TEMP	00053200
	TEMP=B(MAX)	00053300
	B(MAX)=B(I)	00053400
	B(I)=TEMP	00053500
	DO 3000 J=IP,MM	00053600
	FACT=A(J,I)/A(I,I)	00053700
	B(J)=B(J)-FACT*B(I)	00053800
	DO 4000 K=1,MM	00053900
	A(J,K)=A(J,K)-FACT*A(I,K)	00054000
4000	CONTINUE	00054100
3000	CONTINUE	00054200
5000	CONTINUE	00054300
	U(MM,L)=B(MM)/A(MM,MM)	00054400
	DO 6000 I=2,MM	00054500
	K=MM-I+2	00054600
	U(K-1,L)=B(K-1)	00054700
	DO 7000 J=K,MM	00054800
7000	U(K-1,L)=U(K-1,L)-A(K-1,J)*U(J,L)	00054900
6000	U(K-1,L)=U(K-1,L)/A(K-1,K-1)	00055000
	DO 8000 K=1,NZ	00055100
	DO 8500 I=1,NNZ(K)	00055200
	IOUT=IOUT+1	00055300
	H(I,K)=U(IOUT,L)	00055400
8500	DHDN(I,K)=U(IOUT+NNZ(K),L)	00055500
	IOUT=IOUT+NNZ(K)	00055600
8000	CONTINUE	00055700
	IOUT=0	00055800
C		00055900
C		00056000
C	OUTPUT SOLUTION ON BOUNDARY.	00056100
C		00056200
C		00056300
	DO 9000 K=1,NZ	00056400
	WRITE(6,40)L	00056500
40	FORMAT(1H1,'TIME STEP IS',X,I3)	00056600
	WRITE(6,50)K,T(L)	00056700
50	FORMAT(1H0,'SOLUTION FOR ZONE',X,I2,X,'AT TIME =',X,F10.5)	00056800
	WRITE(6,60)	00056900
60	FORMAT(1H0,4X,'I',6X,'X(I)',8X,'Y(I)',8X,'H(I)',9X,'DH/DN(I)')	00057000
	WRITE(6,70)(I,X(I,K),Y(I,K),H(I,K),DHDN(I,K),I=1,NNZ(K))	00057100
70	FORMAT(1H0,3X,I3,3X,F8.5,5X,F8.5,5X,F8.5,5X,F9.5)	00057200
9000	CONTINUE	00057300
	DO 80 K=1,NZ	00057400
	DO 80 I=1,NNZ(K)	00057500
	H(I,K)=0.0	00057600
	DHDN(I,K)=0.0	00057700
80	HW(I,K)=0.0	00057800
	DO 90 I=1,MM	00057900
	B(I)=0.0	00058000
	DO 90 J=1,MM	00058100
90	A(I,J)=0.0	00058200
C		00058300

```

C
C CALCULATE H AT INTERNAL POINTS.
C
C
DO 901 K=1,NZ
IF (NP(K).EQ.0) GO TO 904
DO 902 KT=2,L
DELT1=T(L)-T(KT)
DELT2=T(L)-T(KT-1)
DELT3=T(KT)-T(KT-1)
DO 902 I=1,NP(K)
DO 902 J=1,NNZ(K)
JM=J-1
IF (J.EQ.1) JM=NNZ(K)
DS=0.5*(S(J,K)+S(JM,K))
IF (JD(J,K).EQ.1) DS=0.5*S(JM,K)+DSM(J,K)
IF (JD(JM,K).EQ.1) DS=0.5*S(J,K)+DSP(JM,K)
IF (L.EQ.KT) VAL1=0.0
IF (L.EQ.KT) GO TO 903
V1=R(NNZ(K)+NW(K)+I,J,K)**2/(4.0*ASQUAR(K)*DELT1)
VAL1=EXP(-V1)
903 V2=R(NNZ(K)+NW(K)+I,J,K)**2/(4.0*ASQUAR(K)*DELT2)
VAL2=EXP(-V2)
DELEX=VAL2-VAL1
DELE=EONE(NNZ(K)+NW(K)+I,J,K,KT-1,L)-EONE(NNZ(K)+NW(K)+I,J,K,KT,L)
TERM1=COS(RNP(I,J,K))/(R(NNZ(K)+NW(K)+I,J,K)*6.2831853072)
TERM2=R(NNZ(K)+NW(K)+I,J,K)*COS(RNP(I,J,K))/(25.1327412288*ASQUAR
C(K))
TERM3=((U(J+ICYCIC,KT-1)*DELT1)-(U(J+ICYCIC,KT)*DELT2))/DELT3
TERM4=(U(J+ICYCIC,KT)-U(J+ICYCIC,KT-1))/DELT3
TERM5=((U(J+ICYCIC+NNZ(K),KT-1)*T(KT))-(U(J+ICYCIC+NNZ(K),KT)*
CT(KT-1)))/(12.5663706144*DELT3)
TERM6=(U(J+ICYCIC+NNZ(K),KT)-U(J+ICYCIC+NNZ(K),KT-1))/
C(12.5663706144*DELT3)
902 HIP(I,L,K)=HIP(I,L,K)+((TERM5*DELE)+(TERM6*(T(L)+((R(NNZ(K)+NW(K)+
CI,J,K)**2)/(4.0*ASQUAR(K))))*DELE)
C+((TERM6*DELT1*VAL1)-(TERM6*DELT2*VAL2)-(TERM1*DELEX*TERM3)
C-(TERM2*TERM4*DELE))*DS
904 ICYCIC=ICYCIC+2*NNZ(K)
901 CONTINUE
ICYCIC=0
C
C
C OUTPUT H AT INTERNAL POINTS.
C
C
DO 910 K=1,NZ
IF (NP(K).EQ.0) GO TO 910
WRITE(6,912)K
912 FORMAT(1H0,'INTERNAL POINTS FOR ZONE',X,I2,X,'FOLLOW')
DO 913 I=1,NP(K)
HIP(I,L,K)=HIP(I,L,K)+HWP(I,L,K)
WRITE(6,911)I,X(NNZ(K)+NW(K)+I,K),Y(NNZ(K)+NW(K)+I,K),HIP(I,L,K)
911 FORMAT(1H0,3X,I3,3X,F8.5,5X,F8.5,5X,F8.5)
913 CONTINUE
910 CONTINUE
600 CONTINUE
END
C
C *****
C *
C * FUNCTION EONE(I,J,K,LT,L) *
C *
C *****
C
FUNCTION EONE(I,J,K,LT,L)
COMMON/BLOCK1/R(100,100,5),T(20),ASQUAR(5),A0,A1,A2,A3,A4,A5,B1,B2
C,B3,B4,B5,B6,B7,B8
IF (LT.NE.L) GO TO 502
EONE=0.0
GO TO 500
502 D=R(I,J,K)**2/(4.0*ASQUAR(K)*(T(L)-T(LT)))
IF (D.GE.1.0) GO TO 501
EONE=-ALOG(D)+A0+A1*D+A2*D**2+A3*D**3+A4*D**4+A5*D**5
GO TO 500
501 TOP=D**4+B1*D**3+B2*D**2+B3*D+B4
BOT=D**4+B5*D**3+B6*D**2+B7*D+B8
EONE=TOP/(BOT*D)*EXP(-D)
500 RETURN
END

```

```

DO 600 L=2,N
ICYC=0
ICYCIC=0
DO 700 K=1,NZ
DO 800 I=1,NNZ(K)
DO 850 J=1,NNZ(K)
JM=J-1
IF(J.EQ.1) JM=NNZ(K)
IF(I.EQ.J) GO TO 850
VAL=R(I,J,K)**2/(4.0*ASQUAR(K)*(T(L)-T(L-1)))
DS=S(J,K)+S(JM,K)
IF(JD(J,K).EQ.1) DS=S(JM,K)+DSM(J,K)*2.0
IF(JD(JM,K).EQ.1) DS=S(JM,K)+DSM(J,K)*2.0
IF(JD(JM,K).EQ.1) DS=S(J,K)+DSP(JM,K)*2.0
A(I+ICYC,I+ICYCIC)=A(I+ICYC,I+ICYCIC)-COS(RN(I,J,K))*DS/R(I,J,K)
A(I+ICYC,J+ICYCIC)=COS(RN(I,J,K))*EXP(-VAL)*DS/R(I,J,K)
A(I+ICYC,I+ICYCIC+NNZ(K))=A(I+ICYC,I+ICYCIC+NNZ(K))
C+0.5*ALOG(VAL*1.7810723)*DS
A(I+ICYC,J+ICYCIC+NNZ(K))=0.5*EONE(I,J,K,L-1,L)*DS
850 CONTINUE
A(I+ICYC,I+ICYCIC+NNZ(K))=A(I+ICYC,I+ICYCIC+NNZ(K))
C-2.0*SLOG(I,K)-TOTS(K)*ALOG(0.4452681/(ASQUAR(K)*(T(L)-T(L-1))))
800 CONTINUE
ICYC=ICYC+NNZ(K)
ICYCIC=ICYCIC+2*NNZ(K)
700 CONTINUE
ICYC=0
ICYCIC=0
IF(L.EQ.2) GO TO 55
DO 2220 K=1,NZ
DO 2200 KT=2,L-1
DO 2200 I=1,NNZ(K)
DO 2200 J=1,NNZ(K)
JM=J-1
IF(J.EQ.1) JM=NNZ(K)
DS=0.5*(S(J,K)+S(JM,K))
IF(JD(J,K).EQ.1) DS=0.5*S(JM,K)+DSM(J,K)
IF(JD(JM,K).EQ.1) DS=0.5*S(J,K)+DSP(JM,K)
IF(I.EQ.J) GO TO 2150
VAL1=EXP(-(R(I,J,K)**2/(4.0*ASQUAR(K)*(T(L)-T(KT-1)))))
VAL2=EXP(-(R(I,J,K)**2/(4.0*ASQUAR(K)*(T(L)-T(KT)))))
B(I+ICYC)=B(I+ICYC)
C-U(J+ICYCIC+NNZ(K),KT)*(EONE(I,J,K,KT-1,L)-EONE(I,J,K,KT,L))*DS
C-2.0*U(J+ICYCIC,KT)*(VAL1-VAL2)*COS(RN(I,J,K))*DS/R(I,J,K)
GO TO 2200
2150 B(I+ICYC)=B(I+ICYC)-U(J+ICYCIC+NNZ(K),KT)*ALOG((T(L)-T(KT-1))
C/(T(L)-T(KT)))*DS
2200 CONTINUE
ICYC=ICYC+NNZ(K)
ICYCIC=ICYCIC+2*NNZ(K)
2220 CONTINUE
ICYC=0
ICYCIC=0
55 CONTINUE

```

Fig. B.1 Program Segment to Replace Lines 34200 - 43800 (inclusive) to obtain a Listing for Method 1, Chapter 5.